THE DEVELOPMENT OF A MODEL FOR HIGH PRESSURE PROPENE OLIGOMERISATION OVER H-ZSM-5

By

Sarah Jane Sealy
BSc(Chem. Eng.) (University of Cape Town)

Submitted to the University of Cape Town in fulfilment of the requirements for the degree of

Doctor of Philosophy

Department of Chemical Engineering
University of Cape Town
Rondebosch
Cape Town
South Africa

Date : July 1996

ACKNOWLEDGEMENTS

Firstly, I would like to thank my supervisors Professor Cyril O'Connor and Associate Professor Duncan Fraser for their valuable guidance throughout my post-graduate studies and for reading and correcting the many versions of my thesis. Secondly I would like to thank my third, unofficial supervisor, Dr Klaus Möller, for his valuable comments and criticisms.

Next, I should like to thank all the "unsung heros" of the Department of Chemical Engineering, UCT. Without these people, many of the theses completed here would simply not be possible: Mr Bill Randall and Granville de la Cruz of the Electronic Workshop, as well as Tony Barker, Peter Tobias, Joachim Mäcke and James Daniels of the Technical Workshop. Also Pam Link, Leslie Petrik and Maria Josias, as well as others too numerous to mention.

I would also like to thank the Foundation for Research and Development for their financial assistance throughout my PhD studies.

Finally, I would like to thank all my fellow post-graduate colleagues, who made life just that little bit more enjoyable :

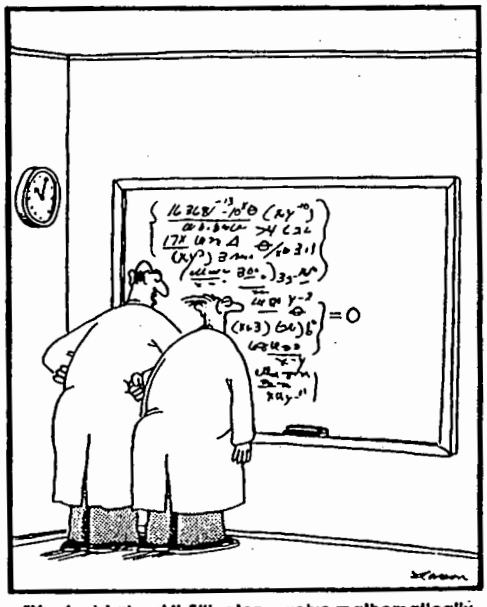

"No doubt about it, Ellington—we've mathematically expressed the purpose of the universe. Gad, how I love the thrill of scientific discovery!"

non-shape selective catalysts and the proposed pathway. The major nonene carbon skeletons observed experimentally were, according to the proposed mechanism, primary products or those that had undergone rapid methyl-shift reactions. The agreement between all the product spectra father pointed to a common reaction mechanism.

TABLE OF CONTENTS

LIST OF TABLES

LIST OF FIGURES

NOMENCLATURE

Symbol	Description
Chapter 1	
b	equilibrium constant of adsorption
C	concentration, mol/length^3
E	activation energy, energy/mol
g	gasoline selectivity
k	rate constant
k^*	elementary rate constant
k_{ij}^f	forward rate constant
k_{ij}^r	reverse rate constant
k_o	pre-exponential factor in Arrhenius equation for rate constant
n_e	number of elementary events
N	number of oligomers
P	pressure
P(X)	probability that reaction will involve molecule X
q_{uv}	scale factor, defined in Equation 1.4
r	reaction rate, units vary according to rate equations
R	reactivity parameter
R_g	universal gas constant, energy/mol/K
T	temperature, K
w(T)	percent of reaction products boiling above T
$w_o(T)$	percent of feedstock boiling above T
x_i	mol fraction of i
x	conversion
Greek	
α	relative rate parameter for disproportionation

ω	carbon number reactivity parameter

Chapter 2

n	number of data points
s	standard deviation, defined by Equation 2.2
V	coefficient of variation, defined by Equation 2.3
x*	mean of a set of data points, defined by equation 2.1
x_i	data point, i = 1...n

Chapter 3

a_m	external surface per unit mass, length^2/mass
C_b	bulk gas concentration, mol/length^3
C_s	surface gas concentration, mol/length^3
D_e	diffusivity coefficient, length^2/time
E_r	activation energy for reaction, energy/mol
E_d	activation energy for diffusion, energy/mol
k	rate constant, units defined by rate equation
K	Henry's Law constant
k_{eff}	effective rate constant, units defined by rate equation
k_i	intrinsic rate constant, units defined by rate equation
k_m	external mass transfer coefficient, length/time
k_o	pre-exponential factor in Arrhenius equation
K_o	pre-exponential factor in Arrhenius equation for K
r	nth order reaction rate, mol/mass cat/time
R	universal gas constant, energy/mol/K
Re	Reynolds Number
R_p	particle radius, length
Sh	Sherwood Number
T	temperature, K
ΔU_o	activation energy for adsorption, energy/mol

Greek

η	effectiveness factor

Chapter 4

G	Gibbs energy, energy/mol
C	concentration, mol/length^3
k	rate constant, units defined by rate equation
K	equilibrium constant of reaction

Chapter 5

A	square matrix, defined by Equation 5.6
A	constant, defined by Equation 5.23
a_i	constant defined by Equation 5.10, i = 1..6
B	constant, defined by Equation 5.23
B_{ij}	element of othogonal collocation matrix **B**
C	concentration, mol/length3
C_i	constant of integration, i = 1..3
const1	constant, defined by Equation 5.22
const2	constant, defined by Equation 5.22
const3	constant, defined by Equation 5.22
const4	constant, defined by Equation 5.22
const5	constant, defined by Equation 5.22
const6	constant, defined by Equation 5.22
const7	constant, defined by Equation 5.22
const8	constant, defined by Equation 5.22
const9	constant, defined by Equation 5.22
constA	constant, defined by Equation 5.83
constB	constant, defined by Equation 5.84
constC	constant, defined by Equation 5.85
constD	constant, defined by Equation 5.86
constE	constant, defined by Equation 5.87
constF	constant, defined by Equation 5.88
constG	constant, defined by Equation 5.89

constH	constant, defined by Equation 5.90
d	matrix defined by Equation 5.97
D	constant, defined by Equation 5.23
D_i	diffusion coefficient, length^2/time
h	vector, defined by Equation 5.7
K	equilibrium constant
k	first order rate constant, length^3/time/mass or relative rate constant
n	number of data points
N	number of collocation points
r	rate of reaction, mol/mass/time
r	radial co-ordinate
R	radius of particle, length
t	time
W	weighting function in orthogonal collocation
X	eigenvector maxtrix
x_i^*	constant, defined by Equation 5.10, i = 1..3
z_i	variable, defined by Equations 5.16 - 5.18, i = 1..3

Subscripts

b,bulk	bulk
cati	surface reaction i, i = 1..3
exp	experimental data
eq	equilibrium
D	doubly methyl branched hexene carbon skeleton
L	linear hexene hexene carbon skeleton
model	model data
p	particle
S2	singly branched hexene carbon skeleton, methyl branch on second carbon
S3	to singly branched hexene carbon skeleton, methyl branch on third carbon
s,sur	surface

v	vacant acid sites

Superscript

*	surface

Greek

η	effectiveness factor, defined by Equation 5.98
θ	dimensionless radial co-ordinate
λ	eigenvector
ρ_p	density of particle

Chapter 6

C	concentration, mol/length^3
k	rate constant, units defined by rate constants
P	pressure
R	universal gas constant, energy/mol/K
t	time
T	temperature, K
Z	compressibility factor

CHAPTER 1 - INTRODUCTION

1.1 Introduction

The primary aim of this thesis is to develop a fundamental, mathematical model for high pressure propene oligomerisation over H-ZSM-5. To this end, this introductory chapter first revises the characteristics and applications of catalysts which have been shown to be active for oligomerisation. This is further split into acid catalysts, heterogeneous nickel catalysts, other transition metal catalysts and finally homogeneous metal catalysts. The next section covers the various mechanisms of oligomerisation on different catalyst types since an understanding of these mechanisms is an important step in the modelling process. Following this, the modelling of oligomerisation reactions is reviewed with an additional section on other complex reaction models. Throughout this chapter heterogeneous acid catalysts are given the most emphasis, especially H-ZSM-5, since this thesis is concerned with modelling oligomerisation over acid catalysts. The final sections of this chapter cover the objectives of this study and the approach to studying this complex reaction in detail.

During oligomerisation light olefins are polymerised into molecules consisting of a small number of monomer units, termed oligomers. This industrially important reaction is used to synthesise motor fuels, plasticizers, medicines, dyes, resins, detergents, lubricants and additives (O'Connor and Kojima (1990)). Alpha-olefins produced via homogeneous ethene oligomerisation have a very wide application as can be seen in the Table 1.1 (Al-Jarallah et al. (1992)).

Heterogeneous acid catalysts, of which zeolites are important examples, are used in the production of hydrocarbon fuels. An example of the commercial application of this reaction is the Mobil Olefins to Gasoline and Distillate (MOGD) process which converts light olefins to synthetic fuels using the shape selective catalyst H-ZSM-5 (Tabak (1984)). Homogeneous catalysts are also widely used in commercial processes. In their review Al-Jarallah et al. (1992) provide examples of the commercial application of homogeneous ethene oligomerisation namely, the Chevron process which utilizes a Ziegler catalyst, the Shell

Table 1.1 Uses of Alpha Olefins (Al-Jarallah et al. (1992))

Alpha Olefin									Reactant	Product	Applications
C4									Polymerize	Polymer	Polybutene
	C6	C8							$CH_2=CH_2$	Comonomers	HDPE, LLDPE
	C6	C8							CO/H_2O	Synthetic Acids	Esters
	C6	C8	C10						$CO/2H_2$	Plasticizer Alcohols	PVC plasticizers
		C8	C10						Oligomerize	Trimers	Sythetic Lube Oils
			C10	C12					CH_3CO_3H	Epoxides	Diols, Hyroxethers, Amines
		C8	C10	C12					H_2S	Mercaptans	Herbicides, Plastics
			C10	C12	C14				CO/H_2	Aldehydes	Acids, Detergents, Alcohols
				C12	C14				C_6H_6	Detergents Alkylates	Surfactants
					C14	C16			H_2SO_4	Alkyl Sulphates	Surfactants
					C14	C16			SO_3	Olefin Sulphonates	Surfactants
					C14	C16			C_6H_5OH	Alkyl Phenols	Surfactants, Lube Oil Additives
						C16	C18		HBr	Alkyl Halides	Amines
						C16	C18		$(CH_3)_2NH$	Tertiary Amines	Cationic Surfactants
						C16	C18		CH_3CN	Nitriles	Amines, Amides
						C16	C18		Maleic-anhydride	Akenyl Succinic-anhydrides	Paper Sizing, Leather, Preservatives
						C16	C18	C20	PH_3	Phosphines	Antistats

Higher Olefin process which oligomerizes ethene using a nickel-ligand catalyst and the EthylCorporation process which uses a modified Ziegler catalyst.

1.2 Catalysts Used For Olefin Oligomerisation

O'Connor and Kojima (1990) reviewed olefin oligomerisation. Along with the kinetics and thermodynamics of the reaction, they thoroughly reviewed catalysts used for catalysing olefin oligomerisation.

1.2.1 Acidic Catalysts

Acidic catalysts can be divided into three major groups namely, zeolites, aluminophosphate molecular sieves and non-zeolitic materials. These are discussed in detail below.

1.2.1.1 Zeolites

Zeolites are crystalline alumino-silicate molecular sieves. They have a porous structure and ion-exchange capacities. These materials may also contain other elements in addition to silicon and aluminium in their framework structures. Acid sites present in the zeolite structure are responsible for their catalytic activity. The original model of the Brønstead acid site proposed by Uytterhoeven et al. (1965) (Figure 1.1a), has recently been shown to be simplistic and the acidic zeolite cluster shown in Figure 1.1b (Kramer et al. (1993)) is more likely to be representative of this site. The interaction of the acidic cluster with a hydrocarbon uses two oxygen atoms of the zeolite. One behaves as an acid, the other as a base. Zeolites also possess Lewis acidity which is associated with extra framework aluminium species.

Some zeolites used for olefin oligomerisation are discussed below :

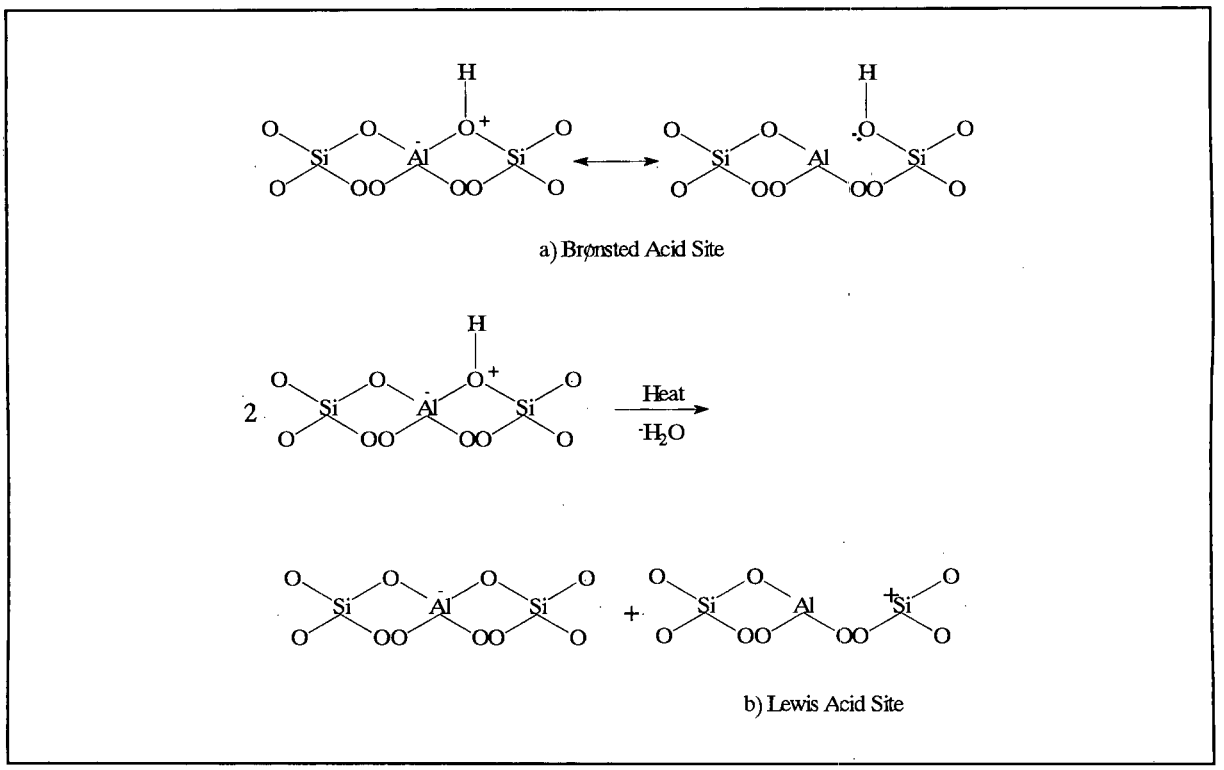

Figure 1.1a : Types of Acid Sites in Zeolites as proposed by Uytterhoeven et al. (1965)

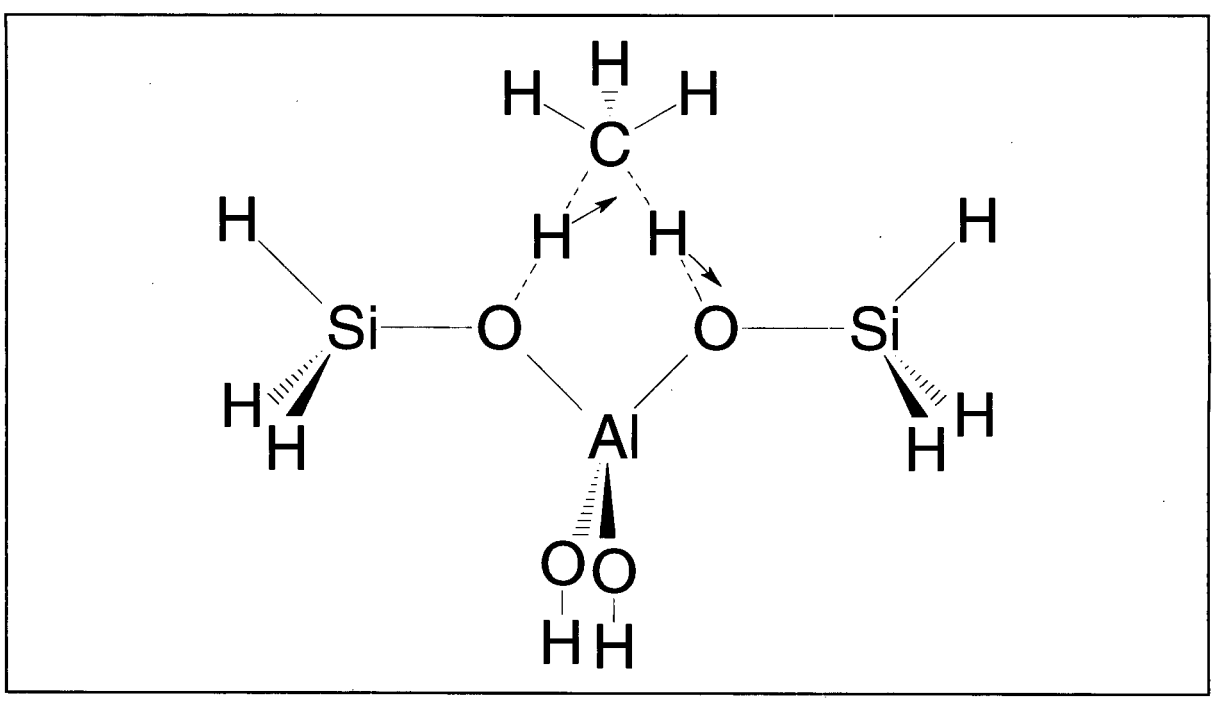

Figure 1.1b : Interaction of a Methane Molecule with an Acid Zeolite Cluster - Kramer et al. (1993)

1) H-ZSM-5, which is used in the MOGD Process, is a medium pore zeolite and a member of the pentasil family (Garwood et al. (1972), Garwood and Lee (1980), Tabak (1984)). The framework structure of this catalyst is shown in Figures 1.2 and 1.3. The pentasil framework structures are formed by linking chains of 5-membered ring secondary building units. H-ZSM-5 has two perpendicularly intersecting 10-ring channel systems. One channel is straight with almost circular openings (5.3 x 5.6 Å) and the other is sinusoidal with elliptical openings (5.1 x 5.6 Å). The intersections of these channels provide a free volume slightly larger in size - approximately 9Å. The geometrical constraints imposed by the 10 membered oxygen ring pores hinder coke formation since large polynuclear hydrocarbons have difficulty forming.

The silica-alumina ratio of H-ZSM-5 ranges from about 20 to above 8000 (essentially Al free). Those materials with a high silica-alumina ratio are highly hydrophobic, thermally stable and more resistant to coke.

Oligomerisation reaction conditions and the nature of the reaction products obtained for this catalyst are discussed in detail in section 1.3.

2) H-Beta was chosen for this study as an example of a large pore zeolite for comparison with H-ZSM-5 and is not widely used to oligomerise light olefins. It has two intersecting pore systems that consist of 12-member rings. The pores are 6.5 x 5.6 Å and 7.5 x 5.7 Å.

3) H-ZSM-12 is an example of a large pore zeolite with a one dimensional channel system. The pores consist of 12-membered rings, 5.5 x 5.9 Å in size. This catalyst oligomerised straight and branched chain olefins in the range C_2 to C_6 (Tabak (1981). Preferred reaction conditions were 38 to 149°C and weight hourly space velocities (WHSV's) between 0.1 and 5 hr^{-1}. Pressures sufficiently high enough to maintain liquid phase were used and depended on the carbon number of the feed and the reaction temperature and thus ranged from 0 to 20 MPa. The silica-alumina ratio used was between 20 and 100.

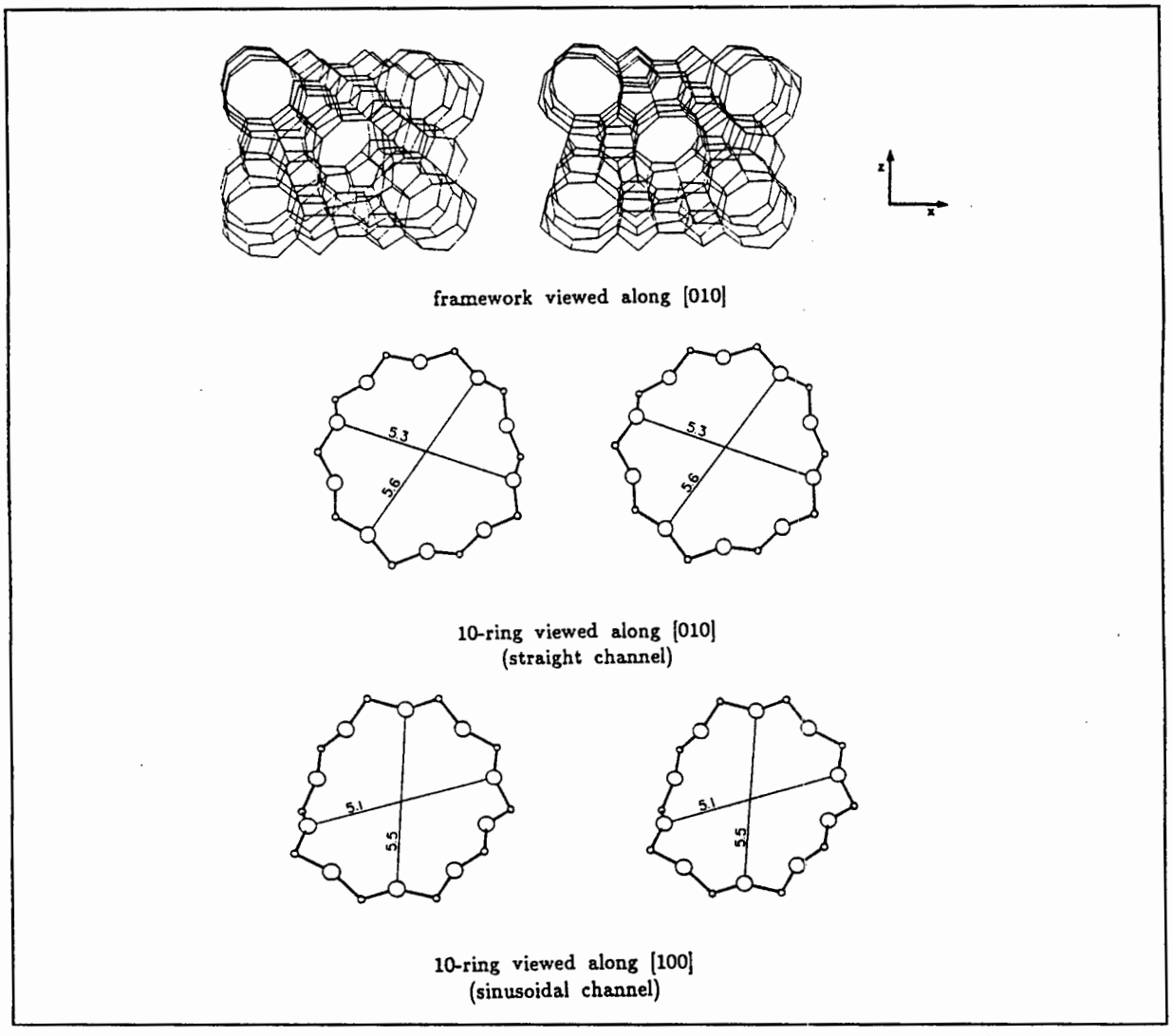

Figure 1.2 : Structure of H-ZSM-5 (Meier and Olson (1992))

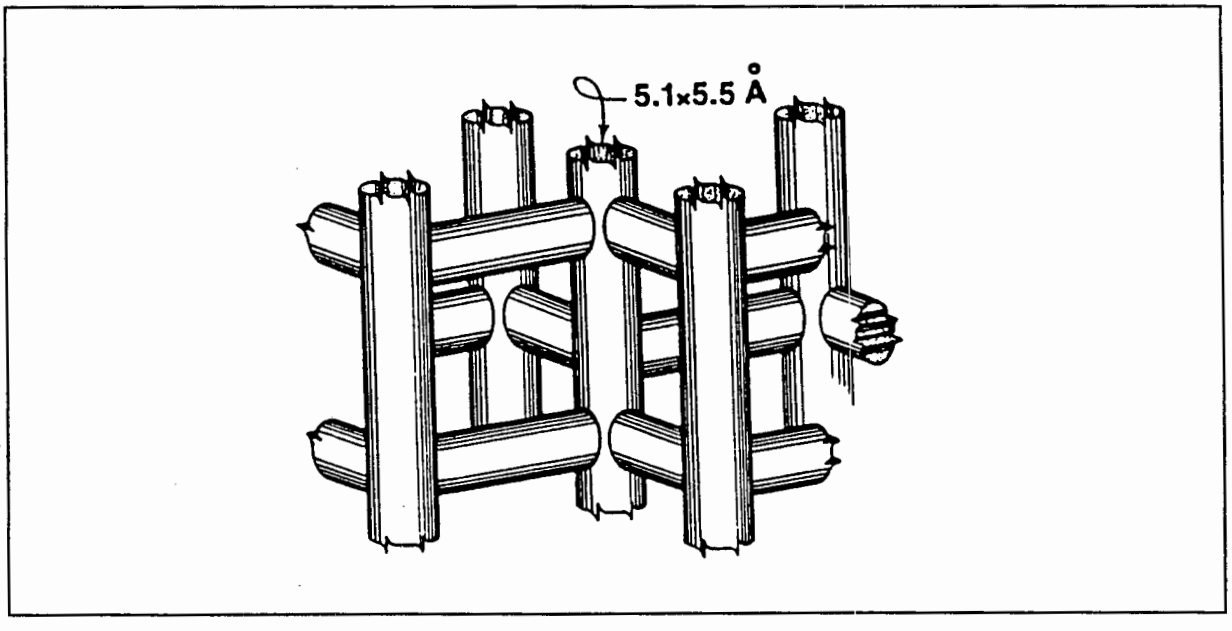

Figure 1.3 : The Pore System in H-ZSM-5 (Meisel et al. (1976))

4) H-ZSM-48 is a medium pore zeolite with a one dimensional pore system. The pores consist of 10 membered rings and are 5.3 x 5.6 Å in size. This catalyst oligomerised light olefins (C_2 - C_8) to gasoline and distillate range hydrocarbons as well as a high-boiling lube fraction. The reaction was conducted in the vapour phase at 204 to 260°C and between 4.8 and 6.8 MPa. WHSV's in the range 0.3 to 4 hr^{-1} were used (Chu and Valyocsik (1987)).

Ocelli et al. (1985) conducted a comparative study on several zeolites capable of catalysing propene oligomerisation. Pilot plant studies were conducted at 3 to 5 MPa and 100 to 400°C. It was found that the molecular size of the oligomers produced was controlled by the zeolite pore size. The catalysts studied by these researchers are listed below. The performance of these catalysts was compared to that of H-ZSM-5.

5) The H-Boralite used by Ocelli et al. (1985) was a borosilicate isomorphous with H-ZSM-5. At high conversions the major product was olefinic (> 90wt%). This catalyst produced more linear isomers than any of the other catalysts studied. No significant deactivation was observed over the temperature range studied.

6) H-Offretite is a large pore zeolite. This catalyst has 12-member ring channels of 6.7Å and intersecting channels consisting of 8-member rings, 3.6 by 4.9Å. The olefinic content of the liquid product from this catalyst was lower than for H-Boralite (~80wt%) with a correspondingly higher content of saturates and aromatics. This catalyst was found to minimize the formation of C_7 and C_8 products.

7) HY is also a large pore zeolite with a three dimensional pore system. The channels consist of 12-member rings with a diameter of 7.4 Å. The product obtained from this catalyst was similar to that obtained using H-Offretite with respect to the olefin/paraffin/aromatic ratios.

8) H-Mordenite is classified as a large pore zeolite with a two dimensional pore system. One channel consists of 12-membered rings while the other is made up of 8-membered rings. The dimension of the largest channel is 6.5 x 7.0 Å. The liquid product produced using this catalyst was similar in composition to that obtained using

H-Offretite.

9) H-Omega is a large pore zeolite with a unidimensional pore system consisting of 12-member ring pores, 7.5Å in diameter. This catalyst had a higher content of paraffins and olefins and a lower content of olefins than H-Offretite, HY and H-Mordenite. At high conversion the liquid product from this catalyst had the highest carbon number of all the catalysts studied.

The liquid product obtained from the catalysts was analysed for degree of branching. Branched primary and tertiary carbon-containing oligomers were found to increase with increasing pore size. (The pore size was based on the kinetic diameter of the largest molecule sorbed.) Additionally, the larger oligomers had a higher ratio of tertiary/secondary carbons. H-Omega produced the most branched product, followed by H-Y, H-ZSM-5, H-M and H-Offretite produced a less branched product than H-Y, while H-Boralite was the most linear.

1.2.1.2 Aluminophosphate Molecular Sieves

Oligomerisation over aluminoposhate molecular sieves has been reported (Long et al.(1985)):

1) SAPO-11, -31, -34
2) MeAPO-11

Aluminophosphate sieves (ALPO's) consist of alternating AlO_2^- and PO_2^+ units. The framework is neutral, with no extra-framework cations and the acidity is negligible. They exhibit reasonable thermal and hydrothermal stability (Venuto (1994)).

Silicoaluminophosphates (SAPO's) are ALPO's with varying amounts of silicon substituted for phosphorous in the $AlPO_4$ framework. This results in weak to moderate acid catalytic properties. The mole fraction of silicon varies from 0 - 1 in $Si_xAl_yP_z$ depending on the synthesis conditions. SAPO's are present in a wide variety of structural and compositional types. For example, SAPO-11 and SAPO-31 have intermediate pore systems while SAPO-34 is an example of a small-pore zeolite, structurally similar to chabazite. In addition, SAPO's exhibit significant thermal and hydrothermal stability.

Metal aluminophosphates (MeAPO's) result when metal atoms are substituted into the $AlPO_4$

framework. Examples of metals used are cobalt, magnesium, iron, zinc and titanium. These compounds usually carry a net electric framework charge which is balanced by cations such as H^+. Thus, MeAPO's display a range of acidities. However, MeAPO's also sometimes show basic properties. Their thermal stability depends on the structure and composition on the material.

Reaction conditions for these catalysts that give a high selectivity to oligomers were reported by Long et al. (1985). These are preferably temperatures between 150 and 315°C, pressures between 0.1 and 10MPa and WHSV's 0.1 and 1.0hr^{-1}. The feed consisted of C_2 to C_{12} olefins. Between 10 and 70wt% of paraffins of the same carbon number and water were employed as diluents.

1.2.1.3 Other Acid Catalysts

Other non-zeolitic acid catalysts that have been successfully employed for olefin oligomerisation are briefly discussed here.

1) Phosphoric acid supported on kieselgur (diatomaceous earth) is used commercially in the Catpoly Process. This solid phosphoric acid catalyst consists of 60% P_2O_5 and 40% Kieselguhr. Liquid phosphoric acid as catalyst for olefin oligomerisation was first reported by Ipatieff (1935). It was found that under relatively mild polymerisation conditions namely, 135 to 200°C and 0.1 to 1.5 MPa, the product consisted of entirely mono-olefins. When the reaction conditions were more severe side reactions gave rise to naphthenes, aromatics and paraffins. When propene was bubbled through 100% orthophosphoric acid at 5.1 MPa and 204°C, 51% conversion was obtained. The liquid product contained olefins of carbon number up to and including C_{15}.

2) The use of ion-exchange resins as catalysts for the oligomerisation of isobutene was reported by Haag (1967). The resin used was a sulphonated styrene-divinyl-benzene copolymer with a macrorecticular pore structure, known commercially as Amberlyst 15. Runs were carried out under batch and continuous flow conditions. Typical reaction conditions for the batch reactor were 20 to 60°C and 0.4 to 0.5 MPa, while

those for the flow reactor were 16 to 60°C, 1 MPa and liquid hourly space velocities between 180 and 3600 hr^{-1}. The product consisted of dimer, trimer and tetramer with very small quantities of higher oligomers.

3) The activity of the layered alumino-silicate, synthetic mica-montmorillonite for propene oligomerisation has been reported by Fletcher et al. (1986). Reaction conditions used were 6.1 MPa, 170°C and a WHSV of 1.6hr^{-1}. The liquid product contained significant quantities of olefins up to and including C_{18}. Small amounts of C_{21} were also observed. Of the oligomers the trimer was present in the greatest amount.

1.2.2 Heterogeneous Nickel Catalysts

1) Nickel supported on various aluminosilicates has been widely used for olefin oligomerisation. (Harms et al. (1989), Garwood et al. (1988), Miller (1985), Imai and Uchida (1964), Imai and Uchida (1966), Imai et al. (1968), Hogan et al. (1955)). The supports include silica-alumina, silica, layered alumino-silicates, H-Mordenite, HY and H-ZSM-5.

2) NiO-TiO_2/SO_4^{2-} was prepared by co-precipitation followed by treatment with H_2SO_4 (Sohn et al. (1987a)). This catalyst was very active for ethene dimerization at room temperature. On the other hand, NiO-ZrO_2 alone was found to be inactive. NiO-ZrO_2/SO_4^{2-} was prepared in a similar manner and also found to be active for ethene dimerisation (Sohn and Kim (1986)). Instead of washing with H_2SO_4, other acids namely, H_3PO_4 and H_3BO_3 were also used. This resulted in the following catalysts: NiO-ZrO_2/PO_4^{3-} and NiO-ZrO_2/BO_3^{3-} (Sohn et al. (1987b)). These catalysts were also active for ethene dimerisation but not as active as NiO-ZrO_2/SO_4^{2-}.

3) The Octol Process, described by Nierlich (1992), oligomerises a 1-butene rich feed at 100°C and sufficiently high pressures to ensure liquid phase operation. This process yields mainly C_8 and C_{12} olefins. The heterogeneous catalyst used is essentially nickel supported on a clay. This catalyst is very sensitive to oxygenates such as water, methanol or dimethylether and it is necessary to remove these before

the feed enters the oligomerisation unit.

1.2.3 Other Heterogeneous Transition Metal Catalysts

1) Propene was reacted over unsupported ReO_3 and WO_3 in order to compare the activities for dimerisation and metathesis. It was found that below 330°C the main reaction was dimerisation for WO_3 while for ReO_3 metathesis was the main reaction (Tsuda et al. (1985)).

2) Cheney et al. (1950) describe a process for oligomerising ethene using a catalyst consisting of cobalt supported on activated carbon. Favourable reaction conditions were temperatures below 150°C and pressures of 0.1 to 10 MPa. The oligomers produced were mainly linear. At 50% conversion the main product was dimer with smaller amounts of trimer and higher boiling compounds.

3) Alkali metals on supports of silicates of alkali and alkaline earth metals, α-aluminas and graphite have also been used for olefin oligomerisation (Pines (1981)). Sodium and potassium supported on K_2CO_3 were highly selective for the dimerisation of propene to 4-methyl-1-pentene. The reaction conditions were 150°C and approximately 10 MPa.

1.2.4 Homogeneous Metal Catalysts

Three classes of catalysts are used for homogeneous ethene oligomerisation (Al-Jarallah et al. (1992):

1) Ziegler types such as trialkylaluminum.

2) Ziegler-Natta types such as transition metals with reducing agents or Lewis acids. These use compounds of three transition metals namely, titanium, zirconium or nickel. $TiCl_4$ is the most frequently used in combination with alkyl aluminum halides. Zirconium in the form of $Zr(OR)_4$ is used together with ethylaluminium sesquichloride ($Et_3Al_2Cl_3$). Nickel derivatives used are nickelocene, nickel acetyl-

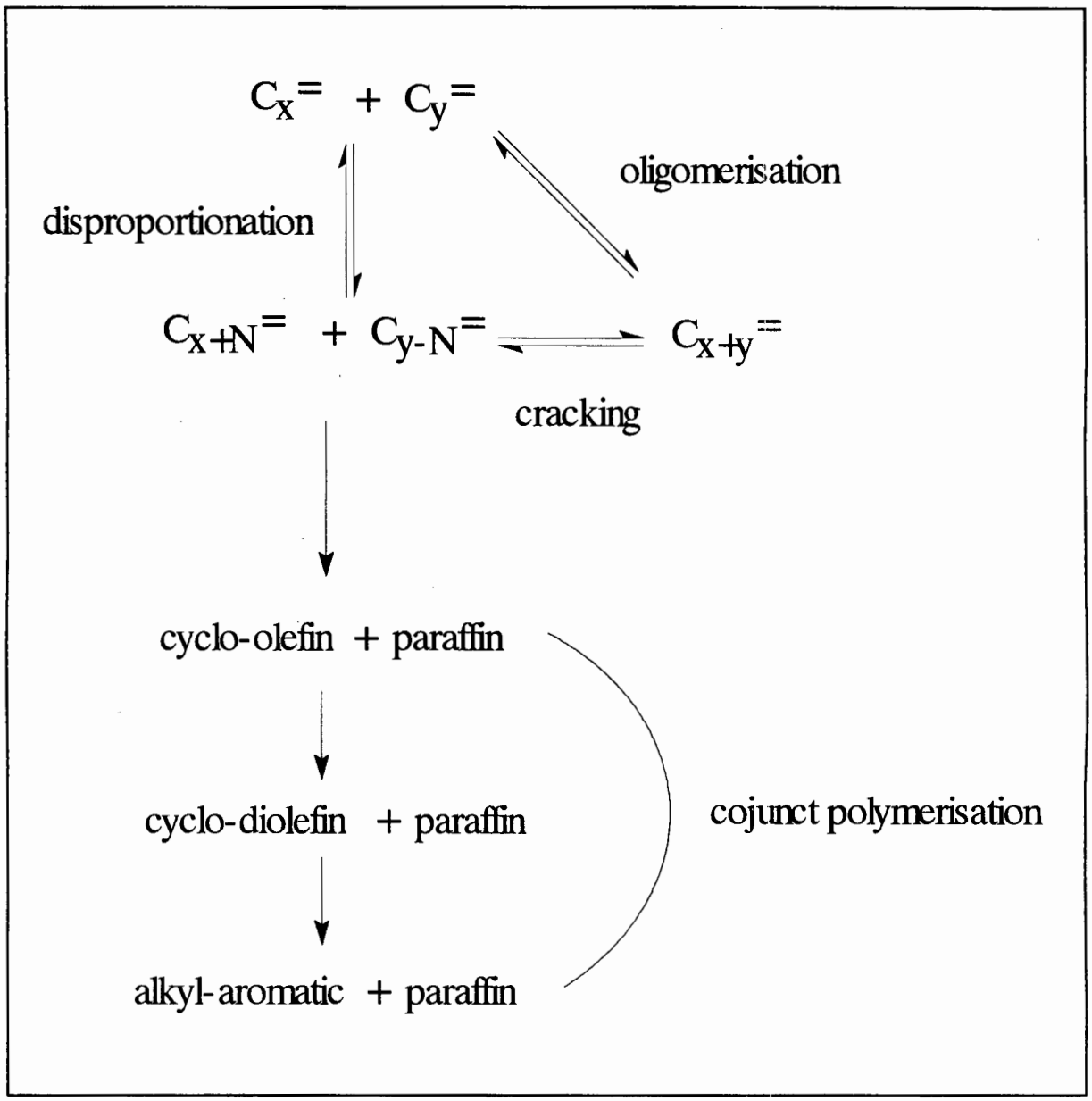

Figure 1.4 : Generalised Reaction Pathway for Oligomerisation (Quann and Krambeck (1990))

acetonates and ylides.

3) Those that can be deduced from the metal complexes (one component catalysts). Complex nickel catalysts have attracted the greatest interest (Keim (1990). An example of a commercial application is the Shell commercial process, SHOP, which uses a non-Ziegler homogeneous nickel ligand catalyst.

1.3 Mechanism of Olefin Oligomerisation

Since the mechanism of hydrocarbon rearrangements that occur during oligomerisation depend on the catalyst type used, this discussion has been divided into sub-sections that cover the major catalyst types and the oligomerisation reactions that occur over them.

1.3.1 Acidic Catalysts

A generalized reaction pathway for oligomerisation is shown in Figure 1.4 (Quann and Krambeck (1990)). Olefins of carbon numbers x and y oligomerise to higher hydrocarbons. These oligomers can crack back to olefins of carbon numbers x+N and y-N. These can undergo disproportionation to two olefins of different carbon numbers. Additionally, cyclic compounds and paraffins are produced via conjunct polymerisation. Each compound formed also undergoes rapid double bond and skeletal isomerisation.

The reaction pathway is clearly a complex one with many reactions occurring simultaneously and many different products being formed. At long reaction times this leads to an almost continuous carbon number spectrum. Indeed, Garwood (1983) has shown that under the same reaction conditions at high conversions, identical product distributions are obtained for C_2 to C_6 and C_{10} olefins.

According to Shephard et al. (1962) Brønsted sites are important for the initiation of the oligomerisation reactions. On the other hand, reactions involving aromatization, hydrogen transfer and coke formation are said to be catalysed by Lewis acid sites.

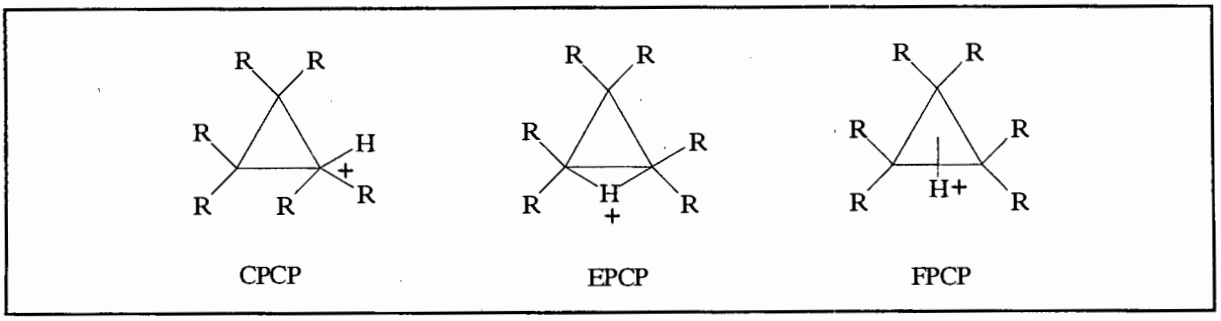

Figure 1.5 : Substituted Protonated Cycloalkanes (Martens and Jacobs (1990))

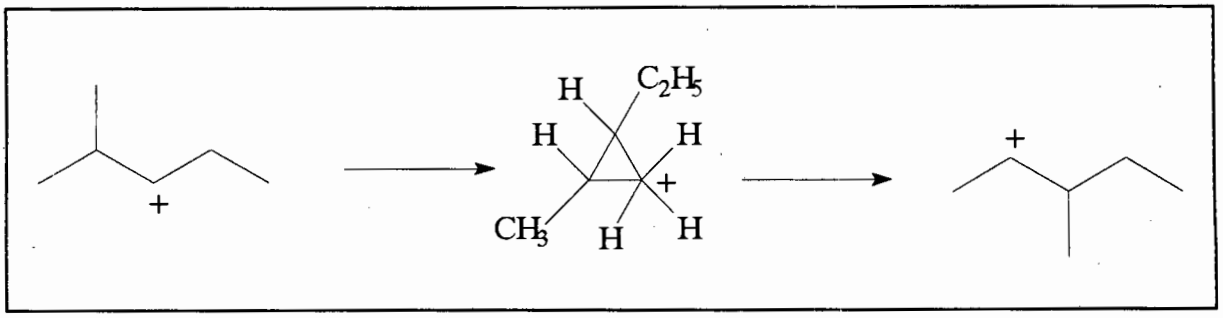

Figure 1.6 : Type A Isomerisation (Martens and Jacobs (1990))

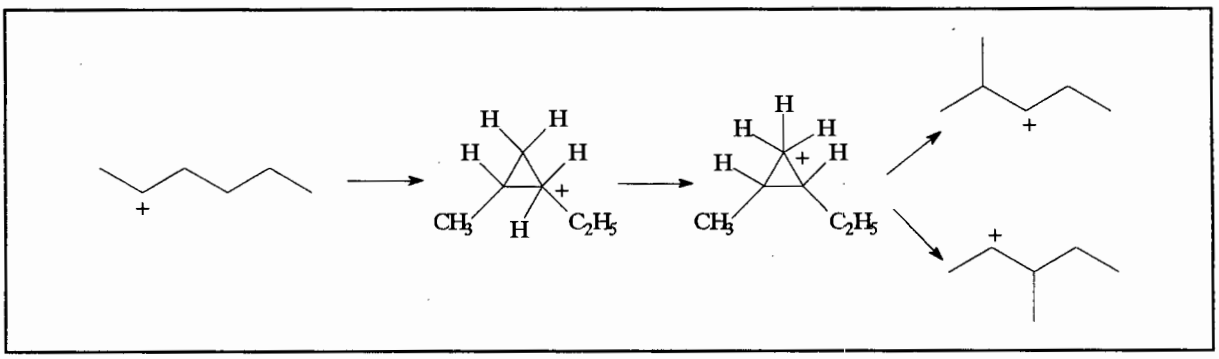

Figure 1.7 : Type B Isomerisation (Martens and Jacobs (1990))

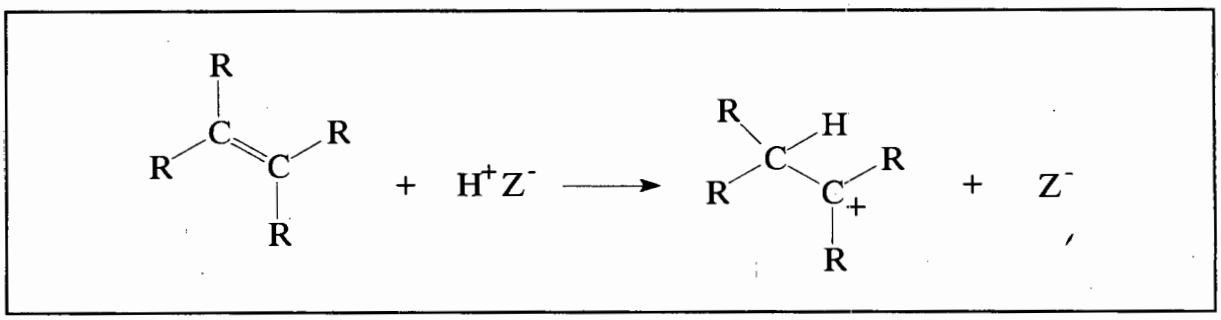

Figure 1.8 : Alkylcarbenium Ion Formation over Brønsted Acid Sites (Martens and Jacobs (1990))

1.3.1.1 Hydrocarbon Rearrangements over Acid Catalysts - Background

Martens and Jacobs (1990) discuss in detail the hydrocarbon rearrangements occurring over heterogeneous acid catalysts. Carbocations formed during hydrocarbon reactions can be divided into two types, namely :

Alkylcarbenium ions - These are ionic species that contain a positively charged carbon atom with three substituents - CR_3^+. This species is sp^2 hybridized and is planar in structure. Alkylcarbenium ions are stable in strong acids and it is possible to study their structure and rearrangements using NMR. These ions are ranked in order of increasing stability as follows:

primary < secondary < tertiary

The alkyl groups are electron donors and thus increase the stability of the ion compared to hydrogen atoms. The authors show that the type of alkyl substituent is less important for stability than the number of substituents. For example, if the substituent was butyl rather than propyl there would be no significant change in stability.

Alkylcarbonium ions - These are positively charged carbon atoms with five substituents namely, CR_5^+. An example of these are **substituted protonated cylopropanes (PCP)** which are postulated intermediates in the isomerisation mechanisms of acylic alkylcarbenium ions. This species can be represented in the following three ways (See Figure 1.5):

1) substituted corner protonated cyclopropane (CPCP)
2) substituted edge protonated cyclopropane (EPCP)
3) substituted face protonated cyclopropane (FPCP)

PCP carbonium ions are not stable in strong acids and their existence has only been inferred from studies concerning the reactions of alkylcarbenium ions. These authors have noted that according to molecular orbital calculations the CPCP and EPCP are more stable than FPCP.

For skeletal isomerisation reactions occurring in strong acids there are two types of reactions, namely :

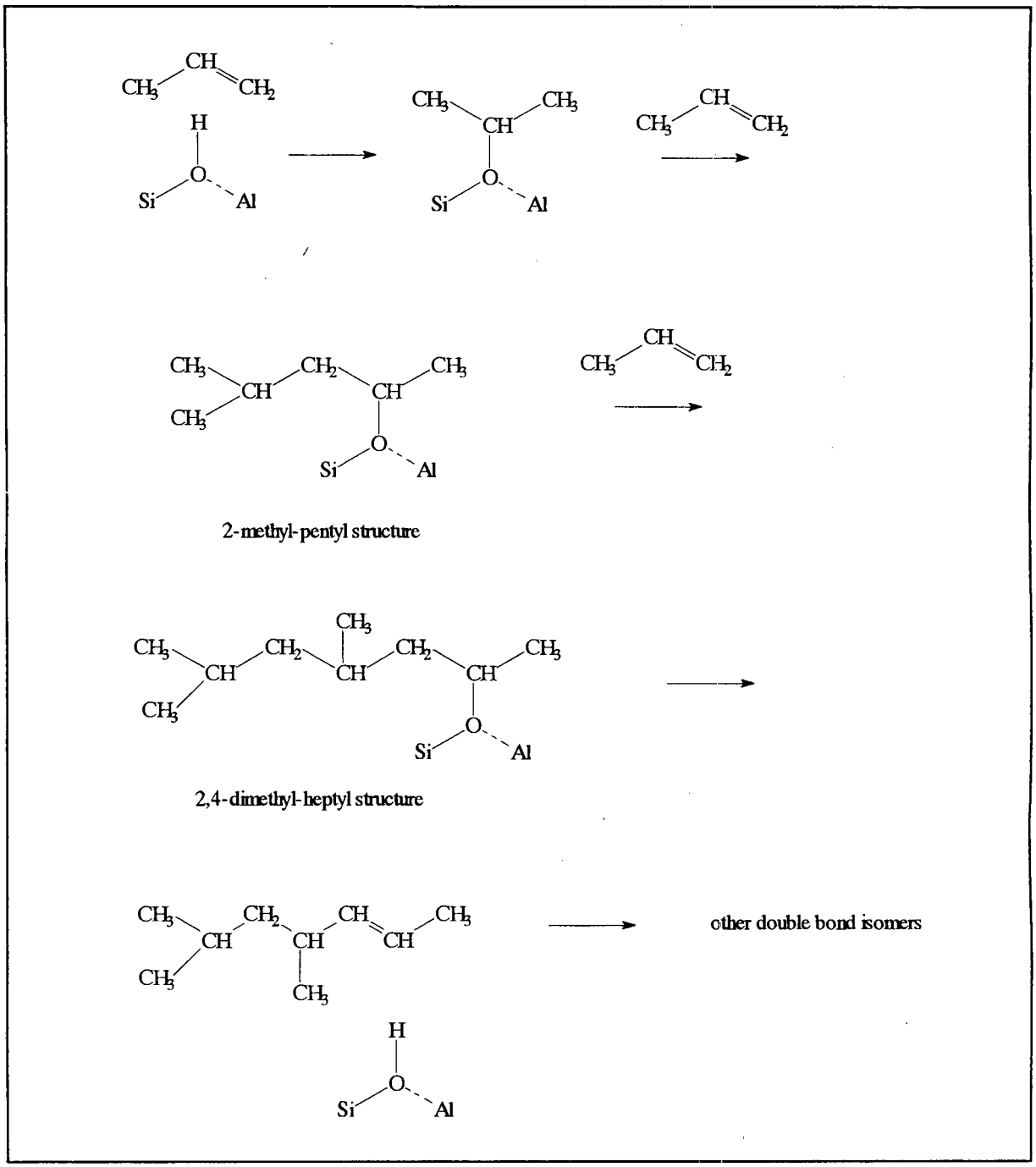

Figure 1.9 : Oligomerisation Scheme from Haw et al. (1989)

Type A - which changes the position of the side chain, leaving the degree of branching unchanged, and

Type B - which increases or decreases the degree of branching (See Figures 1.6 and 1.7).

Type B rearrangements are slower than Type A. The difference in rate of these two reactions is due to the corner-to-corner hydrogen jump in Type B.

The formation of alkylcarbenium ions over heterogeneous catalysts with Brønsted acid sites is shown in Figure 1.8. Support from the literature was presented for the occurrence of alkylcarbenium ions in solid acid catalysts. It was shown that the activation energies for hydrocarbon rearrangements was similar for both homogeneous and heterogeneous acid catalysts. However, the true nature of the reaction intermediates on solid acid catalysts is still uncertain and Martens and Jacobs (1990) noted that no direct evidence for the presence of carbocations ions on the surface of heterogeneous catalyst has been provided.

Haw et al. (1989) propose that long-lived alkoxy species (possibly alkyl silyl ethers) are catalytic intermediates during hydrocarbon reactions on solid acid catalysts. Thus, the authors state that the word "carbocation" is inappropriate. These species are formed by the covalent bonding of "incipient carbocations" to framework oxygen sites. Evidence for the alkoxy species is provided by following the reaction of isotopically labelled propene over HY zeolite using ^{13}C CP/MAS NMR. This led the authors to propose the mechanism for oligomerisation over solid acid catalysts shown in Figure 1.9.

Evidence for the presence of carbenium ions has recently been provided in part by Stapanov et al. (1994). This contribution provides evidence for carbenium ion properties of 1-octene adsorbed on H-ZSM-5. The authors reached the following conclusions regarding the nature of the adsorbed 1-octene:

1) ^{2}H NMR shows that there is H transfer from the catalytic acid sites, $\equiv$Al-OH-Si$\equiv$, to the $CH_2=$ group of the olefin.
2) ^{13}C NMR data shows that scrambling of the ^{13}C label occurs over the hydrocarbon skeleton.
3) They proposed two models to explain the experimental observations :

a) The carbenium ion is the main state of 1-octene adsorption in zeolite channels.
b) The carbenium ion is in equilibrium with an octyl silyl ether or octene.

4) Activation barriers for carbon scrambling and the thermodynamic parameters for the scrambling agree with those for carbenium ions in liquid and solid states.
5) The structure of the carbenium ion is controlled by the zeolite framework, causing it to be linear rather than branched.

While the hydrocarbon rearrangements occurring over heterogeneous acidic catalysts are similar to those occurring in homogeneous acid catalysts, there are additional complications that arise in heterogeneous catalysts with a well defined pore system such as zeolites. The products formed are influenced by shape selectivity and a number of products that would form over amorphous acidic catalysts are not present due either to their bulky size or to the size of their intermediates. (Shape selective effects of zeolites are discussed in more detail in Chapter 3.)

1.3.1.2 Oligomerisation Reactions

A carbenium ion, formed via addition of a proton to the double bond of an olefin molecule by a Brønsted acid (HX), can undergo the following reactions:

1) reaction with a negative ion e.g. X^{-1} (simple Markownikov addition of HX to the double bond),
2) reversal of the process i.e. loss of the proton which gives rise to the same olefin or a double bond isomer,
3) isomerisation followed by proton loss to give a new olefin, and
4) oligomerisation which occurs via addition to an olefin monomer via Markownikov addition.

1.3.1.2.1 Equilibrium Predictions for Oligomerisation

Tabak et al. (1986) and Quann et al. (1988) provide some general details regarding the thermodynamics of oligomerisation over H-ZSM-5. During their studies they assumed the isomerisation reactions were significantly faster than other reactions such as cracking and oligomerisation. Thus they concluded that isomerisation reactions were at equilibrium. The

isomers could then be grouped into a smaller number of pseudocomponents or lumps. Using these lumps they predicted their composition at equilibrium using a method developed by Alberty (1983). Ideal mixtures and ideal gases were assumed. Their calculations showed that when bulky isomers were excluded from the lumps the best agreement between predicted and experimental compositions was obtained. In other words, the shape selectivity of H-ZSM-5 had an influence on the equilibrium product spectrum.

The equilibrium calculations are discussed in more detail by Alberty (1987a). Products from oligomerisation studies over H-ZSM-5 were analysed and the following was found :

1) The product from H-ZSM-5 were mainly linear with methyl branches every five carbons.
2) Single ethyl or longer chains occurred every two or three carbons.
3) The concentration of cis-isomers was low.

Several equilibrium calculations were performed by progressively excluding more and more bulky isomers from the isomer groups, starting with the cis-isomers and ending with highly branched ones. Equilibrium predictions showed that removing bulky isomers from the groups resulted in a shift in concentration to lower carbon numbers. Indeed, by examining the experimental product distributions from propene and hexene oligomerisation it was noted that there was a sharp drop in product concentration with increasing carbon number compared to what is expected for unrestricted equilibrium (Quann et al. (1988)). Thus, the oligomers produced over H-ZSM-5 are subjected to a restricted form of equilibrium from which bulky isomers are excluded.

Experimental hexene isomer distributions at high and low conversions were compared with equilibrium values. Quann et al. (1988) concluded that, even at low conversion, isomerisation was almost at equilibrium. In addition, double-bond isomerisation occurred faster than skeletal isomerisation.

1.3.1.2.2 Temperature and Pressure Effects

Temperature and pressure effects were discussed by Tabak et al. (1986) and Quann et al. (1988). The effect of temperature on the product spectrum was complex. According to equilibrium calculations conducted using restricted isomer groups, low temperatures favoured

a high molecular weight product while high temperatures resulted in a decrease in the molecular weight of the product (Quann et al. (1988)). However, the authors stated that at low conversions the reaction rates were not fast enough with the result that fewer heavy compounds were produced than predicted. Experimentally this caused the molecular weight of the product to pass through a maximum as temperature was increased. At low temperatures, mainly oligomerisation reactions occurred. Randomisation occurred at intermediate temperatures due to an increase in cracking and disproportionation. High temperatures resulted in more complex reactions such as cyclization and hydrogen transfer occurring.

The effect of pressure is less complex and it was found that increasing pressure favoured increasing molecular weight. A combination of high temperature and low pressure resulted in light olefins predominating while the reverse conditions, low temperature and high pressure, resulted in heavy olefins predominating.

The following experimental examples illustrate the effects of temperature and pressure. At 100kPa, for temperatures of 277°C and above the product is C_{10} and lighter (gasoline). On the other hand, if the temperature is kept constant at 277°C increasing pressure results in more distillate production (C_{11} - C_{20}). In general, the possible range of operating conditions for H-ZSM-5 is large. Tabak et al. (1986) state that temperatures and pressures start low at 37°C and 7kPa. Temperatures are only limited by practical constraints while pressures can go as high as 14MPa. Thus, the reaction conditions can be tailored to suit product requirements by adjusting temperature, pressure and catalyst.

1.3.1.2.3 Structure of Product Oligomers

In the papers reviewed below, the authors present detailed analyses of the oligomerisation product. These analyses provide important information regarding the skeletal structure of the product molecules and thus aid in elucidating oligomerisation reaction pathways. The work discussed below covers both non-shape selective and shape selective catalysts (silica-alumina and H-ZSM-5 respectively). At the end of this section general trends observed regarding the nature of the product skeletal structures are summarised.

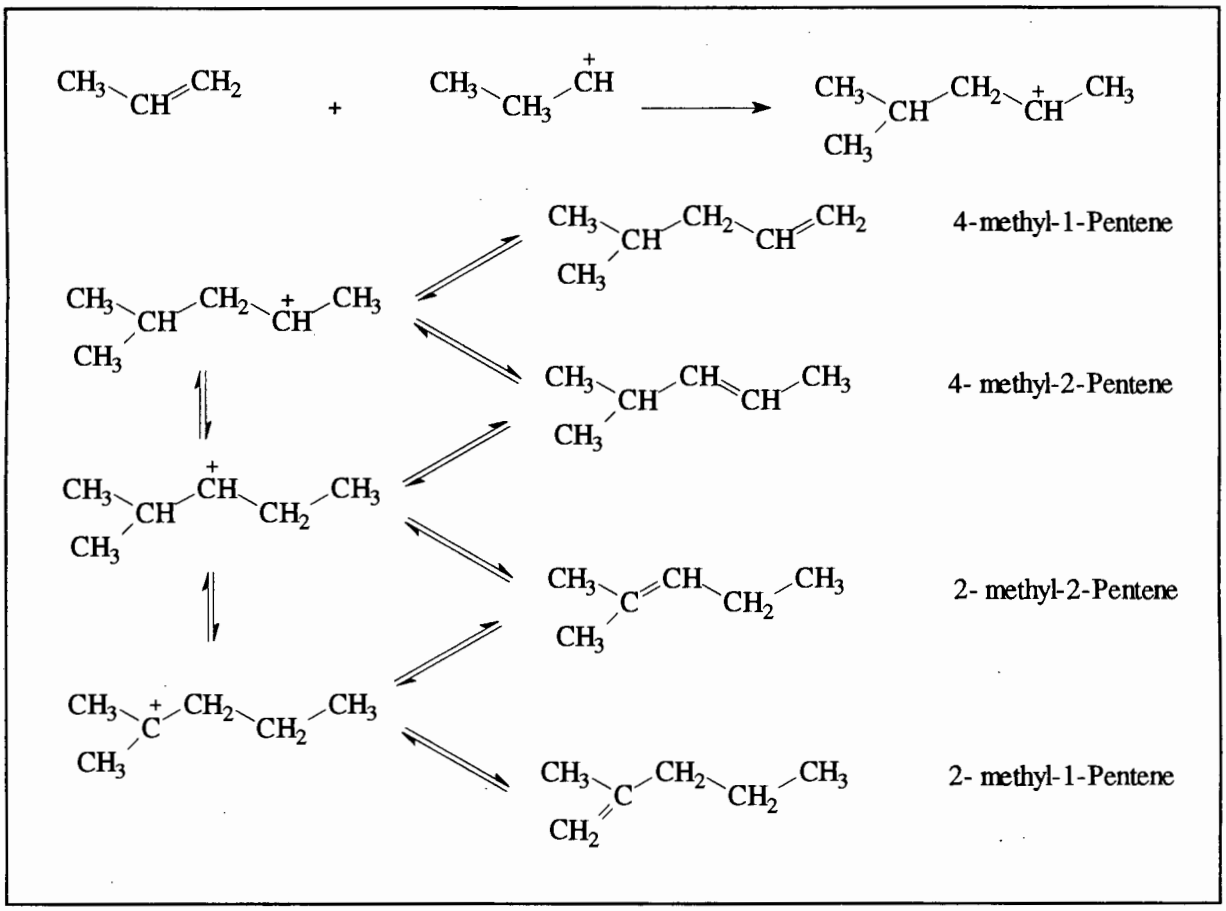

Figure 1.10 : Formation of Primary Hexene Isomers (Fel'dblyum and Baranova (1971))

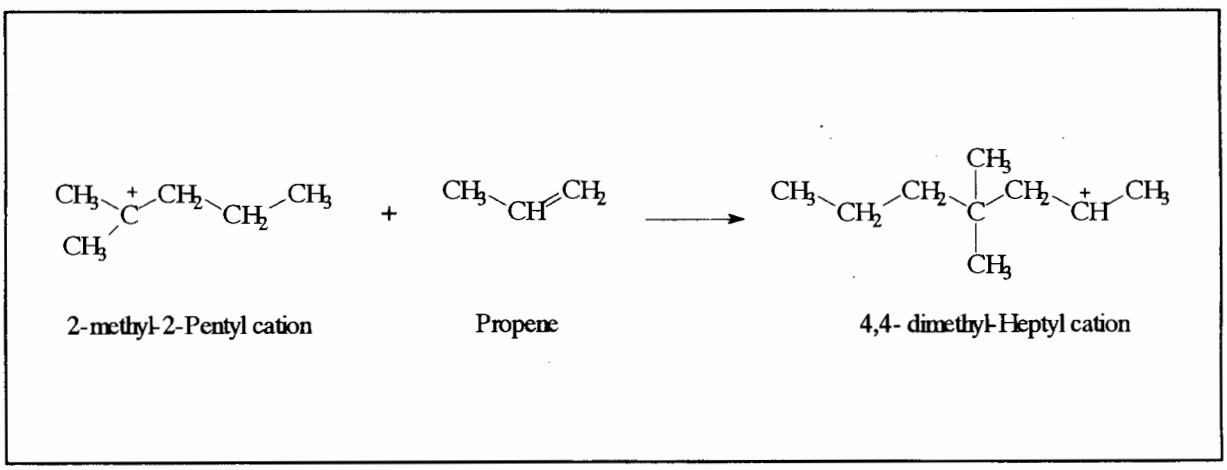

Figure 1.11 : Reaction Scheme for the Formation of 4,4-dimethyl-Heptane (Fel'dblyum and Baranova (1971))

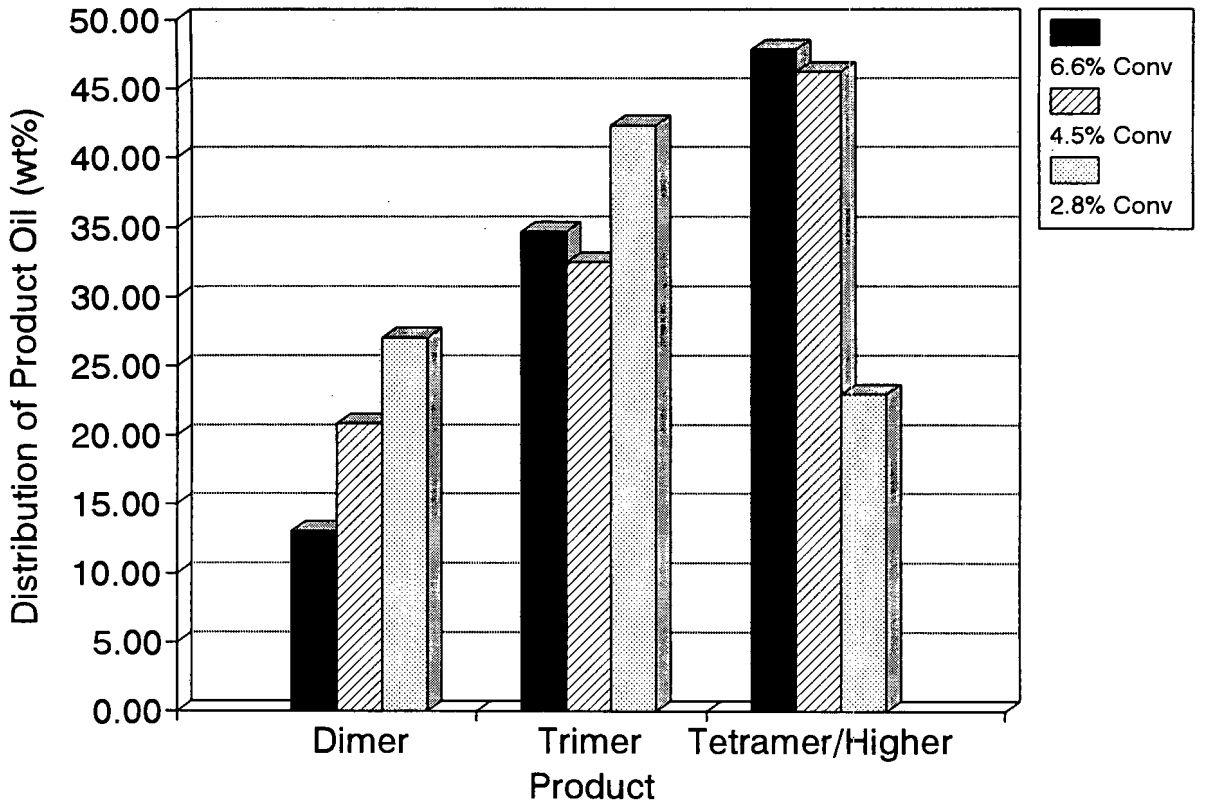

Figure 1.12 : Effect of Conversion Levels on Product Distribution (Takahashi et al. (1972))

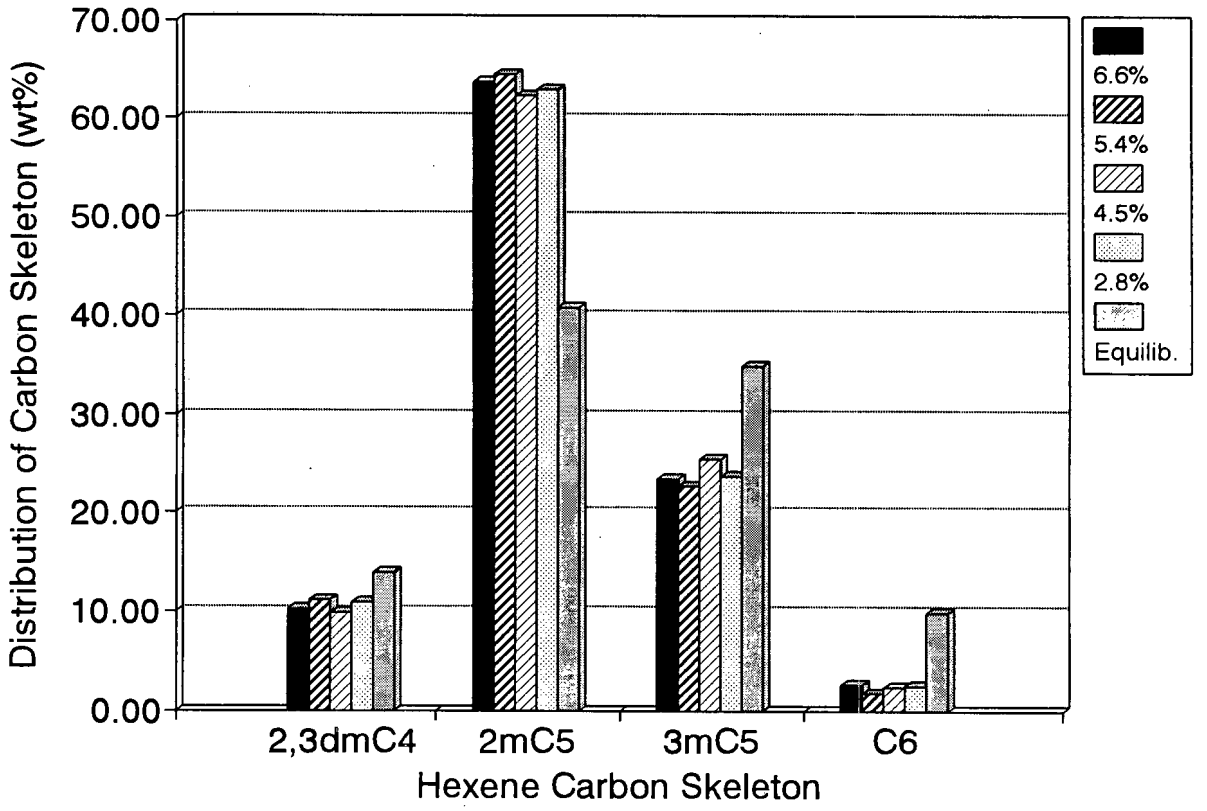

Figure 1.13 : Effect of Conversion Levels on Hexene Isomer Distribution (Takahashi et al. (1972))

Fel'dblyum and Baranova (1971) studied propene oligomerisation over silica-alumina and nickel on silica-alumina at 5MPa and 64°C. For silica-alumina, the conversion of the feed was low, 6%, and the major product was trimer. They found that the dimer product had a high content of 4-methyl-1-pentene and 4-methyl-2-pentene. On the other hand, the linear hexenes were present in small amounts. 2,3-dimethyl-butenes were also observed in low concentrations but there were no 3-methyl-pentenes. The reaction scheme for the formation of the primary hexene isomers presented by Fel'dblyum and Baranova is shown in Figure 1.10. In this reaction scheme a propene molecule adds to a propene carbenium ion to form a 2-methyl-1-pentyl cation which can react further to produced to the various double bond isomers of this skeleton.

Fel'dblyum and Baranova (1971) also hydrogenated and analysed the trimer product from their propene oligomerisation runs. Four peaks were observed, three of which were identified as 4-methyl-octane, 2,4-dimethyl-heptane and 4,4-dimethyl-heptane. The 4,4-dimethyl-heptane is produced when the 2-methyl-2-pentyl cation (produced by dimerisation) reacts with propene. A reaction scheme for the formation of 4,4-dimethyl-heptane is shown in Figure 1.11.

Takahashi et al. (1972) oligomerised propene at 2.5 to 5.0 MPa, 80 to 350°C and liquid hourly space velocities (LHSV's) 5000 to 10000 hr^{-1}. The catalysts used were also silica-alumina and nickel on silica-alumina. Detailed analyses of the dimers were given. The effect of different space velocities and temperatures were investigated. The results are shown in Figures 1.12 to 1.15 for silica-alumina.

Figure 1.12 plots the amount of each oligomer formed for different conversion levels obtained by varying the LHSV and keeping the reaction temperature and pressure constant at 250°C and 5MPa, respectively. This graph shows that at low conversions the major product was trimer and as the conversion increased the major product shifted to the higher molecular weights. Figure 1.13 shows that there is no significant difference in the composition of the carbon skeletons at the low conversions presented. Predicted equilibrium concentrations, also plotted on the same graph for comparison, indicate that the hexene iso-

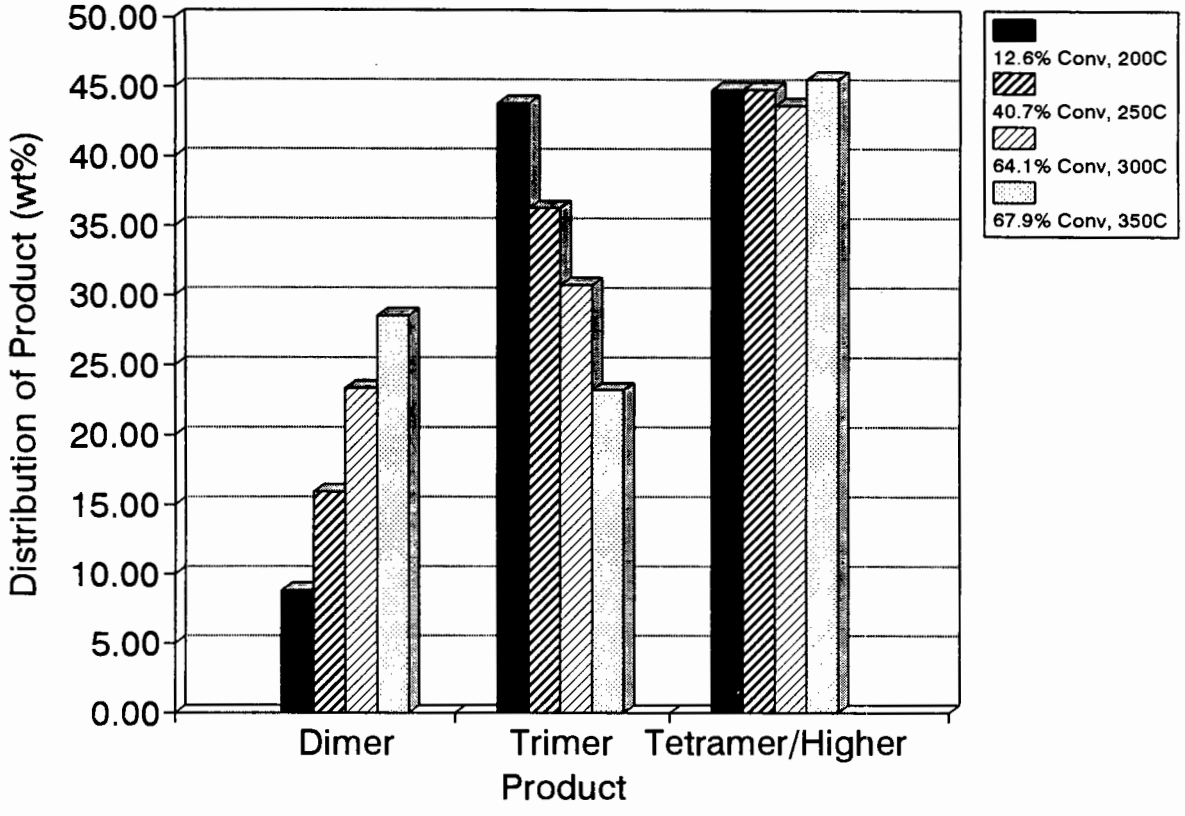

Figure 1.14 : Effect of Temperature on Product Distribution (Takahashi et al. (1972))

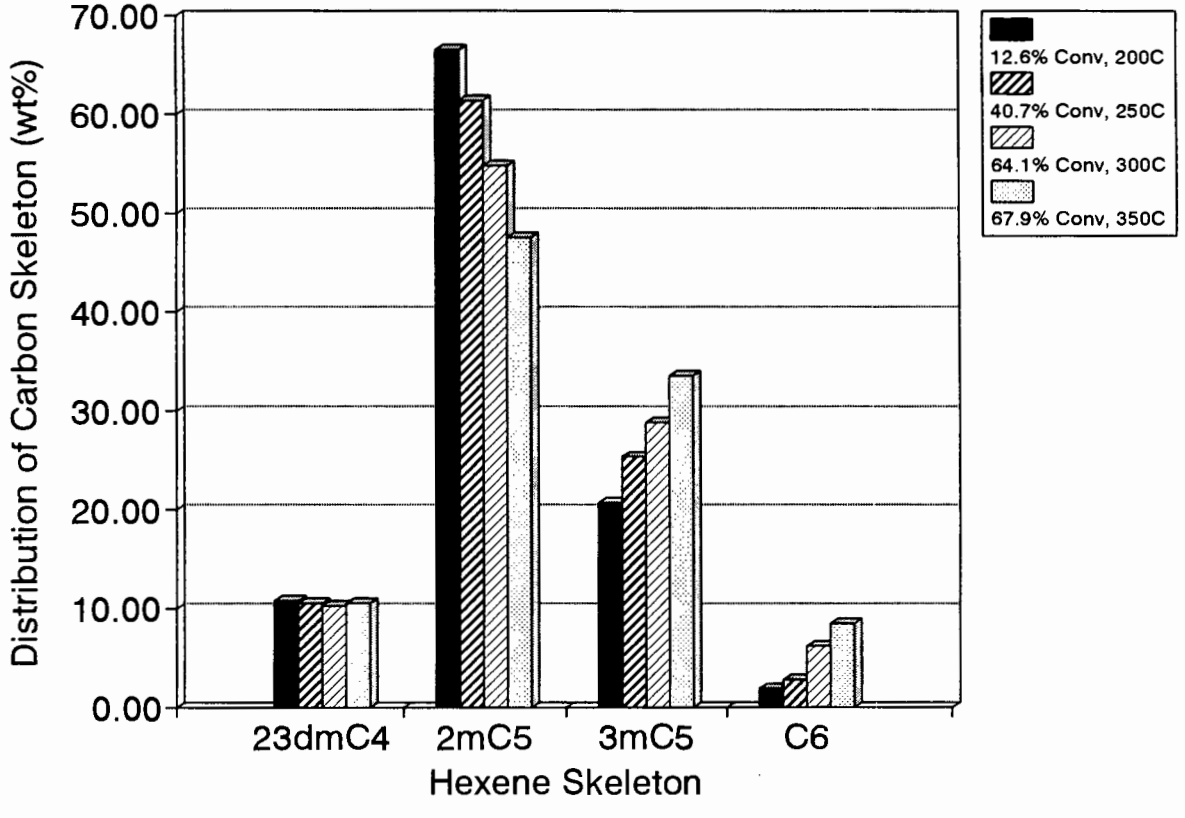

Figure 1.15 : Effect of Temperature on Hexene Isomer Distribution (Takahashi et al. (1972))

mers were not at equilibrium with respect to their skeletal structure. (The predicted equilibrium distributions were obtained using methods described in Chapter 4.) The major product was the 2-methyl-pentane skeleton followed by the 3-methyl-pentane skeleton. The doubly-branched isomers exceeded the linear isomers in composition. Additional information showed that within the 2-methyl-pentane structure 2-methyl-2-pentene dominated, while within the 3-methyl-pentane structure the 3-methyl-2-pentenes dominated. Of the doubly-branched isomers, 2,3-dimethyl-2-butene was present in the greatest amount. In the linear products 2-hexene and 3-hexene were present.

In Figure 1.14 the effect of varying temperature at 5MPa is shown. Unfortunately, the conversions were not kept constant and the effects seen may well be a result of changing conversion. As conversion or temperature increased there was a corresponding increase in the dimer and a decrease in the trimer. This could be due to an increase in secondary cracking reactions. There was no change in the composition of tetramer and higher molecular weight products. In Figure 1.15 the composition of the dimer product is shown. Again, the changes observed may in part be due to changing conversions. Over the temperature range studied the doubly-branched isomers remain unchanged. This trend appears anomalous and no explanation is given. It is possible that these isomers are produced in greater quantities via cracking reactions compared to the other hexene skeletons. There is an increase in both the 3-methyl-pentanes and linear hexanes while the 2-methyl-pentanes decrease. The dominant hexene isomers are the same as for conditions of varying LHSV.

Liquid phase propene oligomerisation over H-ZSM-5 was carried out at 54°C by Miller (1988). Selectivity to dimers was 40 to 45% and conversion after 20 hours on stream was less than 20%. Of the dimer product the 2-methyl-pentane skeletons were present in the greatest amount. However, the next major products were the 2,3-dimethyl-butane structures followed by the 3-methyl-pentane structures. Linear hexenes were present only in small amounts.

Ethene and propene oligomerisation over H-ZSM-5 were studied by Bessel and Seddon (1987). The reactions were carried out at high pressure (~3.4 MPa), low temperature

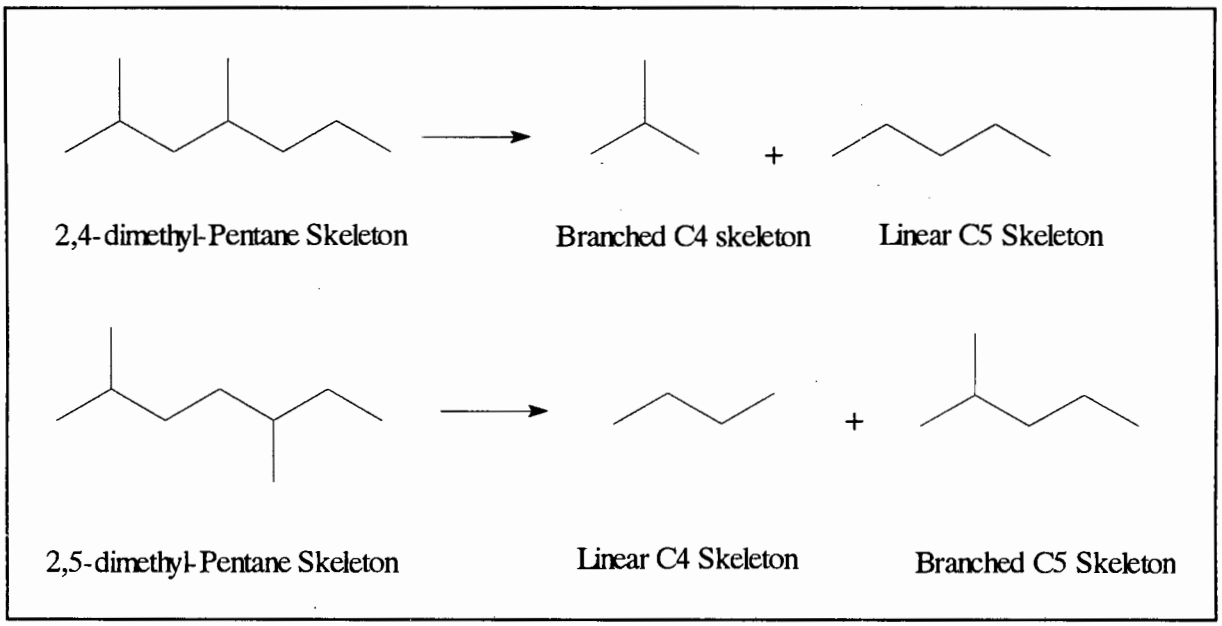

Figure 1.16 : C_9 Precursors for Cracked Products (Bessel and Seddon (1987))

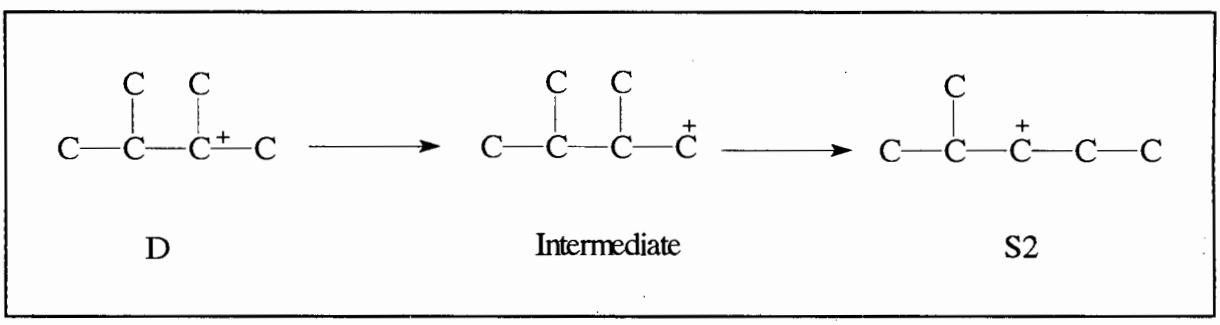

Figure 1.17 : Isomerisation of 2,3-dimethyl-Butenes to 2-methyl-Pentenes (Pines (1981))

(<300°C) and low conversions, generally less than 5%. They found that aromatic formation was not significant below 300°C. The main products observed were oligomers and their cracked products. The major oligomer was the dimer. An increase in cracking products with increasing alumina content was linked to an increase in activity.

Interesting evidence regarding the structure of the trimer was provided by Bessel and Seddon (1987). It was found that on silicalite and low-alumina H-ZSM-5 the C_4 and C_5 olefins produced via cracking were in equal proportions. This implies they may stem from a common C_9 intermediate. As the reaction temperature increases the selectivity to linear C_4 and branched C_5's vs branched C_4 and linear C_5's increases. The authors postulated that there was a change in the C_9 precursor from a 2,4-dimethyl-heptane structure to a 2,5-dimethyl-heptane structure. This is shown in Figure 1.16 together with the cracked product structures produced. Their sorption experiments showed that both these structures were accessible to the zeolite channel. However, the 2,4 isomer was slightly less accessible than the 2,5 structure.

Quann et al. (1988) analysed the dimer product, obtained from high and low 1-hexene conversion at 227°C and 4.2 MPa over H-ZSM-5, in detail. At low conversion the major product was the 2-methyl-pentane skeleton, followed by the 3-methyl-pentane skeleton. The 2,3-dimethyl-butane structure occurred in the lowest concentration. At high conversion the 2-methyl-pentane skeleton did not change much, instead more of the feed was converted to 3-methyl-pentanes and 2,3-dimethyl-butenes.

Wilshier et al. (1987) carried out high pressure (~2.4 MPa) propene oligomerisation over H-ZSM-5. The authors hydrogenated their liquid product and were thus able to present detailed analyses regarding the skeletal structure of all products up to C_9. Firstly, experimental runs were carried out using H-ZSM-5 with 1.22 wt% aluminium at two different temperatures, namely 189 and 284°C. For both runs the conversion to liquid product was 90 wt%. In both cases the dominant skeletal structures contained only methyl branches. Small amounts of linear products and those with ethyl branches were also present. This clearly indicates that there is some degree of shape selectivity occurring, contrary to the

conclusions drawn by the authors.

At the lower temperature the major product was the trimer and oligomers were present in the greatest amounts. Of the dimer product, the 2-methyl-pentane skeleton was the main product, followed by the 3-methyl-pentane skeleton and the 2,3-dimethyl-butane skeleton. The linear hexane was present in the smallest amount. Of the trimer product, the dominant skeletons did not have more than one methyl group per carbon : 2,3-dimethyl-heptane, 2,4-dimethyl-heptane, 3,4-dimethyl-heptane and 3,5-dimethyl-heptane. The linear C_9's were present in small amounts.

An increase in temperature resulted in an increase in non-oligomers and a broadening of the product spectrum. At the dimer level, the concentration of the 2-methyl-pentane skeleton increased while that of the 2,3-dimethyl-butane skeleton decreased. The 3-methyl-pentane and linear product remained unchanged. Concerning the trimers, the main dimethyl-heptanes were the same as before. However, there was a significant increase in the linear product. This was also noted for the C_8 products.

It was concluded by the authors that at low temperatures the reaction takes place on the outer surface of the zeolite, resulting in a more branched product. However, it is also possible that linear products are selectively produced at higher temperatures due to the diffusion of branched products becoming rate limiting. In fact this theory is further supported by additional experiments carried out on low aluminium H-ZSM-5 (0.10 wt%). Although the low aluminium zeolite was prepared in a similar manner to that used for the previous experiments, the crystals (as seen from SEM photographs) were larger in size. These runs showed an increase in shape selectivity, or a shift to linear products. On the other hand, poisoning the outer surface with 4-methylquinoline or treating the catalyst with hexamethyldisilazane vapour or feeding hydroxylic iso-propanol instead of propene all lead to an increase in shape selectivity of the product. This indicates that the reaction occurs to some extent on the external surface.

For all the studies discussed above, the 2-methyl-pentane carbon skeleton was the primary

dimer product. This is produced by Markownikov addition of a propene carbenium ion to a propene molecule. At low temperatures the 2,3-dimethyl-butane skeleton was the major secondary product for both amorphous silica-alumina and H-ZSM-5. The 3-methyl-pentane and hexane skeletal structures were either in small amounts or non-existent. At high temperatures, however, the 3-methyl-pentane skeleton was the major secondary product. It is possible that at low temperatures the doubly-branched isomers form as a result of anti-Markownikov addition since if isomerisation was occurring then the 3-methyl-pentenes should form more readily than the 2,3-dimethyl-butenes (Fel'dblyum and Baranova (1971)).

Data regarding the structure of the nonene isomers is less plentiful. It is interesting to note that the 4,4-dimethyl-heptane skeleton, produced by adding propene to the dominant C_6 carbenium ion, the 2-methyl-2-pentyl ion, is only found in significant amounts when non-shape selective silica-alumina is used. On the other hand, the major trimers obtained when H-ZSM-5 is used are more linear, often containing only one or two methyl groups. Thus, the trimer product is more influenced by shape selectivity than the dimer product.

1.3.1.3 Isomerisation Reactions

As mentioned earlier, isomerisation occurs simultaneously with oligomerisation reactions. Depending on the level of conversion or the approach to equilibrium, entirely different product spectra are obtained. Pines (1981) presents results of the isomerisation of 3,3-dimethyl-1-butene over alumina catalyst at 350°C. The product distributions at several liquid hourly space velocities are compared with equilibrium values. This is shown in Table 1.2 :

Table 1.2 Isomerisation of 3,3-dimethyl-1-Butene, Pines (1981)				
	Product Distribution			
	LHSV (hr^{-1})			
Carbon Skeleton	6.0	2.0	0.5	Equilibrium
3,3-dimethyl-Butenes (DD)	21.0	2.7	1.9	0.5
2,3-dimethyl-Butenes (D)	73.0	39.3	23.0	11.5
2-methyl-Pentenes (S2)	6.0	37.2	42.6	40.5
3-methyl-Pentenes (S3)	-	19.8	31.0	33.5
linear Hexenes (L)	-	1.0	1.5	14.1

According to Pines (1981), the isomerisation of DD to D occurs faster than the isomerisation of D to S2. This is because the latter involves the formation of an unstable, primary carbenium ion intermediate during the reaction (see Figure 1.17). The reaction of S2 to L is also slow due to formation of an unstable, primary carbenium ion intermediate. It was also noted that D is the primary isomerisation product. In addition, the author stated that double-bond isomerisation is faster than migration of methyl groups since S2 were nearly equilibrated before significant amounts of S3 were formed. The rearrangements occur via 1,2-methyl shifts since S3 are formed from S2.

More recently, Martens and Jacobs (1990) present an alternative reaction pathway for the isomerisation of hexenes and this is shown in Figure 1.18. This occurs via PCP intermediates, as discussed earlier. If this mechanism is assumed then, as was observed by Pines (1981), the formation of S2 from D is slower than the formation of D from DD. However, this is due to the type of isomerisation reactions involved rather than the formation of unstable, primary carbenium ion intermediates. S2 is formed via the slower Type B reaction compared to D which forms via Type A.

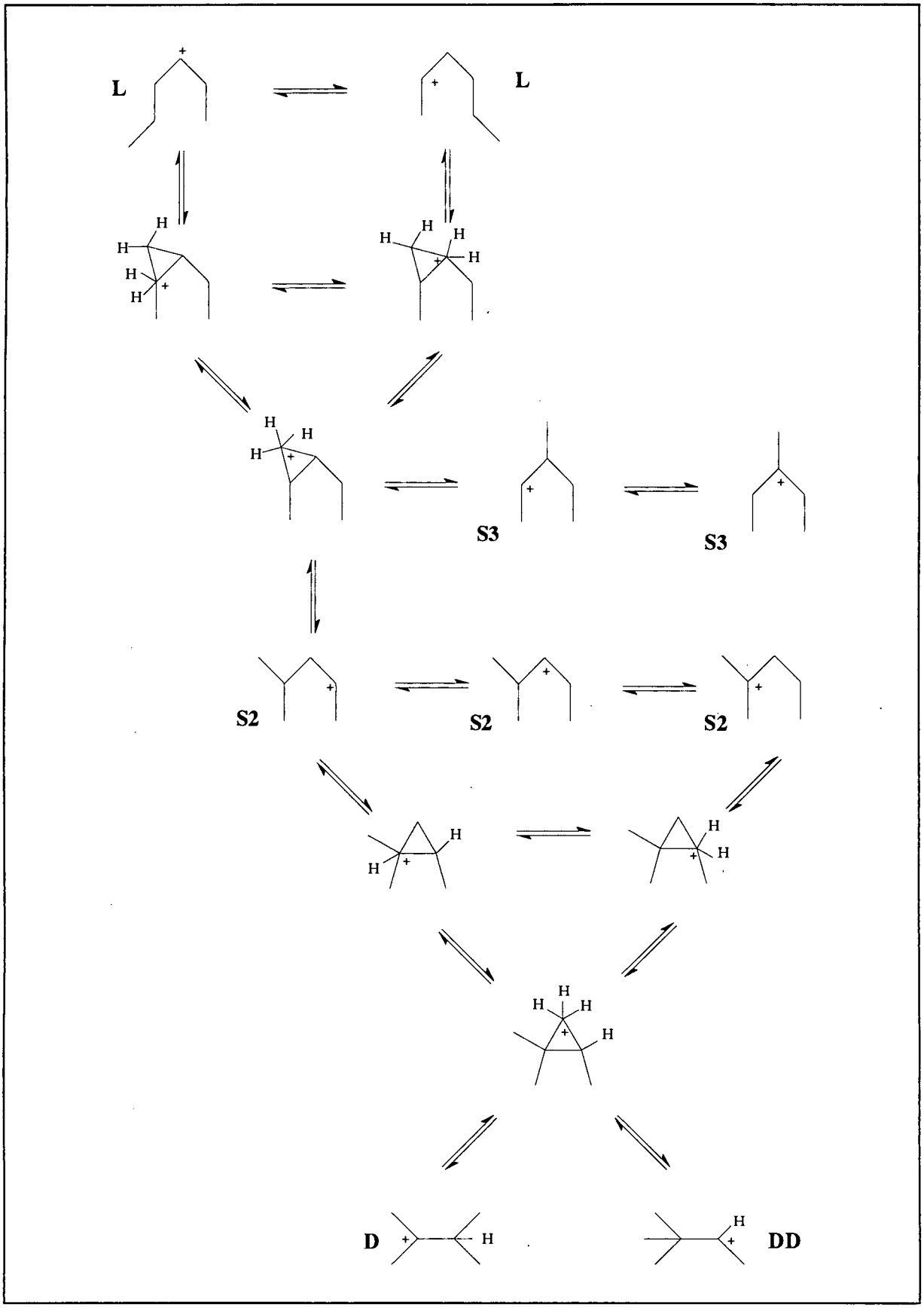

Figure 1.18 : Hexene Isomerisation Scheme from Martens and Jacobs (1990)

1.3.2 Heterogeneous Nickel Catalysts

A number of workers have studied oligomerisation over heterogeneous nickel catalysts and their work is discussed below. In all the papers discussed the addition of nickel to an aluminosilicate support results in a predominance of dimer product. Also, within the dimer product, the selectivity to linear isomers is increased. Addition of nickel results in the generation of a different form of active centre, believed to be a combined nickel ion/ Brønsted site (O'Connor and Kojima (1990)).

The kinetics and product composition pertaining to ethene and propene oligomerisation over nickel-oxide on silica-alumina was studied by Hogan et al. (1955). This study was motivated by the presence of refinery cracked gas containing significant quantities of ethene, hitherto not recoverable by commercial catalysts. Propene diluted with 77% propane and reacted at 70°C and 4MPa gave a conversion of 68%. The major product was dimer. As the conversion decreased, the dimer content increased. The composition of the dimer fraction at 80% conversion was given. The major carbon skeleton was the 2-methyl-pentane structure. The other product formed was the linear hexane structure. No 3-methyl-pentane or 2,3-dimethyl-butane skeletons were evident. The branched chain hexenes were thought to be more reactive and converted further to nonenes, leaving the less reactive linear hexenes behind. The trimer fraction consisted of dimethyl-heptenes and trimethyl-hexenes. There were few linear nonenes.

Ethene, diluted with 55% hydrogen, was reacted at 40°C and 2MPa. Hydrogen was chosen as a diluent because it aided in the removal of impurities from the ethene by selective hydrogenation and because it was present in the refinery cracked gas. The average conversion was 97% and the major product was again the dimer. The dimer fraction consisted only of linear butenes - no isobutene was detected. The trimer consisted of 60 to 70% hexenes and 30 to 40% 3-methyl-pentenes. The tetramer consisted of 40 to 45% 3,4-dimethyl-hexenes, 30 to 35% 3-ethyl-hexenes, 2 to 4% 3-methyl-3-ethyl-pentenes and only 20% linear octenes.

Fel'dblyum and Baranova (1971) also studied nickel oxide on aluminosilicates along with

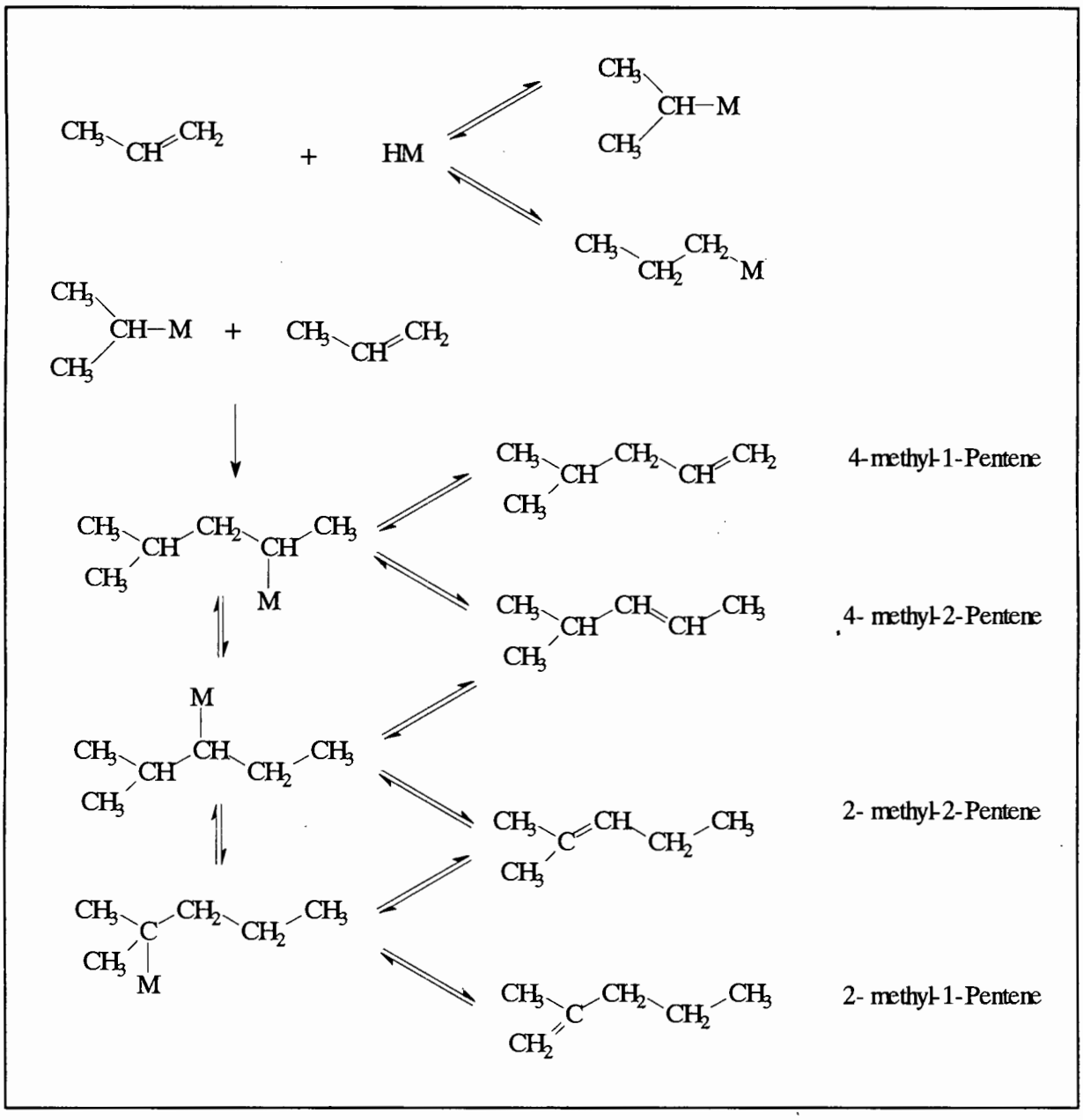

Figure 1.19 : Formation of 2-methyl-Pentenes over Nickel Oxide on Silica-Alumina (Fel'dblyum and Baranova (1971))

silica-alumina as catalysts for propene oligomerisation (64°C, 5MPa). In the introduction to their paper they note that hexenes are formed in large quantities during propene oligomerisation over nickel oxide on silica-alumina in contrast to silica-alumina alone. It was proposed that there are two types of catalytic centres responsible for the reaction. Interestingly it was also stated that the reactivity of ethene, propene and 1-butene varies in the following ratio 100:10:1, which is opposite to that which occurs on acidic catalysts. By examining the reaction products in detail, the authors hoped to elucidate the reaction mechanism.

As mentioned, the product spectrum was different compared to that for the acid catalyst. Firstly, the main reaction product was the dimer compared to the trimer for silica-alumina. It was thought that the 2-methyl-2-pentyl cation was less stable than on the silica-alumina and desorbed instead of reacting further to the trimer. Secondly, the linear hexene content in the dimer product increased. Again, as with the silica-alumina no 3-methyl-pentenes were formed. There were two main trimer skeletons, namely 2,4-dimethyl-heptane and 4-methyl-octane. The proposed reaction pathways are shown in Figures 1.19, 1.20 and 1.21. Complex hydrides of the nickel (HM) are assumed to be responsible for the catalytic action.

Hassan et al. (1977) studied propene oligomerisation using a selection of metals on zeolites X and Y at atmospheric pressure, 190°C and a space velocity of 40 ml/ml catalyst/hr. The overall order of activity was found to be LaY ≈ LaX ≈ CeX ≈ MgY > NiY > CoY > AlY > MgX > MnY > NiX > CoX > CaX. All catalysts except NiX produced only paraffins, however, the source of hydrogen for the formation of these paraffins was not clear. The majority of isomers formed had a single or double methyl branch. The proportion of linear products was low. The presence of C_6 and C_9 paraffins indicated that hydrodimerisation and hydrotrimerisation had taken place. There were also non-oligomer paraffins present indicating that cracking also occurred. NiY and LaX gave more dimers while AlY and CaX gave more trimers. NiX gave pure olefin oligomers, the majority of which were dimers. In addition the quantity of linear isomers increased. Hassan et al. also proposed a mechanism for hydrocarbon rearrangements occurring during propene oligomerisation over heterogeneous nickel catalysts. Two postulated intermediates are formed

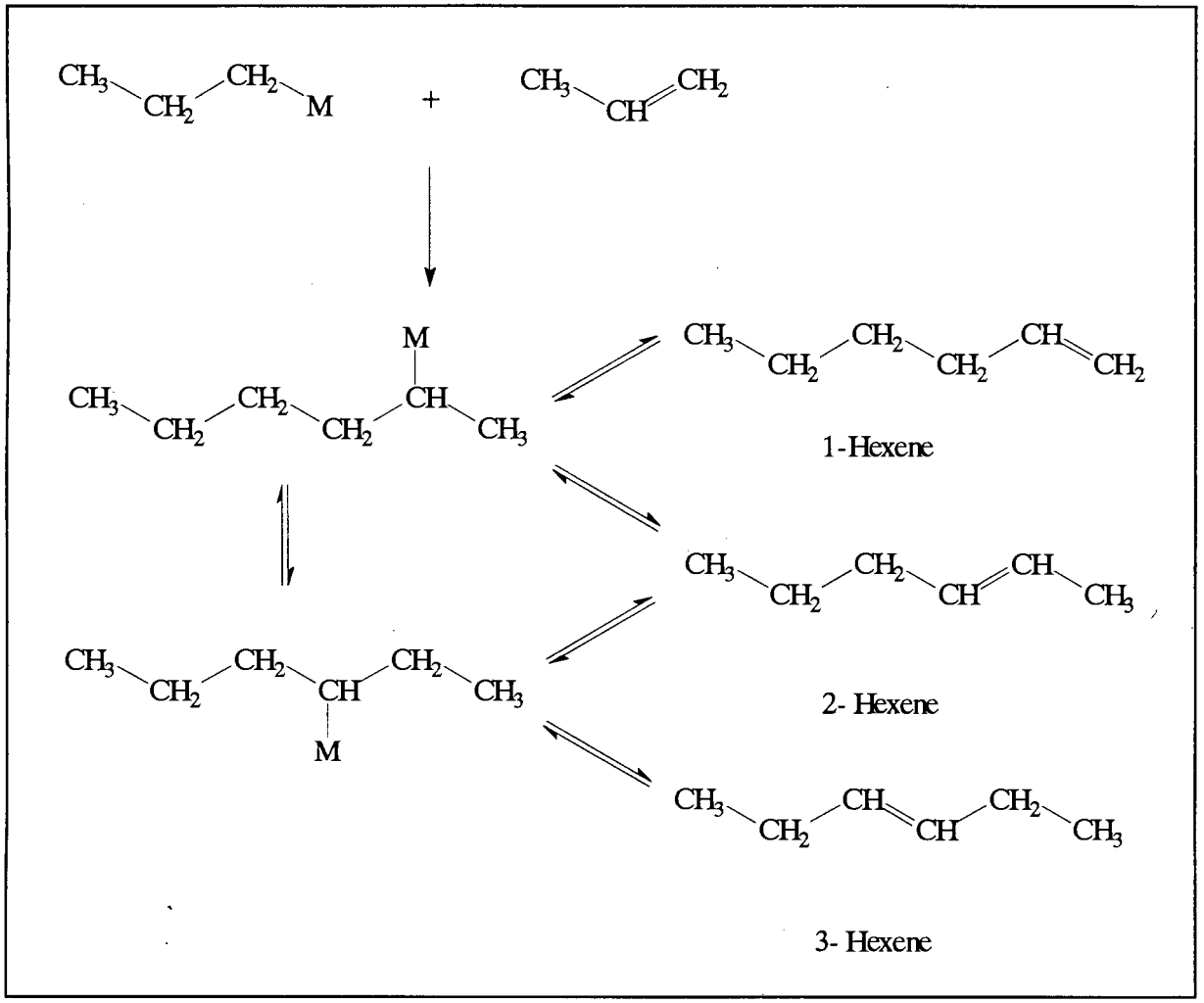

Figure 1.20 : Formation of Linear Hexenes over Nickel Oxide on Silica-Alumina (Fel'dblyum and Baranova (1971))

when two propene molecules react on the zeolite surface (see Figure 1.22). These unstable intermediates then undergo a series of rearrangements which lead to the various hexene or hexane isomers. If bonds 1,2 or 3 in the first intermediate break then 4- or 2-methyl-pentenes are formed. If bonds 1,2 or 3 in the second intermediate break then linear hexenes, 3-methyl-pentenes or 2,3-dimethyl-butenes are formed. Unfortunately, the role of the active sites in the reaction is not clear.

Miller (1988) also studied the effect of metal addition to zeolites on the product spectrum. Addition of 3 wt% nickel to H-ZSM-5 resulted in an increase in catalyst activity along with improved selectivity to the dimer product during liquid-phase propene oligomerisation at 54°C. Within the dimer product there was a significant increase in the amount of linear hexenes. This was also found for amorphous $NiSO_4$ on alumina where the product spectrum was very similar to that of Nickel-ZSM-5. The increase in linear hexenes was thought to be due to the presence of the metal and occurred via an insertion mechanism.

Beltrame et al. (1994) reacted 1-butene over high and low alumina Ni-ZSM5 at 4 and 8 MPa and 100 to 200°C. Runs with nickel oxide on silica-alumina and CoO on carbon were also carried out for comparison. The authors found that under conditions that limit the carbenium ion mechanism and favour the coordinative mechanism of dimerisation on nickel, 1-butene produced more linear products and these are prevented from isomerising further. It was stated that the production of linear dimers depended on the correct balance of dimerisation and isomerisation activities. They noted that the best results were obtained at 8 MPa and low temperatures (120 to 140°C) with a low alumina zeolite. These conditions gave only approximately 37% linear isomers within the C_8 fraction. Unfortunately, the authors did not compare catalysts at the same conversion levels. The reduction in selectivity to linear dimers at lower pressures and higher temperatures may, at least in part, have been due to an increase in conversion.

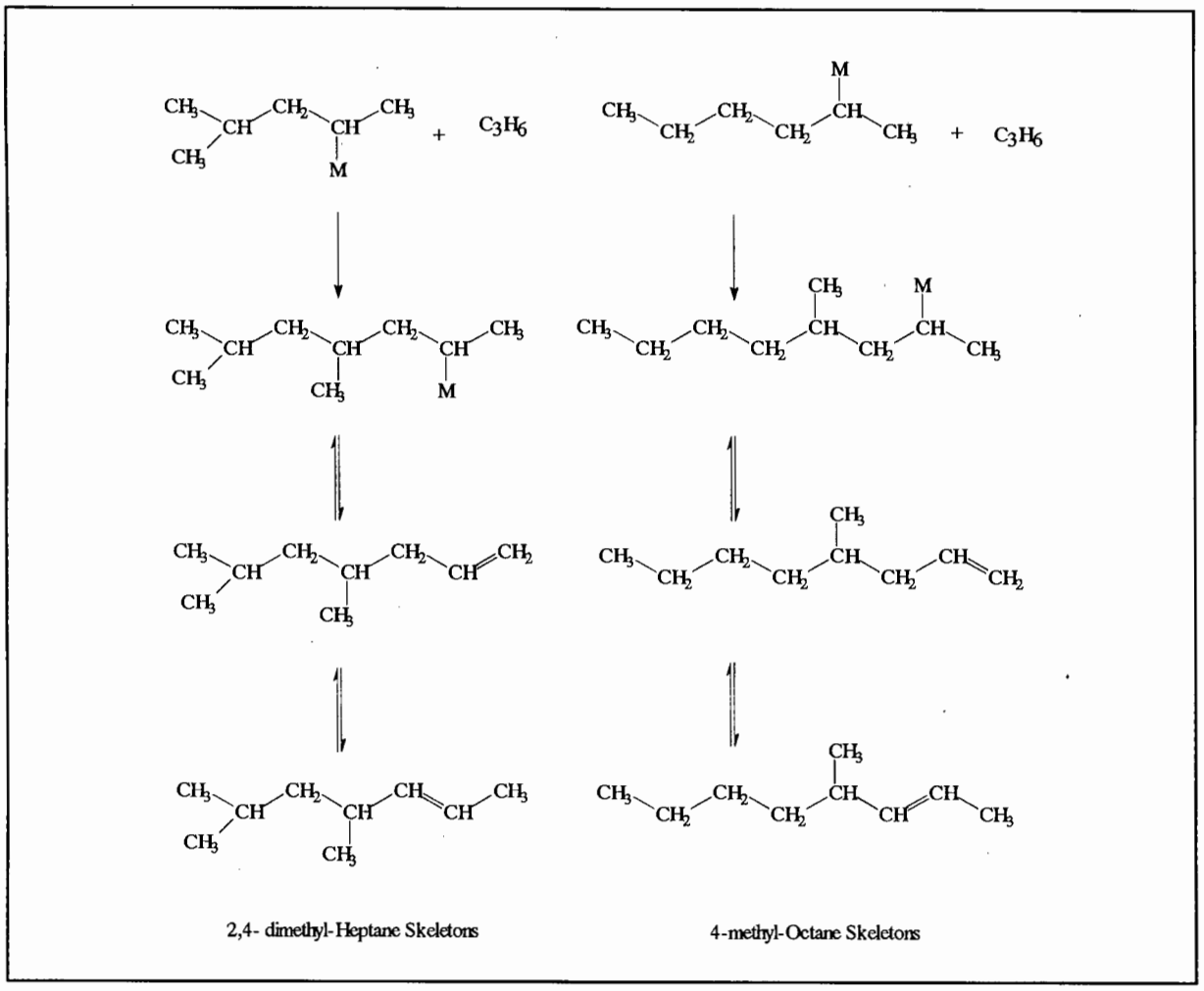

Figure 1.21 : Formation of Nonenes over Nickel Oxide on Silica-Alumina (Fel'dblyum and Baranova (1971))

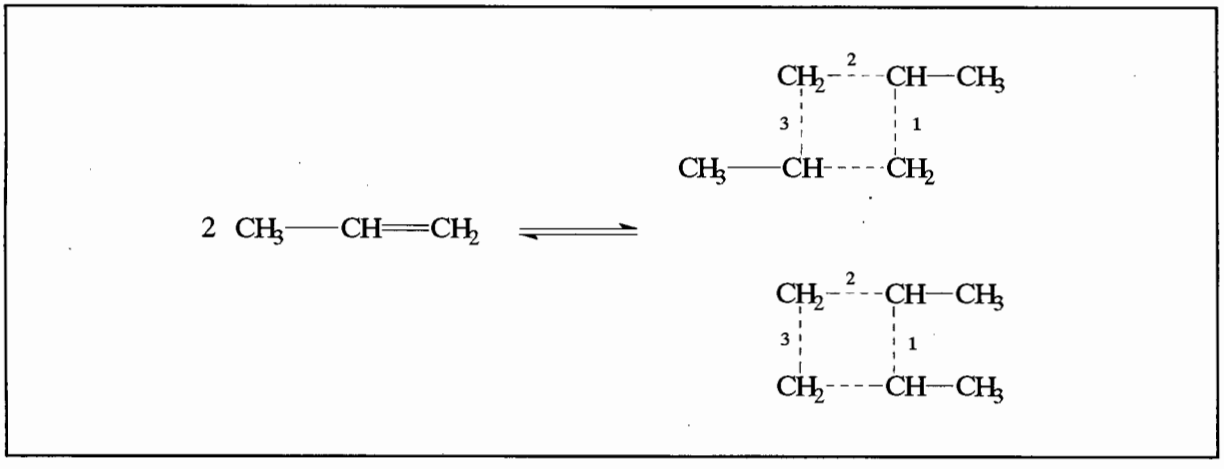

Figure 1.22 : Reaction Intermediates Formed During Oligomerisation (Hassan et al. (1977))

1.3.3 Homogeneous Metal Catalysts

The reaction mechanisms for homogeneous catalysts are different to those occurring over acid catalysts. These mechanisms are discussed below in order to obtain a better understanding of the models over metal catalysts that are described in the following section. In their comprehensive review on ethene dimerisation and oligomerisation, Al-Jarallah et al. (1992), discuss in detail the reaction mechanisms occurring during these reactions. The chemistry of ethene dimerisation and oligomerisation is common to all processes producing alpha olefins. There are two well known mechanisms for ethene dimerisation, namely the hydride and the cyclic intermediate mechanisms. The hydride intermediate mechanism is the one most generally accepted (See Figure 1.23) and consists of the following steps :

1) Insertion of the ethene into the metal-hydride bond (rate constant k_i).
2) Propagation which leads to further insertion of ethene into the metal-alkyl bond and chain growth (rate constant k_p).
3) Elimination which occurs via β-hydrogen elimination and allows L_nMH to re-enter the catalytic cycle (rate constant k_e).

If $k_p >> k_e$ Polymerisation predominates
If $k_p \approx k_e$ Oligomerisation predominates and products have a Schultz-Flory distribution
If $k_e >> k_p$ Dimerisation predominates

Whether polymerisation, oligomerisation or dimerisation prevails depends on the nature of the metal and its oxidation state, the nature of the ligand and the reaction conditions.

Oligomerisation can be divided into two parts, namely chain growth and displacement. The reaction takes place at an organometallic site (M-R). Figure 1.24 shows the metal hydride mechanism for ethene oligomerisation. Depending on whether ethene adds via Markownikov or anti-Markownikov addition, linear or branched products result. The product distribution during catalytic ethene oligomerisation is described by a Schultz-Flory distribution. The growth factor, K, is defined as follows :

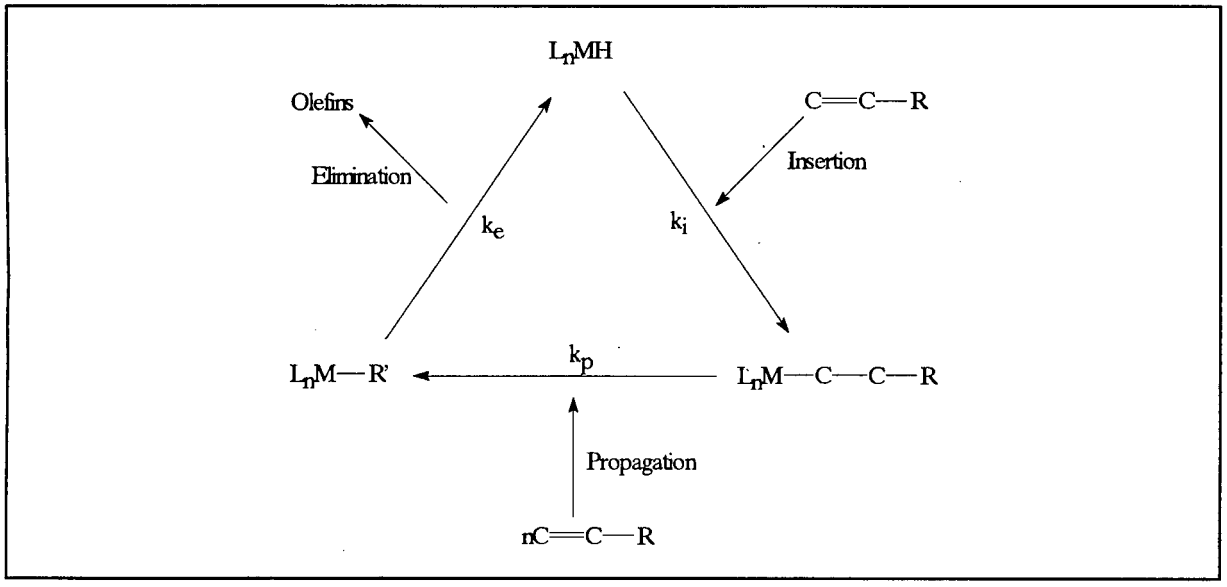

Figure 1.23 : Hydride Intermediate Mechanism for Homogeneous Catalysts

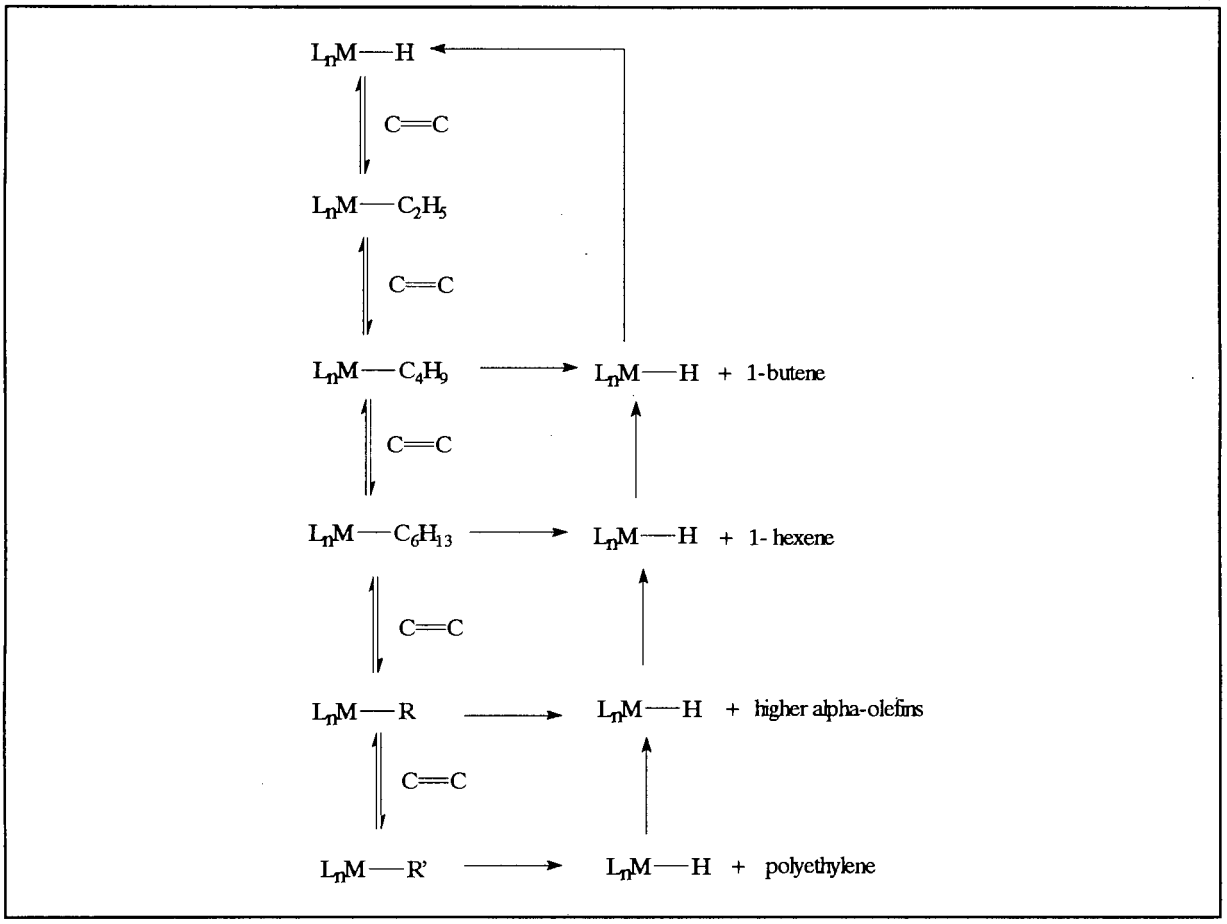

Figure 1.24 : Metal Hydride Mechanism for Ethene Oligomerisation

$$K = \frac{C_{n+2}}{C_n} \quad , K < 1 \qquad (1.1)$$

C_n is the number of molecules of α-olefins with chain length n

C_{n+2} is the number of molecules of α-olefins with chain length n+2, the next member of the series.

The product distribution can also be described using the Poisson distribution if large quantities of catalyst are used (stoichiometric reaction).

1.4 Modelling of Oligomerisation

1.4.1 General Approaches to Modelling Complex Reactions

Complex reaction mixtures are by their very nature difficult to model. Reaction networks for such mixtures may involve thousands of components and reactions. Examples of complex reaction mixtures are the pyrolysis of minerals and biomass, combustion, fermentation, polymerisation and smelting. Krambeck (1992) discusses various ways of simplifying the modelling procedure for complex mixtures. The first method involves lumping or grouping reaction products into smaller numbers of pseudo-components. Three main factors need to be considered when choosing the lumping scheme, namely measurability, adequacy and accuracy.

One example of lumping is the grouping of isomers of the same carbon number obtained from petrochemical reactions. Lumping of these isomers is justified if they are all at equilibrium with one another. However, even though the isomers have the same chemical composition they may have different reactivities due to their structure, especially if shape selective catalysts are being used. Thus the type of grouping employed requires care.

Another approach is to tackle the problem from a more positive side and use a large number of components to advantage. This can be achieved by treating the reaction mixture as a continuum rather than a discrete set of components. The reaction rates are then a continuous

function of some molecular property such as molecular weight, boiling point etc.

Finally, there exists another more elegant approach to the kinetic modelling of complex reactions. Froment (1991) advocates a fundamental method whereby detailed reaction networks are retained to a maximum extent by breaking the reaction down into a series of elementary steps and their single events. Froment believes that although these type of models have more parameters than the lumped approach, their fundamental nature gives them wider applicability. To explain further, fundamental models are not specific to the feed mixture and do not require extensive experimentation each time a new feed is introduced as does the lumping method. In fact, this detailed, fundamental approach can reduce the number of parameters required to model the complex reaction. In this case more is very often less.

Whichever method of modelling is chosen is problem specific. If one wishes to model say, the flow patterns in the reactor, then a highly complex model is neither practical or desirable. On the other hand, if one wishes to understand more about the reaction rather than the reactor then detailed modelling may be required. These methods could therefore be broadly classified into "industrial" versus "academic" approaches. This is clearly outlined in the panel discussion in the last pages of *Chemical Reactions in Complex Mixtures* (Sapre and Krambeck (1991)).

In the sections following, various types of oligomerisation models will be reviewed. This is further split in to several subsections relating to the type of catalysts used since, as already mentioned, the reaction mechanism depends strongly on the class of catalyst used. Almost without exception all the oligomerisation models reviewed adopt the lumped approach in some form whereby all olefin isomers of the same carbon number are assumed to be at equilibrium with one another and lumped together. In the final section some other examples of complex reaction models are presented. One example treats the reaction mixture as a continuum and the other adopts the fundamental approach.

1.4.2 Oligomerisation Models

One of the more unusual models for oligomerisation is presented by McCoy (1993). This model applies the idea of continuous mixtures to model most of the reactions occurring when

olefins are reacted over acid catalysts, namely oligomerisation, cracking and disproportionation. Since no mention is made of the type of catalyst or structure of the product produced it is assumed that this is a general model for a number of possible oligomerisation systems. The model considers each chemical species as a continuous mixture which covers a molecular weight range. This molecular weight distribution of each species is represented by either a Gamma or Gaussian distribution. The concept that the products from oligomerisation reactions tend towards equilibrium distributions at long times is also incorporated into the model. One drawback is that all reacting species are classified according to their carbon number only and no mention is made of skeletal structure. This is important when modelling oligomerisation over shape selective catalysts such as H-ZSM-5.

In addition to oligomerisation, two types of cracking reactions are covered, namely proportioned and random fission. During proportioned fission the molecule can only split into molecules of selected molecular weights. If the initial condition consists of delta-function molecular weight distributions then by definition the distributions must remain delta functions for all time since only certain specified oligomers are allowed. Random fission means that the molecule can split into any pair of fragments. This type of cracking results in a broadening of the product spectrum with time. In this paper the effect of these two types of fission on the product distribution is shown. The rate constants chosen for the simulation were proportional to j^{-3}, where j is the carbon number. Unfortunately, no comparison with experimental data is given so the applicability of the model cannot be evaluated.

1.4.2.1 Acid Catalysts - Zeolites

Quann and Krambeck (1991) developed a three parameter model for olefin oligomerisation over H-ZSM-5 for a wide range of temperatures and pressures. This model was required to evaluate the effect of various process variables such as temperature, pressure and recycle ratio and was used in the design and development of the MOGD process. To reduce complexity, all isomers of the same carbon number were lumped together into a single pseudo-component. The authors assumed that all isomerisation reactions were faster than oligomerisation or cracking reactions and thus they were justified in lumping according to carbon number only since the isomers were at equilibrium. Oligomerisation, cracking and disproportionation were included in the model. Cojunct polymerisation, however, was not

taken into account. The forward rate constant for oligomerisation was dependent on the carbon number of the reactants and a carbon number reactivity parameter:

$$k_{ij}^{f} = k_o(ij)^{-\omega} e^{-E/R_g T} \qquad (1.2)$$

ω - carbon number reactivity parameter

k_0 - pre-exponential factor

The reverse rate constants (or cracking rate constants) k_{ij}^{r} are related to the forward rate constants via equilibrium constants for the reaction.

The third model parameter, α, was the relative rate parameter for disproportionation and was employed as follows. Disproportionation was assumed to occur as a two-step reaction,

$$C_i + C_j \rightarrow [C_z] \rightarrow C_u + C_v$$

The rate of formation of the complex C_z was then related to the oligomerisation rate,

$$r = \alpha P k_{ij}^{f} x_i x_j \qquad (1.3)$$

Additionally, the complex cracking rate must be divided among all the possible combinations of u and v whose sum is equal to z. A scale factor q_{uv} was introduced to scale the rate of complex splitting to the cracking rate of the olefin of carbon number z to olefins of carbon numbers u and v :

$$q_{uv} = \frac{k_{uv}^{r}}{\sum_{l+m=z} k_{lm}^{r}} \qquad (1.4)$$

and,

$$\sum_{l+m=z} q_{lm} = 1 \qquad (1.5)$$

Finally, the rate of formation of u and v via disproportionation is given by:

$$r'_{uv} = q_{uv}\sum r_{lm} - r_{uv} \qquad (1.6)$$

The authors found that the reversible oligomerisation/cracking reactions were not sufficient to model the experimental data and disproportionation needed to be included in order to account for the randomisation of carbon numbers. In addition, they found that isomerisation was not as rapid as was first assumed.

Additionally, they state that while lumping according to carbon numbers may be thermodynamically correct, it may not be a consistent kinetic lump. Each carbenium ion may crack at different rates according to their structure.

While the fit of the model is good and it is able to predict the effect of operating conditions such as temperature, pressure and recycle cut point, using a small number of adjustable parameters, it gives no information regarding the behaviour of different skeletal structures for each carbon number. This model also does not provide an understanding of the underlying reaction mechanisms and, although more time consuming, a fundamental approach to modelling this reaction would be useful in this regard.

Alberty (1987b) also modelled propene and butene oligomerisation over H-ZSM-5 at 327°C and 0.01 and 0.5 MPa. Again, the main assumption was that isomerisation reactions were at equilibrium and therefore justified grouping the product according to carbon number only. The author considered all possible bimolecular reversible reactions between all carbon numbers up to $C_{13}H_{26}$. This gave rise to a 30-step mechanism. If the reactants or products had isomers then the rate constants were weighted averages, according to the equilibrium distribution of the isomers. The reaction was then simulated using one of the following assumptions :

1) The bimolecular rate constants are all equal and the cracking rate constant for each step is calculated using Gibbs Free energies of formation of the isomer groups included in that step.
2) The cracking rate constants are all equal and the bimolecular rate constants for each step are calculated from the Gibbs Free energies of formation.

Alberty believed that in the absence of detailed data both these assumptions were plausible. Additionally he felt that both assumptions were justified because all bimolecular and cracking reactions are similar.

The simulated concentration profiles versus dimensionless time at 327°C for two different pressures 0.01 and 0.5 MPa, two different feed olefins, namely propene and butene, and the two model assumptions, were shown. By examining the simulated product spectra it was possible to clearly distinguish between the two model assumptions. For propene as the starting product, a reaction pressure of 0.01MPa and equal bimolecular rate constants the C_6 dimer formed rapidly and then cracked to C_2, C_3 and C_4 olefins. A small amount of C_9 trimer and no C_{12} tetramer formed. Cracked products C_4 and C_5 were present in significant amounts. Raising the pressure to 0.5MPa resulted in an increase in C_9 and C_{12} olefins, both of which passed through a maximum. The non-oligomer concentrations grew slowly due to the low cracking rate constants. The trends observed for the butene feed were similar.

If cracking rate constants are assumed equal then different composition profiles are predicted. The rate of removal of propene at 0.01 MPa is much higher than for assumption 1 because the effective rate constant increases. As the pressure is increased to 0.5 MPa this trend is even more obvious. The concentration of the C_6 dimer increases much more and cracks far less than for assumption 1 under the same conditions. This led Alberty to question the accuracy of the Gibbs Free energy of formation of the hexene isomer group. The dimer for butene does pass through a maximum as for assumption 1 due to a net increase in its rate of formation. A similar trend is observed for the C_9 trimer for the propene feed.

The validity of the model could not be assessed due to the lack of experimental data with which to compare product compositions. For this model homogeneous reactions were assumed i.e. adsorption or diffusional effects were not included. Ideal gases and gas mixtures were also assumed. However, the shape selective effects of H-ZSM-5 could be included by omitting the most bulky isomers from the isomer groups.

A kinetic study of the oligomerisation of isobutene over H-Mordenite was presented by Ngandjui and Thyrion (1992). This study was very similar to that performed by Haag (1967) using cation exchange resins which is to be reported in the next section. The mordenite used

was a highly dealuminated form having only 1wt% alumina. This meant that the number of acidic sites were low but these were assumed to be very strong. Reactions were carried out in the liquid phase at several temperatures between 40 and 140°C in an agitated batch reactor.

Initially, experiments were conducted to determine mass transport effects. It was found that no extra- or intra-granular diffusion limitations were present when particles less than 90μm and stirring speeds greater than 1000 rpm were used and therefore this particle size was chosen for all the experimental runs. It was found that at initial conditions first-order kinetics with respect to isobutene prevailed. These first-order kinetics were found to be consistent with a Langmuir-Rideal mechanism in which the reaction occurred between one adsorbed molecule and one in the gas phase.

A graph of the product distribution up to 80% conversion was provided for both an industrial extrudate and powder catalyst at a reaction temperature of 80°C. In both cases only oligomers up to the tetramer were formed with no cracked products. For the powder catalyst, the dimer concentration always exceeded that of the trimer while for the extrudate catalyst they were similar. They noted that all oligomers were present as soon as the reaction started. This was taken to provide evidence for a parallel instead of a purely consecutive reaction scheme. Since the tetramer was present only in small amounts the following reactions were considered :

monomer + monomer → dimer
dimer + monomer → trimer
dimer + dimer → tetramer

The Langmuir-Rideal equations for the rate of formation were formulated for all four reacting groups using the above reactions. The ratios of the adsorption coefficients b_T/b_M and b_D/b_M were obtained by feeding different molar ratios of monomer and trimer, and monomer and dimer and studying the initial rates. These ratios reduce the number of parameters in the model and simplified the fitting procedure. The above set of differential equations was solved using a Runge-Kutta method. The model was able to predict the concentration of the reacting species as a function of time. The model concentrations compared well with experimental

data.

1.4.2.2 Acid Catalysts - Non-Zeolitic

Haag (1967) studied isobutene oligomerisation over cation exchange resins (Amberlyst 15). This study grouped the products according to carbon number and the skeletal structure of the products was not specified. Also, non-oligomer groups did not appear in the model. The reaction pathway is shown in Figure 1.25.

The reactions were carried out in both batch and continuous flow reactors. The reaction conditions for the batch reactor were approximately 500 kPa and 25 to 60°C while those for the flow reactor were 1 MPa, 16 to 60°C and liquid hourly space velocities of 180 to 3600 hr^{-1}. The heaviest product produced in significant amounts was the tetramer.

The dimerisation reactions,

$$\text{monomer} + \text{monomer} \rightarrow \text{dimer}$$
$$\text{dimer} + \text{dimer} \rightarrow \text{tetramer}$$

were successfully modelled using a Langmuir-Rideal type mechanism. Surprisingly, the author found that the equilibrium constant for adsorption for the monomer was almost 10 times that for the dimer. The trimers could form by either of the two ways shown in Figure 1.26. $A_3(A)$ is formed via the addition of a dimer to an adsorbed monomer. On the other hand, A3(B) is formed when a monomer adds to an adsorbed dimer. This reaction competes with the desorption of the dimer. The tetramer only forms once the monomer is reduced to a low level since the monomer and dimer undergo competitive adsorption.

Paynter and Schuette (1971) discuss the development of a model for the kinetics of propene and butene co-dimerisation over supported phosphoric acid. Initial product selectivities were studied in order to gain information regarding the rate constants. By using statistical arguments the authors were able to predict co-dimerisation rate constants from the individual dimerisation rate constants. They tested this relationship successfully using experimental data. This additional information was useful in reducing the number of model parameters. The product spectrum was lumped according to carbon number. The model only considered

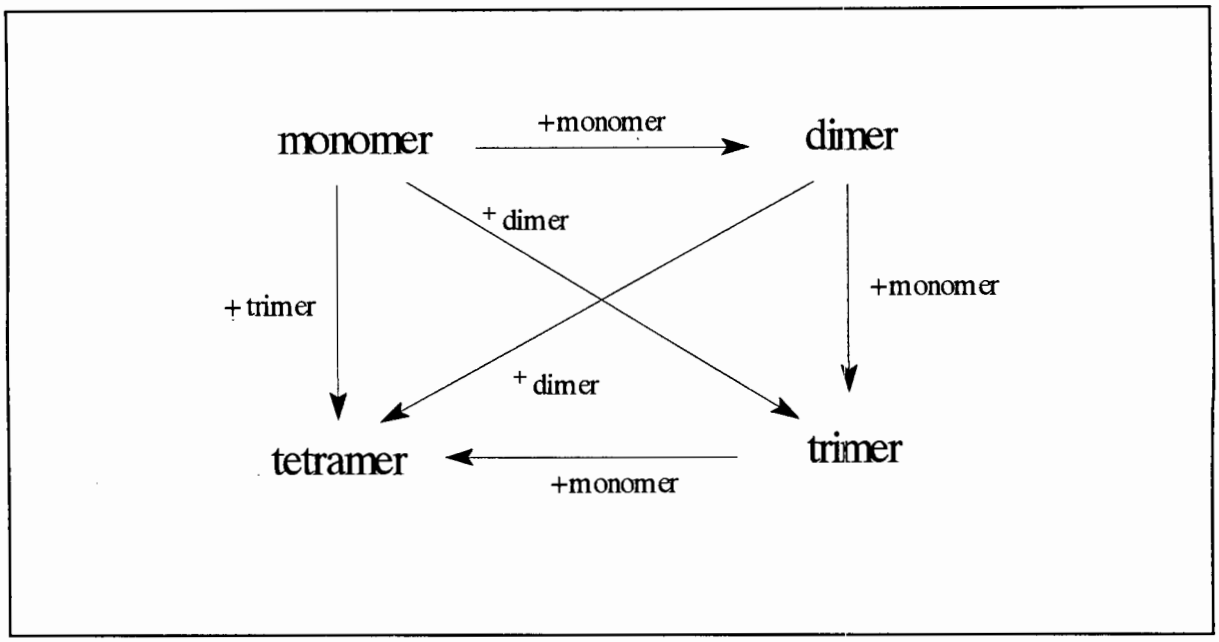

Figure 1.25 : Oligomerisation Reaction Pathway (Haag (1967))

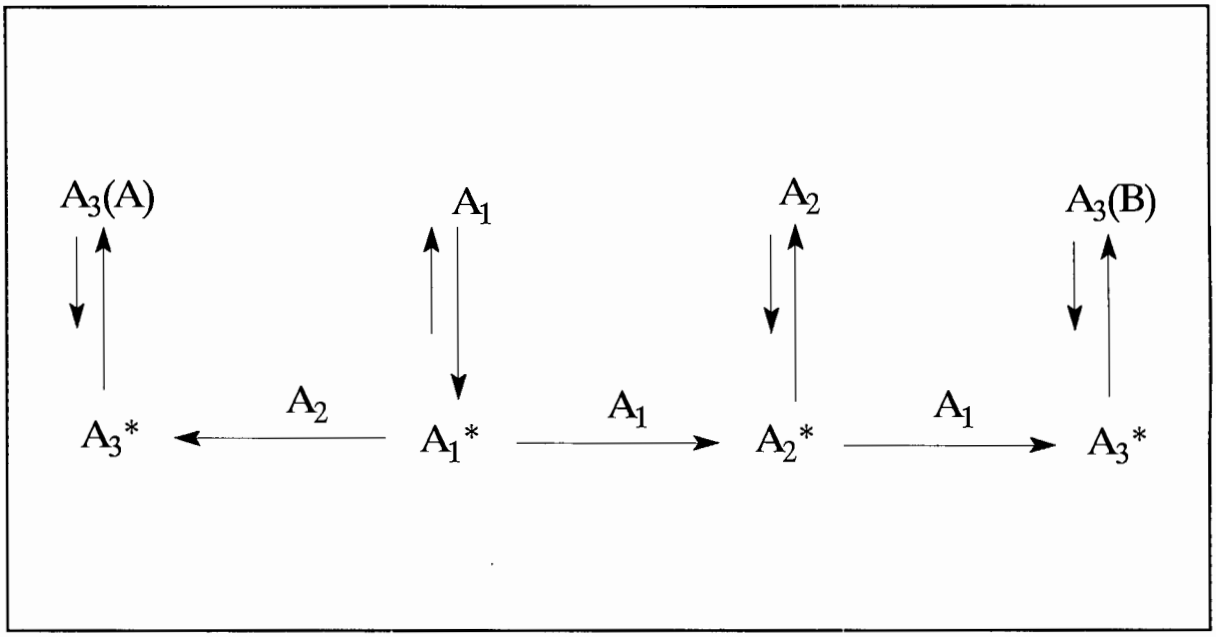

Figure 1.26 : Oligomerisation over Ion Exchange Resins (Haag (1967))

compounds up to and including C8 - everything heavier was combined into one lump. No cracking reactions were considered, only straight-forward chain growth. Finally, the system was described using a set of seven, coupled, non-linear differential equations for which eight rate constants were required. The relationships above reduced the number of rate constants required to four. The fit obtained was reasonable but it was not able to predict the C_{9+} lump at low conversions.

Cao et al. (1988) developed a lumped model for oligomerisation of propene-butene mixtures over a supported phosphoric acid catalyst. Each component was classified according to the number of carbon atoms (n). All components containing n carbon atoms were further split into two groups C_n or $C_{n,1}$. $C_{n,1}$ were molecules that could grow in size by addition of a monomer unit while C_n could not do so. $C_{n,1}$ could react via isomerisation to C_n. These lumping criteria were proposed in order to simulate the situation during the reaction where different olefin isomers exhibited different levels of reactivity towards oligomerisation. No cracking reactions were considered. The authors introduced two kinetic criteria :

1) All reactions $C_{n,1} \rightarrow C_n$ was assumed first order and had the same rate constant
2) The addition reaction $C_{n,1} + C_{m,1} \rightarrow C_{n+m,1}$ was second order and the rate constant was the product of the two intrinsic reactivities. These intrinsic reactivities were adjustable parameters of the model. This assumption was useful since there were more reactions than reacting components and helped to simplify the modelling procedure. Theoretically, as long as the number of reacting components stays constant any number of reactions could be included eg. cracking.

Inter- and intraparticle mass transport resistances were ignored. Only molecules up to C_{11} were considered as inclusion of heavier molecules did not result in an improvement in fit. Additionally, olefins containing more than 7 carbon atoms were assumed not to react in all cases. Concentration profiles versus time were simulated and compared to experimental data from Paynter and Schuette (1971). The resulting fit was good.

1.4.2.3 Heterogeneous Metal Catalysts

The kinetics and mechanism of propene dimerisation to 4-methyl-1-pentene over supported

and promoted metallic sodium was studied by Forni and Invernizzi (1973). The support used was K_2CO_3 and the promoter Hg. Reaction conditions were 130 to 150°C, 1.7 to 7.7 MPa and a range of weight hourly space velocities. The experiments were conducted using a fixed-bed, flow-through reactor. Initially, runs were carried out to assess the influence of mass transport effects. No influence of external diffusion was found. Since the catalyst had large pores ($\geq$ 10 000 Å) it was assumed that there were no internal diffusion restrictions.

The reaction products consisted only of dimers, the main dimer being 4-methyl-1-pentene. Other hexene isomers were formed in small amounts. The products were then grouped into four main lumps : propene, 4-methyl-1-pentene and branched and linear hexene isomers.

Langmuir-Henshilwood type mechanisms were chosen to model the data. In order to determine the rate-limiting step, runs at various reactant partial pressures were carried out. The assumption that the adsorption of propene was rate controlling was found to fit the data best. Additionally, it was assumed that linear dimers form via the same mechanism as 4-methyl-1-pentene while branched dimers form via the isomerisation of 4-methyl-1-pentenes. Since the other hexene isomers were in such small concentration, their influence could be neglected and their rate of formation expressed according to first order rate equations :

$$r_1 = \frac{k_1 P_P}{1 + b_P P_P + b_D P_D} - k_2 P_D \qquad (1.7)$$

$$r_2 = k_2 P_D \qquad (1.8)$$

$$r_3 = k_3 P_P \qquad (1.9)$$

where, r_1 = rate of formation of 4-methyl-1-pentene
r_2 = rate of formation of branched hexene isomers
r_3 = rate of formation of linear hexene isomers

Experimental runs were performed using both differential and integral reactor mode. Using the information obtained from the differential reactor runs, the authors were able to reduce the number of parameters required to fit the integral data. The fit of the model to the

experimental data was good. Additionally, the authors were able to calculate activation energies of the reactions along with the standard enthalpy and entropy of adsorption for 4-methyl-1-pentene.

Espinoza et al. (1987) developed a random dimerisation and co-dimerisation model for the oligomerisation of ethene over a nickel-exchanged amorphous silica-alumina. The silica-alumina mole ratio of the catalyst was 50 and contained 0.27 wt% nickel. Runs were carried out using a fixed-bed, tubular reactor and the effect of operating conditions studied by systematic variation of temperature, pressure and WHSV. Temperatures from 120 to 380°C, pressures from 0.16 to 2.1 MPa and WHSV's from 0.5 to 12 hr^{-1} were covered. Their data showed that an increase in either pressure or temperature resulted in a slightly heavier product. An increase in space velocity resulted in an increase in ethene dimers and a reduction in cracked products. It was thought that acid catalysis contributed to the oligomerisation of the C_{2+} species. The reactivity of light olefins was also studied. Propene and ethene had the same level of reactivity while that of 1-butene was half that of ethene. It was also noted that isomerisation of the butenes was occurring simultaneously with dimerisation. The presence of the acid sites was thought to contribute to the fast establishment of isomer equilibrium.

A model was proposed that represented a concentration-driven random dimerisation and co-dimerisation of the alkenes and adjustments were made for major kinetic differences between the various alkenes. Cracking reactions were ignored. P(X), the probability that the reaction will involve molecule X was defined as :

$$P(X) = \frac{\textit{Number of Molecules with Carbon Number } X}{\textit{Total Number of Molecules}} R \qquad (1.10)$$

where, R reactivity parameter = 1, except for C_{4+} species where it is 0.55
The change in the number of oligomers in any small time increment is :

$$\begin{aligned} \Delta N(2) &= -2[P(2).P(2) + P(2).P(4) + P(2).P(6).....] \\ &= -2\Sigma[P(2).P(x)] \end{aligned} \qquad (1.11)$$

$$\Delta N(4) = P(2).P(2) - 2\Sigma[P(4).P(x)] \quad etc. \qquad (1.12)$$

The mass percent of the products versus conversion of the feed was calculated and compared with experimental data. The fit to the experimental data was good. It was also added that cracking could be incorporated into the model if required.

Another example of kinetic and mechanistic studies performed on a supported nickel catalyst is that by Forni et al. (1975). The catalyst used in this study was 13X molecular sieve containing 4.9 wt% nickel and 1.5wt% Li_2O. Studies were carried using a fixed-bed, flow reactor at 160 to 200°C and approximately 4MPa, using a 1-butene feed. At each temperature the residence time was varied to obtain at set of conversions from approximately 10 to 70% conversion. The major product was the dimer along with 2-butenes. When the C_8 fraction was hydrogenated and analysed it was found that over the reaction conditions studied the linear C_8 content remained constant at 30%. In order to model the reaction, the product spectrum was divided into three groups, namely 1-butene, 2-butene and C_8's. The reactions considered were the isomerisation of 1- to 2-butene and the dimerisation of these two isomers to C_8. Any heavy byproducts were ignored. The authors concluded that despite the simple nature of the model, the fit was adequate and a more complex model was not required. They were also able to calculate the activation energies of the reactions. The low values of the activation energies led to the suggestion that the reaction was mass transfer controlled. The mass transfer resistance was caused by the gaseous reactant having to diffuse through a liquid film before reaction could take place.

1.4.2.4 Homogeneous Catalysts

Galtier et al. (1988) modelled homogeneous ethene oligomerisation occurring during the Dimersol and Alphabutol Processes. It was assumed that oligomerisation could be modelled as a form of polymerisation with two types of reaction steps, namely chain growth and chain termination. Here also, isomers were grouped according to carbon number and isomerisation reactions were ignored. Essentially, this model is an extension of the Schultz-Flory model. According to the model mechanism polymerisation of the monomer and the first oligomers can occur i.e. mixed homo- and co-polymerisation. However, the authors assumed only the dimer and trimer were reactive when fitting the data. The values of the rate constants were adjusted by trial and error until the model fitted the data points. The model fit was good.

1.4.3 Models of Other Complex Reactions

Krambeck (1991) discusses the continuous mixtures approach to modelling fluidized catalytic cracking reactions (FCC). Here the product from FCC is classified as that boiling below 200°C (gasoline). Anything above 200°C is unconverted material. It was found that the unconverted material disappears according to a second order rate law even though the individual species disappear via first order. This is because the fastest reacting compounds are removed first leading to a faster decline in reaction rate than would be expected. This phenomenon is also discussed by Ho and Aris (1987).

Gasoline selectivity was modelled using the following equation, assuming that the gasoline fraction is cracked according to a second order rate law:

$$g = \frac{(1 - k_g)(100 - x)}{100 - (1 - k_g)x} \qquad (1.13)$$

where

g is the gasoline selectivity

x is the conversion

k_g rate coefficient for the gasoline fraction

This model was compared to data from several feedstocks and catalysts and the agreement was good. This model can be extended further to predict the entire boiling point range :

$$\frac{w_o(T)}{w(T)} - 1 = \frac{k(T)x}{(100 - x)} \qquad (1.14)$$

where,

$w_o(T)$ is the percent of feedstock boiling above temperature T

w(T) is the percent of reaction products boiling above T

k(T) is the second order rate constant

Similarly, this model was able to predict experimental data well. However, Krambeck notes

that the performance of the system varies with the feed and there is no simple way of incorporating this effect into the model. Only by adopting a more fundamental approach is one able to solve this problem.

Froment (1991) used the fundamental approach when modelling hydrocracking on metal-loaded zeolites. Here the kinetics of reaction is expressed in terms of fundamental elementary steps. These elementary steps are further broken down into single events :

$$k^* = n_e k \qquad (1.15)$$

where ,

k^* is the elementary rate coefficient

n_e is the number of single events

k is the rate coefficient of the single event

For n-octane feed there were 383 elementary chemical steps, however, 383 rate constants were not required to model the reaction. Using several simplifying assumptions and thermodynamic constraints only 17 independent rate coefficients were required to model the reaction : 2 for protonation, 2 for deprotonation, 2 for hydride shift, 3 for methyl shift, 3 for PCP isomerisation and 4 for β-scission. These rate constants were independent of carbon number and could be determined either from C_8 or C_{10} hydrocracking. The rate equations used to describe the reaction then consisted of the individual elementary steps. The addition of a rate determining step and the effect of physisorption simplified the model still further. Unfortunately, no experimental data was provided with which to test this fundamental approach.

1.5 Objectives of This Study

While the models for oligomerisation reviewed in this chapter are able to predict concentrations well, all lump the products according to their carbon number. This is because for the majority the aim was to predict product properties such as viscosity and boiling point and the effect of reaction conditions such as temperature and pressure for industrial

applications. However, no information is provided by these models on the interconversion of the different skeletal structures which have very different reaction rates.

Thus, the first aim of this thesis was to understand the underlying reaction pathways for high pressure propene oligomerisation over H-ZSM-5 by adopting a fundamental approach. The second aim was to use the information obtained regarding the reaction pathways to develop a mathematical model to describe the oligomerisation process as a whole.

1.6 Problem Solving Methodology

In view of the complex nature of propene oligomerisation, a systematic approach was necessary in order to establish the reaction pathways and to develop a mathematical model for this reaction. The problem was divided into a series of sub-problems, each laying the groundwork for the next. The aim was to obtain as much information about the reaction as possible, in order to make the modelling process more tractable.

1. Reaction conditions of 250°C and 5MPa were chosen for this study since they fell within the range of industrially relevant conditions that maximised oligomer formation.

2. In order for the kinetic studies to have any value, the experimental data needed to be accurate and reproducible. Mass balances and the reproducibility of the experimental data are covered in Chapter 2.

3. Prior to collecting experimental data, it was important to ensure that the reaction was not influenced by external mass transfer limitations and was operating under isothermal conditions. The subject of external mass transfer and isothermal behaviour is covered in Chapters 2 and 3.

4. A study on the effect of reaction temperature for propene oligomerisation over H-ZSM-5 showed that the reaction products were influenced by diffusion and adsorption. Additionally, the shape selective effects of H-ZSM-5 were confirmed by comparison of the reaction products with those from non-shape selective catalysts. The results of these studies are

presented in Chapter 3. This section highlights the influence of diffusion, adsorption and shape selective effects on the reaction products from propene oligomerisation over H-ZSM-5.

5. The next step in the problem solving process was the equilibrium studies, covered in Chapter 4. In order to study the isomerisation reactions, experiments needed to be conducted at conditions of low conversion since the hexene dimers were at equilibrium with respect to their double bonds but not with respect to their skeletal structures. Low conversion also minimised side reactions such as cracking, disproportionation and aromatization. These studies illustrated the importance of operation under conditions of low conversion when studying the kinetics of oligomerisation. In addition, the equilibrium studies also justified the development of a model that lumped the reaction products according to their skeletal structure. Finally, at less than 10% conversion, the reactor could be treated as a differential one and this simplified the development of subsequent oligomerisation models.

6. Under conditions of low conversion the dominant product oligomers were dimers and trimers. The isomerisation of the dimers was studied first and the results are presented in Chapter 5. It was intended that once the relative rate constants for hexene isomerisation, were established this information could be extended to nonene isomerisation. Several models, of increasing complexity, were developed to describe hexene isomerisation.

7. The final step of this study covered the trimerisation step in propene oligomerisation and its inclusion in a model for oligomerisation. This is presented in Chapter 6. Here an isomerisation pathway for the nonenes is presented based on similar isomerisation schemes for the hexenes. Several problems regarding the overall modelling of oligomerisation are highlighted in this section.

CHAPTER 2 - EXPERIMENTAL APPARATUS AND PROCEDURE

2.1 Experimental Apparatus

A diagram of the experimental apparatus used for the oligomerisation of propene is shown in Figure 2.1. Saturated liquid propene, 99.9% pure, was fed via a high pressure, Lewa, diaphragm pump to the reactor system from a No. 7 CADAC gas cylinder. The main impurities present in the propene feed were propane and isobutane along with traces of ethene, ethane and methane.

Liquid propene was supplied at vapour pressure and room temperature, namely 0.9MPa and 25°C. Before entering the pump the propene passed over 17g of 3A molecular sieve of particle size 1 to 2mm in order to remove any water vapour. Next, any particulate matter was trapped using a 0.5 micron filter. As a safety measure there was a 1.5MPa relief valve upstream of the pump. The pressure was monitored upstream and downstream of the pump by pressure gauges. In addition, there were non-return valves on either side of the pump to prevent backflow. The pump head was cooled to 5°C using ethylene glycol in order to prevent cavitation. Downstream of the pump there was a 7MPa bursting disc.

High purity nitrogen could also be fed along with the propene feed stream. The flowrate of nitrogen to the system was controlled by a 5850 TR series Brooks massflow controller (MFC), with a flow range of 0 to 1000ml/min. The massflow controller kept the flowrate of gas constant regardless of downstream pressure fluctuations. Before the MFC there was a 0.5 micron filter to remove any particulates from the gas stream. Pressures upstream and downstream of the MFC were monitored using pressure gauges.

The propene and nitrogen streams passed together through a small packed bed of 1mm glass beads in order to ensure adequate mixing. The mixer and the line downstream to the reactor inlet were heated to 200°C. Before and after the reactor were three-way valves that allowed the feed stream either to enter the reactor or bypass it.

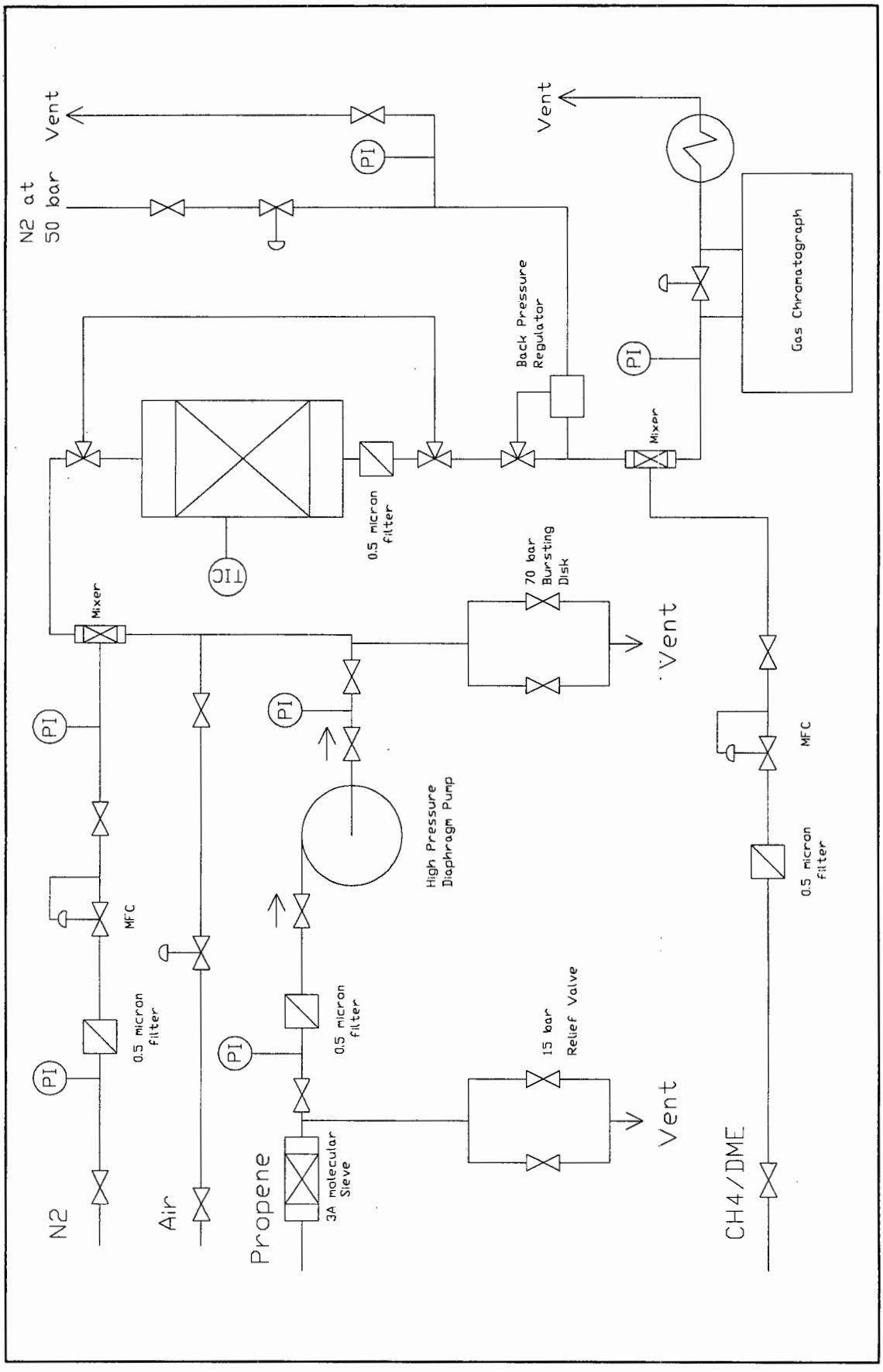

Figure 2.1 : Experimental Apparatus Used for High Pressure Propene Oligomerisation

Synthetic air, 21 mol % oxygen and 79 mol % nitrogen, could also be fed to the system for use during calcination. The air flow was controlled via a needle valve.

The reactor was a tubular, stainless-steel packed-bed reactor (see Figure 2.2). Heat was supplied via a heating block containing four 500W cartridge heaters. The temperature of the heating block was controlled by a PID controller, accurate to 1°C, with a thermocouple mounted in the centre of the heating block. The temperature of the catalyst was measured by a thermocouple in an axially-mounted thermowell. At the reactor exit there was a 0.5 micron filter to prevent any catalyst particles from blocking the downstream lines. The line from the reactor to the condenser was heated to 200°C to prevent any condensation of liquid product. Between the reactor and the gas chromatograph (G.C.) there was a back pressure regulator. This maintained the reactor at the required operating pressure while reducing the pressure of the product stream back to atmospheric pressure.

After the back pressure regulator the reactor product stream was mixed with the internal standard stream using a packed bed of 1mm glass beads. The internal standard, methane or dimethyl ether, was also fed by a 5850 TR series Brooks MFC, with a flow range of 0 to 50ml/min. A 0.5 micron filter was situated upstream of the MFC. The pressure in the product line was also monitored using a pressure gauge.

Samples of the product stream were taken using an online G.C. sampling system. The amount of product stream diverted to the sampling system was controlled using a needle valve. The sampling system consisted of a Varian 3700 G.C. with a flame ionisation detector, linked to Varian Vista CDS 401 integrator. A 50m, Hewlett Packard, Special Performance, PONA capillary column was used. This column had an inner diameter of 0.21mm and a film thickness of 0.5 micron. The stationary phase was crosslinked methyl silicone.

Apart from the normal mode of analysis, the product stream could also be hydrogenated before entering the G.C. column. The hydrogenation was achieved by placing a small packed bed of 5wt% platinum on alumina in the heated injection port of the G.C. and changing the

carrier gas to hydrogen. The temperature of the injection port was 220°C. A typical temperature program for the column was the following : hold at 30°C for 5 minutes, ramp at 5°C/min to 250°C, hold at 250°C for 10 minutes. This mode of analysis converted all the olefins to paraffins of the same carbon skeleton. In doing so, the number of peaks in the chromatogram was reduced. This facilitated the detailed analysis of complex product spectra. It was confirmed that no reaction other than hydrogenation took place over the hydrogenation catalyst. This is shown in Table 2.1 below :

Table 2.1 : Effect of Hydrogenation on Product Spectrum

Skeletal Group	Hydrogenated	Unhydrogenated
	Conversion : 25.4 %	Conversion 25.2 %
Hexane	74.6	74.8
3-methyl-Pentane	10.0	9.85
2-methyl-Pentane	15.4	15.4

After the G.C. sampling system the product stream passed through a glass condenser kept at 5°C. Liquid product was collected in a small flat-bottomed bulb which could be removed, stoppered and weighed. The gas passed through either a wet gas flowmeter (WGFM) or bubble meter before being vented.

For the hexene isomerisation runs the propene cylinder was replaced by a glass, stoppered vessel containing either 1-hexene or 4-methyl-1-pentene.

2.2 Preparation and Packing of Catalyst

Due to the exothermic nature of the reaction it was important to ensure that the reactor was isothermal. If the temperature in the catalyst bed was not properly controlled the reaction could easily become unstable and temperature runaway would occur. A highly effective method involved diluting the catalyst with quartz sand which resulted in a maximum

temperature variation along the bed of 4°C. This was achieved using the following method developed at the Engler-Bunte-Institute, University of Karlsruhe (van Steen (1993)). Acid washed sand, of particle size 100 to 500 micron was obtained from SAARCHEM. Before using the sand it was repeatedly washed in de-ionized water to remove any residual acidity. If this was not done the sand was found to be mildly reactive under oligomerisation reaction conditions. The sand was also sieved to a +212 to -300 micron size range. The catalyst and sand were then weighed out in a 1:50 mass ratio. (For reactions less exothermic a smaller ratio could be used; however, it was also found that a ratio smaller than 1:10 should be avoided as this prevented intimate mixing of catalyst and sand.) The catalyst and sand were then placed in an evaporating dish along with enough de-ionized water to form a slurry. The dish was then placed on a hotplate and heated gently while stirring continuously until all the water evaporated. The catalyst-sand mixture was then placed in the oven at 100°C for a further half hour to dry fully.

Between 0.1 and 0.5g of the catalyst was packed in the reactor in the following manner (see Figure 2.2). A spacer was first placed at the bottom of the reactor. This was a short section of stainless steel tubing that acted as a support for the catalyst bed. A coarse sieve was then placed on top of the spacer followed by a finer one. This was followed by a plug of ceramic wool which was packed down tightly. This was followed by a number of fine sieves. Next, came the catalyst-sand mixture. The position of the catalyst bed in the reactor was carefully noted in order to measure temperatures down the bed accurately. A few more sieves were placed above the catalyst bed, followed by another plug of ceramic wool. More sieves were placed after the wool followed by a bed of 1mm glass beads that acted as a preheat section. Both the sieves and the ceramic wool prevented the catalyst leaving the reactor.

2.3 Experimental Operation

Prior to an experimental run, the catalyst was calcined as follows. The reactor system was first pressurised with nitrogen to the required operating pressure and checked for leaks. Air at 60ml/min was then passed over the catalyst bed while the reactor was slowly heated to

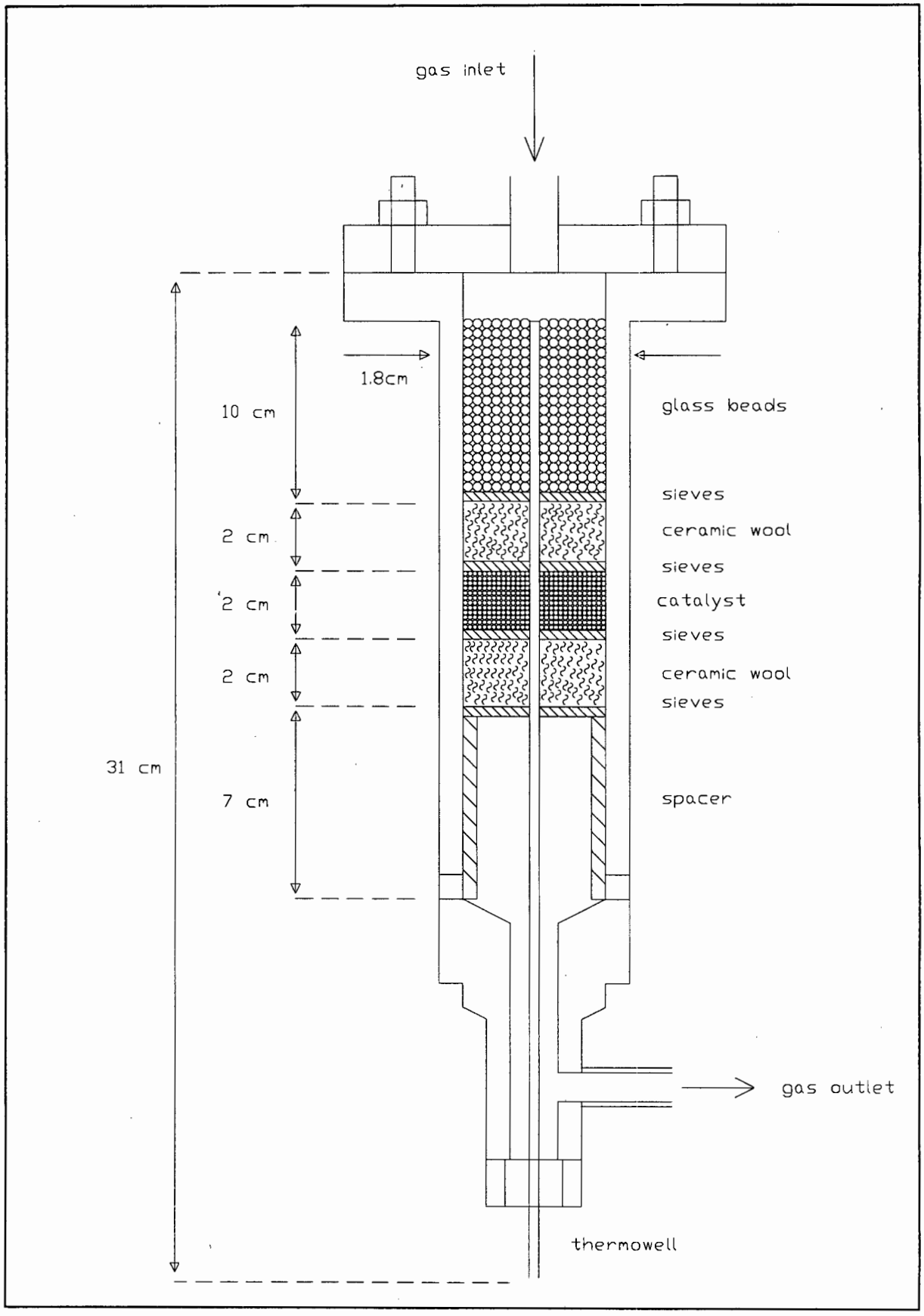

Figure 2.2 : Reactor Layout

500°C. The reactor was left overnight at 500°C, whilst air was continually passed over the catalyst. The lines leading to and from the reactor were heated to 200°C in preparation for the run the following day.

The following morning the reactor was cooled to 120°C and rechecked for leaks. Next, the peristaltic pump for the cooling circuit for the Lewa pump head and catchpot was started. The whole reactor system, from the pump exit up to the back pressure regulator was pressurised using nitrogen. Before starting the run the whole system was flushed with nitrogen in order to remove any air. The three-way valves at the inlet and exit to the reactor were switched to bypass. The propene feed bottle was then opened and the pump started. Once the pump was operating the flow was measured at the exit of the system using either the WGFM or the bubble meter. Once the flowrate was correct, the pump was left for half an hour to stabilize.

If nitrogen was to be co-fed the nitrogen MFC was turned on and flowrate set to the required value. Once the pump was stable several samples of the feed gas were taken using the G.C. sampling system and the mass balance for the feed stream calculated using the internal standard. Following this, the three-way valves were switched to the reactor and the stop-watch started. The temperature of the heating block was then slowly raised until the catalyst bed reached reaction temperature. The reactor was then left for 10 to 15 minutes to ensure that the reactor temperature remained stable. If a low conversion run was to be carried out the internal standard flow was turned on and allowed to stabilize. The reactor temperature and the runtime were then noted and an on-line sample taken.

If a high conversion run was to be carried out then the time and the WGFM reading were noted and a clean, dry bulb connected to the catchpot. For the next hour a number of gas samples were taken and analysed using the Varian G.C. At the end of the hour the WGFM reading was again recorded and the glass bulb disconnected from the catchpot, stoppered and weighed.

At the end of the run the feed pump was stopped and the heating block for the reactor turned

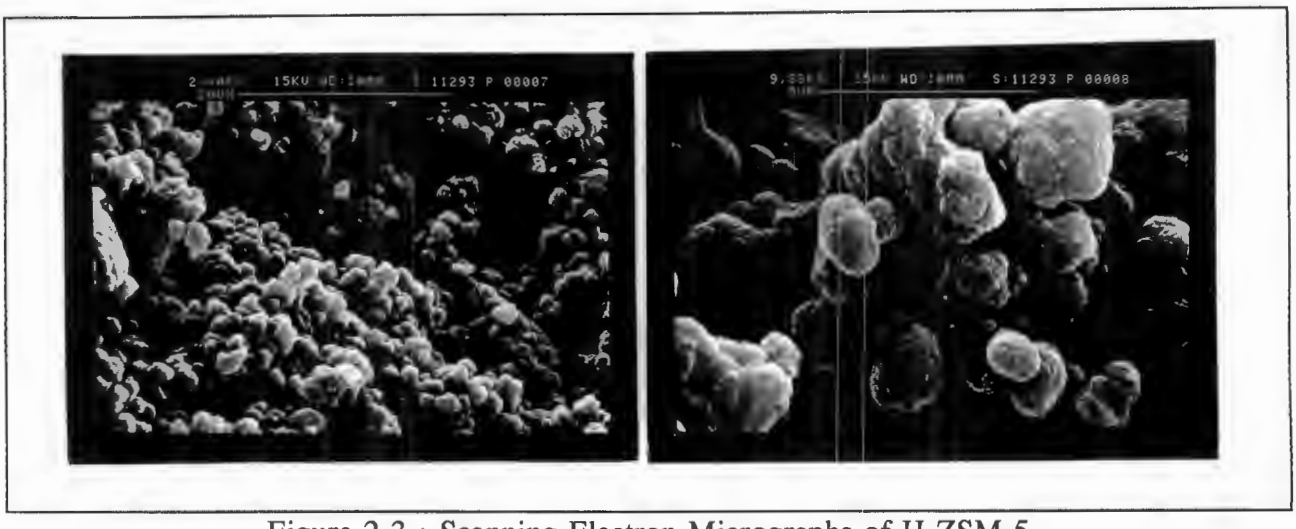

Figure 2.3 : Scanning Electron Micrographs of H-ZSM-5

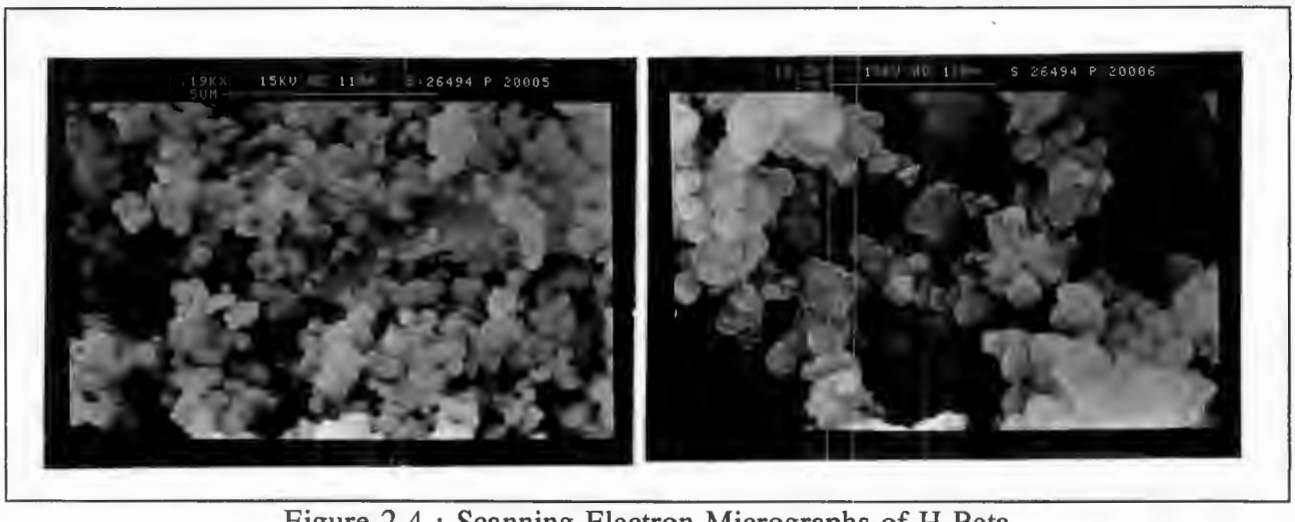

Figure 2.4 : Scanning Electron Micrographs of H-Beta

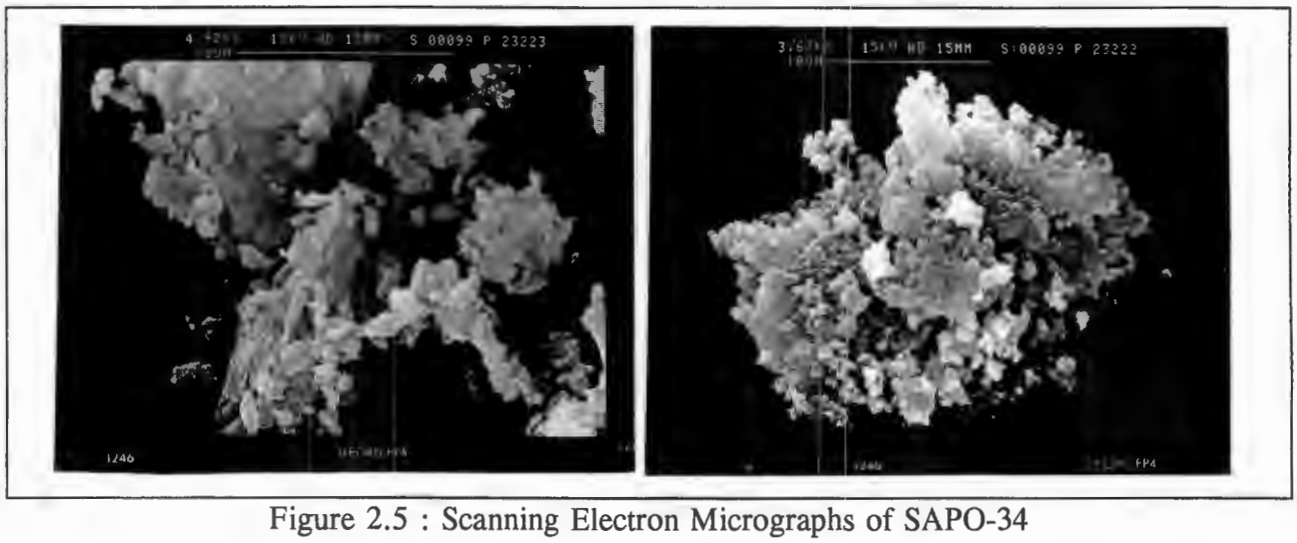

Figure 2.5 : Scanning Electron Micrographs of SAPO-34

off. The nitrogen flow was left on for 15 minutes in order to flush out the system. The nitrogen was then turned off and the system slowly depressurised.

2.4 Catalysts Used

2.4.1 H-ZSM-5

The H-ZSM-5 used in this study was prepared at UCT according to the method of Arguer and Landolt (1972) in a mechanically stirred autoclave. The Si/Al ratio determined by atomic adsorption was approximately 35. The particle size determined from scanning electron micrographs was between 1 and 3 micron. This particle size was the smallest attainable under the synthesis conditions and was chosen to reduce external mass transfer effects. The scanning electron micrographs are shown in Figure 2.3. The X-ray powder diffraction pattern of this catalyst is shown in Figure 2.6. The d-spacings were compared with values given by Szostak (1992)) and can be found in Table A.1, Appendix A.

2.4.2 H-Beta

The H-Beta used in this study was prepared at UCT according to the method of Wadlinger et al. (1967). The Si/Al ratio determined by atomic adsorption was 8. The average particle size determined by scanning electron micrographs was between 0.4 and 0.5 micron. The scanning electron micrographs of this catalyst are shown in Figure 2.4. The X-ray powder diffraction is shown in Figure 2.7. The d-spacings were compared with values given by Szostak (1992) and can also be found in Table A.2, Appendix A.

2.4.3 SAPO-34

This catalyst was prepared at UCT according to the method of Lok et al. (1984). The particle size was approximately 1 to 2 micron. The scanning electron micrographs of this catalyst are shown in Figure 2.5. The X-ray powder diffraction pattern is shown in Figure

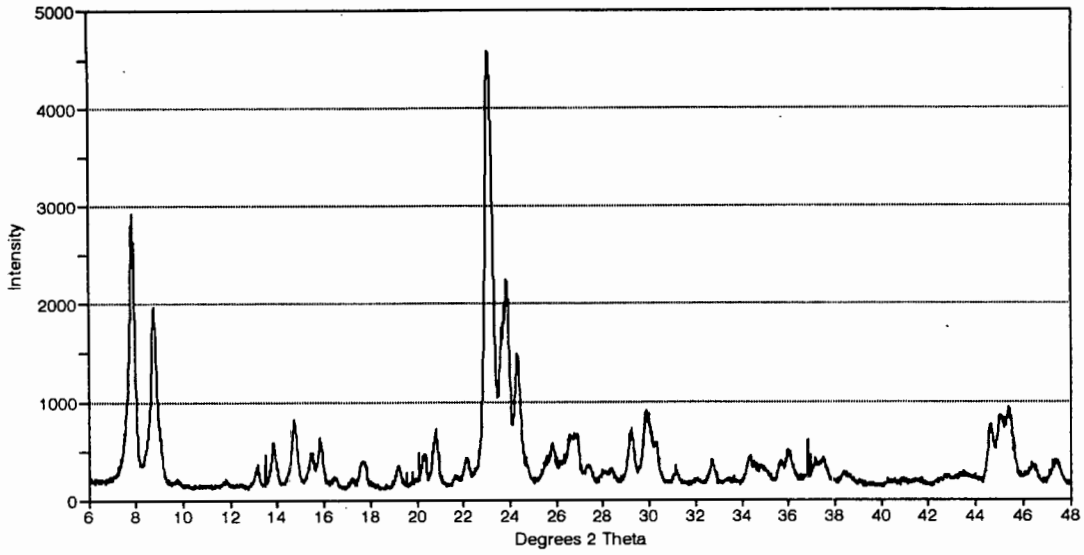

Figure 2.6 : XRD Pattern for H-ZSM5

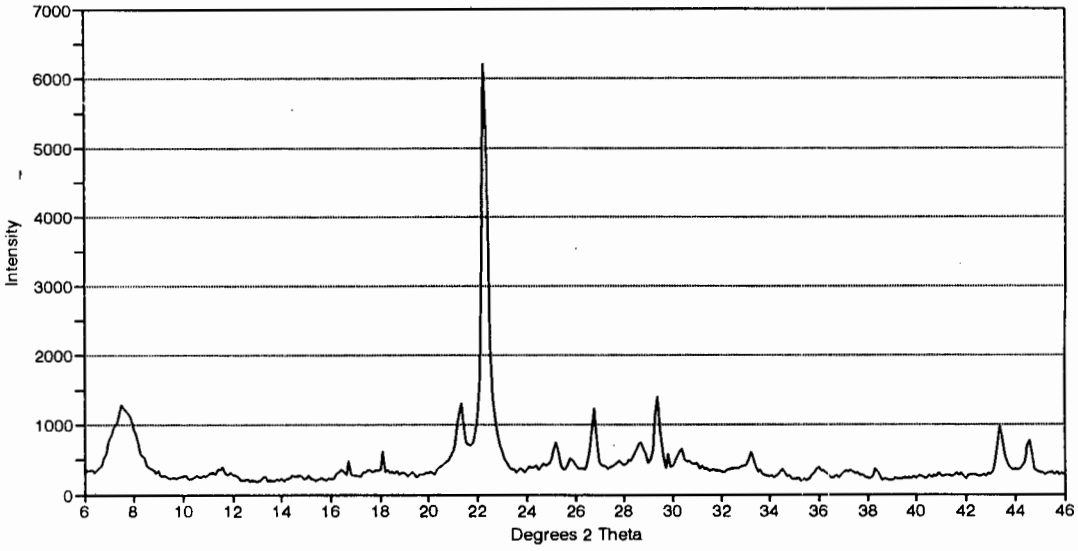

Figure 2.7 : XRD Pattern for H-Beta

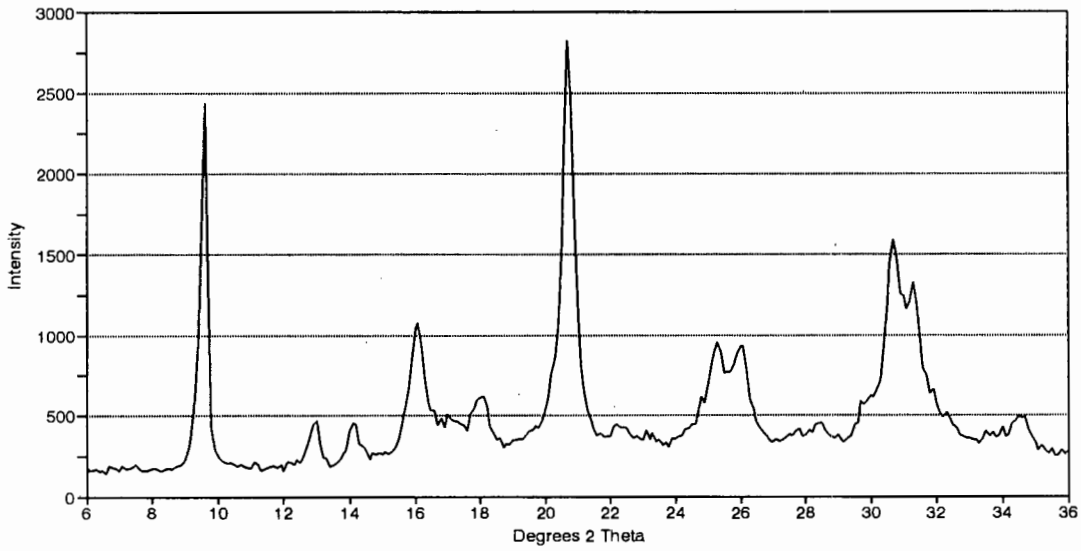

Figure 2.8 : XRD Pattern for SAPO34

2.8. The d-spacings were compared with values given by Szostak (1992) and can also be found in Table A.3, Appendix A.

2.4.4 Amorphous Silica-Alumina

This catalyst was manufactured by Kali-Chemie and had a Si/Al ratio of 9. The catalyst consisted of hard, approximately 3mm beads which were first crushed then ground to a powder of particle size of 30 to 300 micron using a mortar and pestle.

2.5 Data Analysis

Care was taken during this study to ensure good mass balances (> 95%) as these are an important pre-requisite to kinetic studies. Mass balances were performed using an internal standard. This is a non-reactive compound fed into the product line after the reactor and before the G.C. (see Figure 2.1). As the flowrate of this component is known and unchanging it can be used to calculate the flowrate of all components in the product stream. Initially, dimethyl-ether was used as an internal standard because it was not produced during propene oligomerisation. However, the G.C. response factor of this component was significantly different from the rest of the components in the product stream. For runs operating at low conversion methane was used instead as none of this component was produced and its response factor was closer to that of the other components. The internal standard method gave mass balances to within 5%.

At low conversions, the mass% of the components in the product stream were low. In order to obtain accurate product distributions, the sample volume injected into the G.C. had to be increased. However, this resulted in a signal for the propene feed that was too large and mass balances could not be calculated for each sample. As a compromise, one sample was taken for each run with a lower volume injected in order to calculate mass balances while for the other larger volume samples the internal standard was used to calculate conversion.

For high conversion runs large amounts of liquid product were produced. Under these conditions the internal standard could not be used as it did not mix properly with the product. Instead, the total amount of gas and liquid leaving the system was monitored over hourly periods. Deactivation was minimal during the high conversion runs. Mass balances carried out this way also tied to within 5%.

A sample calculation of the mass balance, conversion and selectivity can be found in Appendix A for both high and low conversion runs.

2.6 Reproducibility of Experimental Data

The following definitions are pertinent to the following discussion :
The mean is defined as follows,

$$x^* = \frac{\sum_{i=1}^{n} x_i}{n} \tag{2.1}$$

while the standard deviation is given by,

$$s = \sqrt{\frac{\sum_{i=1}^{n} (x_i - x^*)^2}{n - 1}} \tag{2.2}$$

and coefficient of variation, which represents the variation in several sets of data

$$V = \frac{s}{x^*} \cdot 100 \tag{2.3}$$

The reproducibility of the analysis technique was determined by injecting three successive samples of the same reaction product into the G.C. and calculating the variation in the

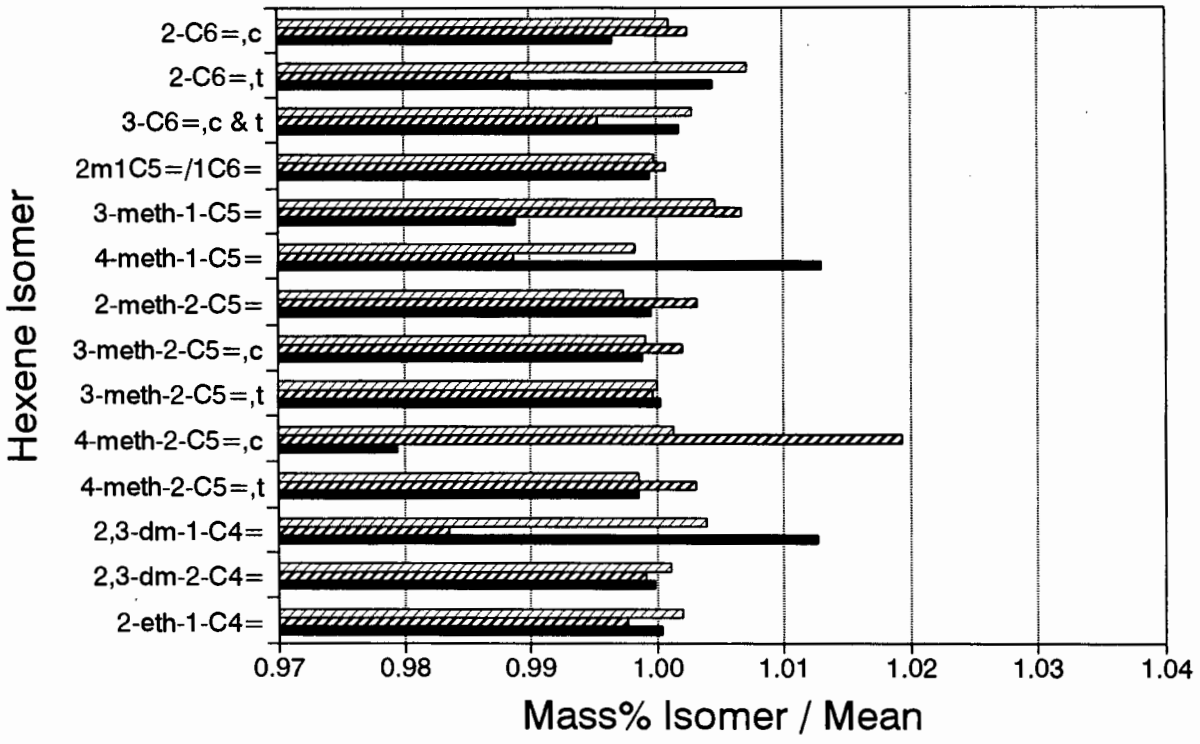

Figure 2.9 : Reproducibility of Analysis Technique

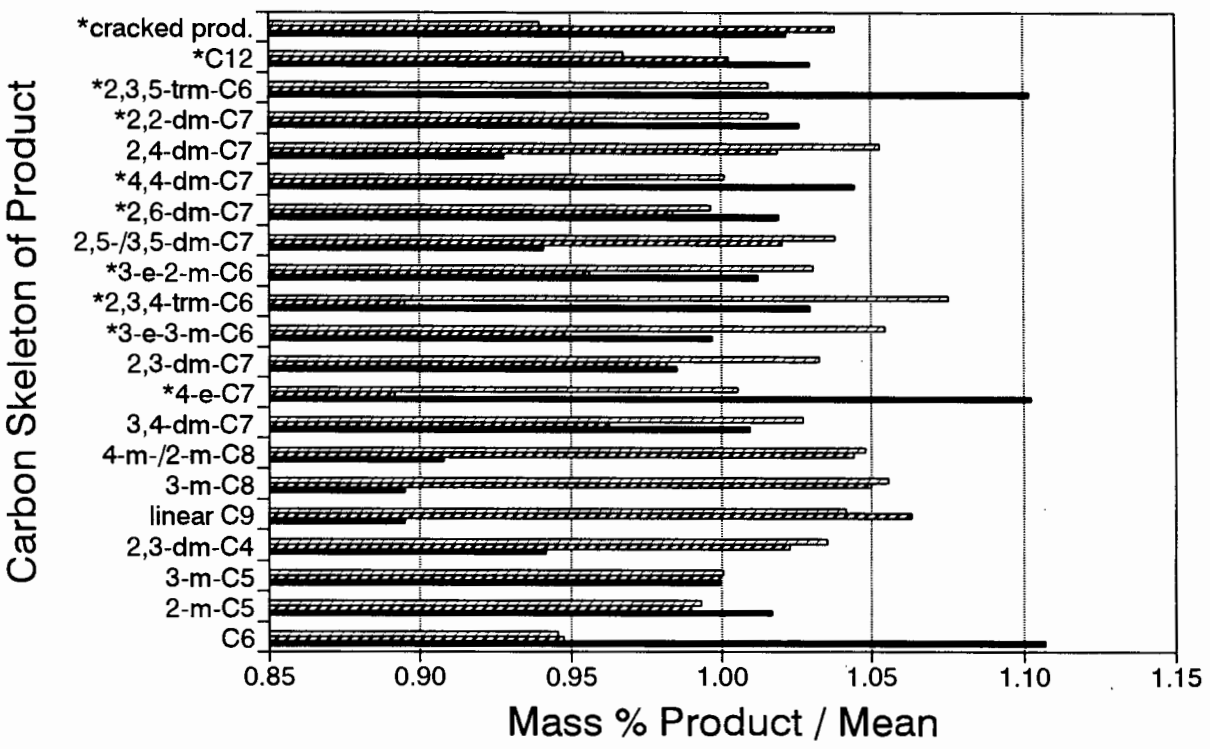

Figure 2.10 : Reproducibility of Experimental Runs

product composition. The results are shown in Figure 2.9. In this figure the ratio of the mass% of the compound to its mean value for the three samples is plotted. (An expanded scale was used in order to highlight the differences.) The average coefficient of variation for the hexene isomers was 0.61%. This indicates that the analysis techniques were reproducible.

The reproducibility of the experimental runs was determined by examining the product distribution from three propene oligomerisation runs performed on separate occasions and conducted at 250°C, 5MPa and 7% conversion. Figure 2.10 plots the ratio of the mass% of the compound to its mean value for the three runs. Those compounds only present in small amounts in the product and thus subject to the greatest variability are marked with a star. The product shown has undergone pre-column hydrogenation before analysis.

The average coefficient of variation was 5.7%. The worst coefficient of variation was approximately 10% for compounds such as 4-ethyl-heptane and 2,3,5-trimethyl-hexane, while the best was approximately 2% for compounds such as 2-methyl-pentane and 2,3-dimethyl-heptane. Thus, it was concluded that the reproducibility of the experimental runs was acceptable.

The data used to assess the reproducibility of the experimental data can be found in Tables A.4 and A.5 in Appendix A.

CHAPTER 3 - PROCESS CONDITIONS

3.1 Introduction

The first section of this chapter presents results of external mass transfer studies. These were conducted prior to any experimental work in order to determine whether gas film diffusion was rate limiting.

Tabak et al. (1986) discuss the effect of temperature and pressure on olefin oligomerisation over H-ZSM-5. The reaction window for H-ZSM-5 is large and Tabak et al. (1986) indicate that oligomerisation at temperatures as low as 37°C and pressures as low as 7kPa and as high as 14 MPa have been observed. However, they note that at temperatures above 327°C equilibrium constraints became significant. Garwood (1983) gives the range of temperatures and pressures that favour high molecular weight products, and thus are of commercial interest, as 200 to 260°C and 2 to 10MPa. Contact times should be high i.e., WHSV of 0.5 to $1hr^{-1}$.

Reactions conditions of 250°C and 5MPa were chosen for this study as these fall within the range of reaction conditions that favour olefin oligomerisation. It was also decided to operate under conditions of low conversion namely, 5%. The reasons for this were mentioned in Chapter 1 and are covered in detail in Chapter 4.

Previous studies on oligomerisation for example, Garwood (1983) and Tabak et al. (1986), have already shown that the effect of increasing pressure is to increase the amount of heavy products, as would be expected thermodynamically. For this reason, the effect of pressure was not investigated during this study. Pressures higher than 5MPa were also not practical with the existing experimental apparatus.

The effect of temperature on the reaction is important in kinetic studies as the rate constants are dependent on temperature via the Arrhenius equation. Thus the reaction temperature was varied from 200 to 280°C and the variations in product selectivity and rate of formation are

presented and discussed in Section 3.3.

The last section in this chapter, Section 3.4, discusses changes in product shape selectivity observed when catalyst type is varied. In this section literature covering shape selective effects in porous catalysts is presented first. Following this, experimental results are presented and discussed.

3.2 External Mass Transfer

A molecule undergoes the following steps during reaction over a solid acid catalyst :

a) transfer from the bulk gas to the external surface of the catalyst particle,
b) diffusion along the catalyst pore to the active site,
c) adsorption on the active site,
d) reaction on the active site to produce the product molecule or molecules,
e) desorption of the product molecule from the active site,
f) diffusion of the product molecule along the catalyst pore to the external surface and
g) transfer from the external surface to the bulk gas.

Any of these steps, not necessarily chemical reaction, may be rate limiting. Figure 3.1 shows how for a non-porous catalyst the surface concentration differs from that of the bulk depending whether transfer to the surface or reaction controls.

For a gaseous reaction on a solid catalyst the following expressions can be written for the rate of reaction at steady state conditions for the following simple reaction (Smith (1981)): (It should be noted that for the purposes of the derivation below internal mass transport resistances are ignored.)

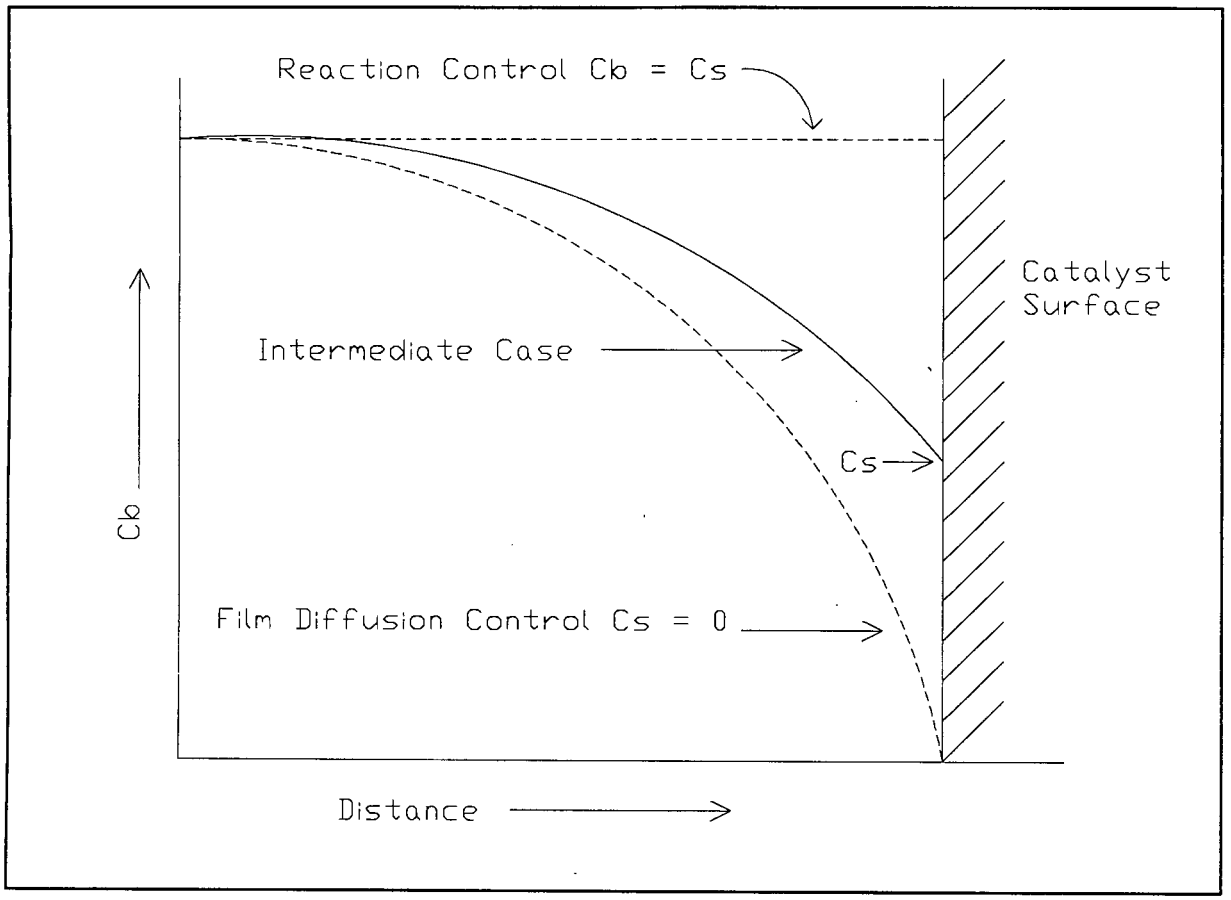

Figure 3.1 : Effect of Different Controlling Mechanisms (after Smith (1981))

$A \rightarrow B$

$$r = k_m a_m (C_b - C_s) \qquad (3.1)$$

$$r = kC_s^n \qquad (3.2)$$

where C_b - concentration in the bulk gas

C_s - the concentration at the surface

k_m - the mass transfer coefficient between bulk gas and surface

a_m - external surface area of catalyst

Combining the above two equations, the following expression for r is obtained :

$$r = \frac{1}{\frac{1}{k} + \frac{1}{k_m a_m}} C_b \qquad (3.3)$$

This equation shows how the overall rate is influenced by two resistances namely, rate of chemical reaction and rate of mass transfer to the surface.

Before conducting kinetic studies it was important to evaluate the extent of external mass transfer resistances on the reaction. A series of experimental runs were carried out at identical WHSV's but at different superficial gas velocities for propene oligomerisation at 5MPa, 250°C. (This was accomplished by varying the catalyst mass and flowrate simultaneously.) If the conversion and the selectivity to the reaction products remained unchanged over a wide set of experimental conditions, it could be assumed that external mass transfer was not limiting. As reaction temperature and pressure did not change, internal mass transfer effects were assumed to be constant during these runs. The external mass transfer coefficients were calculated using one of the few correlations for low particle Reynolds numbers (Wakao and Tanisho (1974)) :

$$Sh = 0.35 Re^2 \; for \; Re = 0.05 \sim 1 \qquad (3.4)$$

The results are shown in Table 3.1. The viscosity of propene at the reaction conditions was calculated using the Lucas method recommended by Reid et al. (1987). The self diffusivity was calculated using a correlation from Lee and Thodos (1983). This correlation is quoted by the authors as having a deviation of 0.51% (for 519 data points) for dilute and dense gaseous states. (Detailed calculations can be found in Appendix B)

Table 3.1 : Estimation of External Mass Transfer Resistances							
Diffusivity of Propene, 5 MPa, 250°C : 0.00377 cm^2/s Viscosity of Propene, 5 MPa, 250°C : 1.68e-5 Pa.s							
WHSV hr^{-1}	Conv. %	Cat Mass g	Vap. Vel. cm/s	Re_p	Sh_p	k_m m/s	$(C_b - C_s)/C_b$
325	5.2	0.05	3.68e-2	0.303	0.0321	4.727e-5	0.1022
340	4.9	0.093	7.16e-2	0.589	0.122	1.790e-4	0.0266
320	6.2	0.28	2.03e-1	1.670	0.976	1.437e-3	0.00397
311	5.2	0.28	1.97e-1	1.623	0.922	1.358e-3	0.00341

For all oligomerisation runs quartz sand particles were used to dilute the catalyst bed and maintain isothermal operation using the method described in Chapter 2. For the purposes of the mass transfer calculations, the catalyst bed was considered as a bed of quartz particles surrounded by a thin layer of small catalyst particles all between 1 and 3 micron in size. Therefore, the particle size used in calculating the particle Reynolds number was the average particle size of the inert quartz sand particles, namely 256 micron.

The last column in Table 3.1 shows that external mass transfer resistances are not significant and can be neglected as the difference between C_b and C_s is less than or equal 10%. This is further supported by the experimental data shown in Figures 3.2 to 3.5. For each experimental run several samples were taken.

Figure 3.2 plots conversion versus run-time, after reaching reaction temperature, for various superficial feed gas velocities. During each experimental run the catalyst underwent deactivation. However, this set of data shows there is no significant change in the conversion versus time profile over the range of gas velocities studied. Figure 3.3 presents the mass selectivity to oligomers as a function of propene conversion for the range of gas velocities covered. This figure again shows there is virtually no effect of gas velocity on selectivity, over the range studied. (As only small amounts of trimer were formed the hexene and nonene

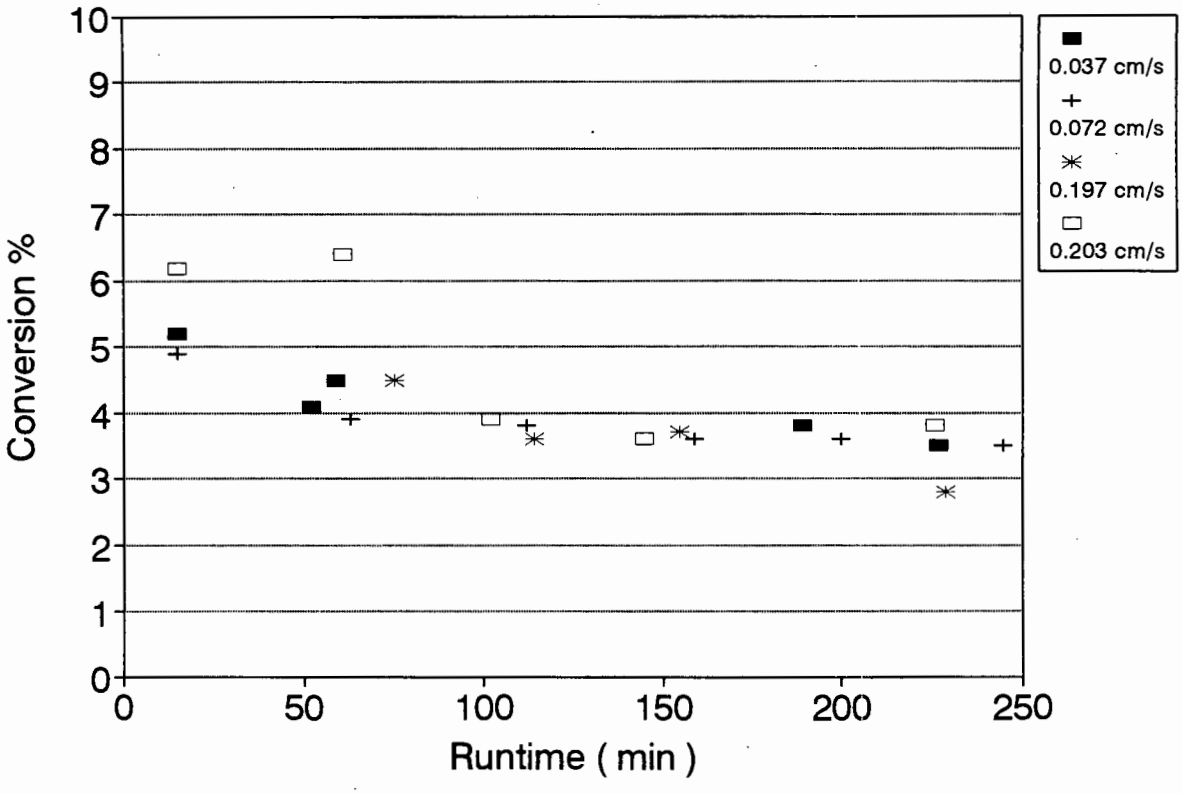

Figure 3.2 : Influence of Superficial Gas Velocity on Propene Conversion

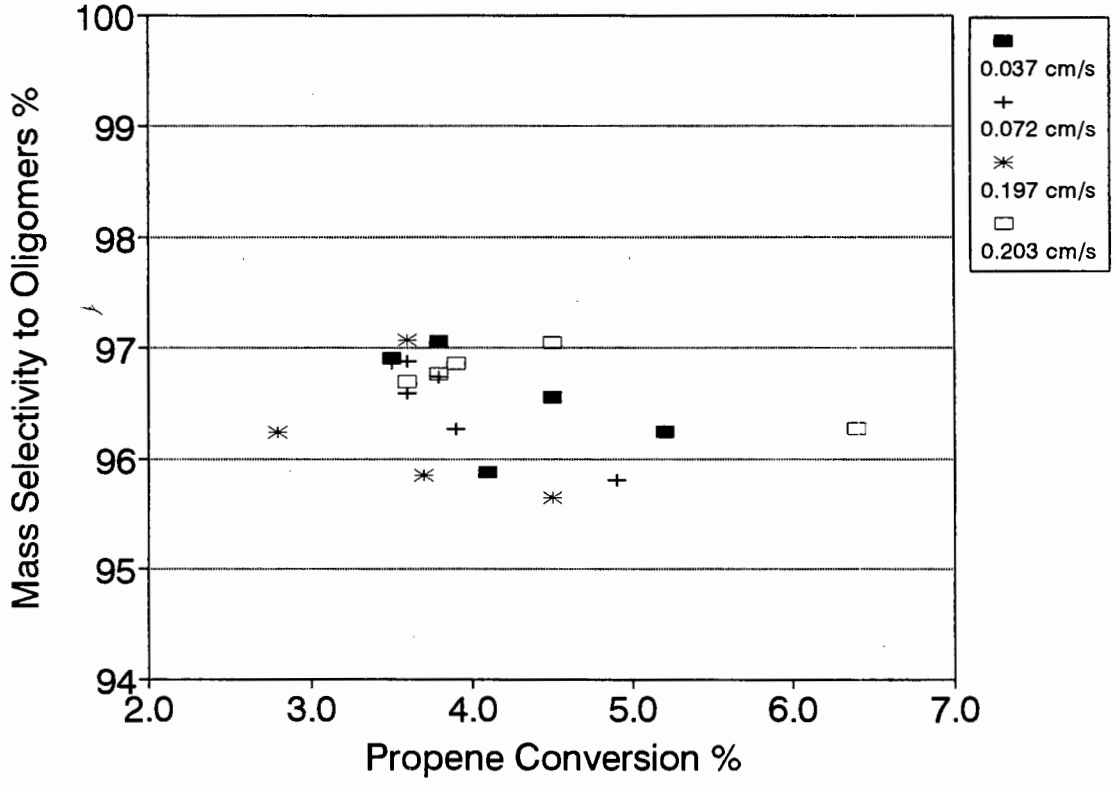

Figure 3.3 : Influence of Superficial Gas Velocity on Selectivity to Oligomers

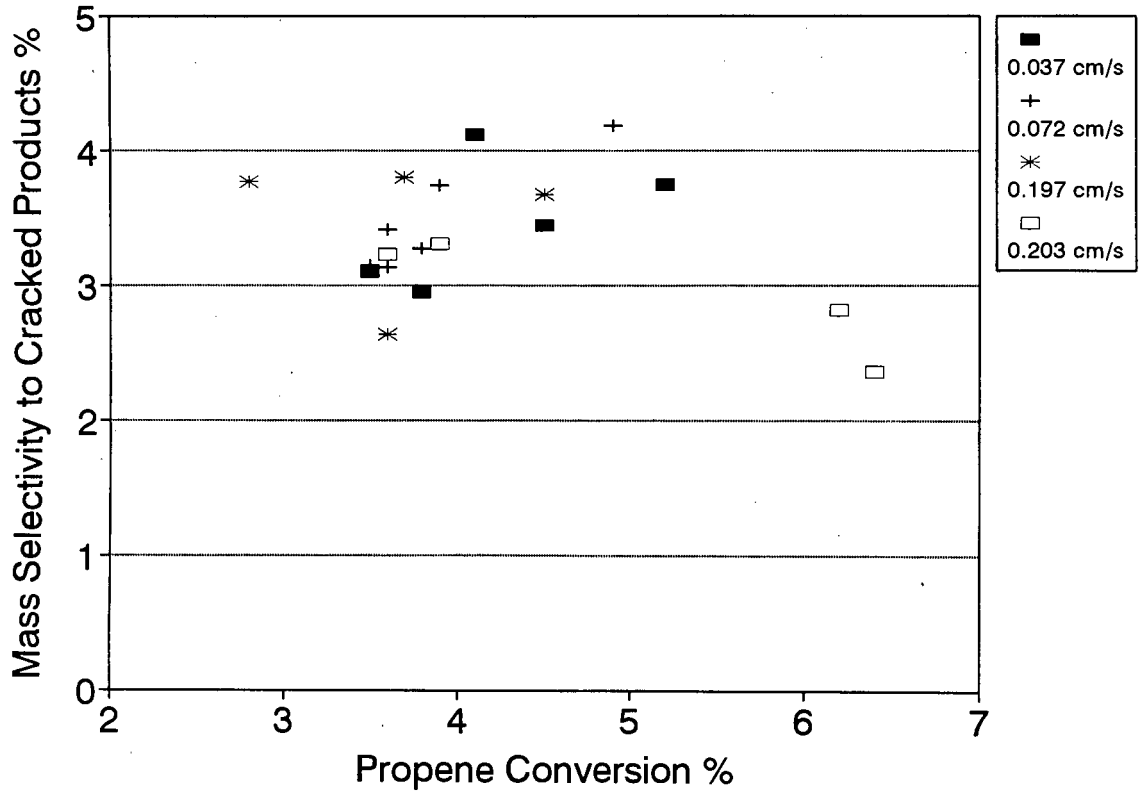

Figure 3.4 : Influence of Superficial Gas Velocity on Selectivity to Cracked Products

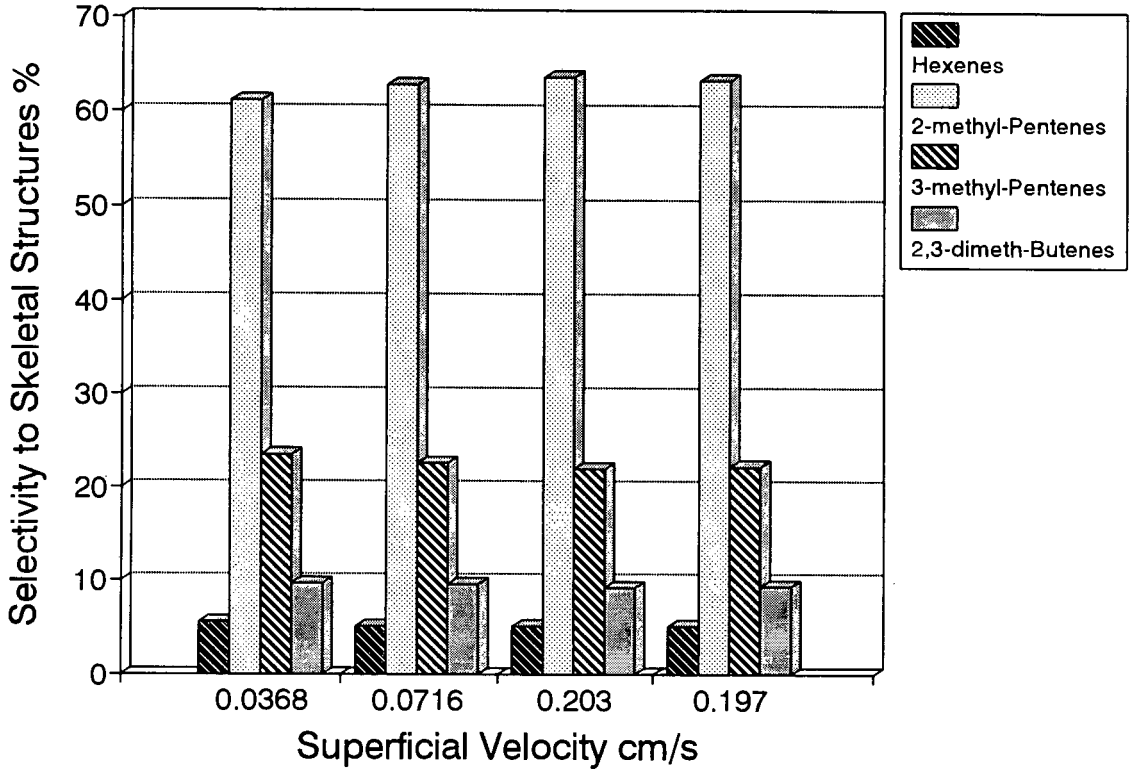

Figure 3.5 : Influence of Superficial Gas Velocity on Selectivity to C6 Skeletons at 5% Conversion

isomers were grouped into one oligomer group.) Figure 3.4 shows the mass selectivity to cracked products as a function of propene conversion. Although this figure does not provide any additional information to Figure 3.3, it was included for completeness.

Figure 3.5 groups the hexene isomers according to their carbon skeleton and compares the selectivities at the different gas velocities at 5% conversion. This figure clearly shows essentially no change in selectivity within the hexene isomer group.

For the above experimental runs the external mass transfer coefficient was varied by approximately 30 times. As no change was observed experimentally and because according to calculations no change was expected, it was concluded that under the experimental conditions used for this study the effect of external mass transfer could be neglected.

The experimental data used to evaluate external mass transfer effects is shown in Tables B.1 to B.4 in Appendix B.

3.3 Effect of Reaction Temperature

Kärger and Ruthven (1992) discuss the temperature dependence of the overall effective rate constant for zeolite catalysts. At low temperatures the reaction is kinetically controlled and the intrinsic rate constant obeys the Arrhenius law :

$$k_i\eta \approx k_i = k_o e^{-E_r/RT} \qquad (3.5)$$

where k_i is the intrinsic rate constant. Under conditions of reaction control the effectiveness factor, η, is close to 1.

As the temperature increases, the rate constant increases faster than the effective diffusivity and a transition to the diffusion controlled regime occurs. The effective rate constant is now defined as follows :

$$k_{eff} \approx (3/R_p)\sqrt{k_i D_e} = (3/R_p)\sqrt{k_o D_e} e^{-E_d/2RT} \quad (3.6)$$

Thus if the temperature dependence of D_e is small (e.g. Knudsen) then the apparent activation energy will be approximately half the true value.

At still higher temperatures external film diffusion becomes controlling and the effective rate constant approaches the following value :

$$k_{eff} \rightarrow 3k_m/R_p \quad (3.7)$$

These different controlling regimes are represented in Figure 3.6.

The above behaviour is typical of macroporous catalysts and cannot be directly applied to zeolites for the following reasons :

1) Intracrystalline diffusion is a function of temperature according to the Arrhenius law and its activation energy may be comparable to that for the chemical reaction.

2) Reaction occurs in the adsorbed phase and as a result the apparent reaction order will be different from the true order outside the Henry's Law region.

If Langmuir equilibrium is assumed and with the further approximation of Henry's Law the rate constant for a simple, first order reaction is :

$$k_i \approx k_i' K \quad (3.8)$$

where K is the Henry's Law constant. The temperature dependence of Henry's Law constant is given by :

$$K = K_o e^{-\Delta U_o/RT} \quad (3.9)$$

Finally the rate constant can be represented by the following equation :

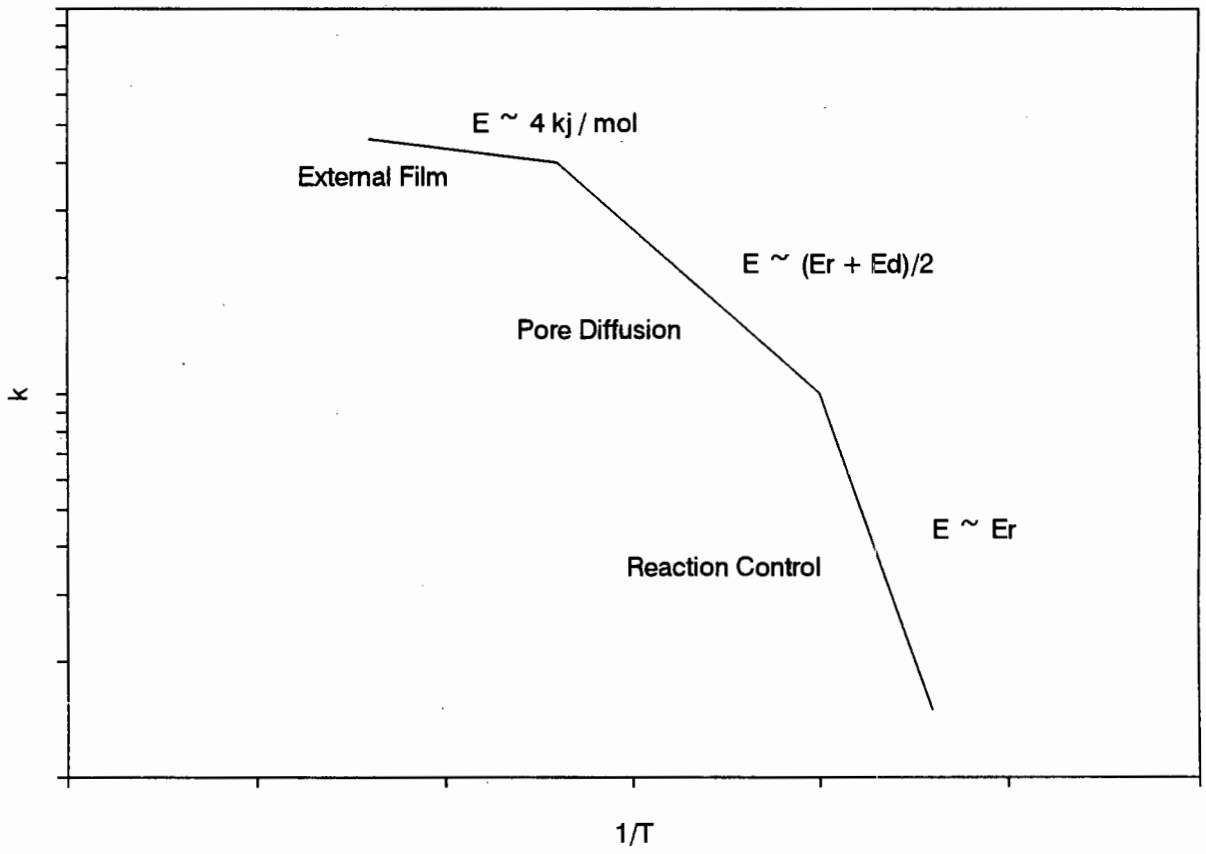

Figure 3.6 : Arrhenius Plot Showing Different Controlling Regimes for Porous Catalysts

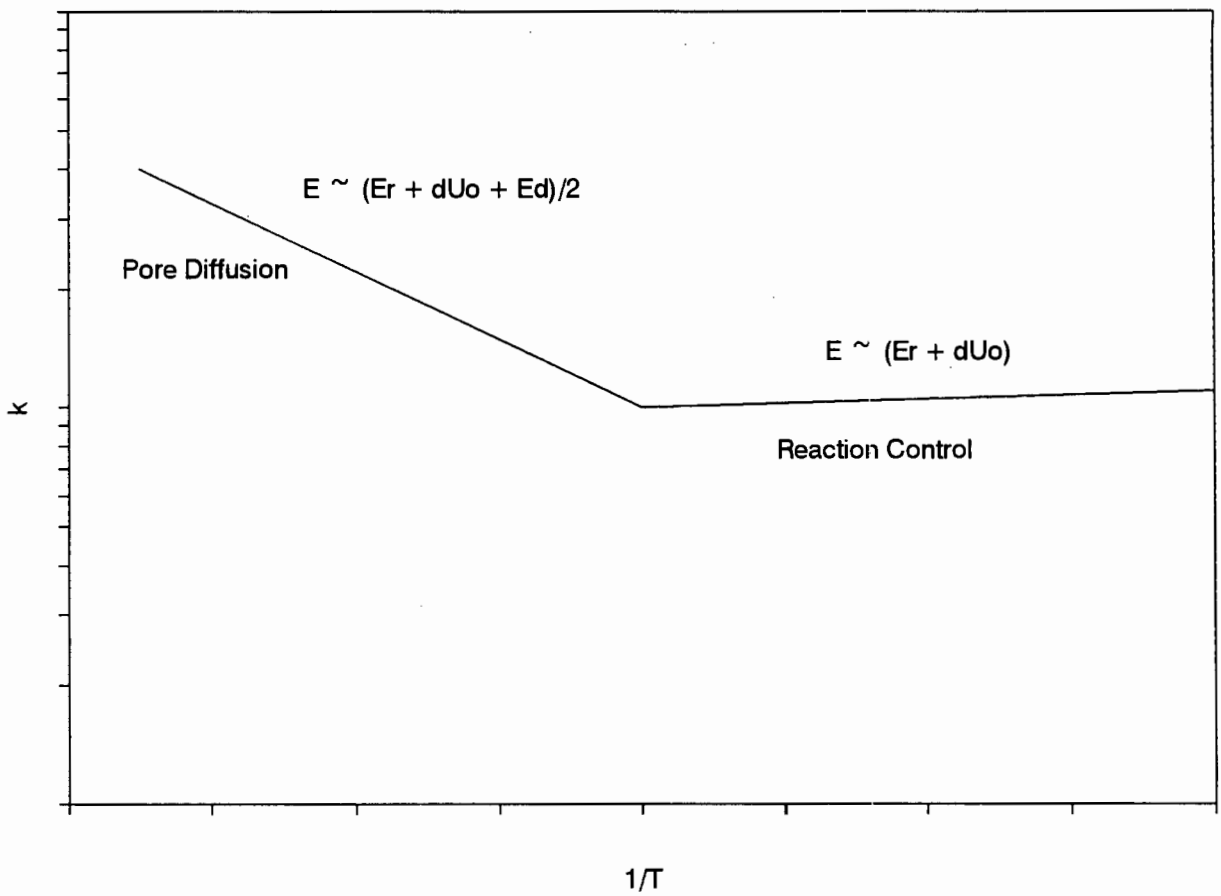

Figure 3.7 : Arrhenius Plot Showing Influence of Strong Adsorption and Diffusion

$$k_i = k_o' K_o e^{-(\Delta U_o + E_r)/RT} \qquad (3.10)$$

This means that the apparent activation energy is now ($E_r + \Delta U_o$). Adsorption is an exothermic process and therefore its activation energy is negative. If the absolute value of activation energy for the reaction, E_r, is smaller than that for adsorption, ΔU_o, the apparent activation energy will be negative. This implies a decrease in reaction rate with increasing temperature. An example of this is provided by Wei (1994). Wei shows how the apparent activation for the cracking of n-paraffins over H-ZSM-5 decreases steadily with increasing carbon number. At n = 16 the apparent activation energy is zero and at n = 20 it becomes -84 kJ/mol.

If diffusion is included, then the activation energy in the kinetic regime, ($E_r + \Delta U_o$), becomes ($E_r + \Delta U_o + E_d$)/2 in the pore diffusion controlled regime. The influence of strong adsorption and diffusion on the Arrhenius plot is shown in Figure 3.7. Therefore, in the light of this discussion, a well-defined transition to an apparent activation energy of about half the true value is unlikely to be observed in a zeolite system.

Propene was oligomerised over H-ZSM-5 at 5MPa, approximately 5% conversion and the temperature varied from 200 to 280°C. Pre-column hydrogenation was used in the G.C. analysis. This procedure hydrogenated the double bonds of the olefins but retained the skeletal structure. The products were thus separated into their skeletal groups. This also ensured that the nonene isomers could be analysed in detail since without hydrogenation the peaks could not be separated and identified accurately. In the graphs that follow the olefins are classified by their alkane skeleton that results from hydrogenation. For example, 2-methyl-1-pentene, 2-methyl-2-pentene and 4-methyl-2-pentene, cis and trans are represented by the 2-methyl-pentane skeleton.

All the experimental runs discussed in sections 3.3 and 3.4 were conducted at the same conversion. This is essential because oligomerisation is a series reaction and comparisons between varying operating conditions should be at the same conversion.

The relative amounts of the skeletal structures within the hexene fraction is shown in Figure 3.8. The conversion for each run is listed next to the reaction temperature in the graph legend. As the temperature decreases there is a steady decrease in the amount of the 3-methyl-pentane structure and a steady increase in the amount of the 2-methyl-pentane structure. At 200°C there is a sharp change in the relative concentrations of both the hexane and 2,3-dimethyl-butane structure. The hexane structure decreases while the 2,3-dimethyl-butane structure increases.

The results are similar for the nonene isomers (Figure 3.9). As the temperature decreases, there is a definite decrease in the amount of linear structures namely, nonane, 3-methyl-octane and 4-methyl-octane/2-methyl-octane. Those dimethyl-heptane skeletons in which the methyl groups are separated via a carbon atom also decrease with decreasing temperature namely, 2,5-dimethyl-heptane, 2,6-dimethyl-heptane and 2,4-dimethyl-heptane. On the other hand, the amount of dimethyl-heptane structures that have adjacent or opposite methyl groups increase with decreasing temperature namely, 3,4-dimethyl-heptane, 2,3-dimethyl-heptane, 4,4-dimethyl-heptane and 2,2-dimethyl-heptane. The highly branched isomers also clearly increase with decreasing temperatures 2,3,4-trimethyl-hexane, 3-ethyl-2-methyl-hexane and 2,3,5-trimethyl-hexane. In view of this noticeable shift in selectivity from linear to branched products it is therefore possible that there is a change in the controlling mechanism of the reaction from diffusion to reaction control as the temperature decreases from 280 to 200°C.

In order to test this theory, Arrhenius plots were generated for all products over the temperature range studied, using differential reaction rates. According to conventional theory, if the reaction becomes increasingly diffusion controlled with increasing temperature, so the slope of the Arrhenius plot should decrease with increasing temperature. The Arrhenius plots are shown in Figures 3.10 to 3.12. Figure 3.10 plots Arrhenius curves for propene and the hexene skeletal structures. "Rate of removal" on the ordinate refers to propene while "rate of production" refers to the hexene skeletal structures. Figures 3.11 and 3.12 present results relevant to the major nonene skeletal structures.

What is most noticeable from these Arrhenius plots is that there is an obvious change in slope

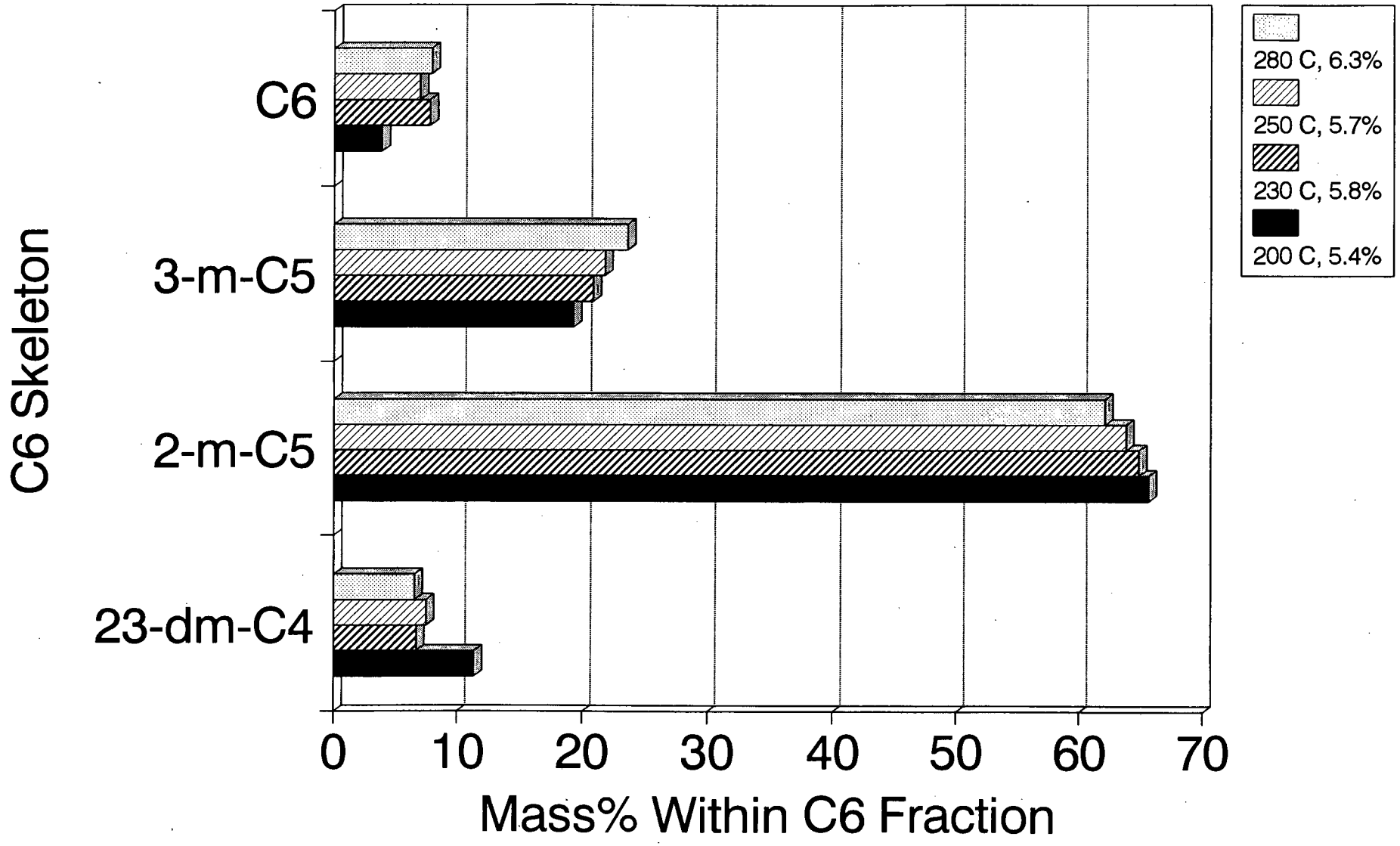

Figure 3.8 : Hexene Selectivity for Different Temperatures (Conversion Shown for Each Temperature)

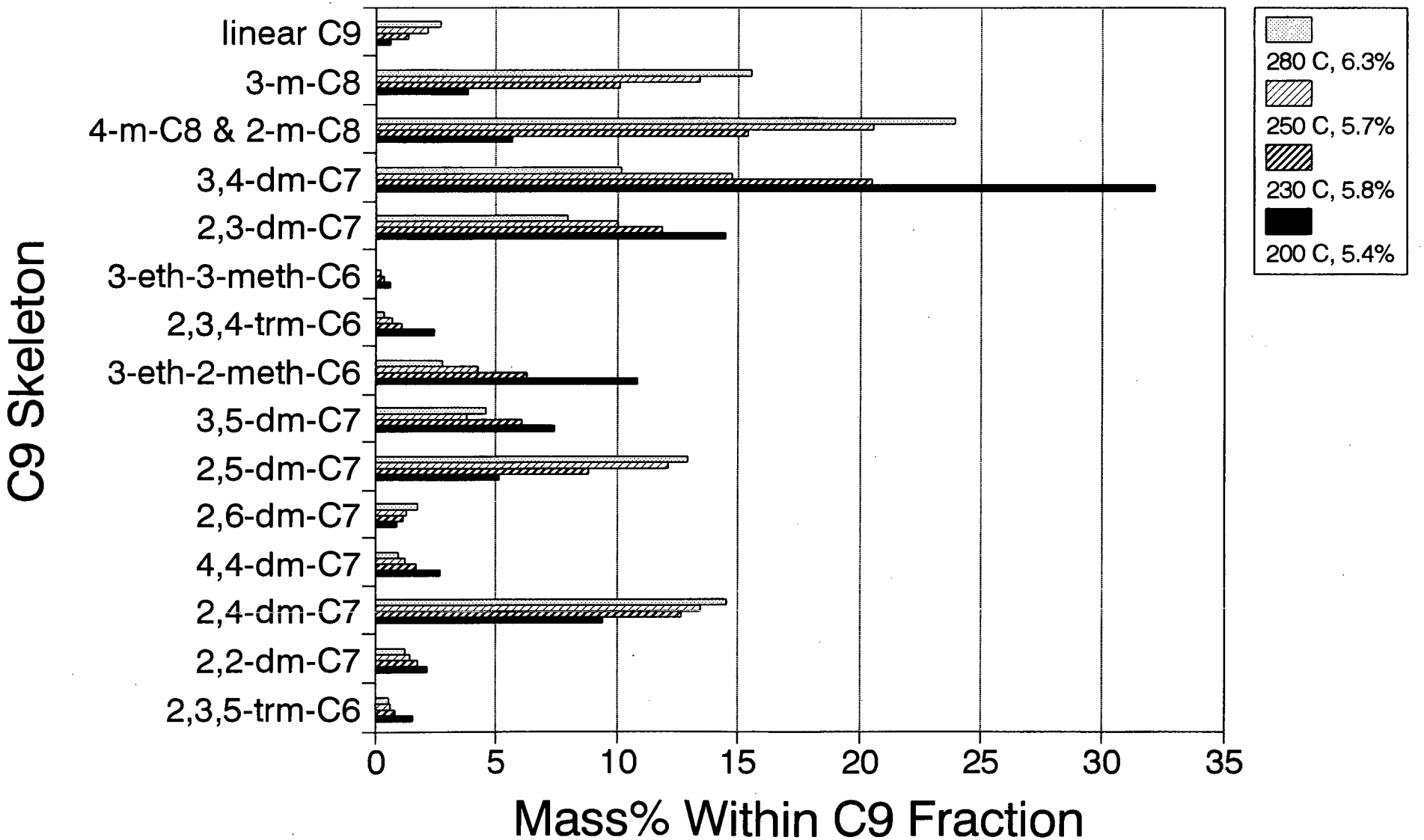

Figure 3.9 : Nonene Selectivity for Different Temperatures (Conversion Shown for Each Temperature)

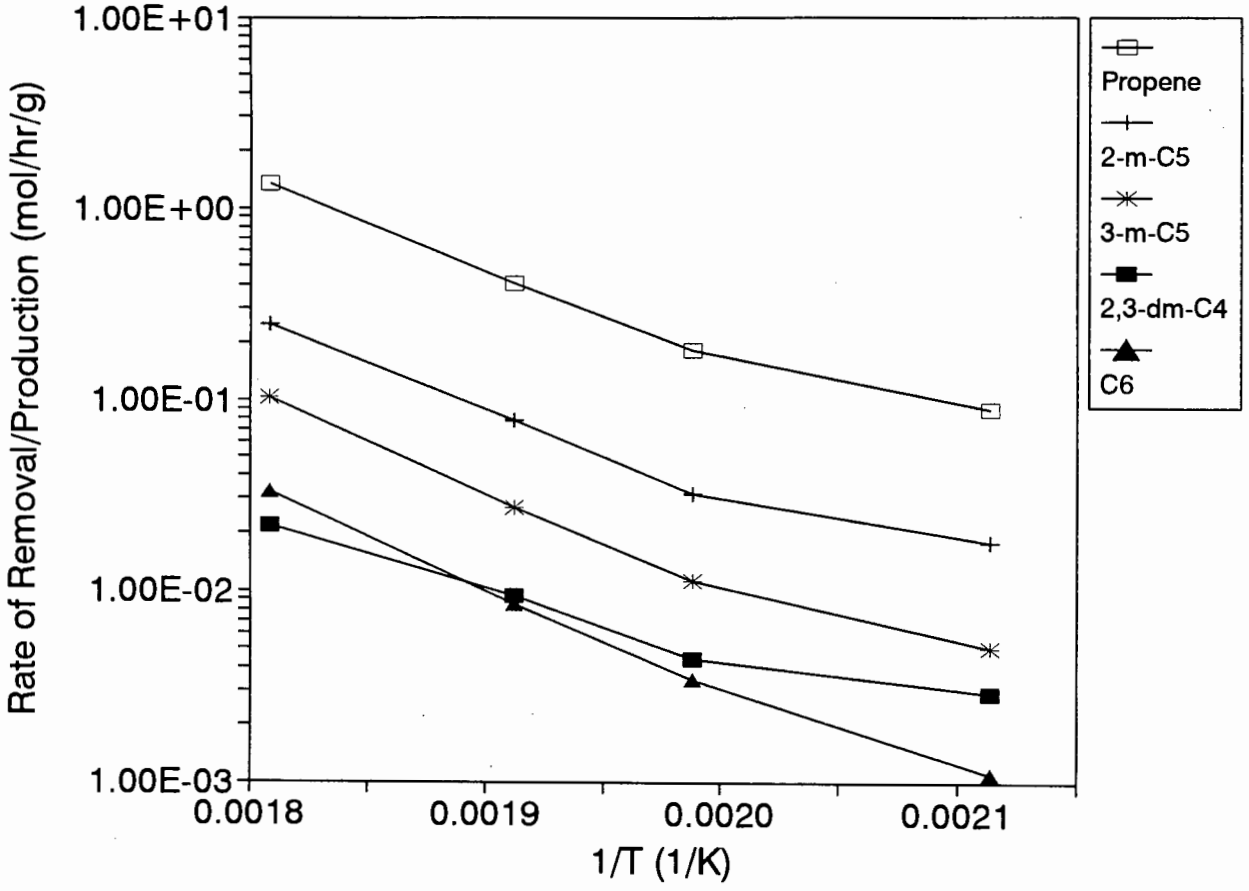

Figure 3.10 : Arrhenius Plots for Propene and Hexene Skeletal Structures

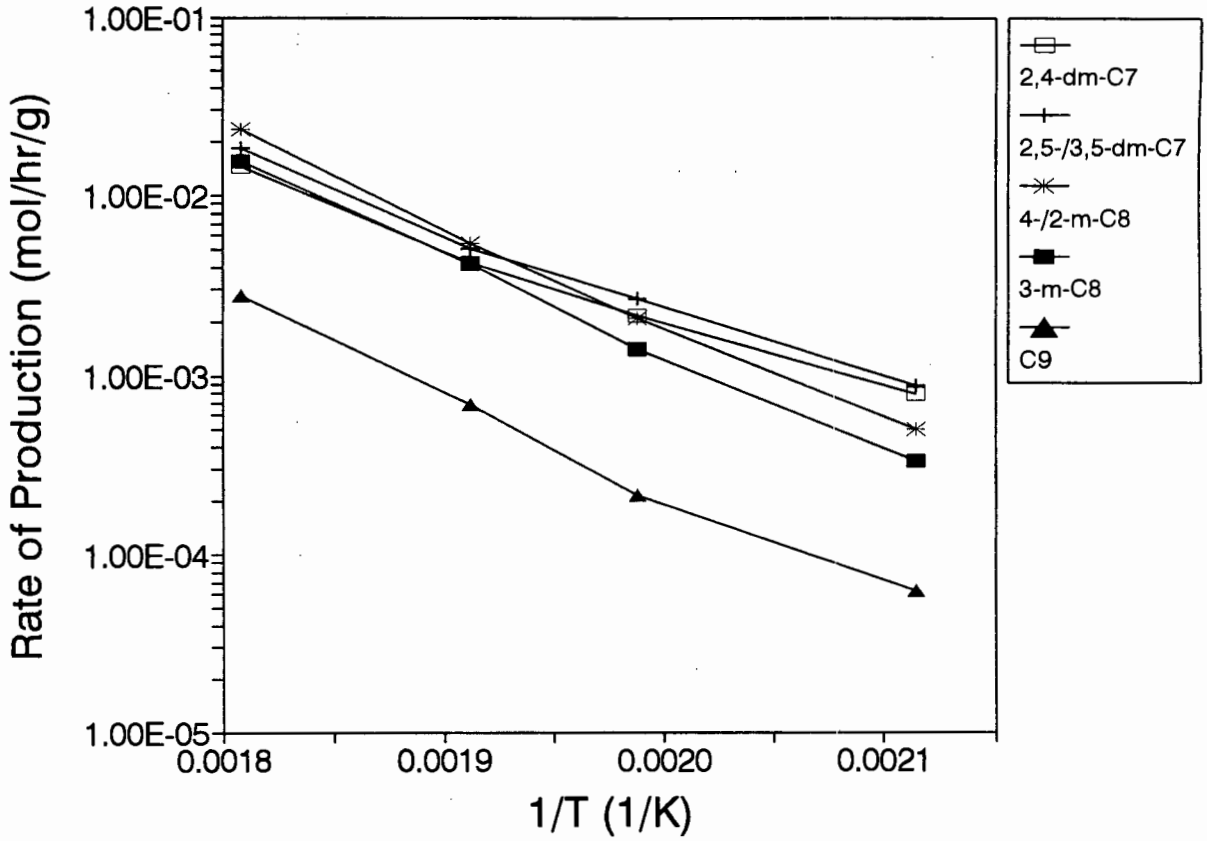

Figure 3.11 : Arrhenius Plots for Nonene Skeletal Structures

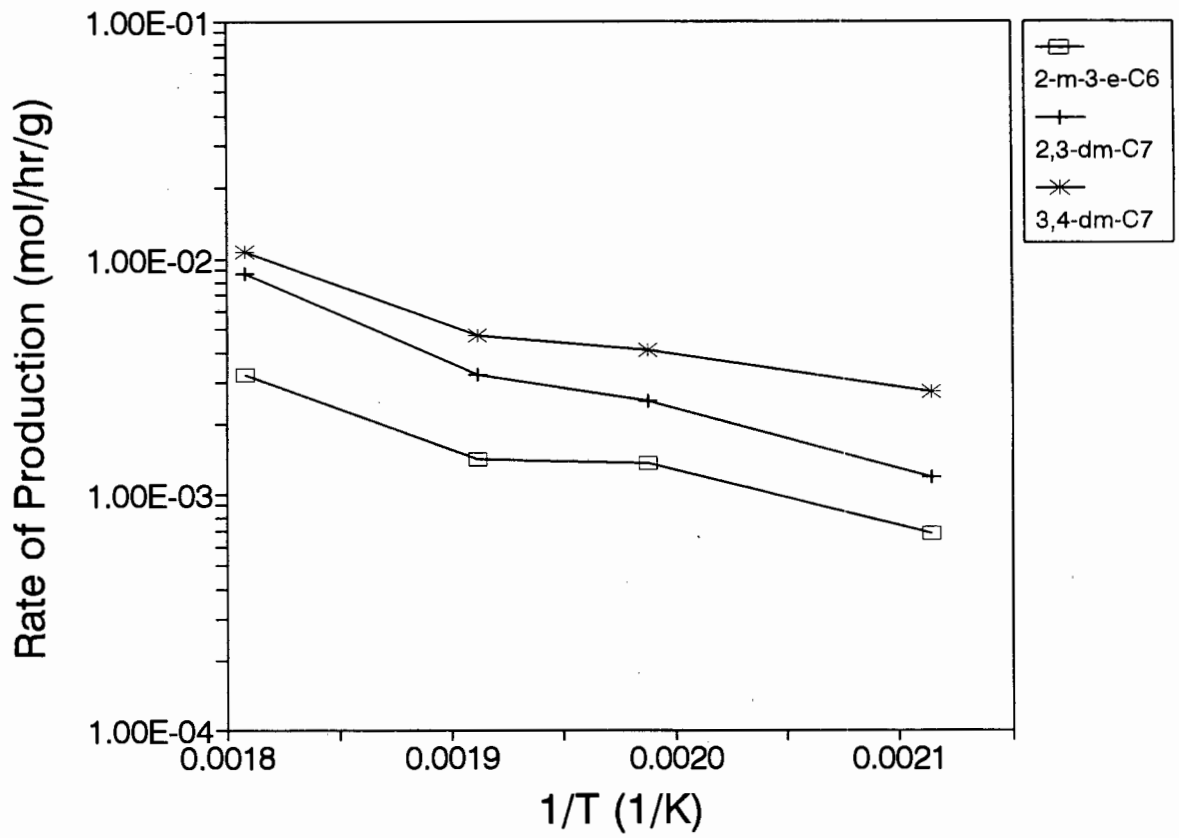

Figure 3.12 : Arrhenius Plots for Nonene Skeletal Structures

over the temperature range studied, even though a clear shift in product selectivity was observed experimentally. The reason for the lack of obvious trend could be the following. Firstly, the temperature range was limited to 200 - 280°C. It is possible that a wider temperature range, or more data points within the existing range, is required in order to observe any change in slope.

Secondly, the reaction could be operating exclusively in one controlling regime, for example, pore diffusion controlling. However, as will be discussed in Section 3.4, when the catalyst was altered from porous (diffusion controlled) to amorphous (reaction controlled), a shift to branched products, similar to that for reduced reaction temperatures, was observed.

Finally, it is possible that the diffusion and adsorption effects are at some intermediate level and are not strong enough to cause a definite change in slope over the temperature range studied.

Therefore, although it is possible that diffusion and/or adsorption were responsible for the change in product selectivity observed with changing reaction temperature, Arrhenius plots of the experimental data could not confirm this.

The experimental data for Figures 3.8 to 3.12 can be found in Appendix B.

3.4 Effect of Catalyst Type

As mentioned previously, four acid catalysts with varying pore sizes and systems were chosen for this study on shape selective effects:

1) SAPO-34 - small pore zeolite with a three dimensional pore system.
- pore size 3.8 x 3.8 Å

2) H-ZSM-5 - medium pore zeolite with a three dimensional pore system.

- pore sizes 5.3 x 5.6Å and 5.1 x 5.5Å

3) H-Beta - large pore zeolite with a three dimensional pore system.
- pore sizes 6.5 x 5.6Å and 7.5 x 5.7Å

4) Silica-Alumina - amorphous acid catalyst.

The structure of these catalysts was discussed in detail in Chapter 1. It should also be noted that the pore dimensions given in the literature are usually based on crystallographic data and are approximate. Often, molecules 1Å larger can quite easily diffuse in and out since the zeolite pore opening itself is not rigid and is subject to vibrations (Haag and Chen (1987)).

Propene was oligomerized at 5 MPa and 250°C using the selection of catalysts listed above. Due to the wide variation in pore sizes of the chosen catalysts a large variation in the shape of the product molecules was expected. Prior to discussing the results of this study, examples from the literature that illustrate the shape selective effects of porous catalysts are presented.

According to Csicsery (1984) there are four types of shape selectivity :

1) Reactant shape selectivity, which occurs when only those reactant molecules small enough to enter the catalyst pores are able to react.
2) Product shape selectivity, which occurs when only those molecules small enough are able to leave the catalyst. The more bulky, branched molecules first have to isomerise to linear, less bulky isomers before they can diffuse out.
3) Transition state selectivity, which occurs when certain transition states are prevented from forming due to steric constraints. Under these circumstances products and reactants can still diffuse freely in and out of the catalyst pores. However, it is not always possible to distinguish between product and transition state selectivity (Venuto (1994)).
4) "Molecular traffic control", which could occur in zeolites with three dimensional pore systems such as H-ZSM-5. Linear molecules can diffuse freely in and out of both the circular, sinusoidal channels and the elliptical, straight channels, while the more branched

molecules are confined to the elliptical, straight channels (Derouane and Gabelica (1980)). Experimental studies were conducted in order to confirm this effect (Derouane et al. (1981)) but unfortunately there is doubt as to whether this phenomenon exists. (Weisz et al. (1981) and Chen et al. (1989)).

The constraint index provides a useful tool for comparing catalysts in terms of their shape selective effects. Frillette et al. (1981) present values for the constraint index for a number of catalysts (See Table 3.2). This parameter approximates the ratio of the cracking rate constant of n-hexane and 3-methyl-pentane.

The Table 3.2 ranks the catalysts according to decreasing shape selectivity. The relevant catalysts are marked in bold. Erionite, while not the same as SAPO-34, is also an example of a small pore zeolite and thus likely to have a similar constraint index.

Chabazite, which is structurally similar to SAPO-34 cannot adsorb molecules with a kinetic diameter greater than 4.3Å (Szostak (1992)).. Venuto (1994) also states that small pore zeolites sorb non-bulky molecules such as n-paraffins or primary alcohols but not branched hydrocarbons. Miale et al. (1966) conducted cracking reactions of n-hexane and 2-methyl-pentane over various catalysts, one of them H-Chabazite. These authors also found that the conversion of the linear hexane was higher than that of the branched isomer for this catalyst.

The kinetic diameter of various molecules is shown in Table 3.3.

Haag et al. (1982) carried out catalytic cracking of C_6 - C_9 hydrocarbons over H-ZSM-5 at 811 K using two crystallite sizes. The authors were able to determine the diffusivities for the hydrocarbons under reaction conditions. Their results are shown in Table 3.4.

The data in Table 3.4 shows that at 811K there is a 10^4 decrease in diffusivities as one proceeds from linear to dimethyl structures. Also, the branching appears to have a greater effect on the diffusivity than the length of the chain. In other words, 2,2-dimethyl-butane has a similar diffusivity to 2,2-dimethyl-heptane. At 811K, the presence of a double bond was

found to have little effect.

Table 3.2 : Constraint Index (Frillette et al. (1981))	
Catalyst	Constraint Index
Erionite (small pore zeolite)	**38**
ZSM-11	8.7
ZSM-5	**8.3**
ZSM-35	4.5
TMA offretite	3.7
ZSM-12	2
ZSM-38	2
Beta	**0.6**
Amorphous Silica-Alumina	**0.6**
ZSM-4	0.5
H-Zeolon (Mordenite)	0.4
REY	0.4

Table 3.3 : Kinetic Diameters of Various Hydrocarbons (Szostak (1992))		
Compound	Structure	Kinetic Diameter,Å
Neopentane	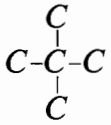	6.2
Isobutane	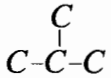	5.0
n-Hexane	*C-C-C-C-C-C*	4.3
n-Butane	*C-C-C-C*	4.3

Table 3.4 : Diffusivities for Hydrocarbons in H-ZSM-5 at 811 K (Haag et al. (1982))		
Carbon Skeleton	Diffusivities - cm^2/s	
	Paraffin	Olefin
C-C-C-C-C-C	-	3e-4
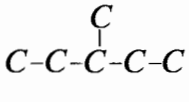	-	4e-5
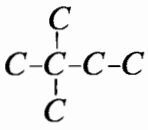	2e-8	7e-8
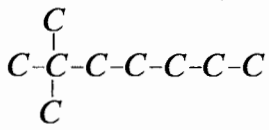	3e-8	-

The catalytic cracking of hexane isomers was also carried out over H-ZSM-5 by Anderson et al. (1979) at 673K. The authors found the following decreasing order of extent of conversion: n-hexane > 3-methyl-pentane > 2,2-dimethyl-butane. They attributed this to the increase in degree of branching and thus reduced accessibility to the zeolite channels. This order was also supported by the decreasing ease of sorption.

Another example of shape selective effects of H-ZSM-5 is presented by Quann and Krambeck (1991). During oligomerisation the degree of branching for the higher carbon numbers found in the reaction product was much less than that for unrestricted propene polymerisation. This could have resulted from restricted transition states and/or product shape selectivity (Venuto (1994)).

Figures 3.13 and 3.14 show the skeletal composition of the two oligomer groupings namely,

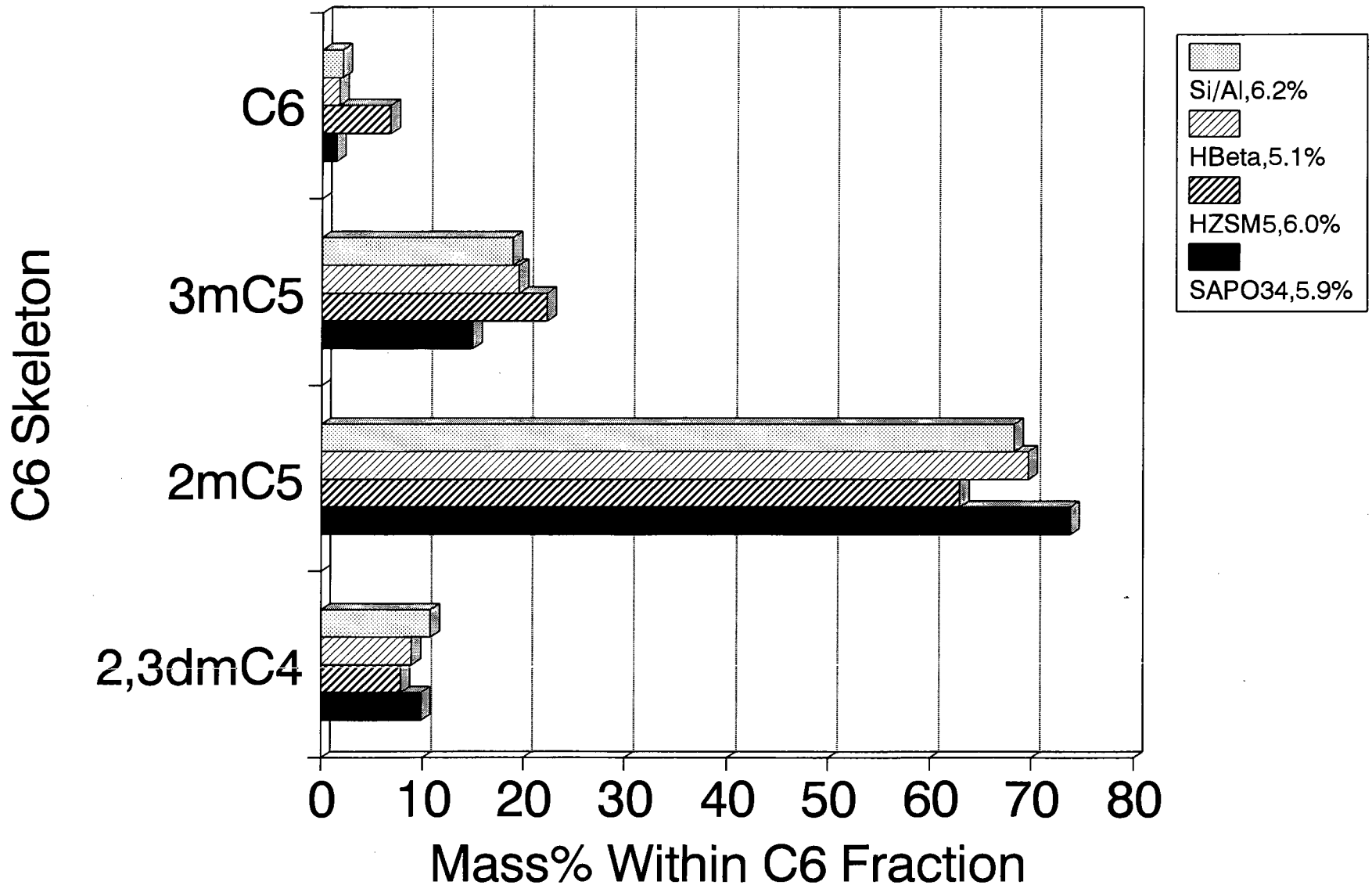

Figure 3.13 : Hexene Selectivity for Different Catalysts (Conversion Shown for Each Catalyst)

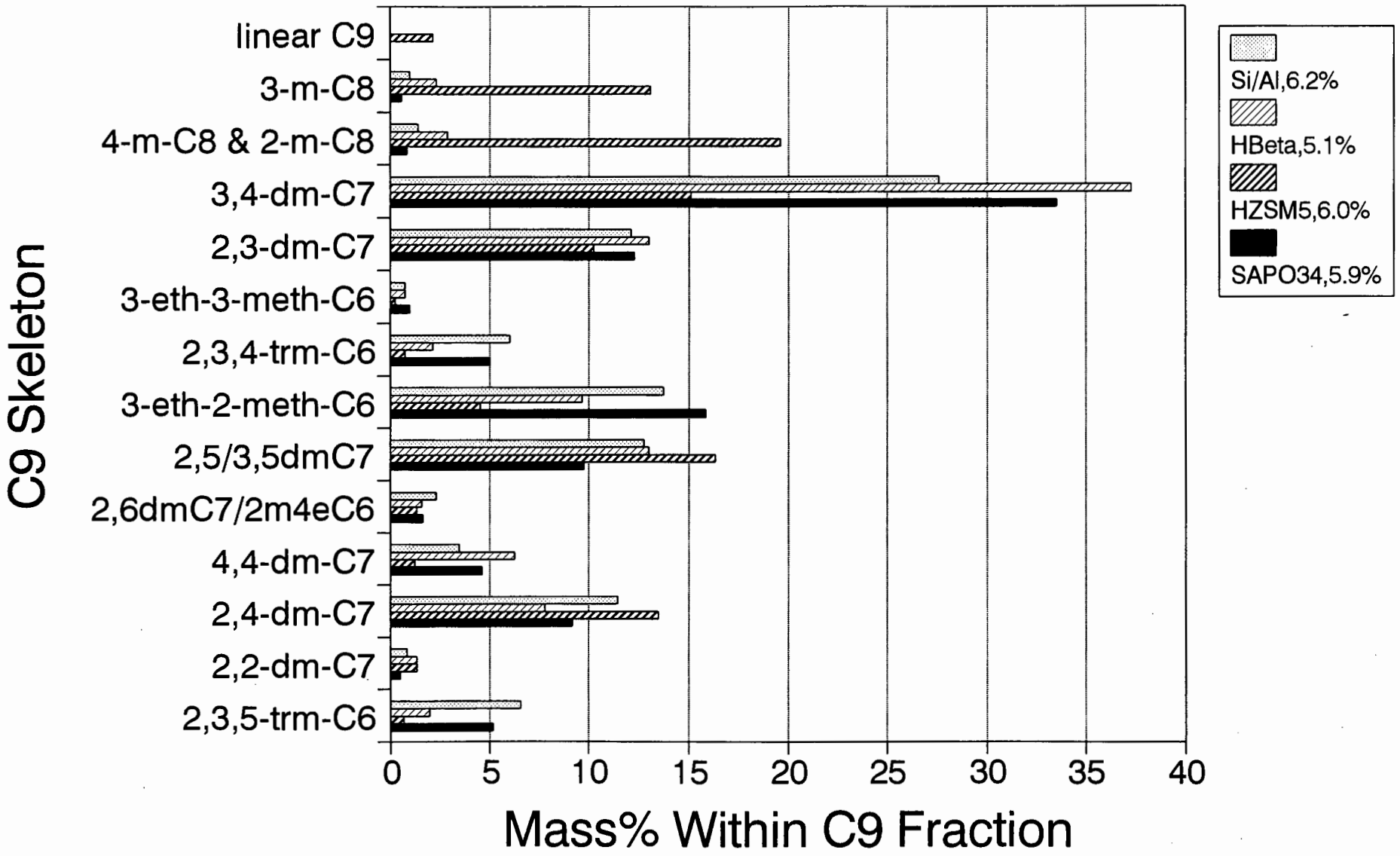

Figure 3.14 : Nonene Selectivity for Different Catalysts (Conversion Shown for Each Catalyst)

hexenes and nonenes, obtained during propene oligomerisation at 250°C and 5MPa for the set of acid catalysts discussed at the beginning of this section. The catalysts listed in the graph legends are ranked in order of decreasing pore size. The actual conversion for each run is given in the legend.

Figure 3.13 shows the relative amounts of the skeletal structures within the C_6 grouping. The most notable product spectrum is that for H-ZSM-5 where there is an increase in the number of linear isomers at the expense of the branched isomers. Surprisingly, the product spectrum for SAPO-34 is similar to the large pore and amorphous catalysts. This could be indicative of reaction occurring mainly on the external surface.

Figure 3.14 shows the relative amounts of the skeletal structures within the nonene fraction. Again, the most notable spectrum is that for H-ZSM-5 where linear structures increase relative to the branched structures. This can be seen especially in the increase in the nonane and methyl-octane structures. Additionally, the skeletons that possess more than two methyl groups are virtually absent from the product spectrum. Among the dimethyl-heptane structures, those that have methyl groups on adjacent carbons, i.e. 2,3-dimethyl-heptane and 3,4-dimethyl-heptane, decrease over H-ZSM-5. On the other hand, those that have methyl groups separated by two or more carbons, i.e. 2,5-dimethyl-heptane, 3,5-dimethyl-heptane and 2,4-dimethyl-heptane, increase over H-ZSM-5. It is possible that those nonenes with methyl groups separated by one carbon atom are able to "twist" and thus diffuse out of the catalyst pores with greater ease than those with adjacent methyl groups. The product spectrum from the SAPO-34 catalyst is again similar to that obtained from H-Beta and Silica-Alumina.

All the above results clearly point to shape selective phenomena occurring over H-ZSM-5 while these effects are not evident for H-Beta, Silica-Alumina and SAPO-34.

The experimental data for this section on catalyst type can be found in Appendix B.

3.5 Conclusions

Based on the results presented in this chapter, the following conclusions can be drawn:

Firstly, the external mass transfer studies presented and discussed in Section 3.2 showed that for the purposes of this study, external mass transfer effects could be ignored.

Secondly, for H-ZSM-5, altering the reaction temperature from 200°C to 280°C showed a clear shift in product selectivity from branched to linear skeletons. It is possible that this shift is caused by strong diffusion and/or adsorption effects but this could not be confirmed by Arrhenius plots of the experimental data.

Finally, the study performed on various acid catalysts with different structures, confirmed the shape selective properties of H-ZSM-5 while H-Beta, Silica-Alumina and SAPO-34 exhibited none.

CHAPTER 4 - EQUILIBRIUM STUDIES

4.1 Introduction

As stated in Chapter 1, this study adopted a fundamental approach to modelling propene oligomerisation. Thus, the aim was to obtain as much information as possible about the reacting system. This information would then aid in developing a simple yet kinetically accurate model rather than an empirical one.

Quann and Krambeck (1991) concluded that isomerisation reactions, both skeletal and double bond, were much faster than oligomerisation reactions. Thus, they were able to simplify the product spectrum by lumping all species with the same carbon number together. However, it was not certain whether at 5% conversion isomerisation reactions were at equilibrium. Indeed it was desirable that they were not so since more information regarding the interconversion of skeletal structures could then be obtained.

Hence, the object of the equilibrium studies was to determine whether at 5% conversion the reaction products approach equilibrium. This was achieved by comparing actual composition data with equilibrium values predicted using various thermodynamic data bases.

4.2 Experimental

Propene oligomerisation runs were carried out at 5MPa and 250°C. The experimental apparatus used was discussed in detail in Chapter 2. Prior to these runs, liquid product from previous test runs had been analysed using three independent methods in order to identify as many of the hexene isomers as correctly as possible. Firstly, high purity G.C. standards were injected and their retention times compared with those of the products. Secondly, the liquid product was analysed using a Hewlett Packard 5890 Series II G.C. with a mass selective detector. Finally, samples of the liquid product were sent to SASOL laboratories for independent analysis. All analysis methods gave consistent results. All but 1 of the 17 hexene

isomers, 3,3-dimethyl-1-butene, were identified in the product spectrum. In addition, two pairs of isomers co-eluted, namely 1-hexene and 2-methyl-1-pentene, and cis- and trans-3-hexene. Additional information regarding the skeletal structure of the C_6 isomers as well as the C_9 isomers was obtained by hydrogenating the liquid product.

4.3 Methods for Predicting Equilibrium Concentrations

Equilibrium is defined as follows (Smith and van Ness (1987)) :

" The equilibrium state of a closed system is that state for which the total Gibbs energy is a minimum with respect to all possible changes at the given T and P. "

In other words :

$$(dG^{total})_{T,P} = 0 \tag{4.1}$$

For an elementary reversible reaction,

$$A \rightleftharpoons B \tag{4.2}$$

the following equation for the rate of removal of A can be written :

$$-\frac{dC_A}{dt} = k_{forward}C_A - k_{reverse}C_B \tag{4.3}$$

At equilibrium both the forward and reverse reaction rates are equal, thus

$$k_{forward}(C_A)_{eq} = k_{reverse}(C_B)_{eq} \tag{4.4}$$

This can also be written

$$\frac{(C_B)_{eq}}{(C_A)_{eq}} = K = \frac{k_{forward}}{k_{reverse}} \qquad (4.5)$$

This means that the ratio of the forward and reverse rate constants can be obtained from equilibrium concentrations - a useful fact when modelling equilibrium reactions.

If hexene equilibrium is to be predicted correctly, it is important that the data for all the hexene isomers originates from the same source. Variations in thermodynamic and physical properties of the isomers are subtle and variations due to different sources could cause erroneous predictions. Therefore it was decided to use a reliable correlation to predict the critical properties since no complete set was available from one source.

Three methods of equilibrium prediction were used. Firstly, data for the heat of formation and Gibbs free energy of formation for each isomer were obtained from Kilpatrick et al. (1946), and are referred to as the National Bureau of Standards (NBS). The critical properties, Pc, Tc and acentric factor, were predicted using a correlation proposed by Lin and Chao (1984). Physical properties were obtained from Rossini et al. (1953). This data was entered into the flowsheeting package PROCESS (1986) and equilibrium concentrations were predicted using a "Gibbs reactor". The equation of state chosen was Soave-Redlich-Kwong. (When calculating equilibrium concentrations using a "Gibbs reactor" PROCESS adjusts the amount of each isomer until the total change in Gibbs Free energy is at a minimum.)

Secondly, the heat of formation and Gibbs free energy of formation values taken from Stull et al. (1969) were used. The same values for the critical and physical properties were used as above. This data was also entered into PROCESS and equilibrium concentrations predicted.

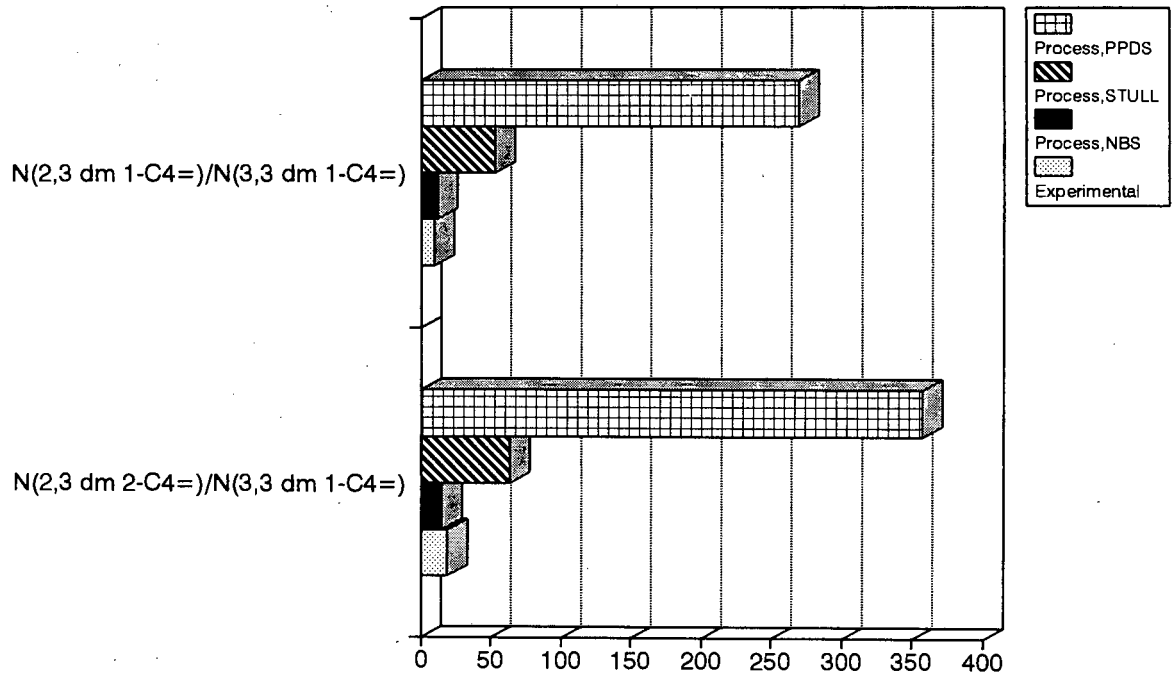

Figure 4.1 : Comparison Between Experimental and Predicted Equilibrium Values for Selected Isomer Ratios (227 C, 0.1 MPa)

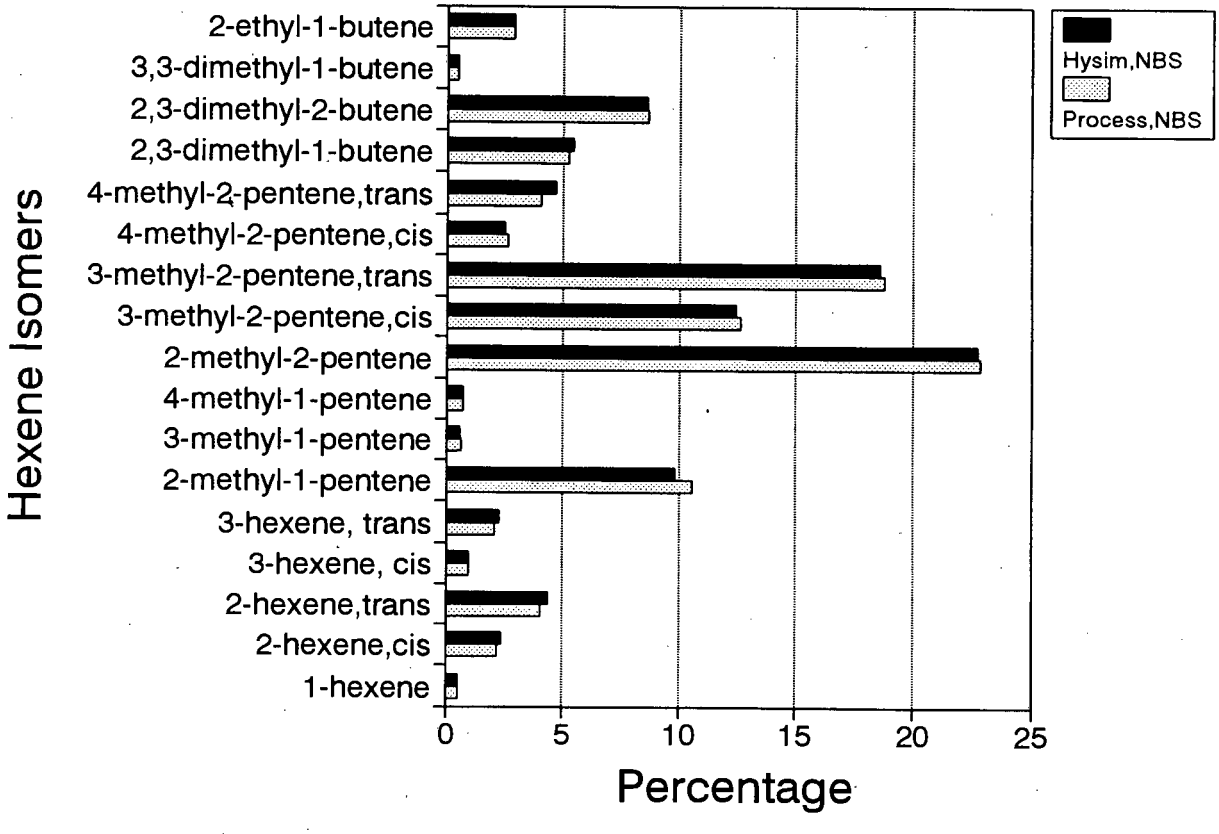

Figure 4.2 : Comparison Between Flowsheeting Packages (Reaction Conditions : 250 C, 5 MPa)

Lastly, data from the PROCESS data bank was used. The source of this data was the Physical Properties Data Service (PPDS).

Figure 4.1 shows the results of the three methods of prediction compared with experimental equilibrium data available from the NBS tables (1946). Unfortunately, no recent equilibrium data could be found in the literature. The figure represents the ratios of 2,3-dimethyl-2-butene to 3,3-dimethyl-1-butene and 2,3-dimethyl-1-butene to 3,3-dimethyl-1-butene. (At equilibrium the ratio of the concentration of any two of these isomers is constant.) Clearly, using data from the NBS tables provides the best estimate of equilibrium compositions. The data from Stull et al. (1969) provides the next best prediction. This figure shows clearly that the accuracy of equilibrium predictions is strongly dependent on the source of data.

Another flowsheeting package, HYSIM (1991) was used together with the NBS data. This gave results similar to PROCESS, using the same data (Figure 4.2). This indicates that the predictions are not dependent on the process simulation programs used.

All thermodynamic and physical properties of the hexene isomers used in these calculations can be found in Appendix C.

4.4 Results and Discussion

Initially, a series of test runs was performed to determine which conditions gave the best selectivity to oligomers. It was found that temperatures of 250°C and pressures of between 2.5 and 5 MPa gave a selectivity to oligomers of about 95% at a conversion of 5%. Figure 4.3 presents results of propene oligomerisation carried out at 250°C and 5 MPa, at 5% as well as at 50% conversion. This figure shows the concentration of each hexene isomer in the total hexene fraction. The product spectra at the two conversion levels indicate a change in selectivity regarding the various hexene isomers. This change is especially obvious for the 2,3-dimethyl-2-butene, cis- and trans-3-methyl-2-pentene, 2-methyl-2-pentene and 2-methyl-1-pentene/1-hexene peaks. Figure 4.3 also shows the predicted equilibrium using NBS data.

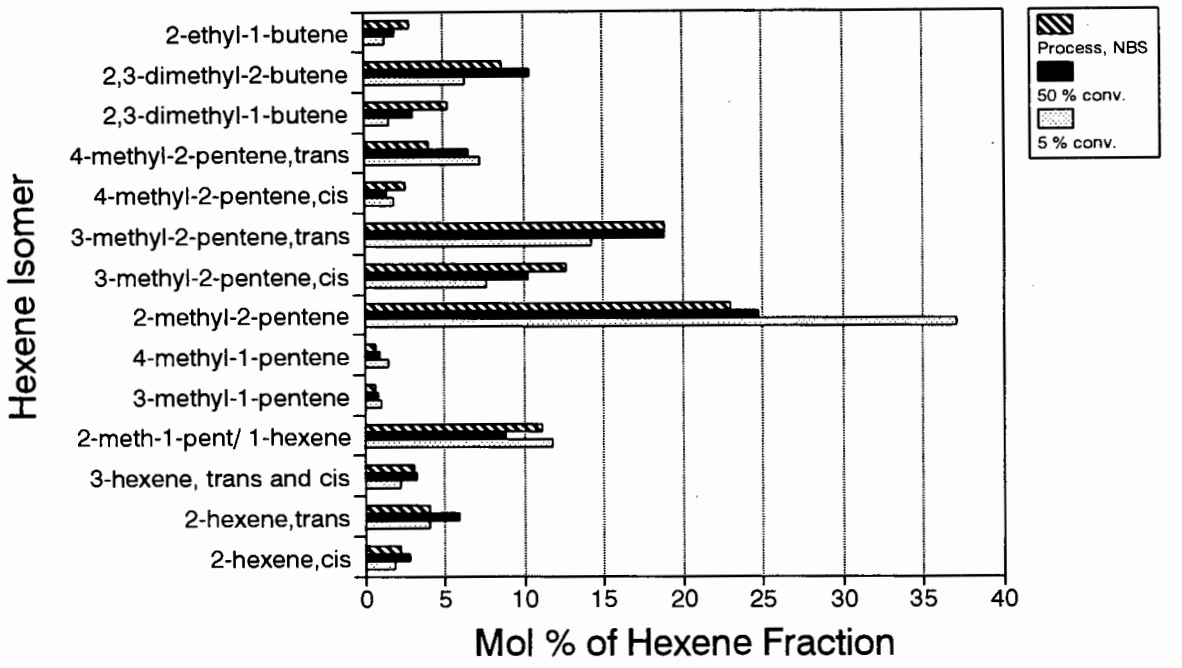

Figure 4.3 : Comparison Between Experimental and Predicted Hexene Isomer Compositions (Propene Oligomerisation : 250 C, 5 MPa)

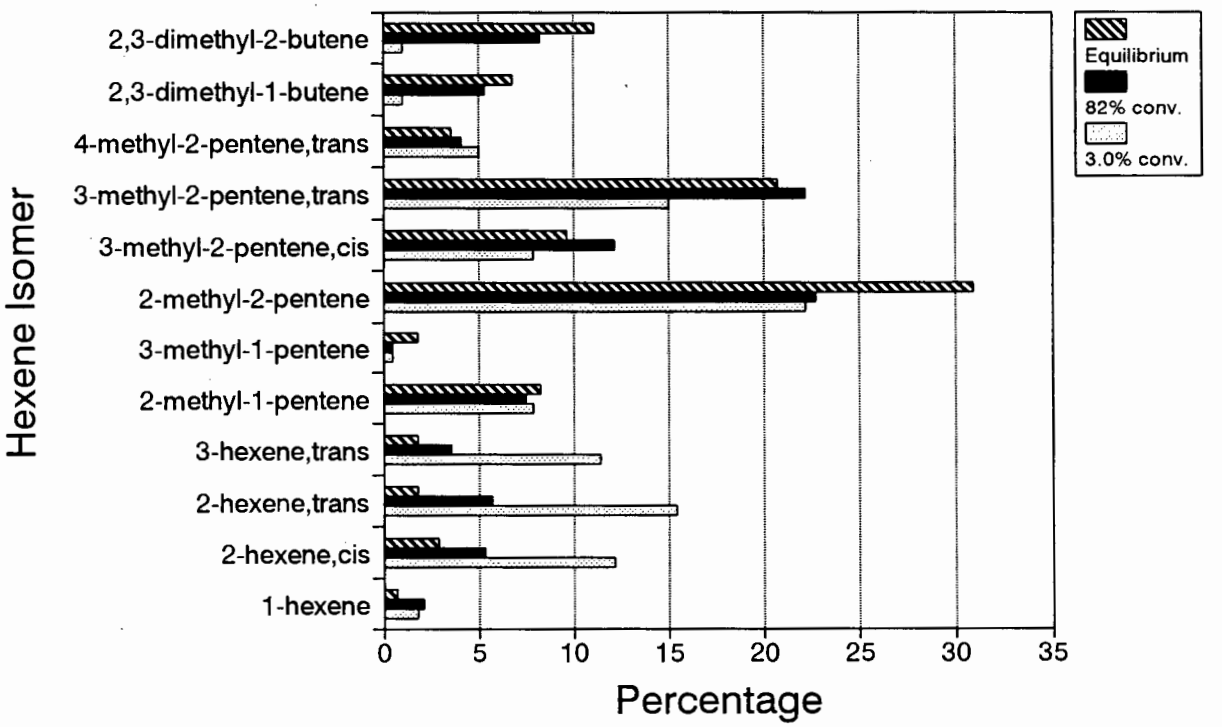

Figure 4.4 : Comparison Between Experimental and Predicted Hexene Isomer Compositions (Hexene Oligomerisation 227 C, 4.2 MPa - Quann et al. (1988))

The composition at 50% conversion agrees reasonably well with this prediction in contrast to that at 5% conversion. As stated in Chapter 2, the reproducibility of the experimental data was good, whereas confidence in predicted equilibria is lower. Therefore, the differences between the 5% and 50% conversion levels are more significant than those between the predicted equilibrium compositions and 50%. It was therefore concluded that at 5% conversion, the hexene isomers are not at equilibrium.

This conclusion is further confirmed by examining the results from Quann et al. (1988) shown in Figure 4.4. This graph compares experimental and predicted hexene isomer compositions for hexene oligomerisation at 227°C and 4.2MPa. Two conversion levels, 3% and 82% are presented, along with their predicted equilibrium compositions. Again, for almost every isomer the high conversion data are closer to equilibrium than the low conversion data.

The rms difference between the compositions at high conversion and the predicted equilibrium compositions is presented in Table 4.1 for this work and for Quann et al. The rms difference is also presented for the low conversion data and predicted equilibrium. The data in this table confirm that the high conversion runs are much closer to equilibrium than those at low conversions. The variations in the rms difference values are much greater than experimental error and thus it cannot be assumed that at low conversions the hexene isomers are converted to their equilibrium distributions as concluded by Quann et al (1988).

Table 4.1 : Comparison of RMS Difference Between High and Low Conversions and Equilibrium Predictions

	This work		Quann et al (1988)	
Conversion	50%	5%	82%	3%
rms difference	1.6	4.5	3.1	7.1

Krambeck and Quann (1991) indicated that double bond isomerisation was much faster than skeletal isomerisation. This means even when the hexene isomers are not at equilibrium with

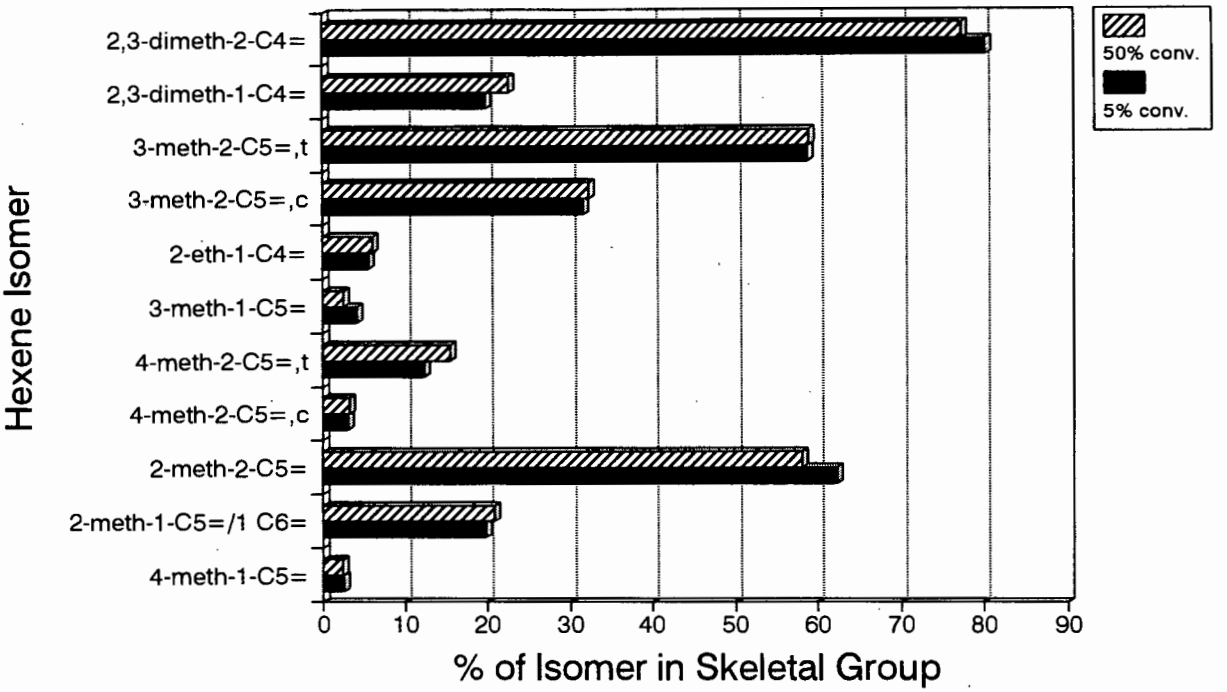

Figure 4.5 : Isomer Compositions within Skeletal Groups for Two Conversion Levels (Propene Oligomerisation 250 C, 5 MPa)

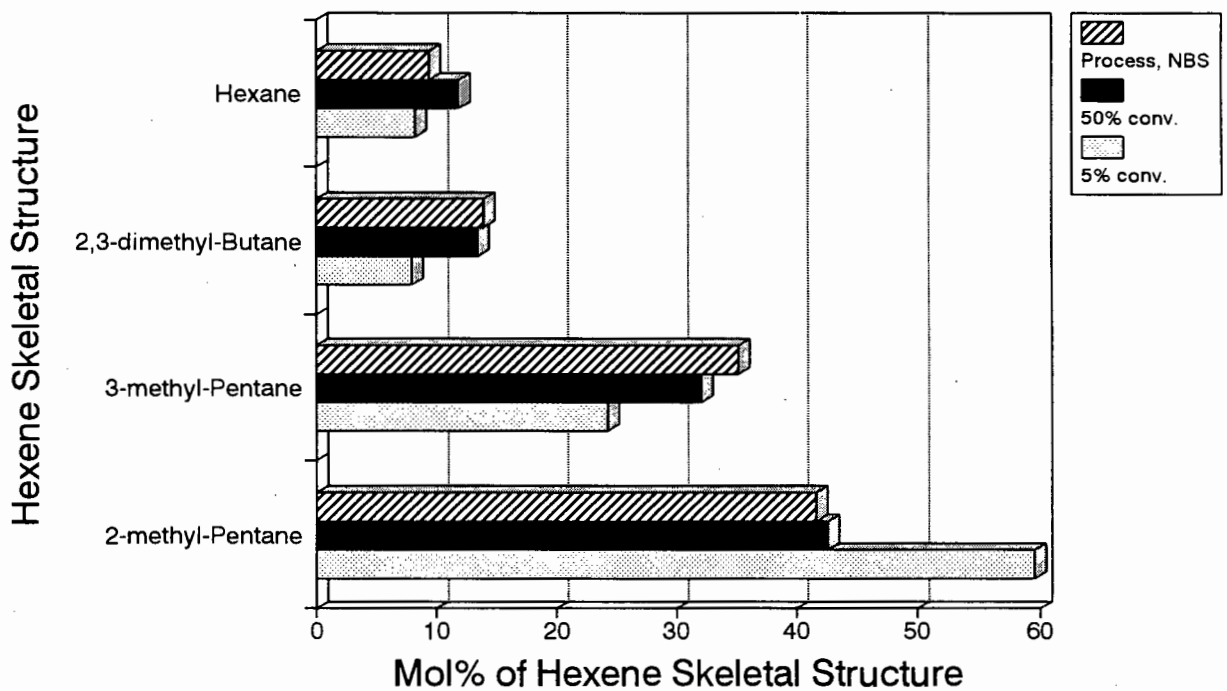

Figure 4.6 : Comparison Between Experimental and Predicted Hexene Skeletal Structure Compositions (Propene Oligomerisation : 250 C, 5 MPa)

respect to their skeletal structure, they could be at equilibrium with respect to their double bonds. In order to test this, the hexene isomers were grouped according to their carbon skeletons :

Olefin	**Carbon Skeleton**
2-methyl-1-pentene	2-methyl-pentane
2-methyl-2-pentene	2-methyl-pentane
4-methyl-2-pentene (cis and trans)	2-methyl-pentane
4-methyl-1-pentene	2-methyl-pentane
2-ethyl-1-butene	3-methyl-pentane
3-methyl-1-pentene	3-methyl-pentane
3-methyl-2-pentene (cis and trans)	3-methyl-pentane
2,3-dimethyl-1-butene	2,3-dimethyl-butane
2,3-dimethyl-2-butene	2,3-dimethyl-butane
1-hexene	hexane
2-hexene (cis and trans)	hexane
3-hexene (cis and trans)	hexane
3,3-dimethyl-1-butene	2,2-dimethyl-butane

There are five major carbon skeletons namely, hexane, 2-methyl-pentane, 3-methyl-pentane, 2,2-dimethyl-butane and 2,3-dimethyl-butane. For the 2-methyl-pentane group the most plentiful isomer was 2-methyl-2-pentene, for the 3-methyl-pentane group it was 3-methyl-2-pentene and for the 2,3-dimethyl-butane group it was 2,3-dimethyl-2-butene. 3,3-dimethyl-1-butene was not identified in the product spectrum.

The fraction of each isomer within its skeletal group was plotted for 5 and 50% conversion. The results are shown in Figure 4.5. This figure shows that at both 5% and 50% conversion the composition of isomers within each skeletal group are similar, and thus it is reasonable to assume they are close to equilibrium with respect to the double bond isomerisation. Figure 4.6 further confirms this when the fractions of each skeletal group at high and low conversion are compared with equilibrium compositions at predicted equilibrium.

All the values for distribution of the hexene isomers shown in Figures 4.1 to 4.6 can be found in Appendix C.

4.5 Conclusions

This investigation has shown that, for propene oligomerisation at 5 % conversion, the skeletal structures of the hexene isomers are not at equilibrium. However, the double bond isomers within each skeletal group are close to equilibrium even at these low conversions. This result validates the use of a model for propene oligomerisation which lumps the skeletal structures at each carbon number. It was also shown that the accuracy of predicted equilibrium concentrations are dependent on the source of the data used.

CHAPTER 5 - HEXENE ISOMERISATION

5.1 Introduction

The next major section of this thesis involved the study of hexene isomerisation, under the conditions of propene oligomerisation. The first aim was to determine whether the hexene isomers followed the same isomerisation pathway over H-ZSM-5 as that presented by Martens and Jacobs (1990) for superacid catalysts. The second aim was to establish the values of the hexene isomerisation rate constants relative to one another. It was intended that once the relative values of hexene isomerisation rate constants were known, this information could be extended to encompass the isomerisation of nonene isomers. For example, once the rate constant for a methyl-shift reaction relative to the rate constant for a reduction in branching was known, this relationship could be applied to the isomerisation of the nonenes. These isomerisation relationships would aid in reducing the number of parameters required to model the reaction, without reducing the complexity of the model.

Several models were developed to model the isomerisation of hexenes. These models are based on the isomerisation of hexene isomers over superacid catalysts presented by Martens and Jacobs (1990). Since it was intended to extend the hexene isomerisation model to model nonene isomerisation, the models developed started with the simplest possible and gradually increased in complexity. Double bond isomerisation was ignored during this study since it was shown in Chapter 4 that, within each skeletal group, the double bond isomerisation is close to equilibrium, even at 5% propene conversion.

The first section of this chapter briefly covers experimental details relevant to the hexene isomerisation runs. Following this, the isomerisation models are presented in order of increasing complexity. The section on each model covers the development of the model, a sensitivity analysis of the model and finally the fit of the model to the experimental data. Finally, conclusions on the hexene isomerisation studies are presented.

5.2 Experimental

The experiments were performed on a high pressure experimental rig described in detail in Chapter 2. Two hexene isomers with different skeletal structures, namely 1-hexene and 4-methyl-1-pentene, were passed separately over H-ZSM-5 at the same reaction conditions as propene oligomerisation i.e. 250°C and 5MPa. The feed stream contained 4 mol% of either one of the isomers in nitrogen. The low partial pressure of the hexene isomer kept dimerisation to a minimum. The characteristics of the H-ZSM-5 used can be found in Chapter 2. The conversion to C_{12} olefins for all data points was less than 9% and for most data points less then 5%.

The WHSV was varied in order to obtain different levels of conversion. A new experiment was carried out for each WHSV, using fresh catalyst each time. This is shown in Table 5.1 below. The WHSVs were chosen to cover as wide a conversion range as possible. However, several factors limited the range of WHSVs chosen. Firstly, for a fixed WHSV the conversion of 4-methyl-1-pentene was higher than 1-hexene and necessitated a wider range of WHSVs. Secondly, oligomerisation had to be kept to a minimum and thus for both feeds the WHSV could not be decreased below $8hr^{-1}$. Finally, the equipment limited the maximum and minimum flow possible.

Table 5.1 : Weight Hourly Space Velocities Used During Hexene Isomerisation Runs

Feed Isomer : 1-Hexene		Feed Isomer : 4-methyl-1-Pentene	
Run Number	WHSV hr^{-1}	Run Number	WHSV hr^{-1}
69	8	75	8
67	10	71	9
68	17	72	17
		76	56

Details regarding each isomerisation run can be found in Appendix D.

5.3 Nomenclature

For this chapter on hexene isomerisation the hexene isomers are grouped according to their skeletal structures. This is because, as shown in Chapter 4, there is equilibrium with respect to the double bonds. These skeletal groups are represented using the nomenclature shown in the table below.

Table 5.2 : Hexene Isomer Skeletal Groups

Carbon Skeleton	Hexene Isomer	Symbol
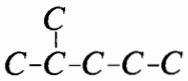	2-methyl-1-Pentene 2-methyl-2-Pentene 4-methyl-2-Pentene,cis and trans 4-methyl-1-Pentene	S2
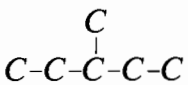	3-methyl-2-Pentene,cis and trans 3-methyl-1-Pentene 2-ethyl-1-Butene	S3
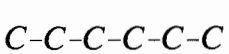	1-Hexene 2-Hexene,cis and trans 3-Hexene,cis and trans	L
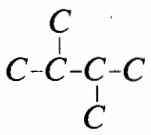	2,3-dimethyl-1-Butene 2,3-dimethyl-2-Butene	D

Key :

S2	-	singly branched, methyl branch on second carbon
S3	-	singly branched, methyl branch on third carbon
L	-	linear structure, no branching
D	-	doubly branched

5.4 Catalyst Deactivation During Hexene Isomerisation

For all hexene isomerisation runs over H-ZSM-5 deactivation occurred throughout the run. This meant that reaction rates were not constant during each run. Since this problem could not be avoided, the experimental data was plotted as concentration of product isomers versus concentration of feed isomer. This meant that the variation in catalyst reactivity with time on stream was, in effect, cancelled out. Also, this method of plotting the data was sufficient to determine the relative reaction rates. This approach was also adopted by Paynter and Schuette (1971) when they modelled olefin codimerisation.

When a catalyst undergoes deactivation during an experimental run, it is possible that a change in the reaction mechanism can occur. Figures 5.1 to 5.4 plot normalised product concentration versus feed isomer concentration for all the isomerisation runs. Figure 5.1 shows the data obtained from 1-hexene isomerisation while Figures 5.2 to 5.4 show the 4-methyl-1-pentene isomerisation data. These graphs clearly show that although the catalyst deactivated during each run, there was no change in the reaction mechanism. Therefore, the isomerisation of hexenes was modelled as product concentration versus feed concentration instead of the usual concentration versus time plots.

5.5 Modelling of Hexene Isomerisation

The hexene isomerisation scheme incorporated in all of the following models is based on the reaction scheme presented by Martens and Jacobs (1990) for superacid catalysts (Figure 5.5). In this scheme the 2-methyl-pentane skeleton (S2) reacts to the dimethyl-branched skeletons namely, 2,3-dimethyl-butane (D) and 3,3-dimethyl-butane (DD) via slow Type B isomerisation. S2 can also react to the 3-methyl-pentane skeleton (S3) via fast Type A isomerisation. S3 in turn reacts to the linear hexane skeleton (L) via Type B isomerisation. The intermediates in all the isomerisation reactions are protonated cyclopropanes (PCP).

This reaction scheme indicates that 3,3-dimethyl-butenes have the same probability of formation as 2,3-dimethyl-butenes. However, none of the former was observed in the

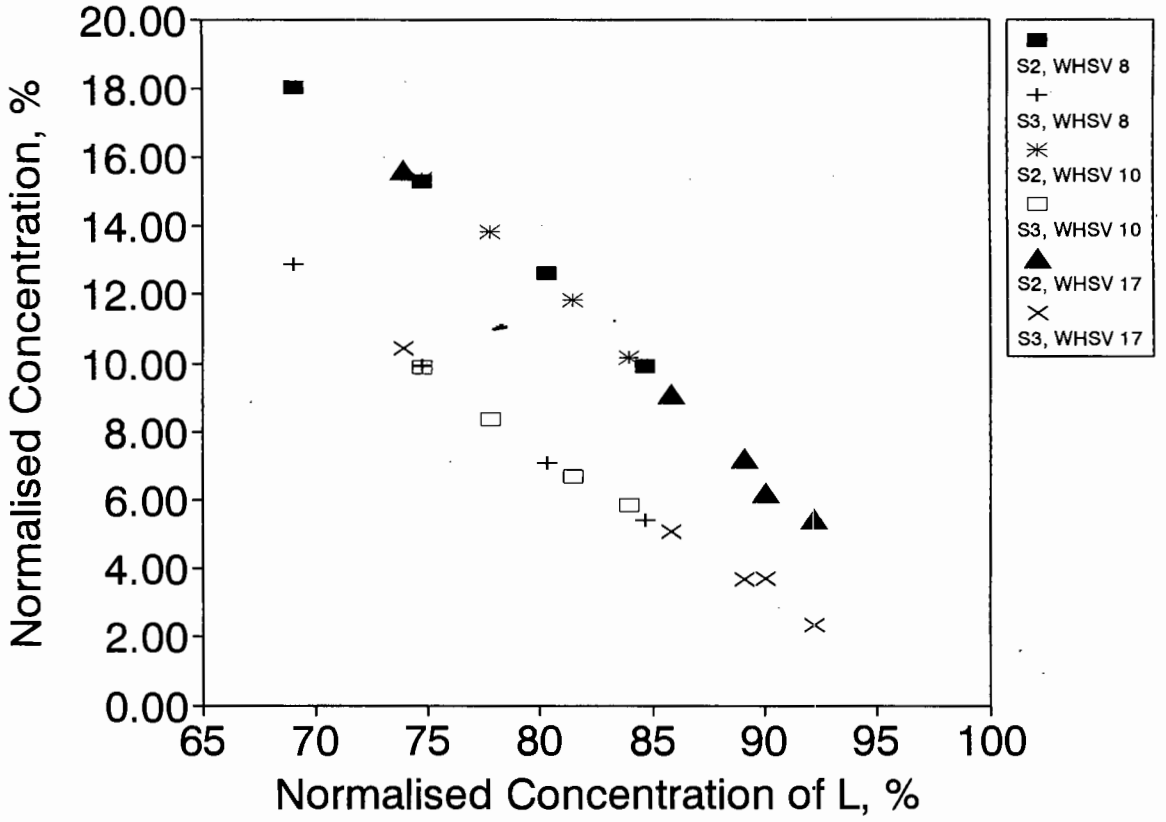

Figure 5.1 : 1-Hexene Isomerisation Experimental Data

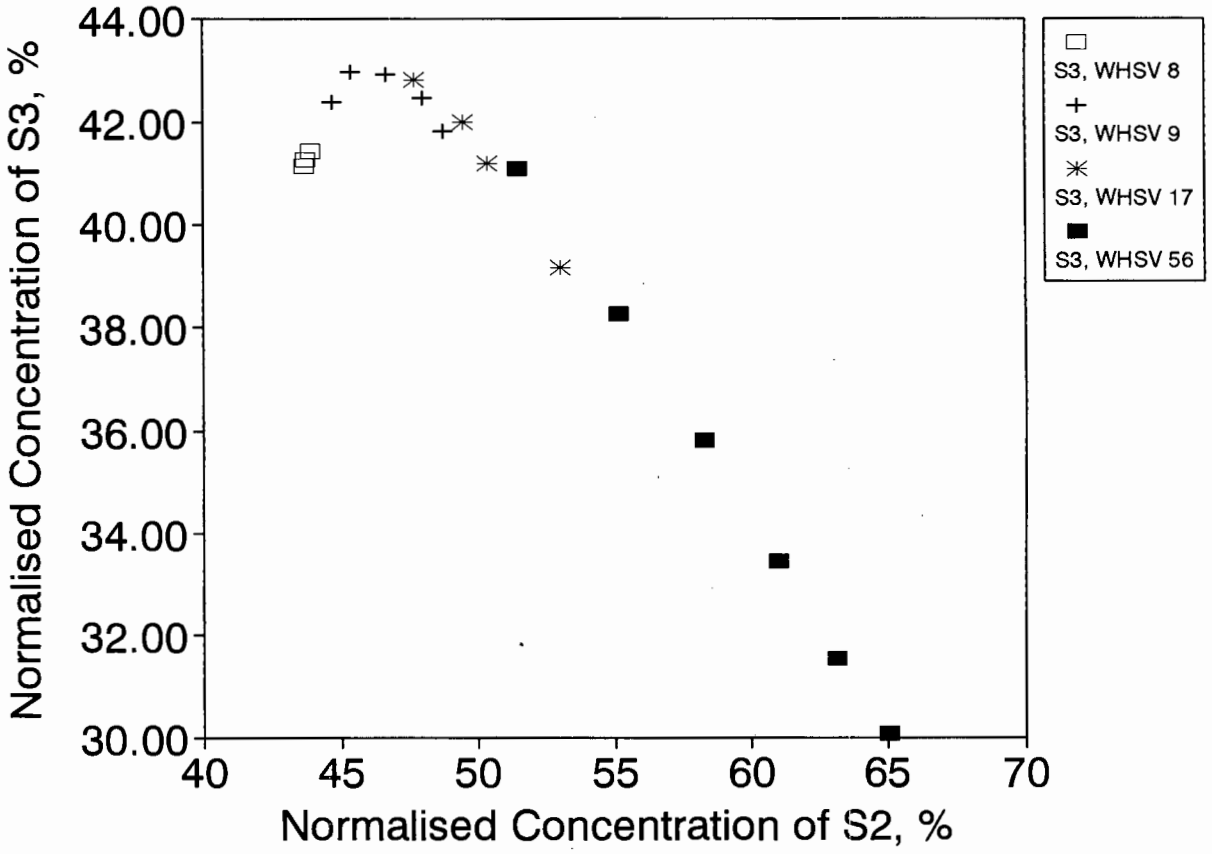

Figure 5.2 : 4-methyl-1-Pentene Isomerisation Experimental Data - Variation of Concentration of S3 with Feed Concentration

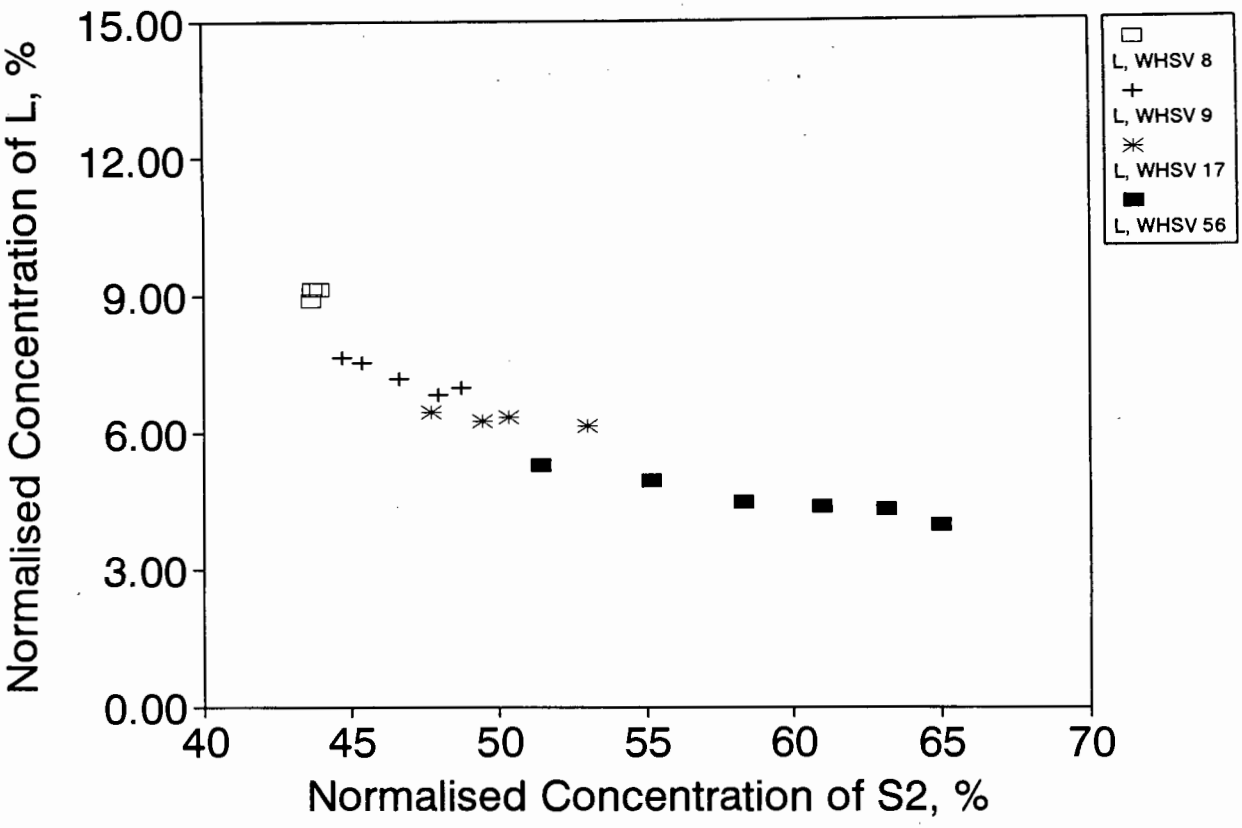

Figure 5.3 : 4-methyl-1-Pentene Isomerisation Experimental Data - Variation of Concentration of L with Feed Concentration

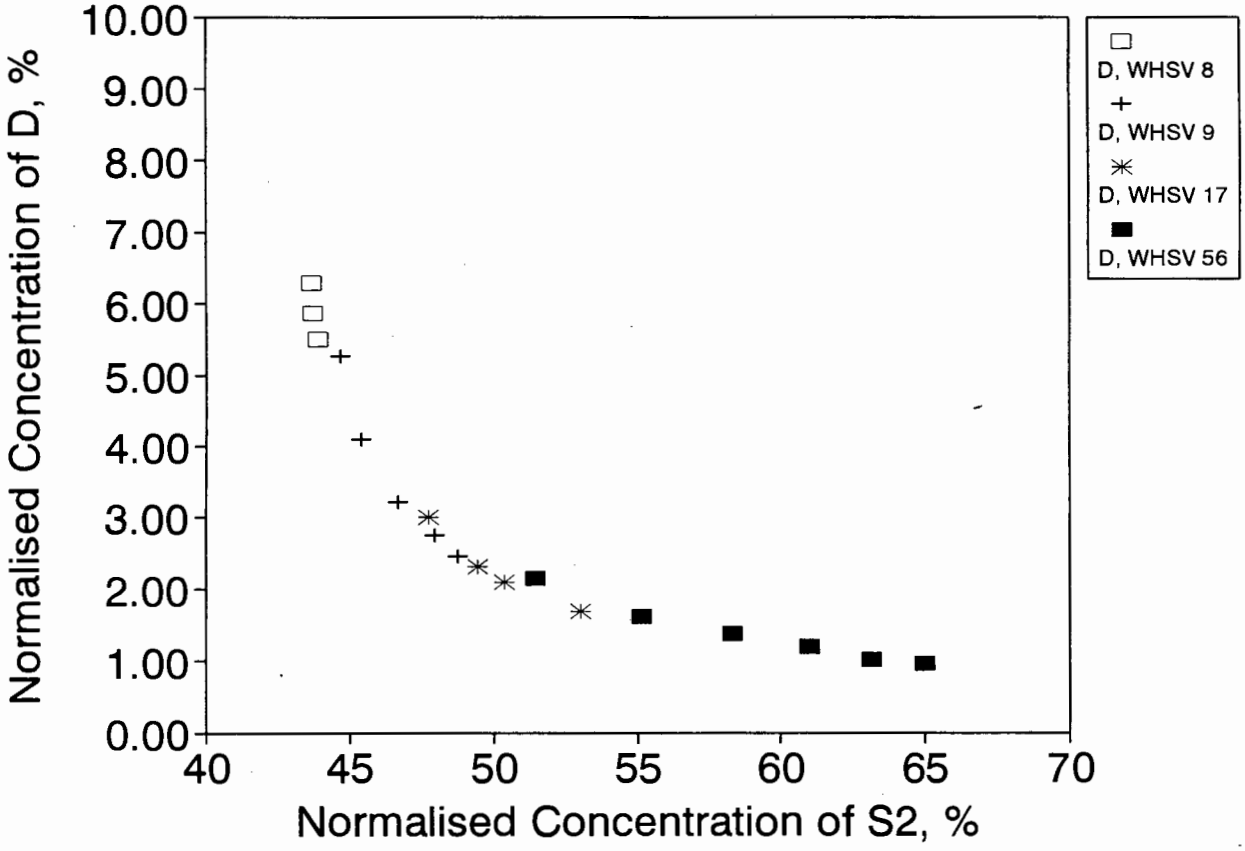

Figure 5.4 : 4-methyl-1-Pentene Isomerisation Experimental Data - Variation of Concentration of D with Feed Concentration

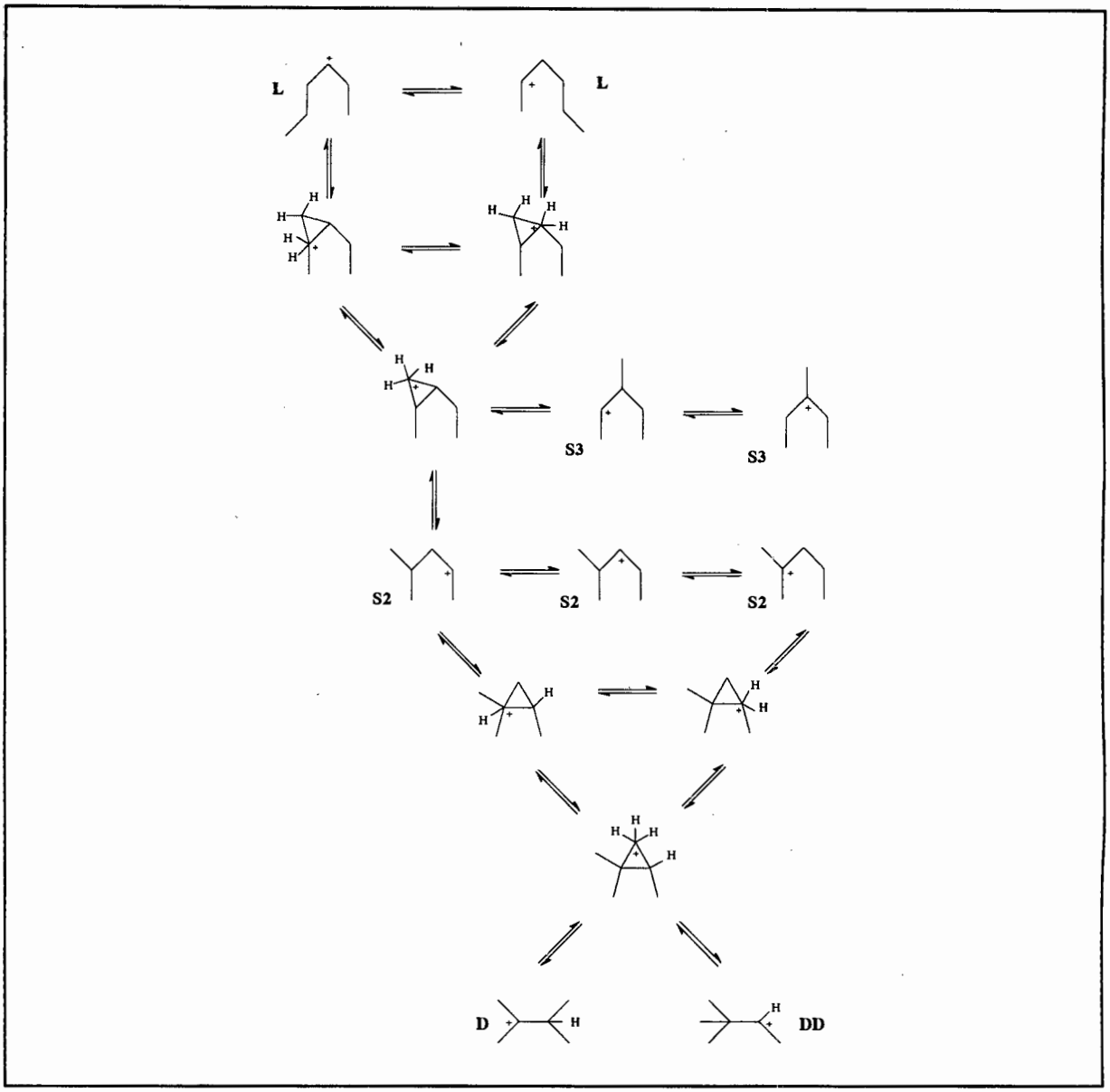

Figure 5.5 : Hexene Isomerisation Mechanism from Martens and Jacobs (1990)

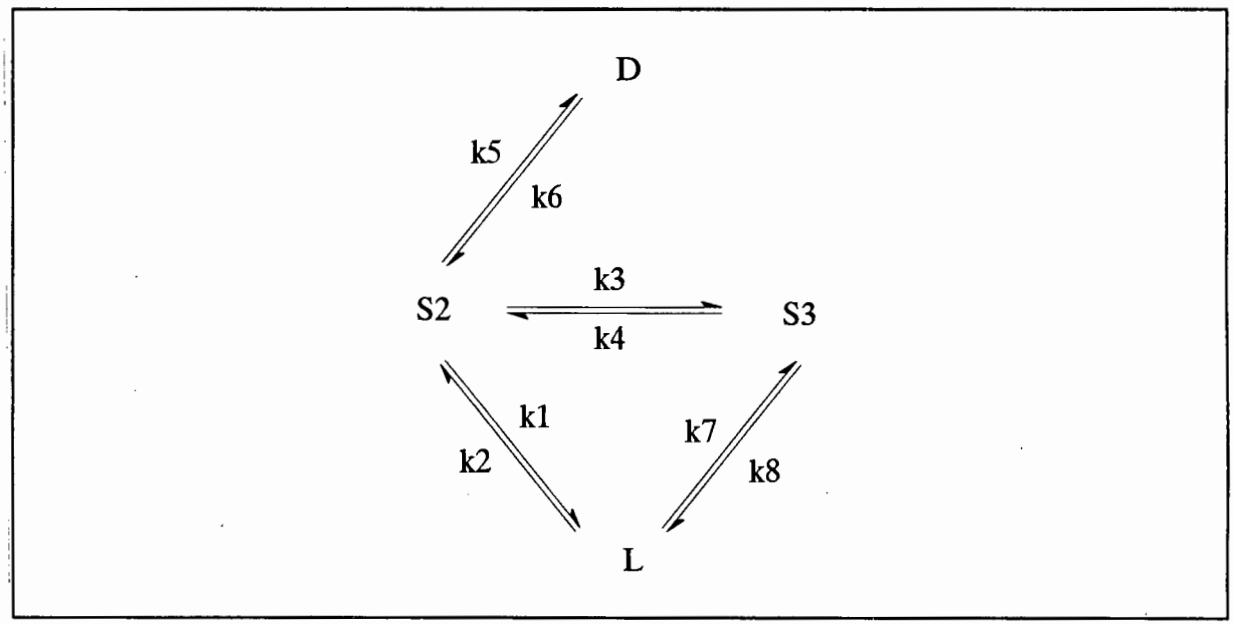

Figure 5.6 : Reaction Pathways for Model A

product spectra, even at high conversions. This could be due to shape selective effects imposed by H-ZSM-5. As shown in Chapter 3, all of the reaction products formed during propene oligomerisation over H-ZSM5 have linear carbon skeletons with no more than one methyl group per carbon atom. In addition, the predicted equilibrium concentration of 3,3-dimethyl-butene is very low, 0.45% (see Figure 4.2), and is therefore not likely to be observed in the product spectrum.

The three models developed will now be presented in turn.

5.5.1 Model A

5.5.1.1 Model Development

A number of workers have successfully modelled oligomerisation over acid catalysts using homogeneous reactions, for example Quann and Krambeck (1991), Cao et al. (1988), Alberty (1987) and Paynter and Schuette (1971). No effect of adsorption of reactants or products or the effect of interparticle mass transfer resistances were included in these models. Since in this present study it was intended to extend the information obtained concerning hexene isomerisation to nonene isomerisation it was decided to begin with as simple a model as possible. Thus Model A was proposed.

The hexene isomerisation reaction scheme for Model A can be represented schematically as shown in Figure 5.6. In this scheme the isomers are grouped according to their skeletal structure. As mentioned previously, both S2 and L were fed separately over the catalyst during the experimental runs. Feeding S2 provides information about its isomerisation to D, S3 and L, while feeding L provides information about its isomerisation to S2 and S3 and the fast methyl-shift reaction between S2 and S3. However, none of these isomerisation runs can provide information concerning the isomerisation of D to S3 since D was not fed. In addition, according to the scheme shown in Figure 5.5, D does not form directly from S3. Therefore the isomerisation of D to S3 was not included in the model.

In homogeneous Model A the reactions are elementary and the reactor is assumed to be plug flow. The rate equations for Model A are as follows :

$$\frac{dC_L}{dt} = k_1 C_{S2} - (k_7 + k_2)C_L + k_8 C_{S3} \tag{5.1}$$

$$\frac{dC_{S2}}{dt} = k_2 C_L + k_4 C_{S3} + k_6 C_D - (k_5 + k_3 + k_1)C_{S2} \tag{5.2}$$

$$\frac{dC_{S3}}{dt} = k_7 C_L + k_3 C_{S2} - (k_4 + k_8)C_{S3} \tag{5.3}$$

Since only C6 isomers are considered, the following mass balance relationship can be used to replace C_D in equation (5.2) above,

$$C_D = 1 - C_L - C_{S3} - C_{S2} \tag{5.4}$$

to give :

$$\frac{dC_{S2}}{dt} = (k_2 - k_6)C_L - (k_5 + k_3 + k_1 + k_6)C_{S2} + (k_4 - k_6)C_{S3} + k_6 \tag{5.5}$$

One possible method of solution for a system of first order, linear, ordinary differential equations is the method of eigenvectors and eigenvalues, described in detail in Kreyszig (1979). (See Appendix D.) This method is applied in solving the above set of differential equations namely, equations (5.1), (5.3) and (5.5) :

$$\boldsymbol{A} = \begin{bmatrix} -(k_7+k_2) & k_1 & k_8 \\ (k_2-k_6) & -(k_6+k_5+k_3+k_1) & (k_4-k_6) \\ k_7 & k_3 & -(k_4+k_8) \end{bmatrix} \tag{5.6}$$

$$h = \begin{bmatrix} 0 \\ k_6 \\ 0 \end{bmatrix} \tag{5.7}$$

The characteristic polynomial, det (**A** - λ**I**) =

$$\begin{aligned} &\lambda^3 + (k_1+k_2+k_3+k_4+k_5+k_6+k_7+k_8)\lambda^2 + \\ &(k_7k_6+k_7k_5+k_7k_3+k_7k_4+k_2k_6+k_2k_5+k_2k_3+k_2k_4+k_2k_8+k_1k_6+k_6k_4 \\ &+k_6k_8+k_5k_4+k_5k_8+k_3k_8+k_1k_4+k_1k_8+k_3k_6+k_7k_1)\lambda \\ &+ (k_7k_6k_4+k_7k_5k_4+k_7k_3k_6+k_2k_6k_4+k_2k_6k_8+k_2k_5k_4+k_2k_5k_8+k_2k_3k_6+k_1k_6k_4+ \\ &k_1k_6k_8+k_1k_7k_6+k_8k_3k_6) \end{aligned} \tag{5.8}$$

Let the roots of this equation be λ_1, λ_2, λ_3. The matrix of eigenvectors corresponding to these λ_i's is :

$$\boldsymbol{X} = \begin{bmatrix} 1 & 1 & 1 \\ a_1 & a_2 & a_3 \\ a_4 & a_5 & a_6 \end{bmatrix} \tag{5.9}$$

$$x_3^* = \frac{k_7k_1+k_7k_3+k_2k_3+k_3\lambda_i}{k_1k_4+k_1k_8+k_1\lambda_i+k_8k_3}, \quad x_2^* = \frac{-k_8x_3^*+k_7+k_2+\lambda_i}{k_1}, \quad i=1,2,3$$

$$a_1, a_2, a_3 = x_2^*, \quad a_4, a_5, a_6 = x_3^* \tag{5.10}$$

Next,

$$\boldsymbol{X}^{-1} = \begin{bmatrix} a_2a_6-a_3a_5 & a_5-a_6 & a_3-a_2 \\ a_3a_4-a_1a_6 & a_6-a_4 & a_1-a_3 \\ a_1a_5-a_2a_4 & a_4-a_5 & a_2-a_1 \end{bmatrix} \frac{1}{\det \boldsymbol{X}} \tag{5.11}$$

and

$$\boldsymbol{X}^{-1}h = \begin{bmatrix} \frac{a_5-a_6}{detX}k_6 \\ \frac{a_6-a_4}{detX}k_6 \\ \frac{a_4-a_5}{detX}k_6 \end{bmatrix} \tag{5.12}$$

Now

$$z_1' - \lambda_1 z_1 = \frac{k_6(a_5-a_6)}{\det \boldsymbol{X}} \tag{5.13}$$

$$z_2' - \lambda_2 z_2 = \frac{k_6(a_6-a_4)}{\det \boldsymbol{X}} \tag{5.14}$$

$$z_3' - \lambda_3 z_3 = \frac{k_6(a_4-a_5)}{\det \boldsymbol{X}} \tag{5.15}$$

Solving for each z :

$$z_1 = \frac{k_6(a_6-a_5)}{\det \boldsymbol{X}\lambda_1} + C_1 e^{\lambda_1 t} \tag{5.16}$$

$$z_2 = \frac{k_6(a_4-a_6)}{\det \boldsymbol{X}\lambda_2} + C_2 e^{\lambda_2 t} \tag{5.17}$$

$$z_3 = \frac{k_6(a_5-a_4)}{\det \boldsymbol{X}\lambda_3} + C_3 e^{\lambda_3 t} \tag{5.18}$$

Finally the concentrations of the hexene skeletal structures as a function of time are given by:

$$C_L = \frac{k_6(a_6-a_5)}{\det \boldsymbol{X}\lambda_1} + C_1 e^{\lambda_1 t} + \frac{k_6(a_4-a_6)}{\det \boldsymbol{X}\lambda_2} + C_2 e^{\lambda_2 t} + \frac{k_6(a_5-a_4)}{\det \boldsymbol{X}\lambda_3} + C_3 e^{\lambda_3 t} \tag{5.19}$$

$$C_{S2} = \frac{a_1 k_6(a_6-a_5)}{\det \boldsymbol{X}\lambda_1} + a_1 C_1 e^{\lambda_1 t} + \frac{a_2 k_6(a_4-a_6)}{\det \boldsymbol{X}\lambda_2} + a_2 C_2 e^{\lambda_2 t} + \frac{a_3 k_6(a_5-a_4)}{\det \boldsymbol{X}\lambda_3} + a_3 C_3 e^{\lambda_3 t} \tag{5.20}$$

$$C_{S3} = \frac{a_4 k_6(a_6-a_5)}{\det \boldsymbol{X}\lambda_1} + a_4 C_1 e^{\lambda_1 t} + \frac{a_5 k_6(a_4-a_6)}{\det \boldsymbol{X}\lambda_2} + a_5 C_2 e^{\lambda_2 t} + \frac{a_6 k_6(a_5-a_4)}{\det \boldsymbol{X}\lambda_3} + a_6 C_3 e^{\lambda_3 t} \tag{5.21}$$

Let

$$const1 = \frac{k_6(a_6-a_5)}{\det \boldsymbol{X}\lambda_1},\quad const2 = \frac{k_6(a_4-a_6)}{\det \boldsymbol{X}\lambda_2},\quad const3 = \frac{k_6(a_5-a_4)}{\det \boldsymbol{X}\lambda_3},$$
$$const4 = \frac{a_1 k_6(a_6-a_5)}{\det \boldsymbol{X}\lambda_1},\quad const5 = \frac{a_2 k_6(a_4-a_6)}{\det \boldsymbol{X}\lambda_2},\quad const6 = \frac{a_3 k_6(a_5-a_4)}{\det \boldsymbol{X}\lambda_3}, \tag{5.22}$$
$$const7 = \frac{a_4 k_6(a_6-a_5)}{\det \boldsymbol{X}\lambda_1},\quad const8 = \frac{a_5 k_6(a_4-a_6)}{\det \boldsymbol{X}\lambda_2},\quad const9 = \frac{a_6 k_6(a_5-a_4)}{\det \boldsymbol{X}\lambda_3}$$

$$A = const1 + const2 + const3$$
$$B = const4 + const5 + const6 \tag{5.23}$$
$$D = const7 + const8 + const9$$

Applying the following boundary conditions when 4-methyl-1-Pentene is fed,

$$t = 0,\ C_L = C_{S3} = C_D = 0 \text{ and } C_{S2} = 1 \tag{5.24}$$

$$C_1 + C_2 + C_3 + A = 0 \tag{5.25}$$

$$a_1C_1 + a_2C_2 + a_3C_3 + B = 1 \tag{5.26}$$

$$a_4C_1 + a_5C_2 + a_6C_3 + D = 0 \tag{5.27}$$

Solving for constants of integration,

$$C_3 = \frac{a_4A - D - \dfrac{(1 - B + a_1A)(a_5 - a_4)}{(a_2 - a_1)}}{\dfrac{(a_1 - a_3)(a_5 - a_4)}{a_2 - a_1} + a_6 - a_4} \tag{5.28}$$

$$C_2 = \frac{1 - B + a_1A + (a_1 - a_3)C_3}{(a_2 - a_1)} \tag{5.29}$$

$$C_1 = -A - C_2 - C_3 \tag{5.30}$$

Applying the following boundary conditions when 1-Hexene is fed,

$$t = 0,\ C_{S2} = C_{S3} = C_D = 0 \text{ and } C_L = 1 \tag{5.31}$$

$$C_1 + C_2 + C_3 + A = 1 \tag{5.32}$$

$$a_1C_1 + a_2C_2 + a_3C_3 + B = 0 \tag{5.33}$$

$$a_4C_1 + a_5C_2 + a_6C_3 + D = 0 \tag{5.34}$$

Solving for the constants of integration,

$$C_3 = \frac{\frac{(a_4-a_5)(a_1A-B-a_1)}{(a_1-a_2)} - a_4(A-1)+D}{\frac{(a_5-a_4)(a_1-a_3)}{a_1-a_2}+(a_4-a_6)} \qquad (5.35)$$

$$C_2 = \frac{(a_3-a_1)C_3+a_1+B-a_1A}{a_1-a_2} \qquad (5.36)$$

$$C_1 = 1-A-C_2-C_3 \qquad (5.37)$$

Since the constants of integration are different for the two sets of boundary conditions, the equations (5.19) to (5.21) give rise to two different sets of concentration curves.

The ratios of the forward and reverse rate constants are equal to the ratios of the equilibrium composition of the isomers. The equilibrium composition used was obtained from the 4-methyl-1-Pentene isomerisation runs. This is shown along with predicted equilibrium concentrations obtained using PROCESS, as discussed in Chapter 4:

Table 5.3 : Equilibrium Composition of Hexene Isomers

Skeletal Group	Mol %, Experimental	Mol %, Predicted
S2	43.3	41.0
S3	40.6	35.0
L	8.75	9.93
D	7.35	13.95

Thus, the ratios of rate constants are as follows:

Table 5.4 : Ratios of Rate Constants for Model A	
k_1/k_2	0.2021
k_3/k_4	0.9381
k_5/k_6	0.1697
k_7/k_8	4.642

5.5.1.2 Sensitivity Analysis

This section covering the sensitivity analysis illustrates and discusses the effects of the rate constants, relative to one another, on the concentration profiles for both starting compounds namely, L (hexenes) and S2 (2-methyl-pentenes). Table 5.5 shows the manner in which the rate constants were varied in order to assess their influence on the product spectrum. For the base case, k4 was chosen to be larger than k2, k6 and k8 because methyl-shift reactions are faster than those involving a change in degree of branching. Due to the form of the experimental data, i.e. normalised concentration versus feed concentration, only relative rate constants could be fitted to the data. Thus, for the sensitivity analysis the values of the rate constants relative to one other is important and not their absolute values.

For each feed compound, the results for each case are presented in the form of two graphs. Firstly, the C/C_{eq} versus time plots are shown. C_{eq} represents the equilibrium concentration of a species. Where clarification is necessary, these graphs contain an insert which shows the behaviour of the curves close to zero time. As C/C_{eq} approaches 1, so each skeletal group approaches equilibrium. Secondly, product concentration versus feed concentration curves are plotted. All concentrations are normalised with respect to the feed concentration. This second set of curves has the same form as the experimental data. Note that for this second graph that as the concentration of the feed compound decreases, the reaction approaches equilibrium.

Table 5.5 : Model A - Parameters Used in Sensitivity Analysis				
Case	k_2 L → S2	k_4 S3 → S2	k_6 D → S2	k_8 S3 → L
1 (Base)	1	10	1	1
2	100	10	1	1
3	1	1000	1	1
4	1	10	100	1
5	1	10	1	100

1-Hexene Isomerisation

The sensitivity analysis for 1-hexene isomerisation is discussed below and the results shown in Figures 5.7 to 5.11.

Case 1 - When the insert in Figure 5.7a is studied, it can be seen that close to the origin S3 has a definite slope while S2 and D do not. Thus S3 behaves as if it were a primary product while S2 and D behave as secondary products. S2 is in fact also primary but appears as secondary because the overall reaction L → S3 → S2 is faster than L → S2. Figure 5.7b shows how both S2 and S3 form rapidly from L and increase to a maximum concentration exceeding their equilibrium concentrations. S2 and S3 establish equilibrium between themselves early on in the reaction, as can be seen by the convergence of their curves at approximately t=1 in Figure 5.7a. Once equilibrium is established, S2+S3 then form and react as one "pseudo-component". S2+S3 then establishes equilibrium with the feed component, L. Again this is illustrated by the coincidence of all three curves. The final group, S2+S3+L, then reacts to form D. In Figure 5.7b the concentration of D remains small throughout most of the reaction and only increases sharply to its equilibrium concentration close to overall equilibrium.

Case 2 - Here the rate constant for the formation of S2 from L was increased by two orders

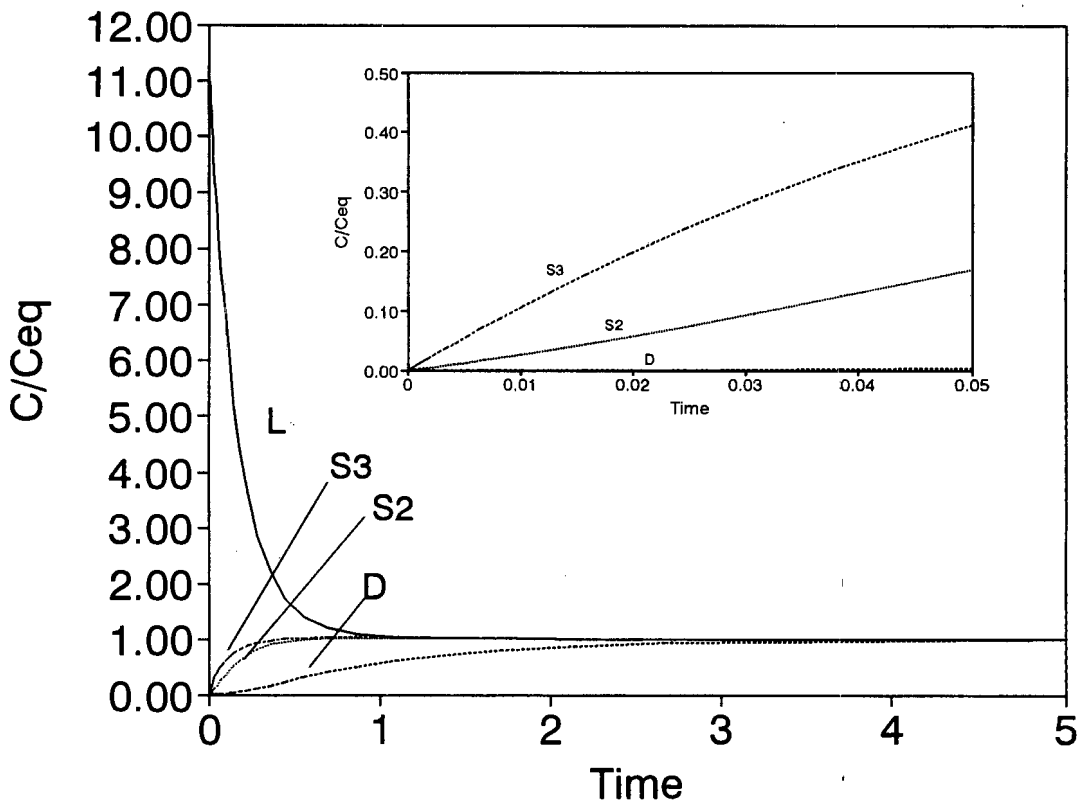

Figure 5.7a : Sensitivity Analysis for Model A, 1-Hexene Feed - Case 1

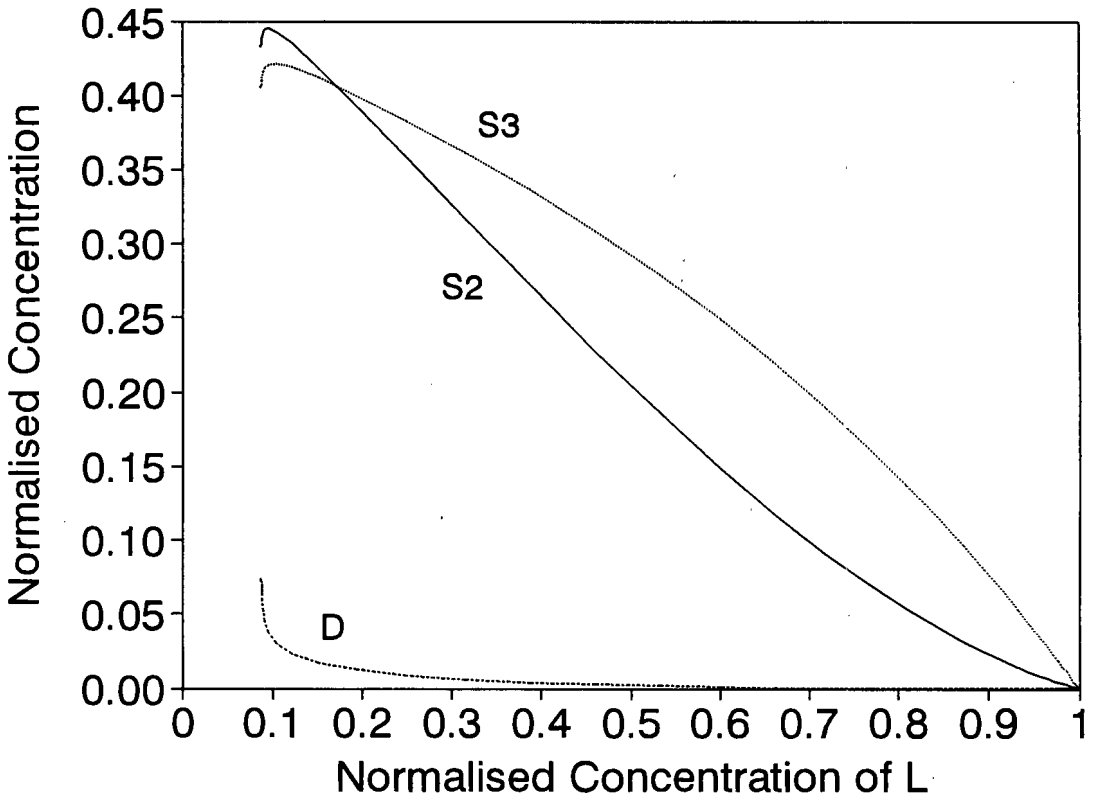

Figure 5.7b : Sensitivity Analysis for Model A, 1-Hexene Feed - Case 1

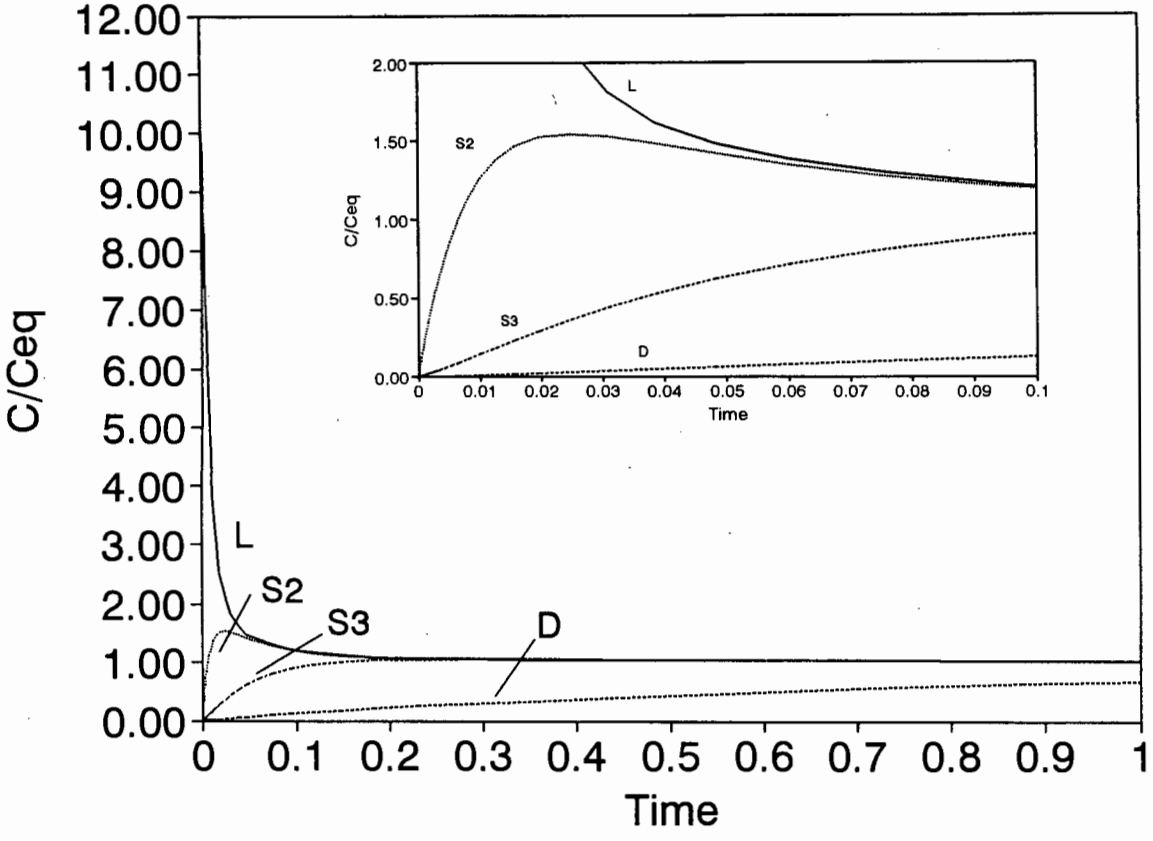

Figure 5.8a : Sensitivity Analysis for Model A, 1-Hexene Feed - Case 2

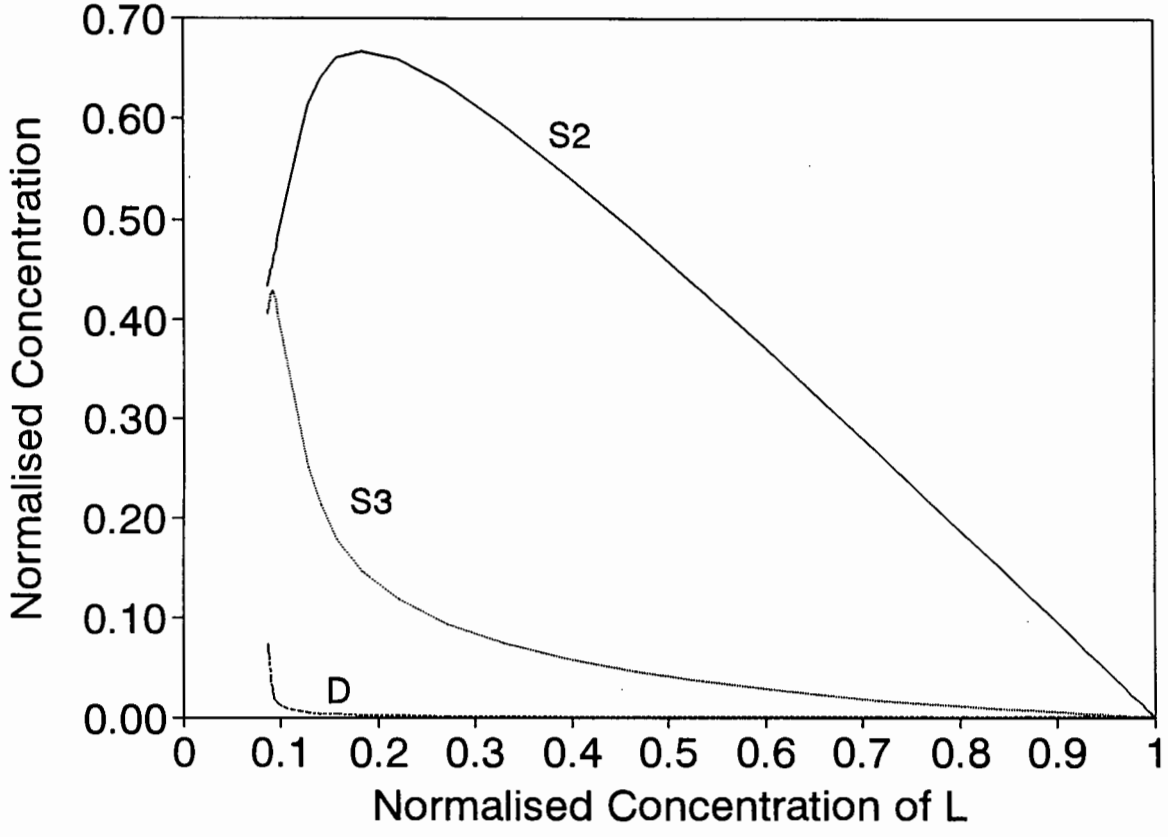

Figure 5.8b : Sensitivity Analysis for Model A, 1-Hexene Feed - Case 2

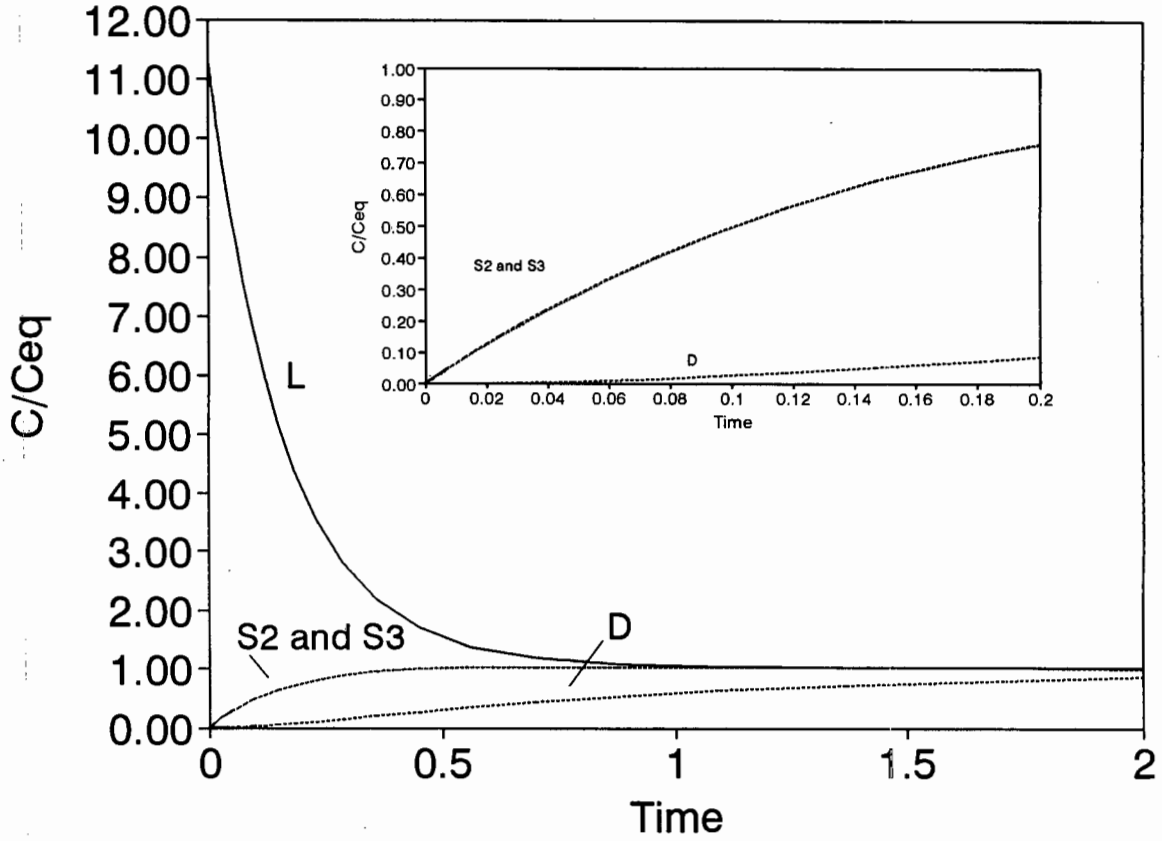

Figure 5.9a : Sensitivity Analysis for Model A, 1-Hexene Feed - Case 3

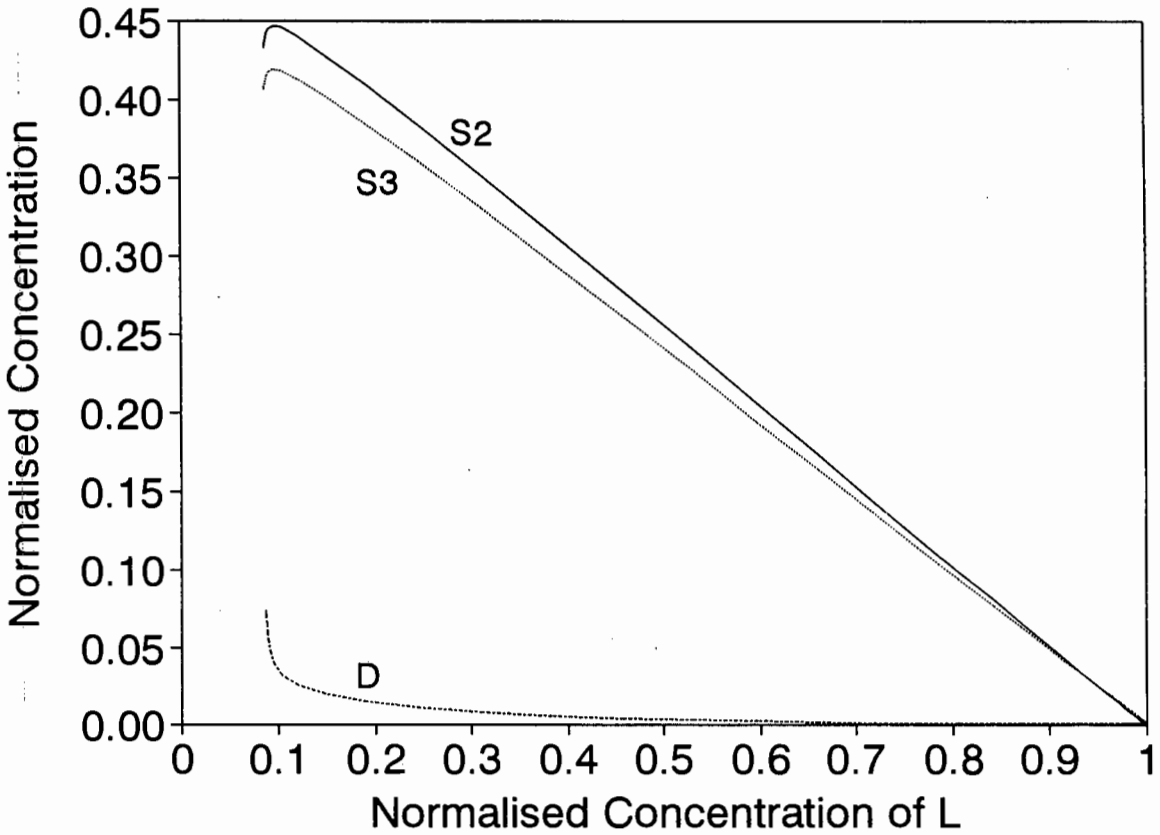

Figure 5.9b : Sensitivity Analysis for Model A, 1-Hexene Feed - Case 3

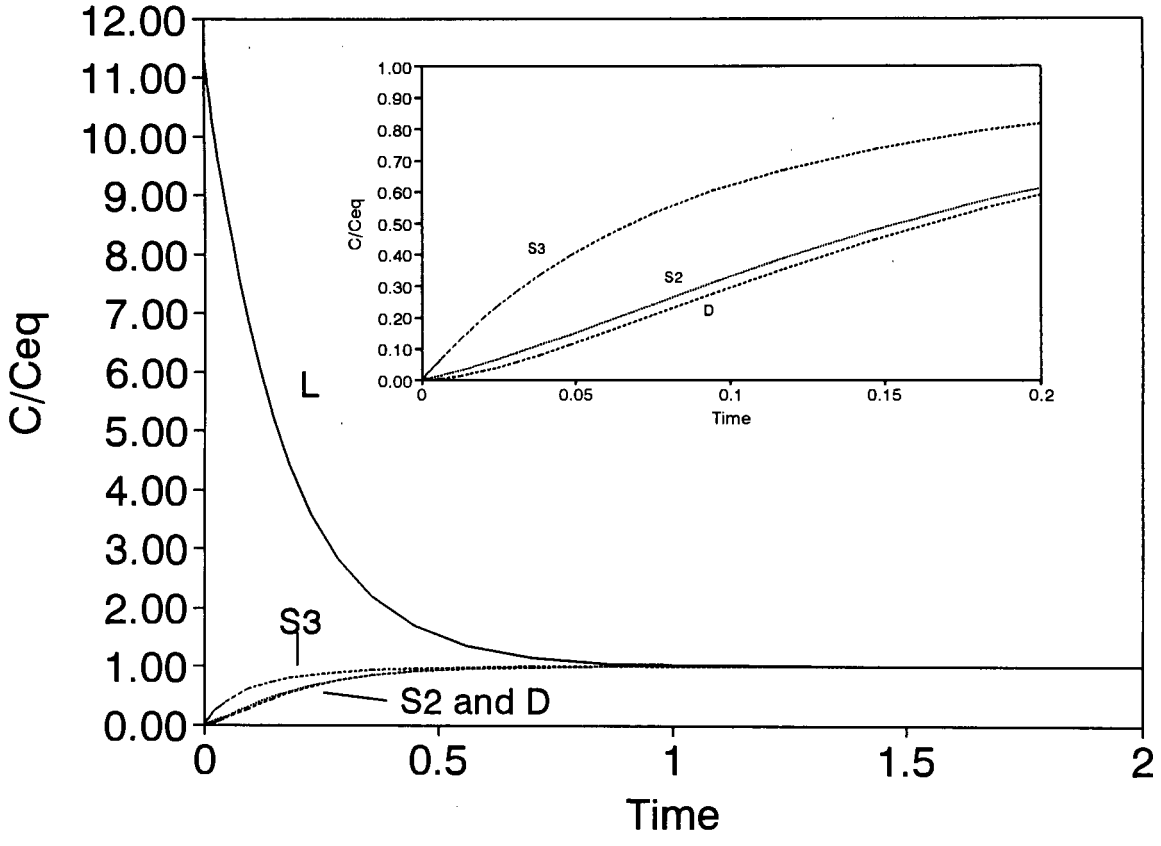

Figure 5.10a : Sensitivity Analysis for Model A, 1-Hexene Feed - Case 4

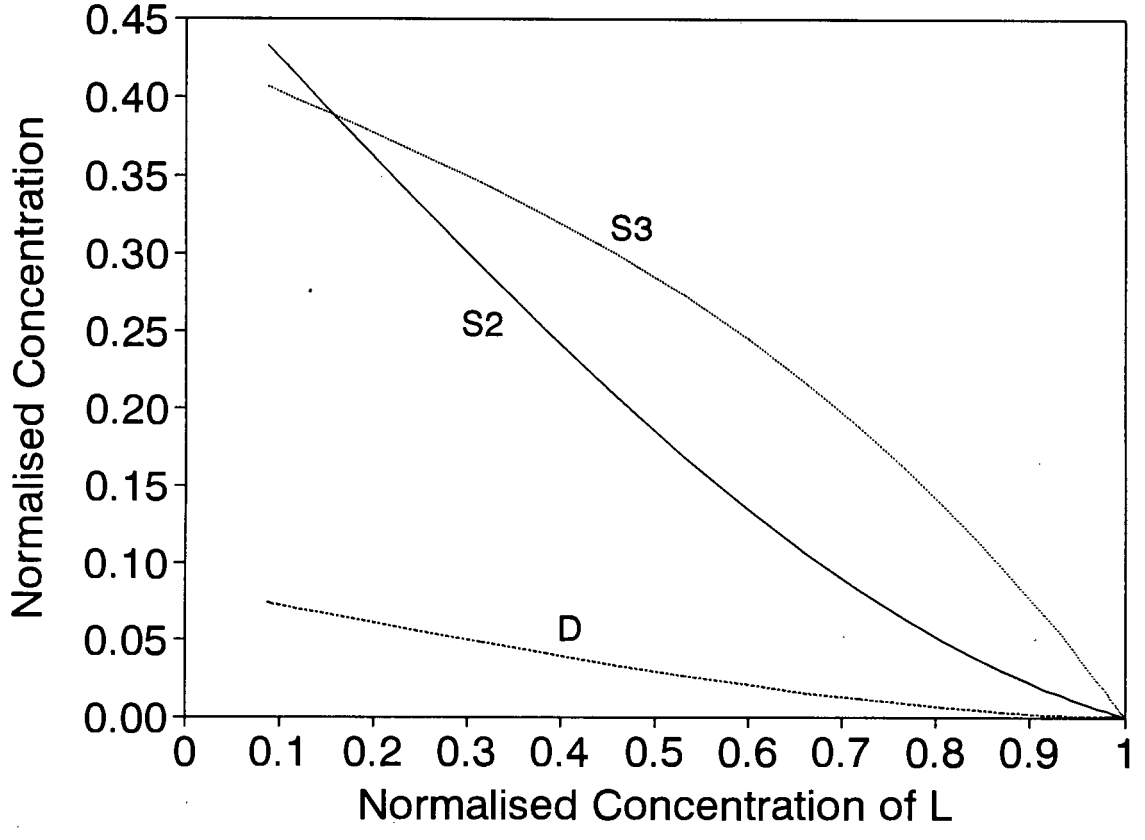

Figure 5.10b : Sensitivity Analysis for Model A, 1-Hexene Feed - Case 4

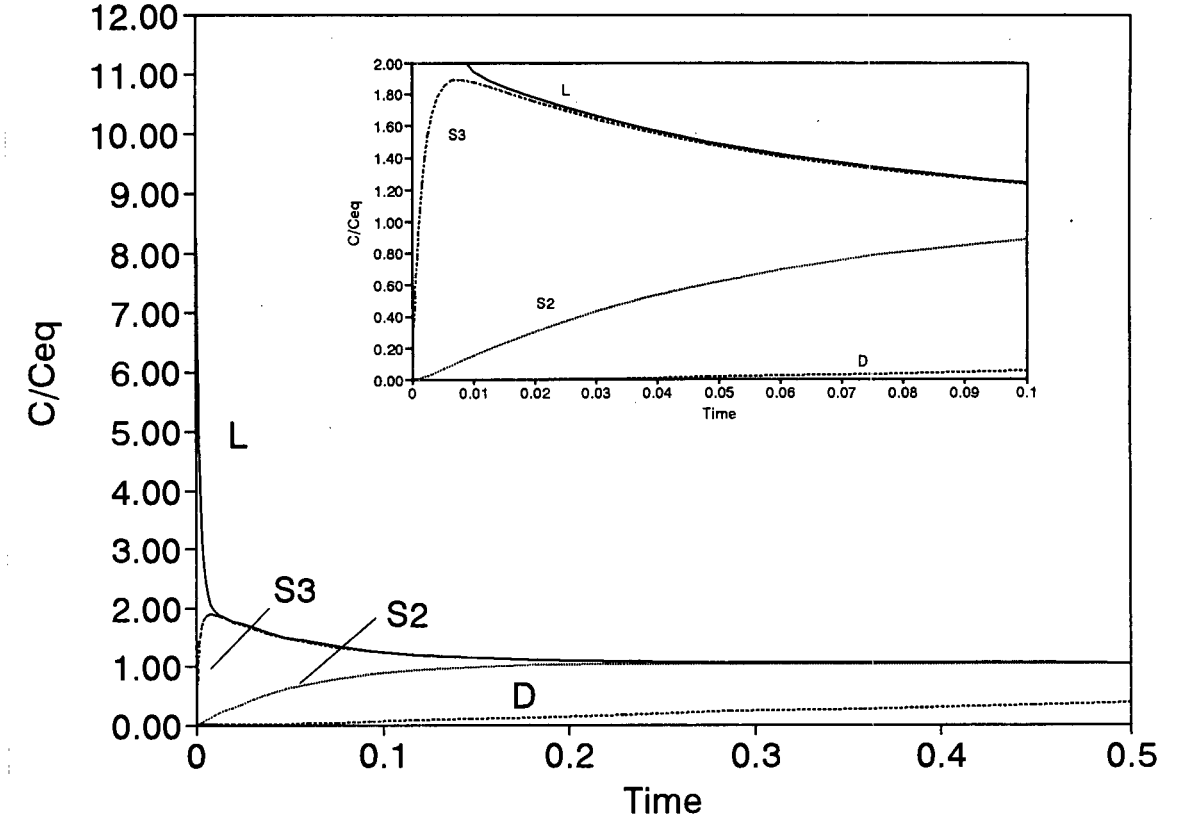

Figure 5.11a : Sensitivity Analysis for Model A, 1-Hexene Feed - Case 5

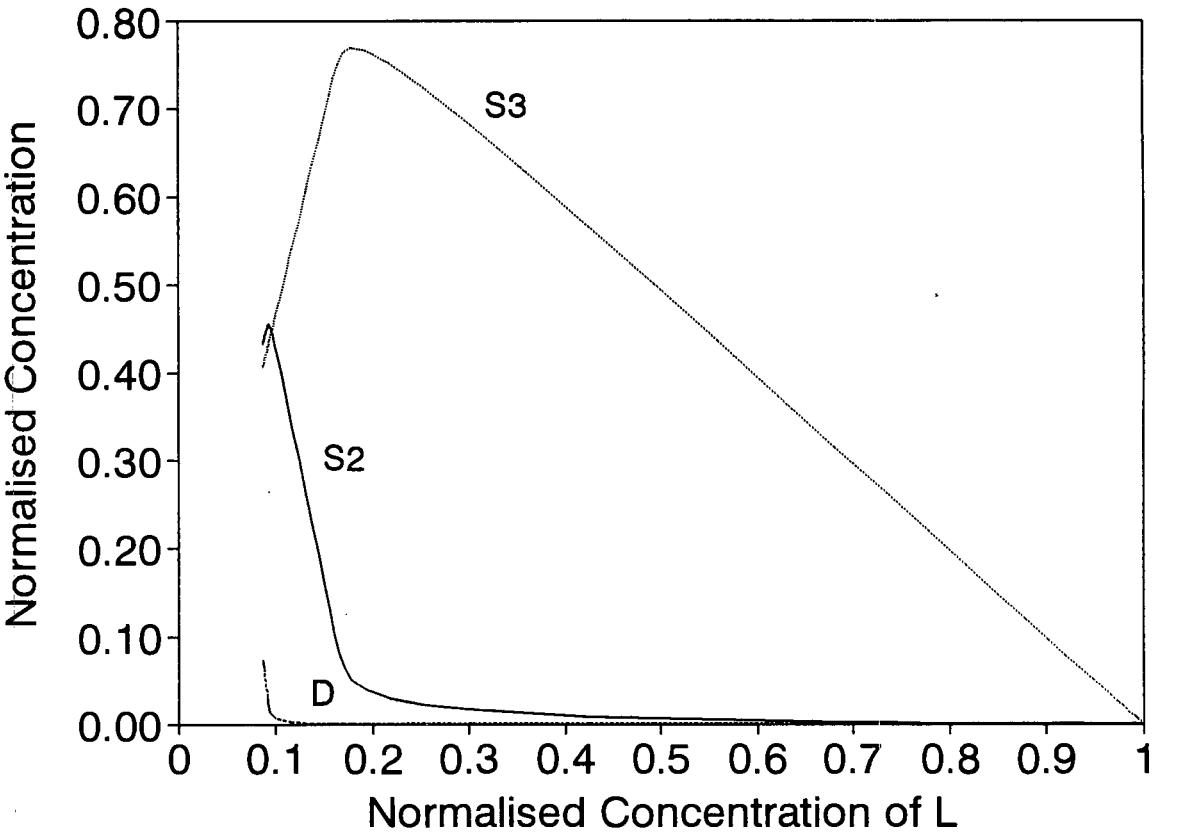

Figure 5.11b : Sensitivity Analysis for Model A, 1-Hexene Feed - Case 5

of magnitude. The behaviour of the reaction products observed in Figures 5.8a and 5.8b can be explained as follows. L now reacts rapidly to form S2 until a concentration exceeding S2's equilibrium value is reached. The rapid interconversion of S2 and L result in these components establishing equilibrium between themselves and then reacting together as one "pseudo-component" to form S3. This is illustrated by the coincident curves of S2 and L from t=0.1 onwards in Figure 5.8a. The S2+L group isomerises to form S3 until a concentration exceeding S3's equilibrium value is reached. A second "pseudo-component", S3+S2+L, now reacts to form D. Again, this can be seen by the merging of the curves for S3, S2 and L at t=0.2 in Figure 5.8a.

Case 3 - Here the rate constant for the methyl-shift reaction was increased. In comparison to **case 1**, there is in an increase in the rate of formation of S2. The C/C_{eq} versus time plot (Figure 5.9a) shows how the curves of S2 and S3 coincide and they behave as one product. Their combined slope close to zero time indicates primary product behaviour. These effects result from the almost instantaneous establishment of equilibrium between S2 and S3. There is no effect on the formation of D compared to **case 1**. Figure 5.9b also shows the similar behaviour of S2 and S3 for example, both of these products overshoot equilibrium to the same extent.

Case 4 - Here the rate constant for the formation of the double-branched isomer, D, is increased. This leads to an increase in the amount of D during the reaction and the approach to equilibrium for this compound is faster. S3 and S2 no longer overshoot equilibrium since S2 reacts more quickly to form D. S2 and D establish equilibrium between themselves early on in the reaction and behave as a single secondary product from a series reaction namely, L → S3 → S2+D. This secondary product behaviour is illustrated by the zero slope of S2+D close to the origin in Figure 5.10a. On the other hand, S3 behaves as the major, primary product. S2+D establish a local equilibrium with S3 before the S2+D+S3 group establishes overall equilibrium with L. This is seen in Figure 5.10a by observing the order in which the concentration curves merge with one another. In Figure 5.10b, S2 and S3 no longer overshoot their

equilibrium concentrations as in **case 1**.

Case 5 - Here the rate constant for the formation of S3 from L is increased. The curves for this case, Figures 5.11a and 5.11b, are identical to **case 2** except S3 has now been interchanged with S2. The explanation for the product concentration behaviour is the same as for **case 2**. L reacts rapidly to form S3, which overshoots its equilibrium concentration. Since the interconversion of S3 and L is rapid, these compounds establish local equilibrium and then react together to form S2 which also reaches a concentration exceeding its equilibrium value. Next, the three species, S2, S3 and L, establish local equilibrium. Following this S2+S3+L then react further to form D and reach overall equilibrium.

4-methyl-1-Pentene Isomerisation

Next, the case where 4-methyl-1-Pentene is the starting isomer is discussed :

Case 1 - S2 is now the starting component. Because the reaction of S2 to S3 is rapid, the concentration of S2 drops quickly with a corresponding sharp increase in the concentration of S3. S3 reaches a maximum concentration exceeding its equilibrium value. Due to the rapid methyl-shift reaction, equilibrium between S2 and S3 is established. This equilibrium between S2 and S3 is illustrated by the convergence of their curves in Figure 5.12a. When the curves for S2 and S3 coincide it implies that the ratio of their concentrations is constant. After equilibrium between them is reached, S2 and S3 react as one "pseudo-component" to form L and D. L is formed quicker than D and also exceeds its equilibrium concentration, but not to such a great extent as S3. L, S2 and S3 then establish equilibrium amongst each other. Again, this can be seen by the convergence of all three curves in Figure 5.12a. The ratios of the concentrations of L, S2 and S3 to each other is then constant for the rest of the reaction. This final "pseudo-component", L+S2+S3, reacts to form D.

Case 2 - For this case, the rate constant for the interconversion of S2 and L was increased.

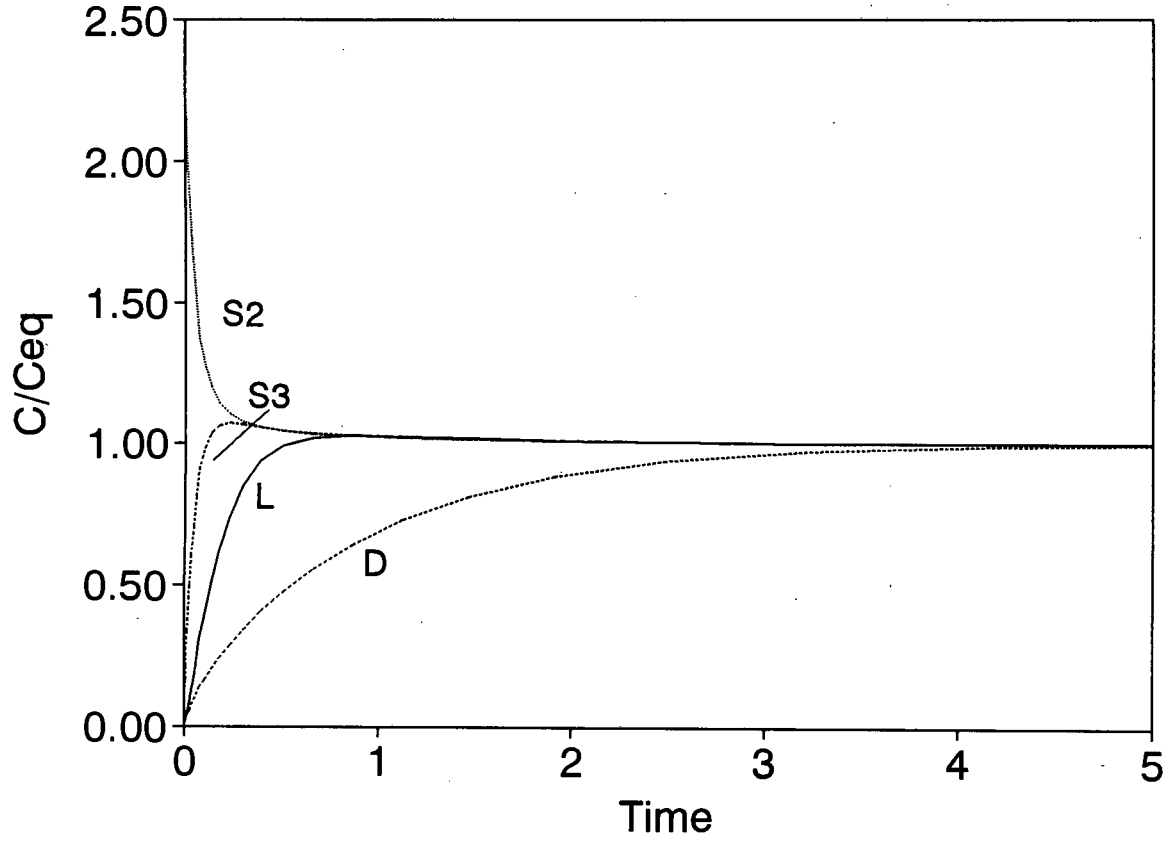

Figure 5.12a : Sensitivity Analysis for Model A, 4-methyl-1-Pentene Feed - Case 1

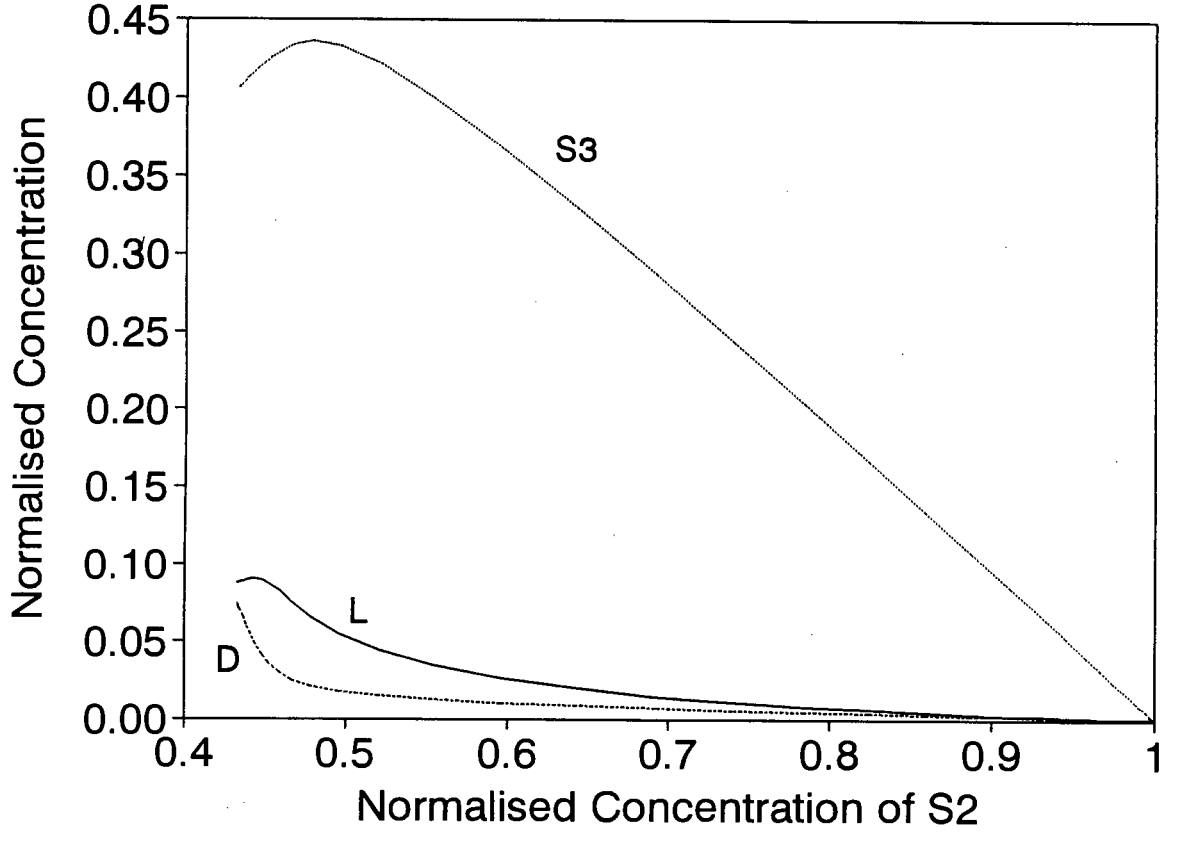

Figure 5.12b : Sensitivity Analysis for Model A, 4-methyl-1-Pentene Feed - Case 1

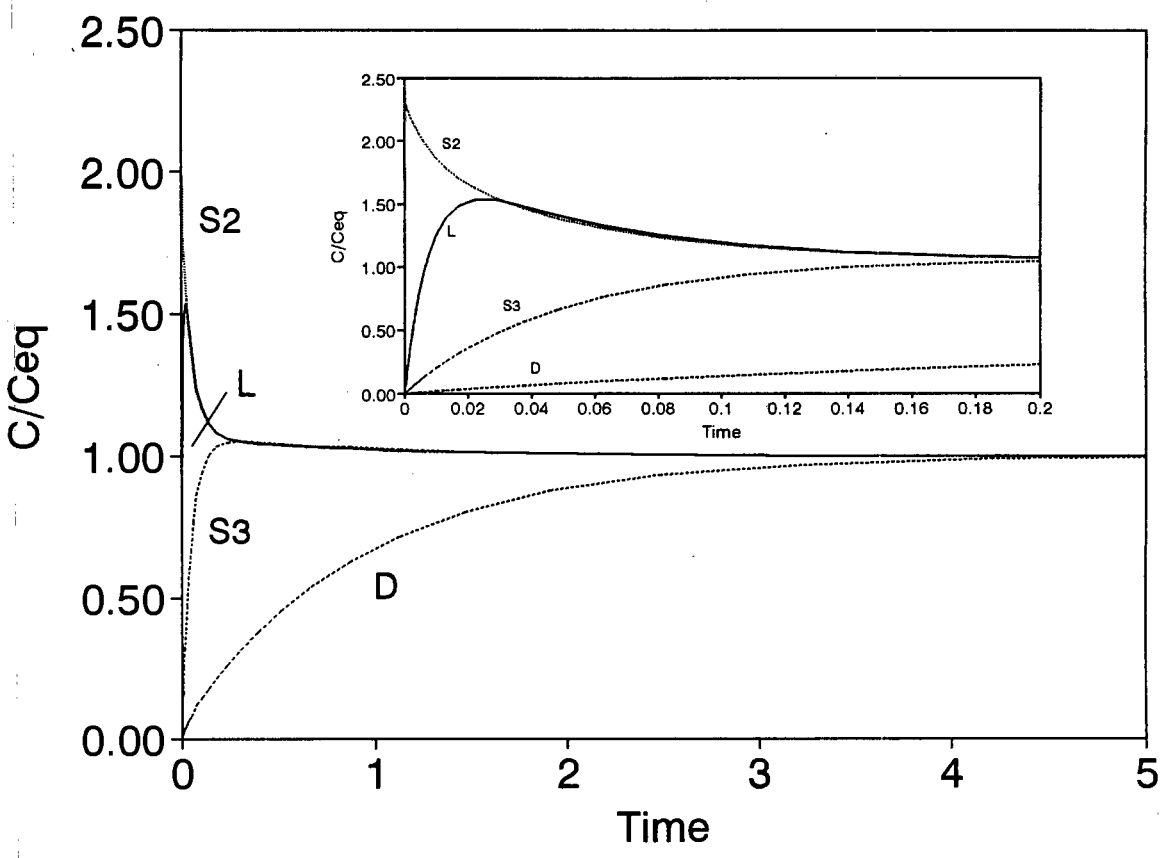

Figure 5.13a : Sensitivity Analysis for Model A, 4-methyl-1-Pentene Feed - Case 2

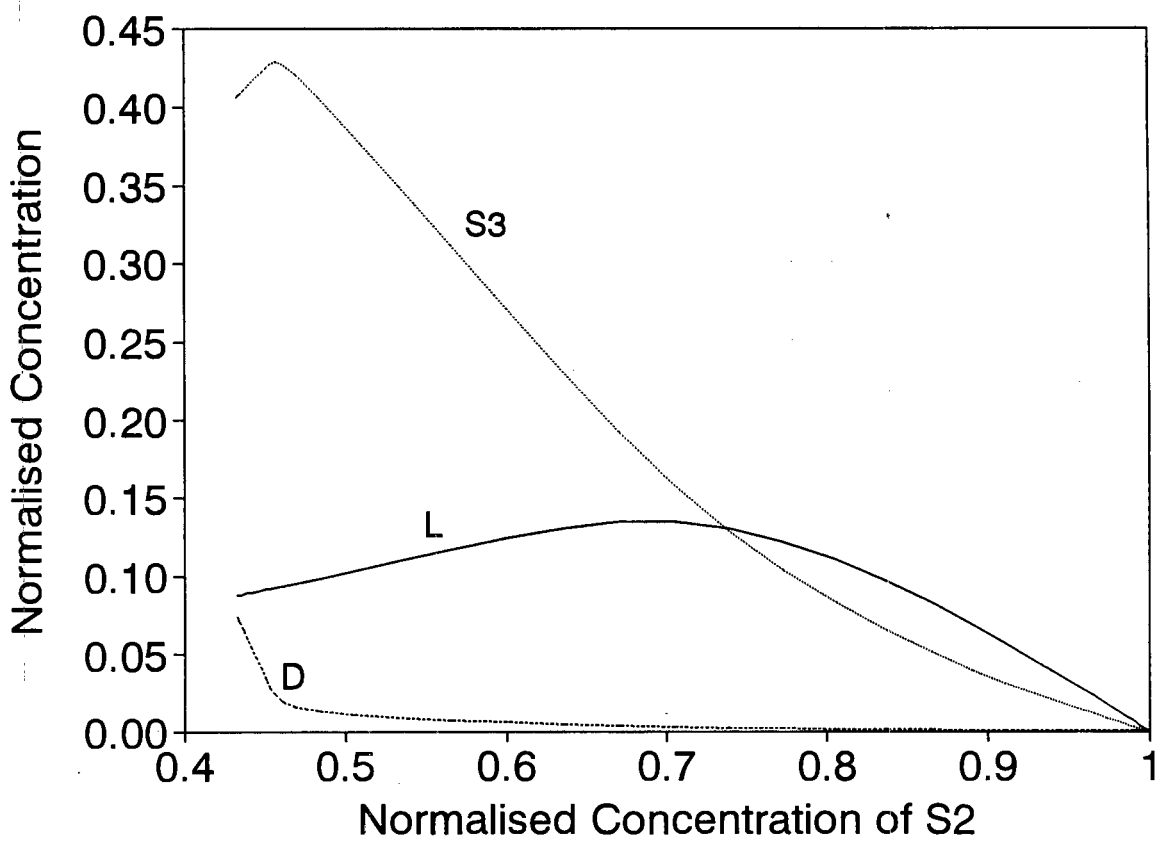

Figure 5.13b : Sensitivity Analysis for Model A, 4-methyl-1-Pentene Feed - Case 2

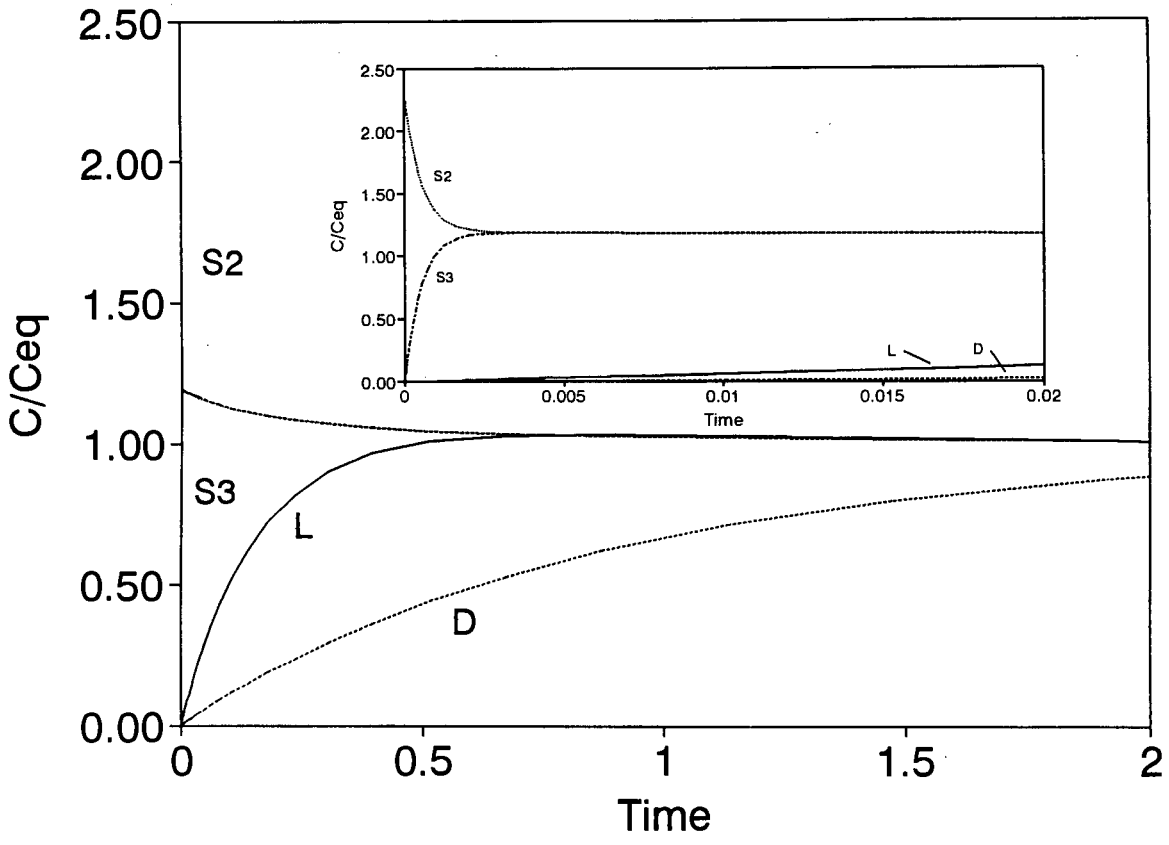

Figure 5.14a : Sensitivity Analysis for Model A, 4-methyl-1-Pentene Feed - Case 3

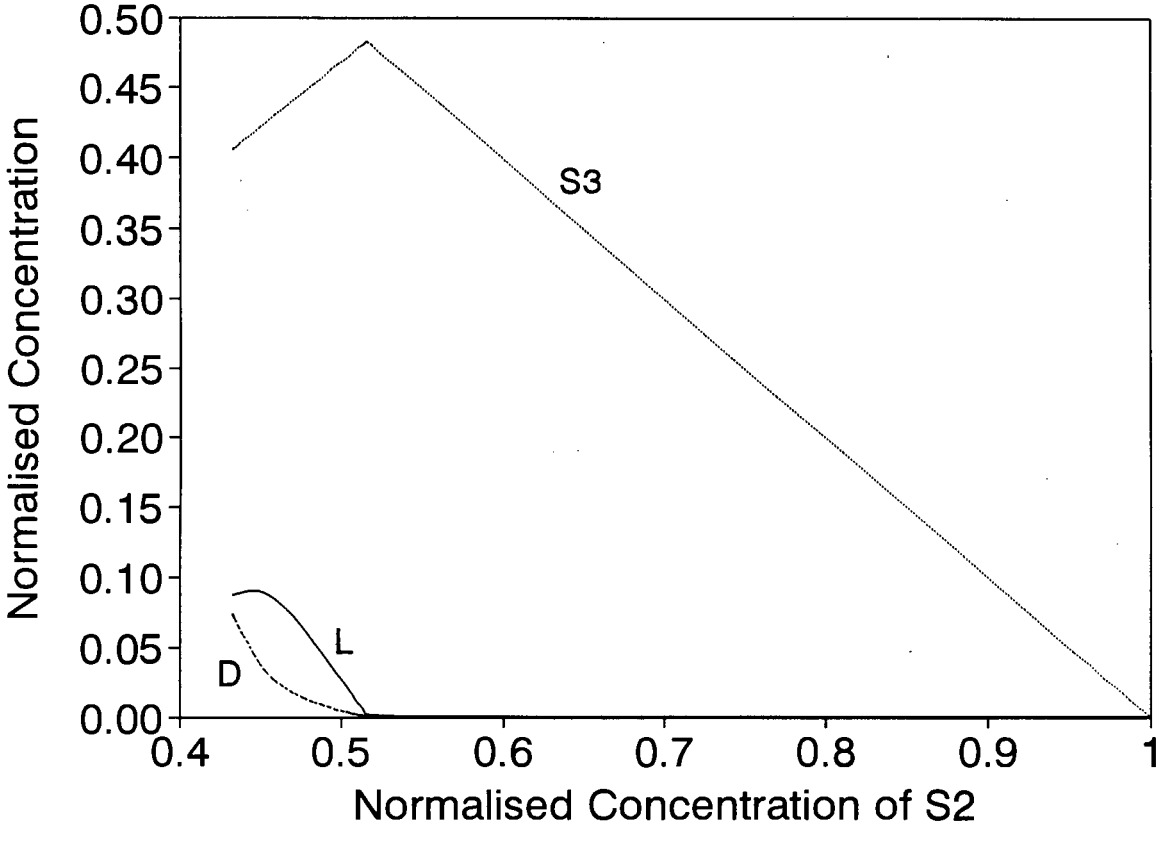

Figure 5.14b : Sensitivity Analysis for Model A, 4-methyl-1-Pentene Feed - Case 3

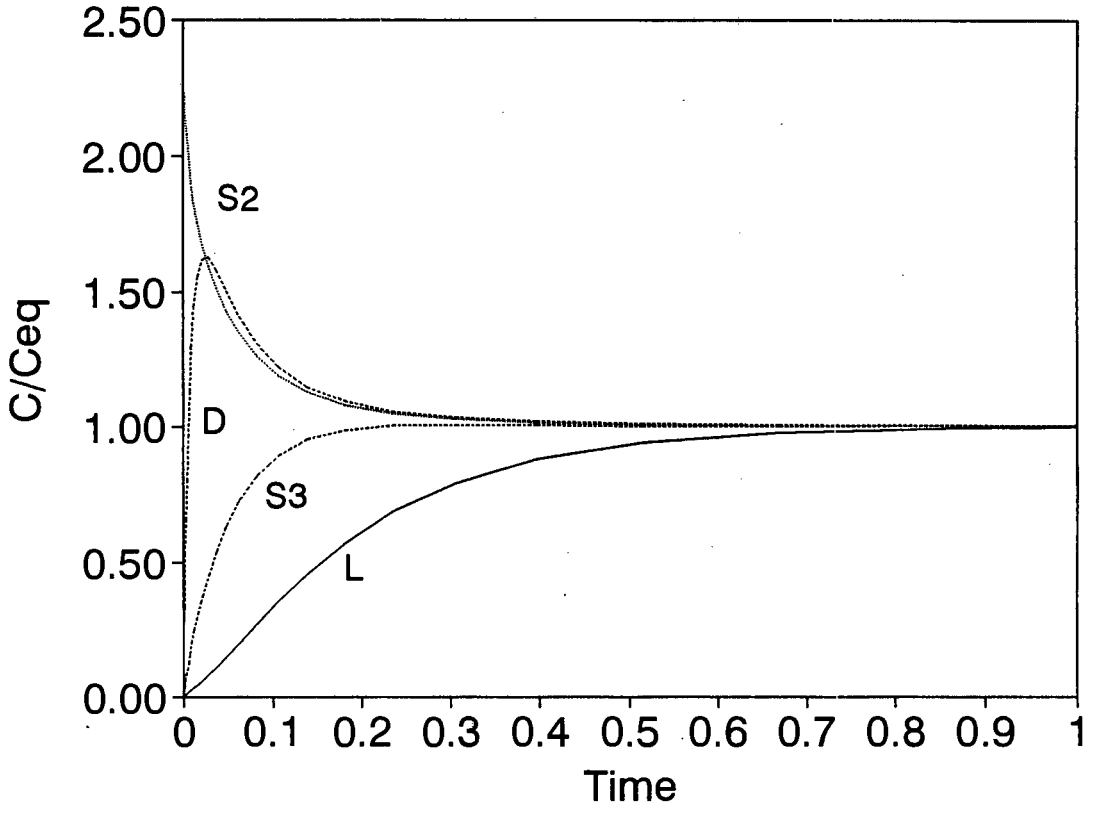

Figure 5.15a : Sensitivity Analysis for Model A, 4-methyl-1-Pentene Feed - Case 4

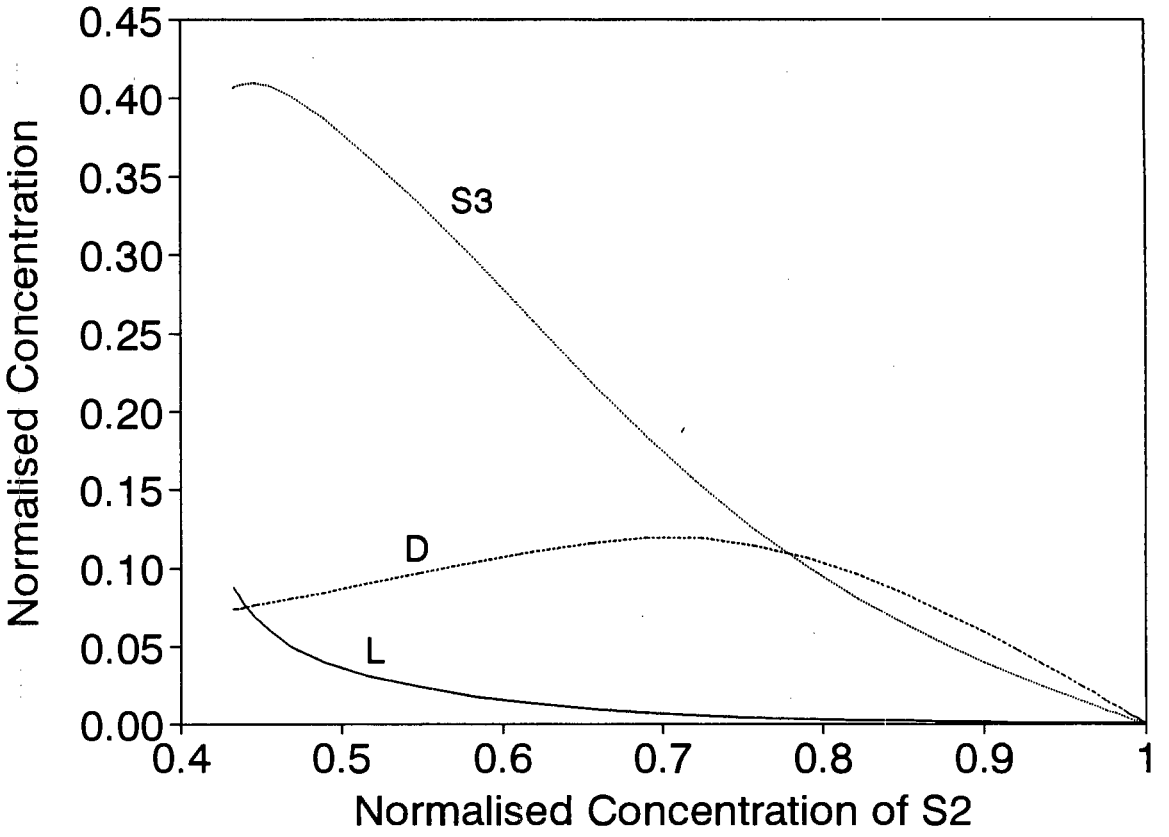

Figure 5.15b : Sensitivity Analysis for Model A, 4-methyl-1-Pentene Feed - Case 4

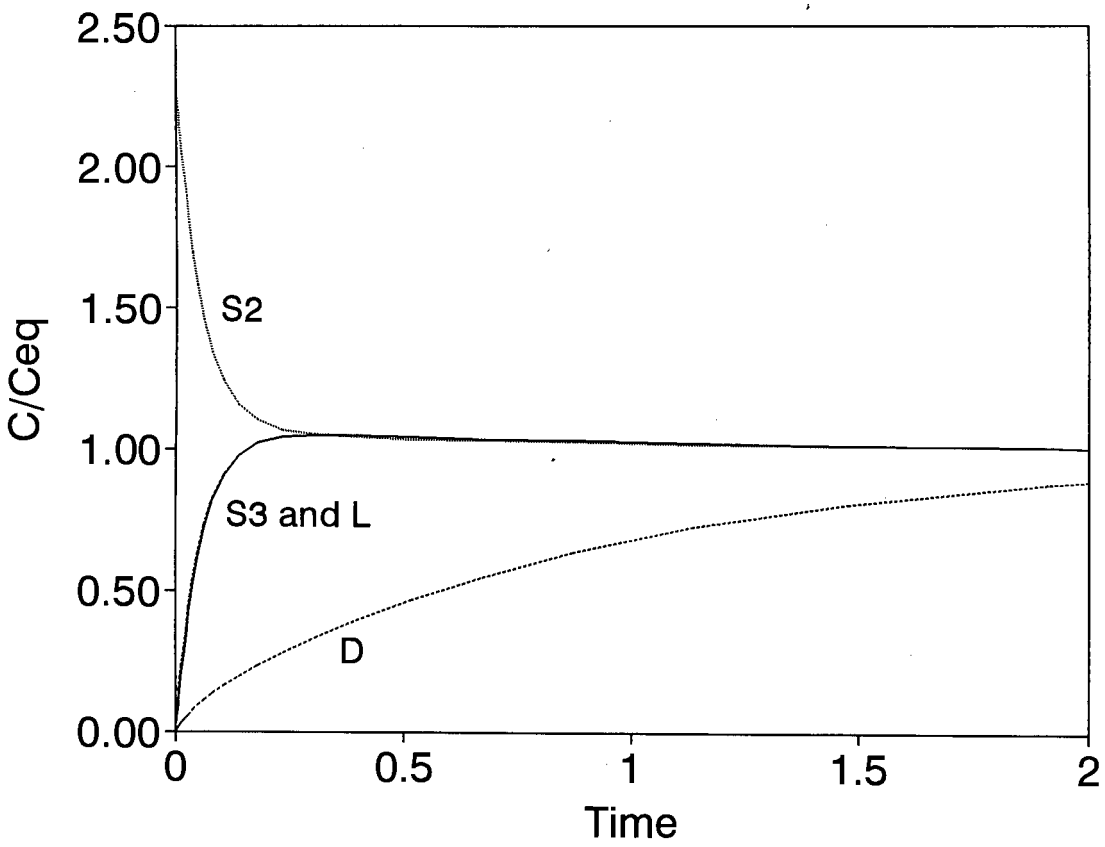

Figure 5.16a : Sensitivity Analysis for Model A, 4-methyl-1-Pentene Feed - Case 5

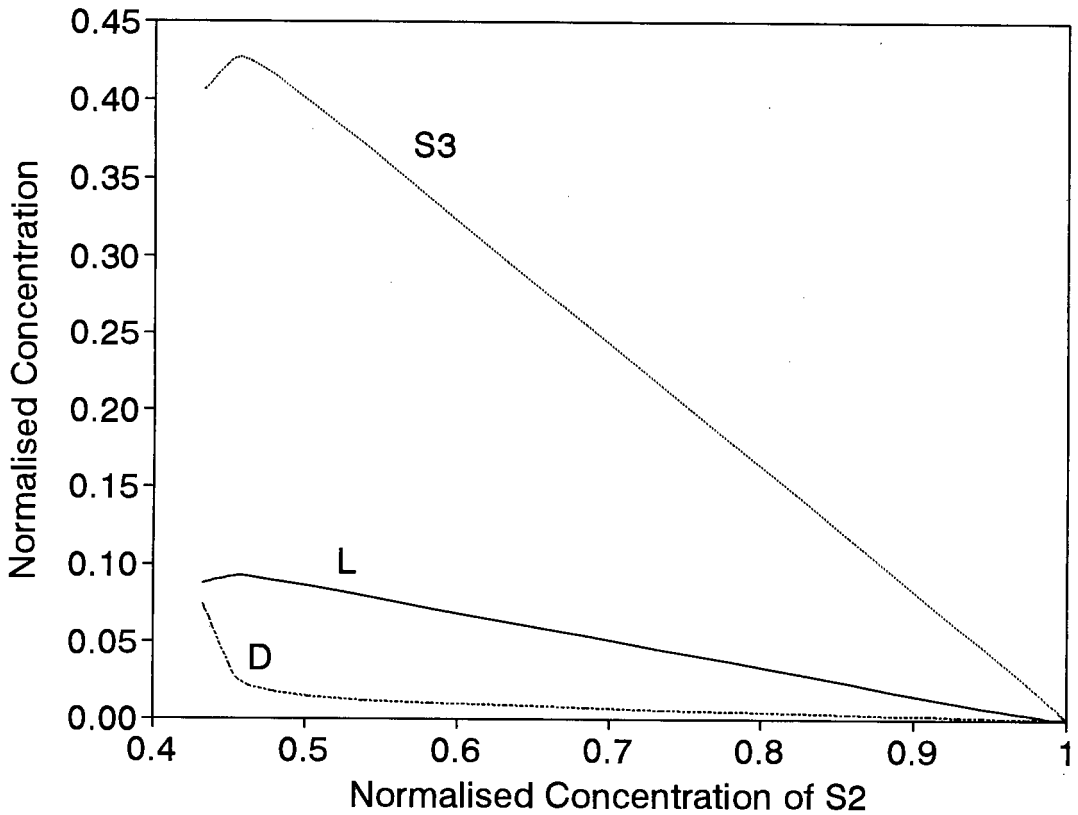

Figure 5.16b : Sensitivity Analysis for Model A, 4-methyl-1-Pentene Feed - Case 5

L is formed rapidly and quickly reaches a concentration exceeding its equilibrium value. Equilibrium between L and S2 is established early on in the reaction and this can be seen by the convergence of their curves in Figure 5.13a. The L+S2 group then isomerises to S3 and D. S3 is formed much faster than D and also exceeds its equilibrium concentration. Equilibrium between S2, S3 and L is now established and this group reacts to form D. Throughout most of the reaction the concentration of D is suppressed compared to **case 1**, due to the increase in the rate of formation of *L* (See Figure 5.13b).

Case 3 - Here the rate constant for the methyl-shift reaction was increased. For this case, equilibrium between S2 and S3 is established almost immediately on reaction of S2. This results in a sharp drop in the concentration of S2 and a sudden increase in the concentration of S3. As for **case 1**, S3 reaches a maximum concentration exceeding its equilibrium value. Once equilibrium between S2 and S3 is established these two compounds react as one to form L and D. In a manner similar to **case 1**, L is formed until it reaches a maximum concentration, exceeding its equilibrium value, and establishes equilibrium with the S2+S3 group. L+S2+S3 then reacts together to form D. Compared to **case 1**, the concentrations of L and D are suppressed during most of the reaction due to the rapid formation of S3 from S2 (See Figure 5.14b).

Case 4 - Here the rate constant for the formation the double-branched isomer is increased. This case is similar to **case 2**, except D and L have been interchanged. D now forms rapidly from S2 to reach a maximum concentration exceeding its equilibrium value. S2 and D then establish equilibrium, as seen by the convergence of their curves in Figure 5.15a. The S2+D group then reacts to form S3 and L. S3 is formed quicker than L and reaches a maximum concentration just exceeding its equilibrium value. S3 next establishes equilibrium with the S2+D group and all three components isomerise as one to form L until overall equilibrium is established.

Case 5 - In this case the rate constant for the interconversion of L and S3 was increased. Now L and S3 establish almost instantaneous equilibrium as can be seen by the

convergence of their curves in Figure 5.16a. S2 reacts to form the S3+L group and D. S3 and L form until they exceed their equilibrium concentrations and establish equilibrium with S2. The S3+L+S2 group then reacts further to form D until overall equilibrium is established.

5.5.1.3 Insights from Sensitivity Analysis

One of the purposes of the sensitivity analysis was to determine whether each model parameter had a distinct effect on the product spectra. If two or more model parameters had similar effects then it would not be possible to determine a unique set of rate constants that would describe the data accurately. The figures shown above for Model A clearly show that, depending on the initial conditions and the values of the rate constants relative to one another, widely differing concentration profiles can be obtained. The rate constant for the interconversion of S2 and S3, k_4, produces the greatest difference in product spectrum. In other words, this parameter should be determined with the greatest accuracy.

The effect of the different rate constants becomes most apparent when the C/C_{eq} versus time curves are studied. The effect of the different model parameters is not as clear over the entire conversion range when the normalised concentration versus normalised feed concentration curves are studied. Therefore when determining the reaction pathways, experimental data in the form of concentration versus time curves is preferred.

If the rate constant for a particular isomerisation reaction exceeds that for all other isomerisation reactions, the species involved in this reaction establish a local equilibrium amongst themselves early on in the reaction. This local equilibrium group then reacts and forms as one "pseudo-component" until overall equilibrium is reached. Once local equilibrium between two of the reacting species is established no information can be obtained regarding the rate constants for their interconversion. Thus, experimental data should be obtained over as wide a conversion range as possible.

Another important result from the sensitivity analysis was that the slopes as $t \rightarrow 0$ do not

always provide an unequivocal indicator as to whether a product is primary or secondary. Large rate constants for the formation of secondary products can lead to the assumption that the product is primary if only the slope close to zero time is considered.

5.5.1.4 Model Parameter Estimation

For Model A a Turbo-Pascal program, including a Nelder-Mead optimization routine (Nelder and Mead (1965)), was written in order to calculate those rate constants that gave the best fit to the experimental data. As mentioned in section 5.4 above, the experimental data was in the form of normalised product concentration versus normalised feed concentration. For a particular set of rate constants, the software integrated the model rate equations analytically, using the method of eigenvectors and eigenvalues outlined above, and compared the experimental with the model concentrations. The values of the rate constants were judged to have converged when the sum of the relative squared error between the model and experimental concentrations were less than 10^{-5}. As the quality of the experimental data was shown to be good (see Chapter 2), it was decided to give all product concentrations equal weighting during the fitting procedure using the relative error. The relative error used is defined as follows:

$$Error = \sqrt{\frac{\sum_{1}^{i=n} (relative\ error)^2}{n}} \tag{5.38}$$

where,

$$relative\ error = \frac{C_{\exp} - C_{model}}{C_{\exp}} \tag{5.39}$$

When fitting the data, care was taken to determine whether the solution obtained was unique. This was done by varying the initial guess over a wide range of starting guesses. As an additional check the experimental data was replaced by model data and the rate constants calculated. If the original solution was unique then the program would produce the rate

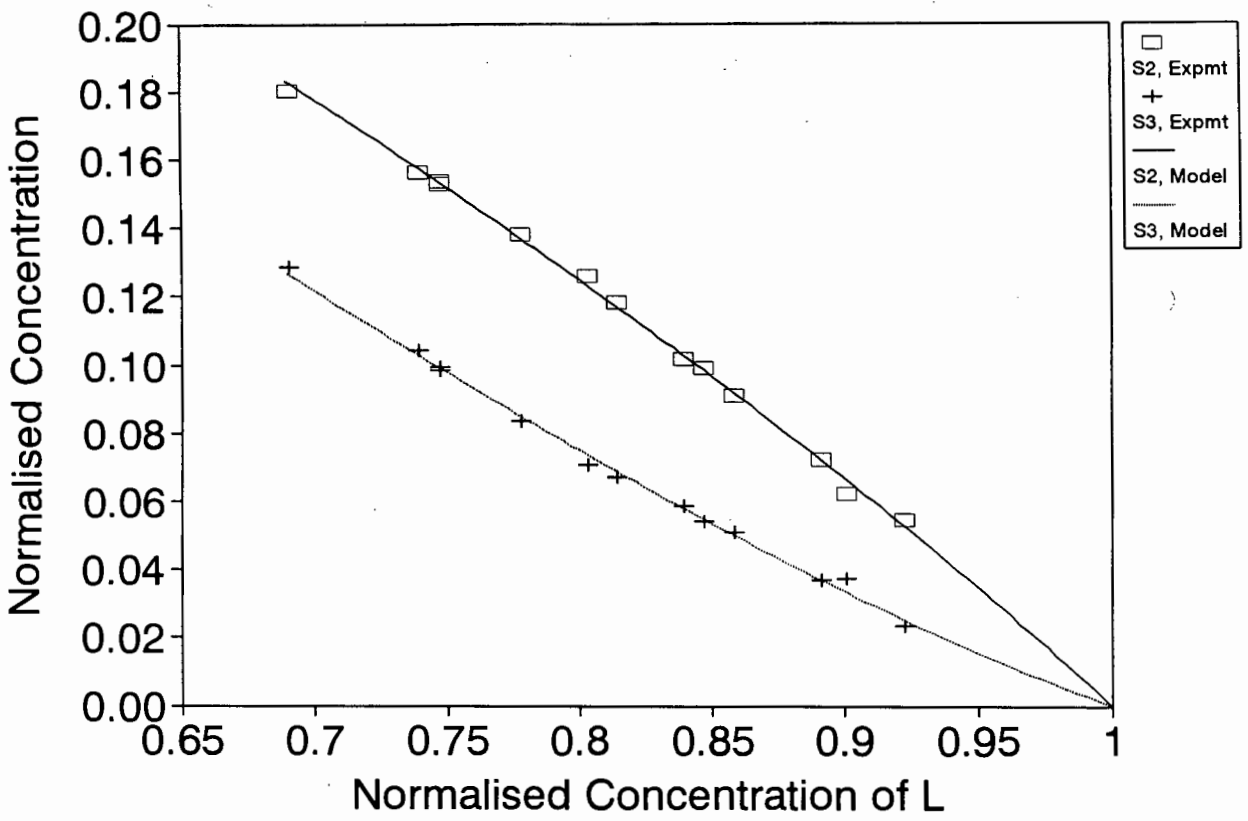

Figure 5.17 : Fit of Model A to 1-Hexene Isomerisation Data

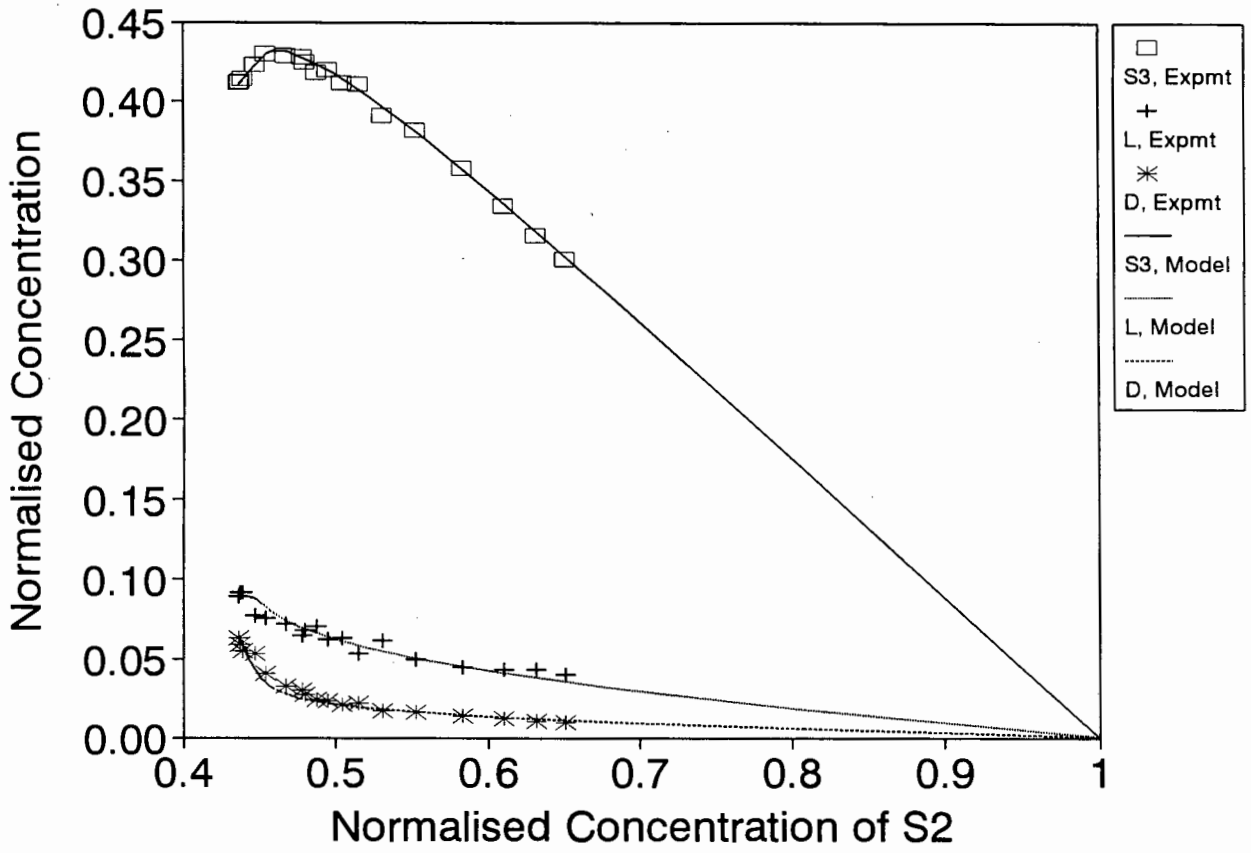

Figure 5.18 : Fit of Model A to 4-methyl-1-Pentene Isomerisation Data

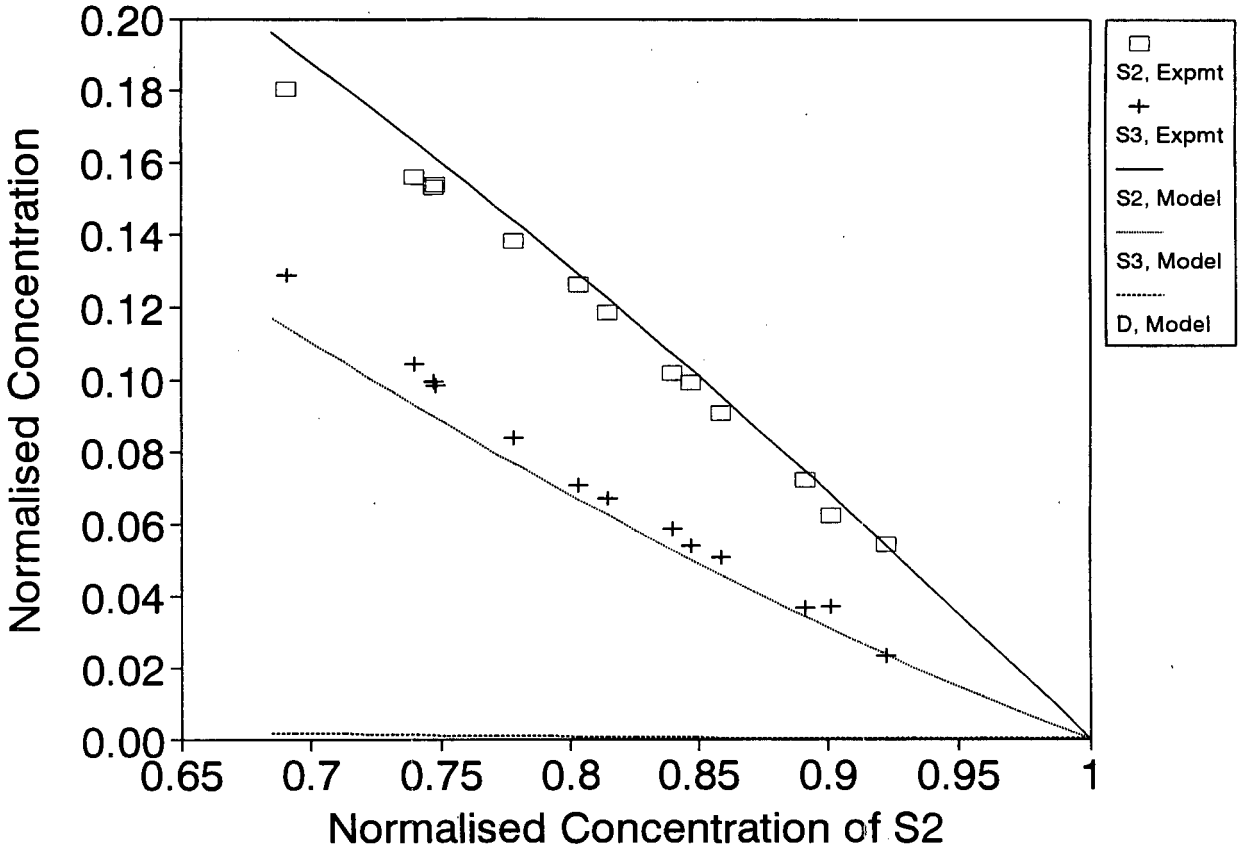

Figure 5.19 : Fit of Model A to 1-Hexene Isomerisation Data - Final Set of Rate Constants

constants that generated the data. This indeed was found to be the case.

Because of the form of the experimental data, namely product concentration versus feed concentration, only relative rate constants could be calculated. When L was fed the concentration of D formed was too low to be detected. However, from the L isomerisation data the rate constants for the isomerisation of L $\rightleftharpoons$ S2 relative to the rate constants for L $\rightleftharpoons$ S3 could be determined. The rate constant for the methyl-shift reaction S2 $\rightleftharpoons$ S3 could also be determined. On the other hand, when S2 was fed the rate constants for S2 $\rightleftharpoons$ D, S2 $\rightleftharpoons$ S3 and S2 $\rightleftharpoons$ L could be calculated. Therefore, the L isomerisation data was fitted first in order to determine the values of k1/k2 relative to k7/k8. The S2 isomerisation data was modelled next, using the values of k1/k2 and k7/k8 obtained from the L isomerisation data. The S2 data gave the values of k3/k4 and k5/k6. Therefore a complete set of rate constants could be calculated using both sets of data.

Once k3/k4 and k5/k6 were established using the S2 isomerisation data, these constants were fixed and then the rate constants k1/k2 and k7/k8 were recalculated from the 1-hexene data. However, no improvement in the final set of rate constants was obtained.

Table 5.6 shows the set of rate constants obtained from fitting the L isomerisation data. The fit of the model to the experimental data is shown in Figure 5.17.

Once the values of k1/k2 and k7/k8 were established from the L isomerisation data, the S2 isomerisation data was used to calculated the remaining constants. This is shown in Table 5.7. The fit of Model A to the S2 isomerisation data is shown in Figure 5.18. Model A fits both sets of hexene isomerisation data well. The isomerisation reaction that is common to both sets of data namely, S2 $\rightleftharpoons$ S3, has similar values for its rate constants from both sets of data. The final unique set of rate constants, shown in Table 5.7, was used to predict the L isomerisation data and this is shown in Figure 5.19. The error between the 1-hexene data and Model A using the final set of rate constants is 10.7%. Although this error is larger than for fitting the 1-hexene data alone, it is still acceptable.

Table 5.8 : Rate Constants for Various Hydrocarbon Rearrangements

	Hexylcarbenium Ions - Martens and Jacobs (1990)		Olefins - This Work
Reaction	$k_{127°C}$ (10^3 s^{-1})	$k_{227°C}$ (10^5 s^{-1})	$k_{250°C}$ (relative)
1,2-methyl shift - Type A e.g. S2 → S3	200	100	11
Di-branched to mono-branched - Type B e.g. D → S2	5	4	1.8
Mono-branched to unbranched - Type B e.g. S2 → L	0.9	1	1

5.5.2 Model B

5.5.2.1 Model Development

In Chapter 3 it was indicated that during propene oligomerisation over H-ZSM-5 the adsorption of the feed and product olefins could influence the rates of reaction. Therefore, the next step in complexity in modelling the isomerisation of hexenes was to account for the effects of hexene isomer adsorption. Thus Model B was proposed, which is a Langmuir-Hinshelwood Model with surface reaction controlling (Smith, (1981), pages 360-367). It was decided only to model the S2 isomerisation data using this model since this set of data contained significant concentrations of product D. Thus, as this experimental data provides no information regarding the isomerisation reaction between L and S3 this reaction was not included in the model.

The following steps occur during the reaction :

$$S2 + X \leftrightharpoons S2{\cdot}X \qquad \textit{Adsorption} \qquad (5.40)$$

$$\left.\begin{array}{l} S2{\cdot}X \underset{k_{cat1}'}{\overset{k_{cat1}}{\rightleftharpoons}} S3{\cdot}X \\ S2{\cdot}X \underset{k_{cat2}'}{\overset{k_{cat2}}{\rightleftharpoons}} D{\cdot}X \\ S2{\cdot}X \underset{k_{cat3}'}{\overset{k_{cat3}}{\rightleftharpoons}} L{\cdot}X \end{array}\right\} \quad \textit{Reaction} \qquad (5.41)$$

X represents an active site on the catalyst.

If surface reaction is controlling then both the adsorption and desorption steps will be at equilibrium i.e.,

$$(C_{S2}^*)_{eq} = K_{S2}C_{S2}C_v^* \qquad (5.43)$$

$$(C_L^*)_{eq} = K_L C_L C_v^* \qquad (5.44)$$

$$(C_{S3}^*)_{eq} = K_{S2}C_{S3}C_V^* \qquad (5.45)$$

$$(C_D^*)_{eq} = K_D C_D C_v^* \qquad (5.46)$$

Where C_i^* is the concentration of adsorbed species i, C_v^* is the concentration of vacant acid sites and K_j is the equilibrium constant of adsorption.

The rate of formation on the surface is given by :

$$\begin{aligned} r_{S2} &= k'_{cat1}C_{S3}^* + k'_{cat2}C_D^* + k'_{cat3}C_L^* - (k_{cat1} + k_{cat2} + k_{cat3})C_{S2}^* \\ &= k_{cat1}\left(\frac{1}{K_{cat1}}C_{S3}^* - C_{S2}^*\right) + k_{cat2}\left(\frac{1}{K_{cat2}}C_D^* - C_{S2}^*\right) + k_{cat3}\left(\frac{1}{K_{cat3}}C_L^* - C_{S2}^*\right) \end{aligned} \qquad (5.47)$$

$$r_{S3} = k_{cat1} C^*_{S2} - k'_{cat1} C^*_{S3} \tag{5.48}$$

$$r_D = k_{cat2} C^*_{S2} - k'_{cat2} C^*_D \tag{5.49}$$

$$r_L = k_{cat3} C^*_{S2} - k'_{cat3} C^*_L \tag{5.50}$$

$$C^*_m = C^*_v + C^*_{S2} + C^*_{S3} + C^*_D + C^*_L \tag{5.51}$$

Where k_{cati} and k'_{cati} are the forward and reverse rate constants for the adsorbed species on the surface and the K_{cati} are the equilibrium constants for the surface reaction.

C_m^* is the total number of acid sites and is equivalent to the total number of Al atoms as obtained from atomic adsorption analysis of the catalyst. $C_m^* = 0.396$ mmol/$g_{cat.}$

Additionally,

$$K_1 = \left(\frac{C_{S3}}{C_{S2}}\right)_{eq} = \frac{C^*_{S3}/K_{S3}C^*_v}{C^*_{S2}/K_{S2}C^*_v} = \frac{K_{S2}}{K_{S3}}\left(\frac{C^*_{S3}}{C^*_{S2}}\right)_{eq} = \frac{K_{S2}}{K_{S3}} K_{cat1} \tag{5.52}$$

or,

$$K_{cat1} = K_1 \frac{K_{S3}}{K_{S2}} \tag{5.53}$$

$$K_{cat2} = K_2 \frac{K_D}{K_{S2}} \qquad K_2 = \left(\frac{C_D}{C_{S2}}\right)_{eq} \tag{5.54}$$

$$K_{cat3} = K_3 \frac{K_L}{K_{S2}} \qquad K_3 = \left(\frac{C_L}{C_{S2}}\right)_{eq} \tag{5.55}$$

Rearranging (5.51) and substituting for C_v^* and for K_{cati} in (5.47) - (5.50) the following equations are obtained:

$$\frac{dC_{S2}}{dt} = \frac{C_m^* K_{S2}\left[k_{cat1}\left(\frac{C_{S3}}{K_1} - C_{S2}\right) + k_{cat2}\left(\frac{C_D}{K_2} - C_{S2}\right) + k_{cat3}\left(\frac{C_L}{K_3} - C_{S2}\right)\right]}{(1 + K_D C_D + K_L C_L + K_{S3} C_{S3} + K_{S2} C_{S2})} \tag{5.56}$$

$$\frac{dC_{S3}}{dt} = \frac{C_m^* K_{S2} k_{cat1}\left(C_{S2} - \frac{C_{S3}}{K_1}\right)}{(1 + K_D C_D + K_L C_L + K_{S3} C_{S3} + K_{S2} C_{S2})} \tag{5.57}$$

$$\frac{dC_D}{dt} = \frac{C_m^* K_{S2} k_{cat2}\left(C_{S2} - \frac{C_D}{K_2}\right)}{(1 + K_D C_D + K_L C_L + K_{S3} C_{S3} + K_{S2} C_{S2})} \tag{5.58}$$

$$\frac{dC_L}{dt} = \frac{C_m^* K_{S2} k_{cat3}\left(C_{S2} - \frac{C_L}{K_3}\right)}{(1 + K_D C_D + K_L C_L + K_{S3} C_{S3} + K_{S2} C_{S2})} \tag{5.59}$$

5.5.2.2 Sensitivity Analysis

A sensitivity analysis was performed to examine the effect of various model parameters on the concentration profiles obtained. The parameters were varied in the manner shown in Table 5.9 :

Table 5.9 Model B - Parameters Used in Sensitivity Analysis				
Case	K_{S2}	K_{S3}	K_D	K_L
1	250	250	250	250
2	2500	250	250	250
3	250	2500	250	250
4	250	250	2500	250
5	250	250	250	2500

The units of the equilibrium constants of adsorption are $cm^3/mmol$. Each case examines the effect of increasing each equilibrium constant of adsorption by 1 order of magnitude. Since all species in this reaction are isomers it is unlikely that their equilibrium constants will differ by more than 1 order of magnitude from one another. The values shown in Table 5.10 are arbitrary since it was not possible to obtain estimates of equilibrium constants of adsorption for C_6 olefins over H-ZSM-5 at 250°C and 5MPa. The following set of relative surface rate constants were chosen based on the values obtained from Model A :

$k_{cat1} = 10.0,\ k_{cat2} = 1.0,\ \ k_{cat3} = 1.0$

The results of this sensitivity analysis are shown in Figures 5.20 to 5.21.

Case 1 - This is the base case and is shown in Figures 5.20a and 5.20b. Since the equilibrium constants of adsorption are the same for all of the hexene skeletal groups, this case is equivalent to the homogeneous model.

Case 2 - Here K_{S2} was increased and the results shown in Figure 5.21a and 5.21b. When the time required to reach equilibrium (C/Ceq = 1) in Figure 5.20a is compared to that in 5.21a, it can be seen that an increase in all reaction rates has occurred. This is due to the increase in the adsorption of the feed molecule. The selectivity to the various isomers however, remains unchanged. (Figure 5.21b)

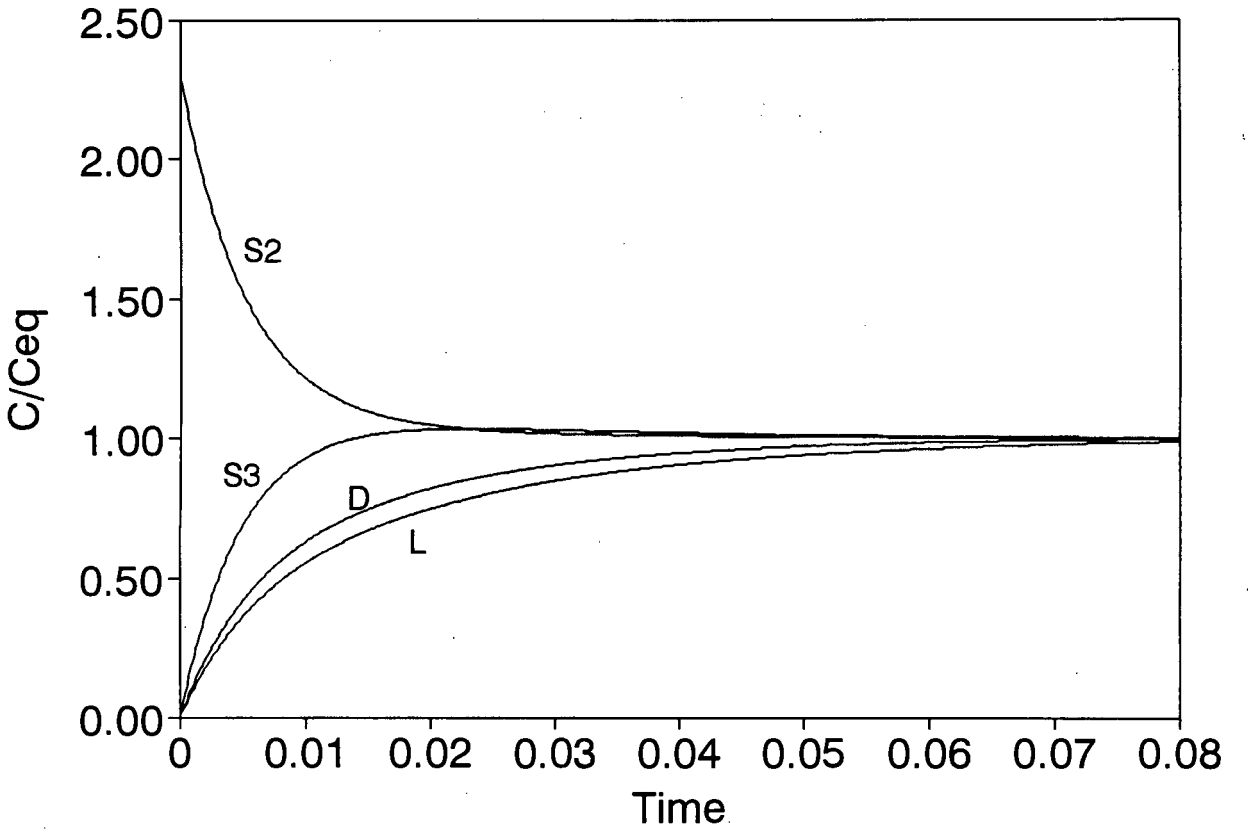

Figure 5.20a : Sensitivity Analysis for Model B - Base Case

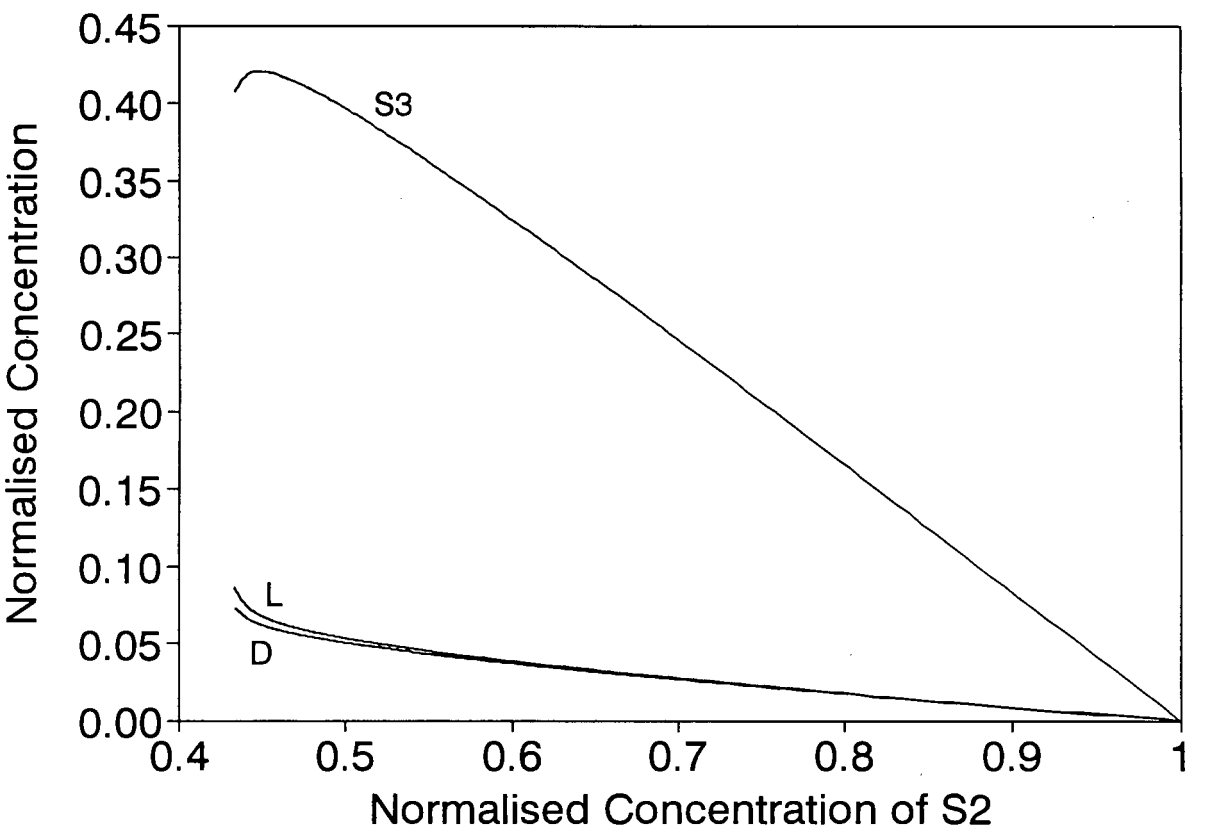

Figure 5.20b : Sensitivity Analysis for Model B - Base Case

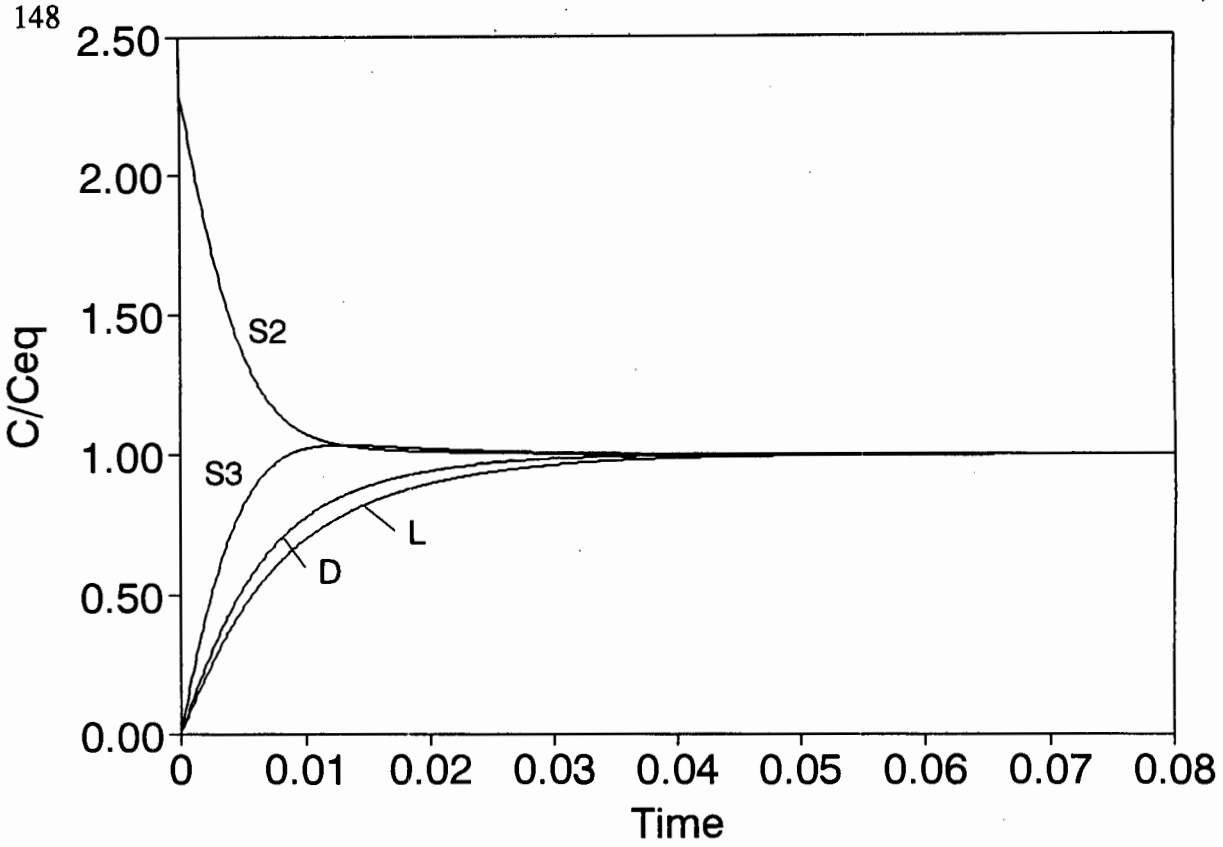

Figure 5.21a : Sensitivity Analysis for Model B - Case 2

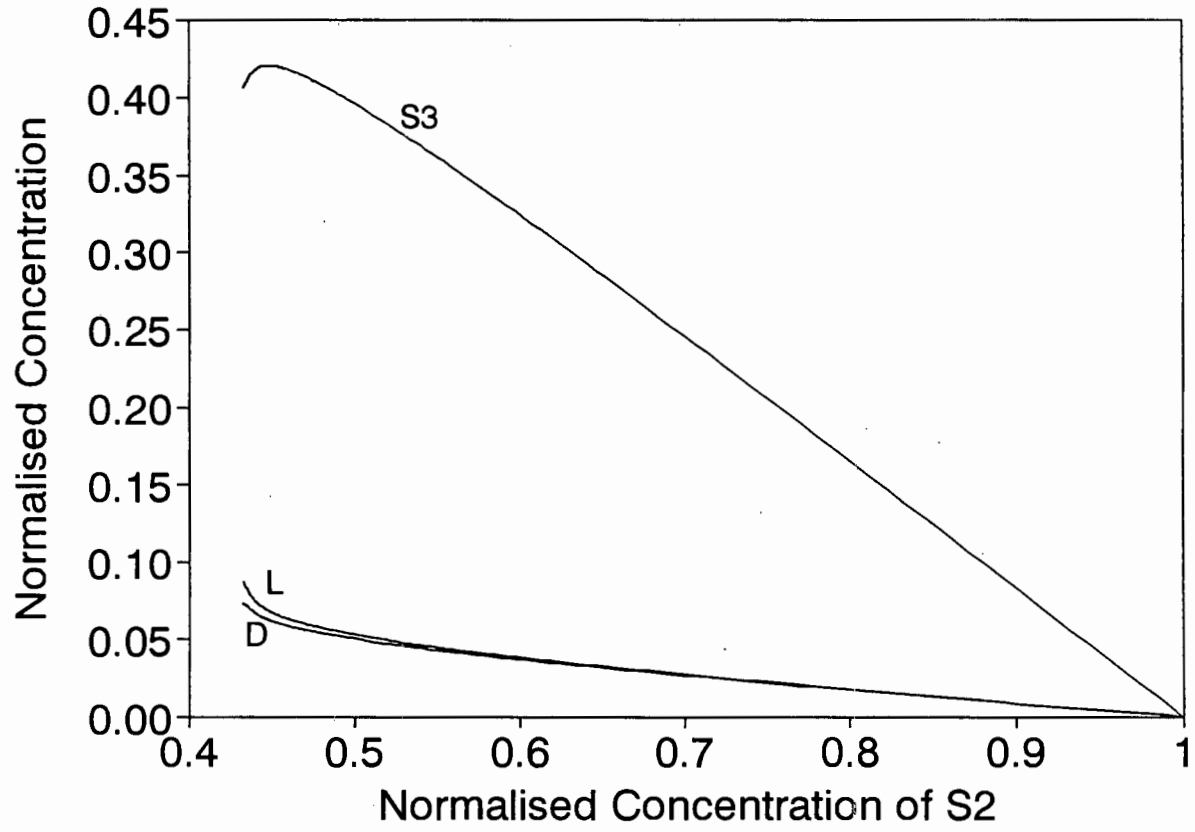

Figure 5.21b : Sensivity Analysis for Model B - Case 2

Case 3 - In this case K_{S3} was increased. A decrease in all the rates of reaction compared to the base case was observed, in a manner similar to that shown in Figure 5.21a. This is due to an increase in the adsorption of the product molecule, S3. Again, there was no change in selectivity to the hexene isomers and for this reason the relevant figures are not shown.

Case 4 and **Case 5** - Here the effects were the same as Case 3. An increase in either K_D or K_L leads to a decrease in all the rates of reaction compared to the base case. No change in selectivity was observed.

Since the effect of individually varying the rate constants for the surface reaction is the same as that for Model A they are not shown here.

Thus the effect of the equilibrium rate constants is to increase or decrease the rate of reaction. There is no change observed for the selectivity to hexene isomers. This can be confirmed when the rate equations for this model, (5.54) to (5.57), are examined. The selectivity to a particular product can be represented as follows :

$$selectivity = \frac{rate\ of\ formation\ of\ product\ i}{total\ rate\ of\ formation\ of\ products} \tag{5.60}$$

For example, the selectivity to S3 can be given by :

$$selectivity = \frac{k_{cat1}\left(C_{S2} - \frac{C_{S3}}{K_1}\right)}{\left(k_{cat1}\left(\frac{C_{S3}}{K_1} - C_{S2}\right) + k_{cat2}\left(\frac{C_D}{K_2} - C_{S2}\right) + k_{cat3}\left(\frac{C_L}{K_3} - C_{S2}\right)\right)} \tag{5.61}$$

It can be seen from (5.61) above that the equilibrium constants of adsorption do not occur in the selectivity relationships and therefore cannot influence the normalised concentration versus normalised concentration of S2 plots, which are also a measure of selectivity.

5.5.2.3 Insights from Sensitivity Analysis

The sensitivity analysis showed that increasing the equilibrium constant of adsorption of the feed increased the reaction rate while increasing the equilibrium constant of adsorption of the products reduced the rate of reaction. However, changing the K_i produced no change in the selectivity to the hexene skeletal structures. Unfortunately, this implies that unless the experimental data is in the form of concentration versus time no information can be obtained regarding the equilibrium constants of adsorption. This was confirmed when various starting guesses were used for the optimization procedure. No unique solution could be found. Therefore the Langmuir-Henshilwood equations, where surface reaction controls, cannot be successfully used to model this particular reaction namely, the isomerisation of hexene isomers, using the present form of experimental data.

5.5.3 Model C

5.5.3.1 Model Development

Model A above does not take into account intracrystalline diffusional effects during the isomerisation reaction. As shown in Chapter 3, H-ZSM-5 has a definite shape selective effect on the product olefins. Thus Model C was proposed in order to include the effect of intraparticle diffusion on the selectivity to the various hexene isomers.

The effect of adsorption of the isomers was not included in this model for the following reasons. If adsorption is accounted for, then the surface concentrations, according to the Langmiur-Hinshelwood model for the surface reaction controlling, are given by :

$$C_{sur} = KC_{bulk}C_v^* \qquad (5.62)$$

It is also not implausible to assume that the equilibrium constants of adsorption (K) are similar for the hexene isomers. Thus, if the K's are all similar, then the surface concentrations relative to one another will be similar to those in the bulk gas, provided

external mass transfer resistances are not significant. (This was shown in Chapter 3.) Additionally, it was not possible to obtain estimates for K's for C_6 olefins at the relevant reaction conditions namely, 250°C and 5MPa.

The model development which follows is for the isomerisation of S2 i.e. 4-methyl-1-pentene feed. Again, as for Model B, it was decided to model the 4-methyl-1-pentene data as this had significant concentrations of D. Thus, as the experimental data provides no information regarding the isomerisation of L to S3, this reaction was not included in this model.

A mass balance over a differential volume element in the catalyst particle is performed first. This gives rise to a set of differential equations that are solved using orthogonal collocation.

For a volume element the following mass balance can be written for species i :

$$\{\textit{rate of i in}\} - \{\textit{rate of i out}\} + \{\textit{rate of production i}\} = \{\textit{rate of accumulation of i}\} \tag{5.63}$$

Figure 5.22 shows a differential volume element in a spherical catalyst particle along with the concentration profile of a reacting component. The balance equations for the hexene isomers over a differential element of the catalyst particle are given by equations (5.64) to (5.67). For the purposes of Model C, for reasons explained above, $C_{bulk} = C_{surface}$.

$$\frac{1}{r^2}\frac{d}{dr}\left(D_{S3}r^2\frac{dC_{S3}}{dr}\right) + \rho_p(k_3C_{S2} - k_4C_{S3}) = 0 \tag{5.64}$$

$$\frac{1}{r^2}\frac{d}{dr}\left(D_Lr^2\frac{dC_L}{dr}\right) + \rho_p(k_1C_{S2} - k_2C_L) = 0 \tag{5.65}$$

$$\frac{1}{r^2}\frac{d}{dr}\left(D_Dr^2\frac{dC_D}{dr}\right) + \rho_p(k_5C_{S2} - k_6C_D) = 0 \tag{5.66}$$

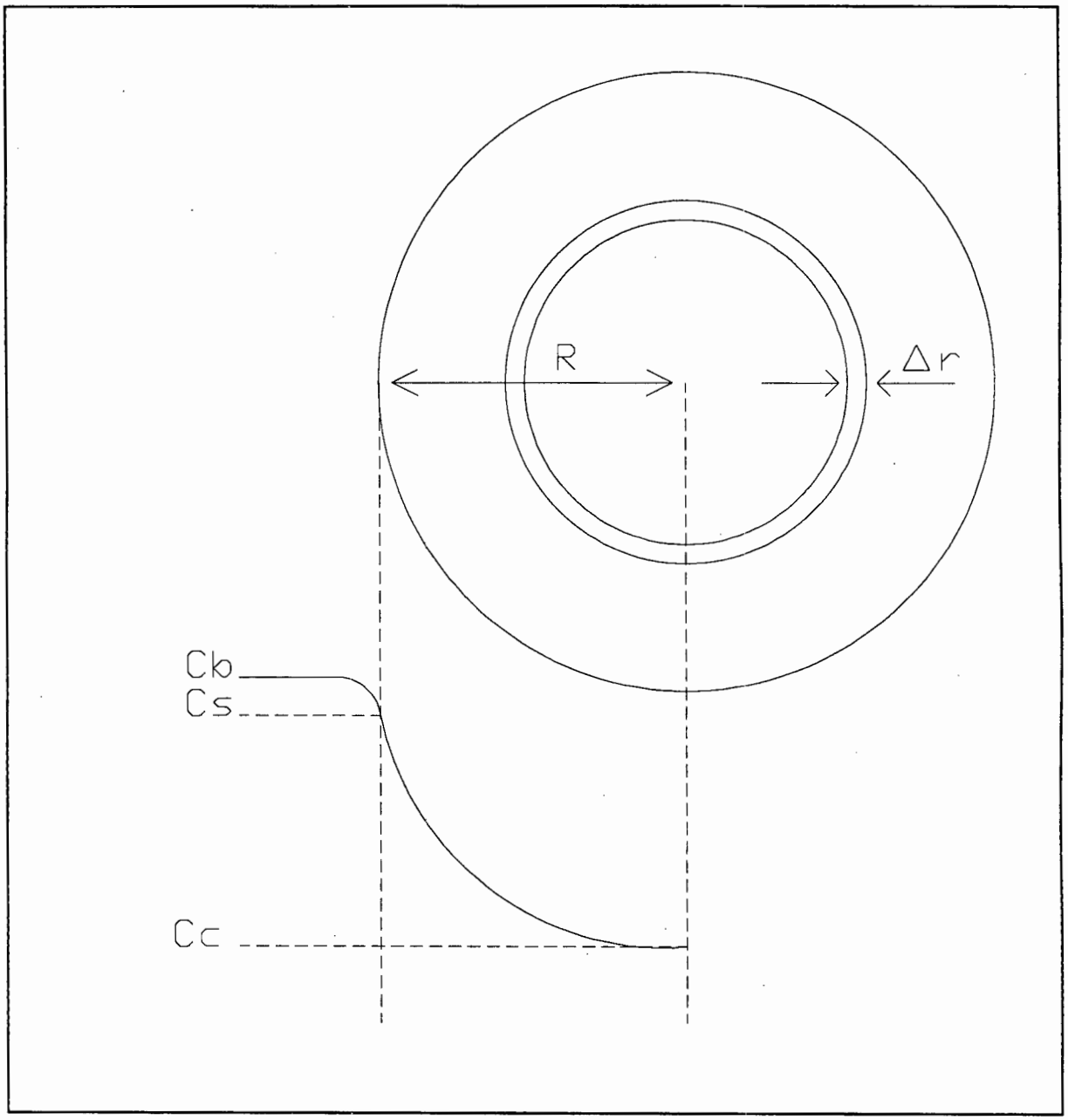

Figure 5.22 : Concentration Profile in Catalyst Particle

$$\frac{1}{r^2}\frac{d}{dr}\left(D_{S2}r^2\,\frac{dC_{S2}}{dr}\right) - \rho_p(\,(k_5+k_3+k_1)C_{S2} - k_2C_L - k_4C_{S3} - k_6C_D\,) = 0 \qquad (5.67)$$

The system is assumed to be at steady state and therefore the accumulation term is zero. The right hand terms represent the rate of production of the isomer via reaction while the left hand terms represent the net rate of diffusion into the differential element. ρ_p is the density of the catalyst particle, C_i the concentration of i inside the catalyst particle at position r and D_i is the diffusivity of component i. The diffusivities are independent, non-interacting and given by Fick's Law.

Next, the non-dimensional variable θ is introduced into equations (5.64) to (5.67). This will be required later for orthogonal collocation.

$$\theta = \frac{r}{R} \qquad d\theta = \frac{dr}{R} \qquad (5.68)$$

This leads to :

$$\frac{1}{\theta^2}\frac{d}{d\theta}(\theta^2\,C_{S3}) + \frac{R^2\rho_p}{D_{S3}}(\,k_3C_{S2} - k_4C_{S3}\,) = 0 \qquad (5.69)$$

$$\frac{1}{\theta^2}\frac{d}{d\theta}(\theta^2\,C_L) + \frac{R^2\rho_p}{D_L}(\,k_1C_{S2} - k_2C_L\,) = 0 \qquad (5.70)$$

$$\frac{1}{\theta^2}\frac{d}{d\theta}(\theta^2\,C_D) + \frac{R^2\rho_p}{D_D}(\,k_5C_{S2} - k_6C_D\,) = 0 \qquad (5.71)$$

$$\frac{1}{\theta^2}\frac{d}{d\theta}(\theta^2\,C_{S2}) - \frac{R^2\rho_p}{D_{S2}}(\,(k_5+k_3+k_1)C_{S2} - k_2C_L - k_4C_{S3} - k_6C_D\,) = 0 \qquad (5.72)$$

The parameters $R^2\rho_p k_i/D_i$ are dimensionless terms and represent the ratio of rate of reaction to rate of diffusion i.e. the larger the term the greater the influence of diffusion and vice versa. These terms are equivalent to the Thiele modulus squared (ϕ^2).

If equations (5.69) to (5.72) are multiplied through by D_i and summed, the reaction terms cancel and the following relationship is obtained :

$$D_{S3}\nabla^2 C_{S3} + D_L\nabla^2 C_L + D_{S2}\nabla^2 C_{S2} + D_D\nabla^2 C_D = 0 \qquad (5.73)$$

that is,

$$\nabla(D_{S3}\nabla C_{S3} + D_L\nabla C_L + D_{S2}\nabla C_{S2} + D_D\nabla C_D) = 0 \qquad (5.74)$$

According to Aris (1975) this implies that

$$D_{S3}\nabla C_{S3} + D_L\nabla C_L + D_{S2}\nabla C_{S2} + D_D\nabla C_D \qquad (5.75)$$

is the gradient of a potential function. If the diffusion coefficients are constant then

$$D_{S3}C_{S3} + D_L C_L + D_{S2}C_{S2} + D_D C_D \qquad (5.76)$$

is itself a potential function and constant for all values of C_i. Thus the following holds true:

$$D_{S3}C_{S3} + D_L C_L + D_D C_D + D_{S2}C_{S2} = D_{S3}C_{S3_s} + D_L C_{L_s} + D_D C_{D_s} + D_{S2}C_{S2_s} \qquad (5.77)$$

where C_{is} is the concentration at the surface.

Equation (5.77) can be rearranged to give the following equation for C_D :

$$C_D = \frac{D_{S3}}{D_D}(C_{S3_s} - C_{S3}) + \frac{D_L}{D_D}(C_{L_s} - C_L) + \frac{D_{S2}}{D_D}(C_{S2_s} - C_{S2}) + C_{D_s} \tag{5.78}$$

Substituting for C_D in equation (5.72) above gives,

$$\nabla^2 C_{S2} - \frac{R^2\rho_p}{D_{S2}}\left(k_5 + k_3 + k_1 + k_6\frac{D_{S2}}{D_D}\right)C_{S2} + \frac{R^2\rho_p}{D_{S2}}\left(k_2 - k_6\frac{D_L}{D_D}\right)C_L + \frac{R^2\rho_p}{D_{S2}}\left(k_4 - k_6\frac{D_{S3}}{D_D}\right)C_{S3} + k_6\frac{R^2\rho_p}{D_{S2}}\left(\frac{D_{S3}}{D_D}C_{S3_s} + \frac{D_L}{D_D}C_{L_s} + \frac{D_{S2}}{D_D}C_{S2_s} + C_{D_s}\right) \tag{5.79}$$

Equations (5.69), (5.70) and (5.79) can be written more simply as :

$$\nabla^2 C_{S3} + constA\,C_{S2} - constB\,C_{S3} = 0 \tag{5.80}$$

$$\nabla^2 C_L + constC\,C_{S2} - constD\,C_L = 0 \tag{5.81}$$

$$\nabla^2 C_{S2} - constE\,C_{S2} + constF\,C_L + constG\,C_{S3} + constH = 0 \tag{5.82}$$

where,

$$constA = \frac{R^2\rho_p}{D_{S3}}k_3 \tag{5.83}$$

$$constB = \frac{R^2\rho_p}{D_{S3}}k_4 \tag{5.84}$$

$$constC = \frac{R^2\rho_p}{D_L}k1 \tag{5.85}$$

$$constD = \frac{R^2 \rho_p}{D_L} k2 \tag{5.86}$$

$$constE = \frac{R^2 \rho_p}{D_{S2}} \left(k_2 + k_3 + k_1 + k_6 \frac{D_{S2}}{D_D} \right) \tag{5.87}$$

$$constF = \frac{R^2 \rho_p}{D_{S2}} \left(k_2 - k_6 \frac{D_L}{D_D} \right) \tag{5.88}$$

$$constG = \frac{R^2 \rho_p}{D_{S2}} \left(k_4 - k_6 \frac{D_{S3}}{D_D} \right) \tag{5.89}$$

$$constH = k_6 \frac{R^2 \rho_p}{D_{S2}} \left(\frac{D_{S3}}{D_D} C_{S3_s} + \frac{D_L}{D_D} C_{L_s} + \frac{D_{S2}}{D_D} C_{S2_s} + C_{D_s} \right) \tag{5.90}$$

The above equations can now be solved using orthogonal collocation (See Finlayson (1980) for a full description of the technique).

(5.80) - (5.82) can be written in the following format :

$$\sum_{i=1}^{N+1} B_{ij} C_{S3,i} + constA\, C_{S2,j} - constB\, C_{S3,j} = 0 \qquad j = 1,2...N \tag{5.91}$$

$$\sum_{i=1}^{N+1} B_{ij} C_{L,i} + constC\, C_{S2,j} - constD\, C_{L,j} = 0 \tag{5.92}$$

$$\sum_{i=1}^{N+1} B_{ij} C_{S2,i} - constE\, C_{S2,j} + constF\, C_{L,j} + constG\, C_{S3,j} = -constH \tag{5.93}$$

In addition there are the following boundary conditions :

$$C_{S3,N+1} = C_{S3_S} \tag{5.94}$$

$$C_{S2,N+1} = C_{S2_S} \tag{5.95}$$

$$C_{L,N+1} = C_{L_S} \tag{5.96}$$

Where C_{is} is the concentration of species i on the catalyst surface. The above equations are written for weighting function, W=1 and N=3 collocation points. The matrix **B** is known.

The above set of equations (5.91) - (5.96) can now be solved for each concentration at each collocation point C_{ij}. Each set of C_{ij}'s is also represented by a series of polynomials, for example,

$$\begin{pmatrix} C_{S2,1} \\ C_{S2,2} \\ C_{S2,3} \\ C_{S2,4} \end{pmatrix} = \begin{pmatrix} d_1 \\ d_2 \\ d_3 \\ d_4 \end{pmatrix} \begin{pmatrix} 1 & \theta_1^2 & \theta_1^4 & \theta_1^6 \\ 1 & \theta_2^2 & \theta_2^4 & \theta_2^6 \\ 1 & \theta_3^2 & \theta_3^4 & \theta_3^6 \\ 1 & \theta_4^2 & \theta_4^4 & \theta_4^6 \end{pmatrix} \tag{5.97}$$

The matrix **d** can then be solved for as both other matrixes are known. Once **d** is known then the concentration of each isomer can be calculated for any point inside the catalyst particle. This means that effectiveness factors can also be calculated. The effectiveness factors are defined as follows :

$$\eta = \frac{\textit{average reaction rate for catalyst crystal with diffusion}}{\textit{rate of reaction evaluated at the surface conditions}} \tag{5.98}$$

or,

$$\eta_{S3} = \frac{\int_0^1 (k_4 C_{S3}(r) - k_3 C_{S2}(r)) r^2 dr}{\int_0^1 (k_4 C_{S3}(1) - k_3 C_{S2}(1)) r^2 dr} \qquad (5.99)$$

$$\eta_L = \frac{\int_0^1 (k_2 C_L(r) - k_1 C_{S2}(r)) r^2 dr}{\int_0^1 (k_2 C_L(1) - k_1 C_{S2}(1)) r^2 dr} \qquad (5.100)$$

$$\eta_D = \frac{\int_0^1 (k_6 C_D(r) - k_5 C_{S2}(r)) r^2 dr}{\int_0^1 (k_6 C_D(1) - k_5 C_{S2}(1)) r^2 dr} \qquad (5.101)$$

$$\eta_{S2} = \frac{\int_0^1 ((k_5 + k_3 + k_1) C_{S3} - k_2 C_L - k_4 C_{S3} - k_6 C_D) r^2 dr}{\int_0^1 ((k_5 + k_3 + k_1) C_{S3}(1) - k_2 C_L(1) - k_4 C_{S3}(1) - k_6 C_D(1)) r^2 dr} \qquad (5.102)$$

The integrals in (5.99) - (5.102) were evaluated using Simpson's Rule.

Thus, for each set of surface concentrations and rate constants the effectiveness factors could be calculated. Once the effectiveness factors are known, the concentration of the hexenes in the bulk gas can be calculated using,

$$\frac{dC_{S2_S}}{dt} = \eta_{S2} \left((k_2 - k_6)C_{L_S} - (k_5 + k_3 + k_1 + k_6)C_{S2_S} + (k_4 - k_6)C_{S3_S} + k_6 \right) \quad (5.103)$$

$$\frac{dC_{L_S}}{dt} = \eta_L \left(k_1 C_{S2_S} - k_2 C_{L_S} \right) \quad (5.104)$$

$$\frac{dC_{S3_S}}{dt} = \eta_{S3} \left(k_3 C_{S2_S} - k_4 C_{S3_S} \right) \quad (5.105)$$

$$C_{D_S} = 1 - C_{L_S} - C_{S2_S} - C_{S3_S} \quad (5.106)$$

Again, as for the previous models, the reactor is assumed to be plug-flow.

5.5.3.2 Sensitivity Analysis

A sensitivity analysis was carried out on Model C and the effect of the various Thiele Moduli studied. The Thiele Modulus can be varied by either varying the rate constants or the diffusion coefficients or both. In this study the diffusion coefficients were varied and the rate constants kept constant. The rate constants used are summarised in the Table 5.10 below :

Table 5.10 : Model C - Rate Constants	
$k_1 = 0.202$	$k_2 = 1$
$k_3 = 9.38$	$k_4 = 10$
$k_5 = 0.170$	$k_6 = 1$

The rate constants chosen were based on the values obtained for Model A. The diffusivities chosen were related to the skeletal structure of the species and are based on the values used during the fitting procedure, shown in Table 5.12 later in this section. The most branched skeletal structure had the lowest diffusivity while the linear skeleton had the highest. Table

5.11 shows how the diffusion coefficients were varied :

Table 5.11 Model C - Parameters Used in Sensitivity Analysis				
	Diffusivity cm^2/s			
Case	S2	S3	D	L
1 (Base)	1e-6	1e-6	1e-9	1e-5
2	**1e-8**	1e-6	1e-9	1e-5
3	1e-6	**1e-8**	1e-9	1e-5
4	1e-6	1e-6	**1e-10**	1e-5
5	1e-6	1e-6	1e-9	**1e-10**

The diffusion coefficients were adjusted until a change in the concentration curves were observed. The effect of varying the diffusion coefficients on the concentration of each hexene skeletal structure is shown in Figures 5.23 to 5.29 along with the concentration curves for Model A. For this sensitivity analysis S2 was the starting compound. The curves pertaining to the variation of a particular diffusion coefficient are labelled accordingly. "Model A" on all the curves refers to the homogeneous reaction without diffusional effects.

In Figures 5.23 to 5.26 C/C_{eq} versus time is plotted. The C's here refer to the concentrations in the bulk gas and C_{eq} refers to the equilibrium concentration of the skeletal group. As C/C_{eq} approaches 1, so the reaction approaches equilibrium. The time scale is chosen to display the behaviour of the curves as clearly as possible. In Figures 5.27 to 5.29, normalised concentration versus normalised feed concentration for all products namely, S3, L and D are plotted. Note that as the feed concentration drops, so the reaction approaches equilibrium.

Case 1 (Base Case) - When diffusional resistances are taken into account, S2 approaches equilibrium slower than for the homogeneous reaction, Model A (Figure 5.23). This is because this compound now has to diffuse into the catalyst particle before it can isomerise. Of the products, S3 and L are favoured over D when case 1 is compared to Model A because

these skeletal groups have much higher diffusivities and are able to diffuse out faster. This is shown by the increase in the concentrations of S3 and L over D when Model A and the Base case are compared in Figures 5.27 to 5.29. The linear structure, L, now approaches equilibrium faster than for the homogeneous reaction. This can be seen in Figure 5.24. On the other hand, the more branched products, S3 and D, approach equilibrium slower than for the homogeneous case (Figures 5.25 and 5.26).

Case 2 - For this case the diffusivity of the feed, S2, was reduced. As expected, S2 now reacts much slower compared to the base case (Figure 5.23). The initial rate of S2 is affected most since this is when its rate of formation is highest. Because S2 isomerises more slowly, so L and S3 form more slowly and their rate of formation is reduced compared to the base case (Figures 5.24 and 5.25). The rate of formation of D is essentially unchanged due to its slow diffusivity and reaction rate (Figure 5.26). In the normalised concentration plot shown in Figure 5.27, the concentration of S3 drops and overshoots its equilibrium concentration less because its rate of formation is slower. The concentrations of L and D now increase relative to S3 although D is less affected because its rate of formation and diffusion is slower than L's.

Case 3 - For this case the diffusivity of S3 is decreased. The rate of S2 is affected most at the start of reaction since this is where the ratio of reaction rate to diffusion is highest (Figure 5.23). S3 undergoes the greatest reduction in its rate of formation at the start of the reaction for the same reason. Figure 5.25 shows how both D_{S2} and D_{S3} have the same effect on S3's concentration profile due to the fast interconversion of S2 and S3. The rate of formation of L and D are now favoured compared to the base case since less S3 is formed (Figures 5.24 and 5.26). In the normalised concentration plots, the concentration of S3 drops relative to the other skeletal groups, L and D.

Case 4 - Here the diffusivity of D is decreased. The rate of S2 is only affected close to equilibrium since this is when D starts to form in appreciable amounts (Figure 5.23). The slow formation of D decreases the rate at which S2 approaches its equilibrium concentration compared to the base case. The reduction in the rate of the formation of D also results in

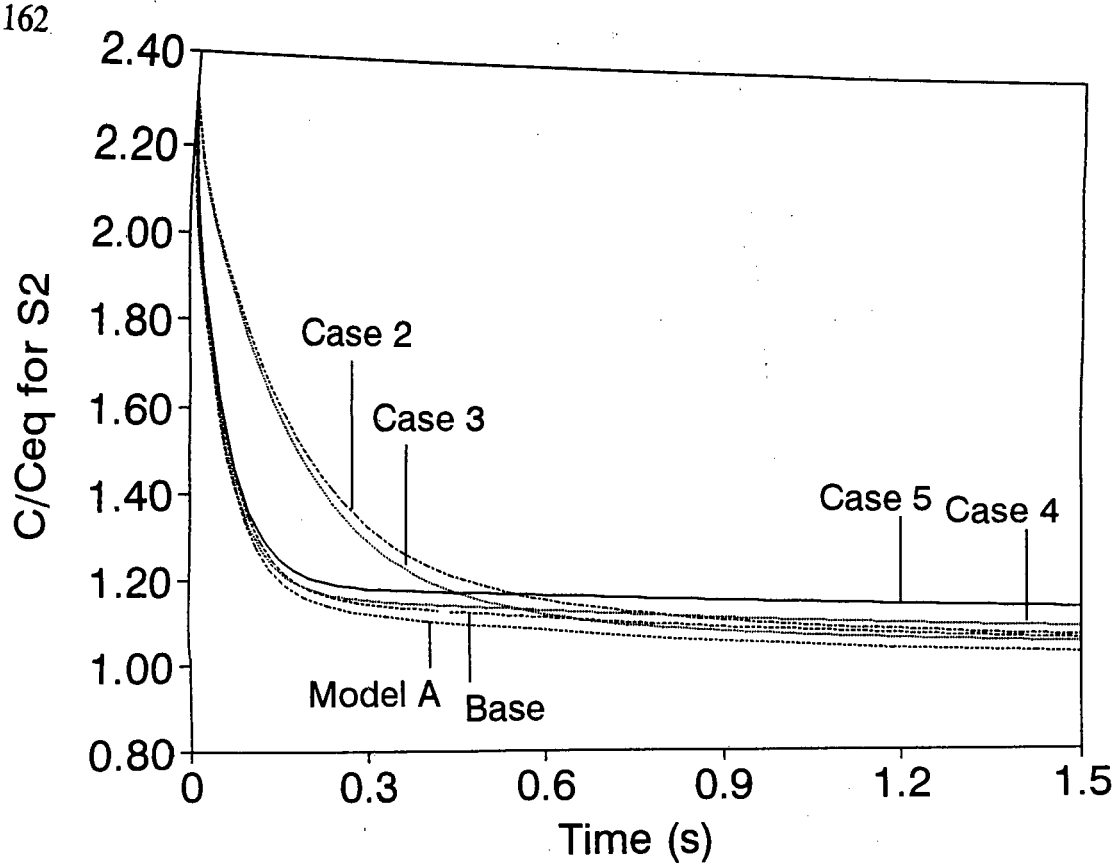

Figure 5.23 : Sensitivity Analysis for Model C - Variation in S2 with the Diffusivities of Hexene Isomers

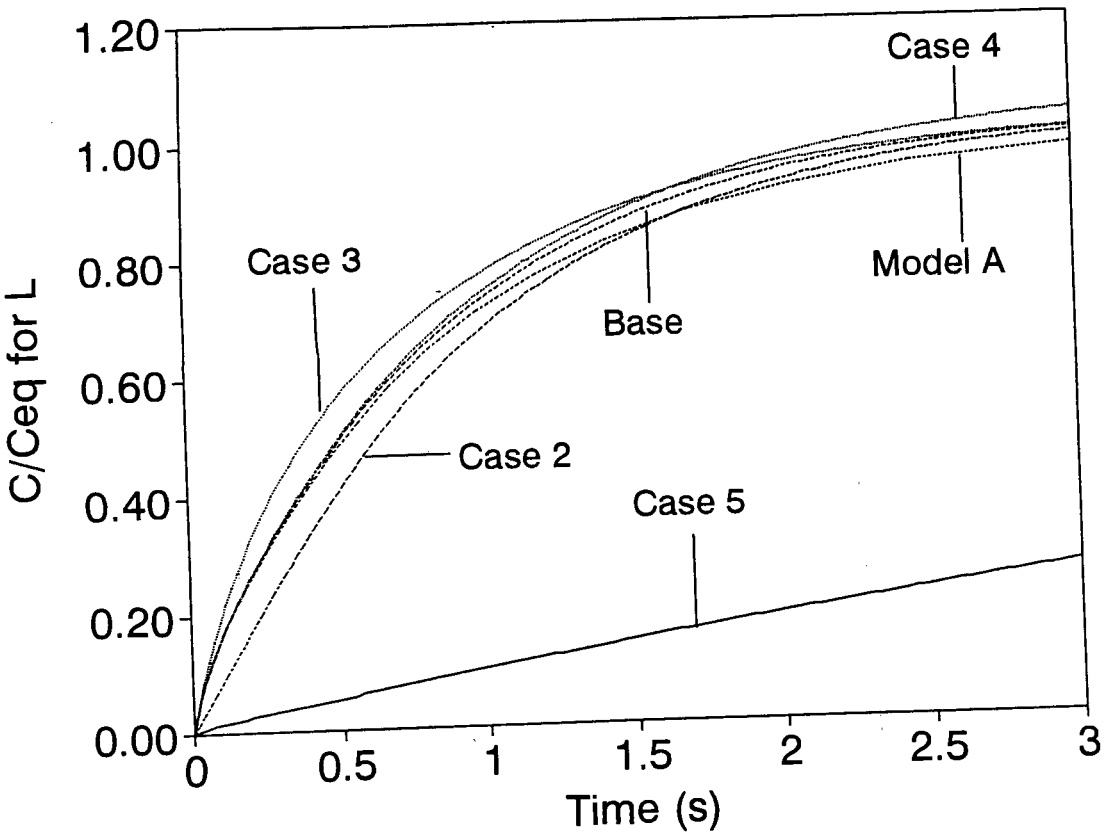

Figure 5.24 : Sensitivity Analysis for Model C - Variation in L with the Diffusivities of Hexene Isomers

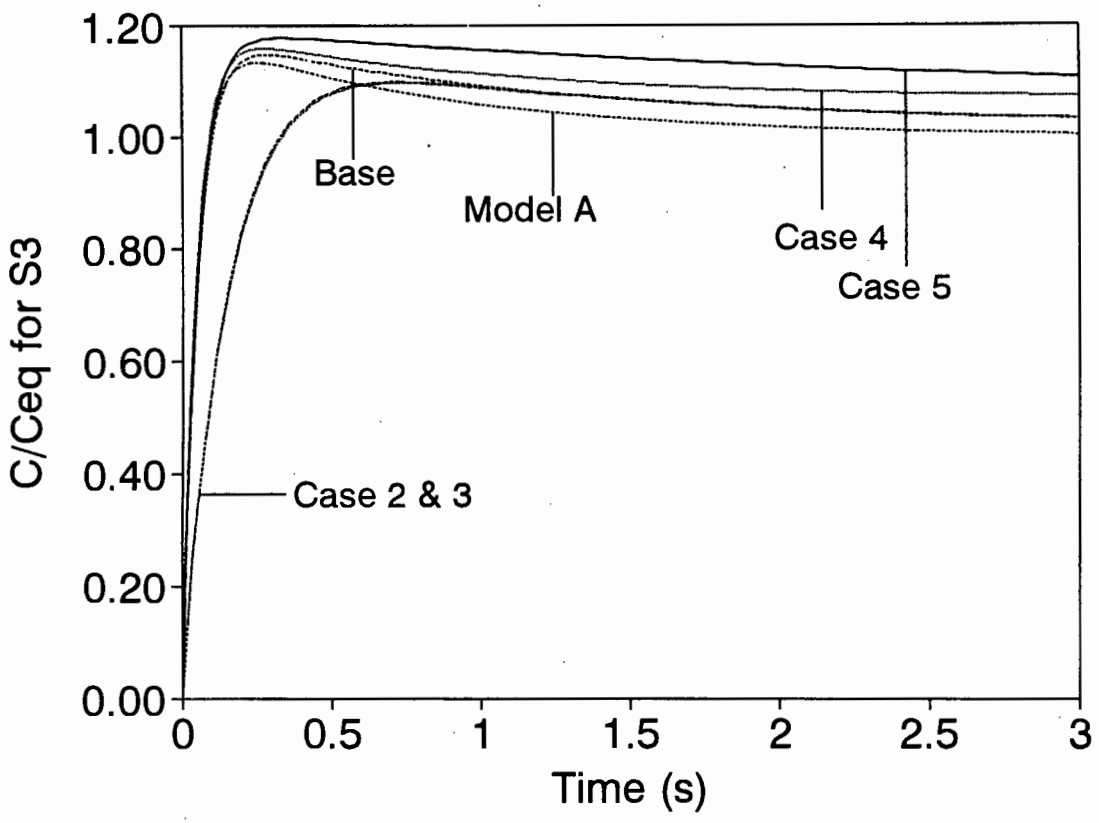

Figure 5.25 : Sensitivity Analysis for Model C - Variation in S3 with the Diffusivities of Hexene Isomers

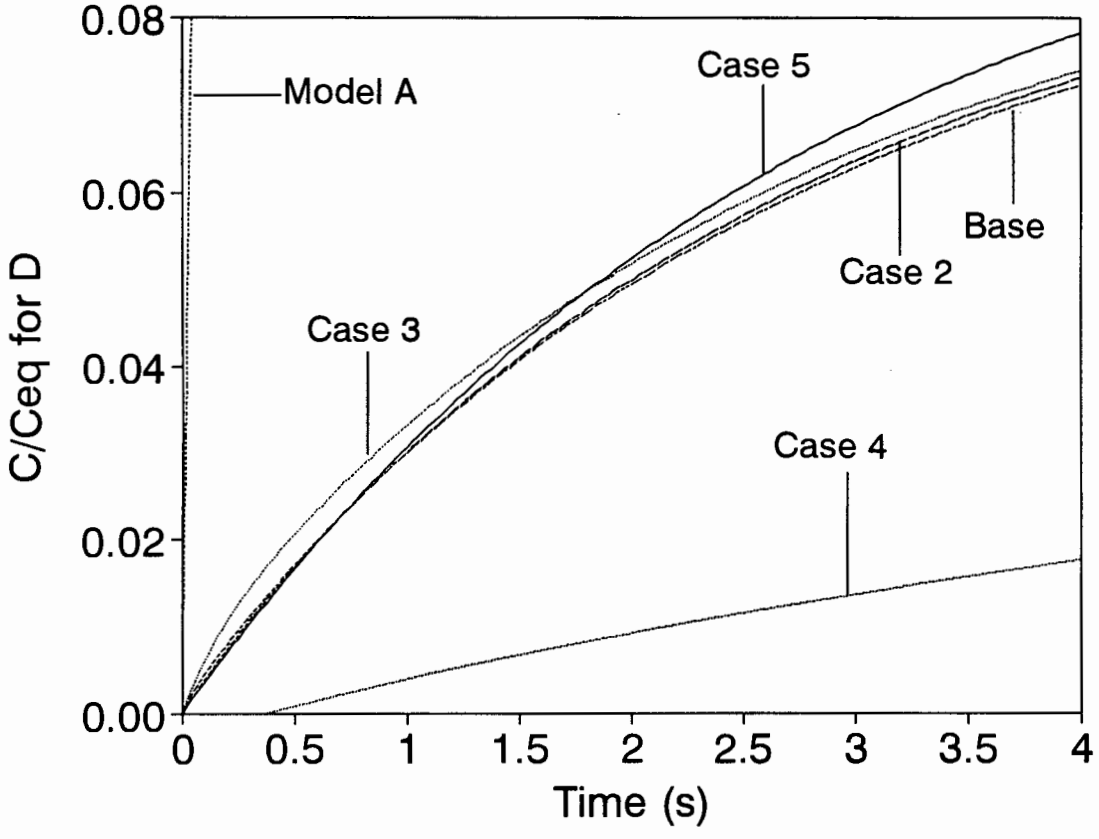

Figure 5.26 : Sensitivity Analysis for Model C - Variation in D with the Diffusivities of Hexene Isomers

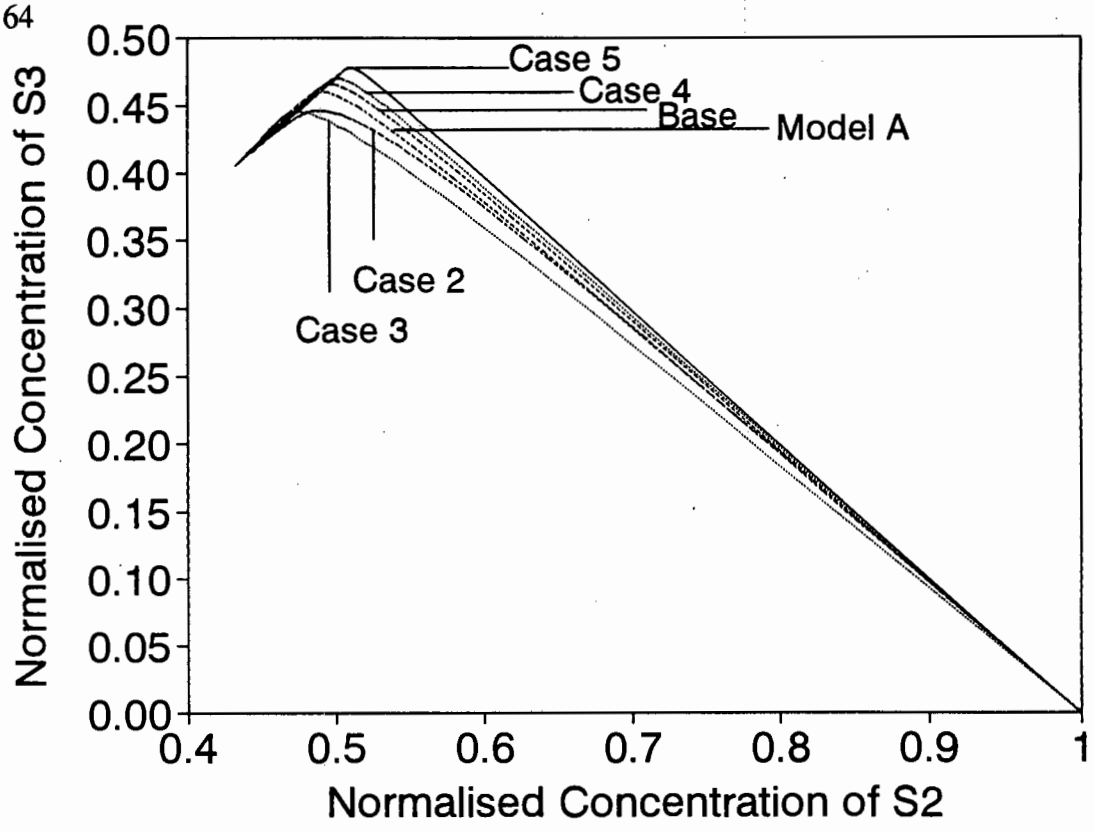

Figure 5.27 : Sensitivity Analysis for Model C - Variation in S3 with the Diffusivities of Hexene Isomers

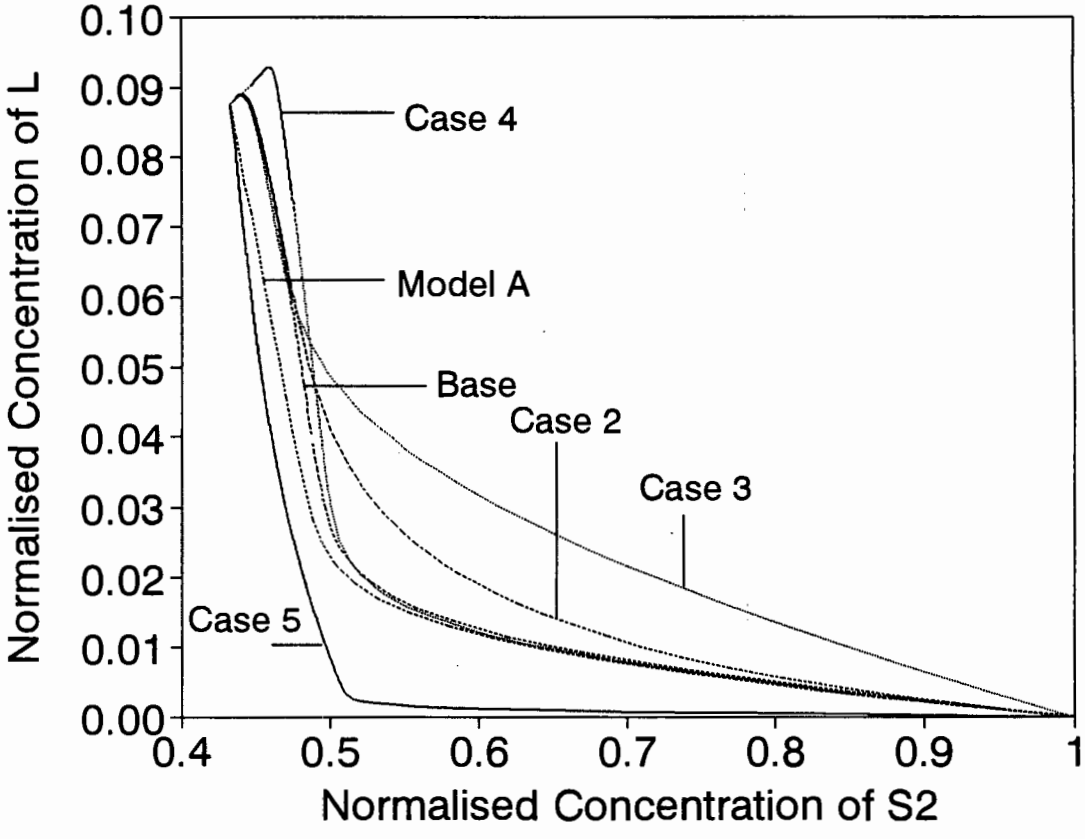

Figure 5.28 : Sensitivity Analysis for Model C - Variation in L with the Diffusivities of Hexene Isomers

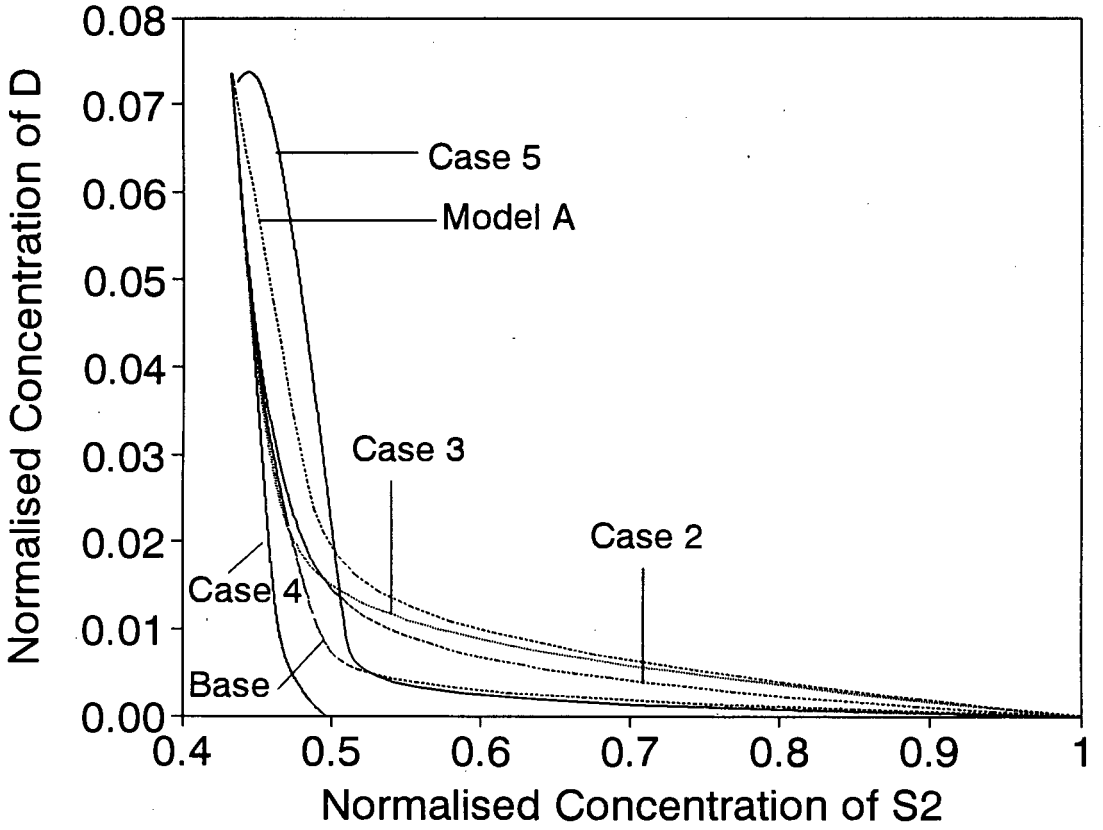

Figure 5.29 : Sensitivity Analysis for Model C - Variation of D with the Diffusivities of Hexene Isomers

corresponding increase in the rate of formation of L and S3 and an increase in their concentrations relative to D. L is now favoured to such an extent that it overshoots its equilibrium value before decreasing to its final equilibrium concentration (Figure 5.28). S3 now also overshoots its equilibrium concentration to a greater extent than for the base case (Figure 5.27).

Case 5 - Here the diffusivity of L is decreased and results in a corresponding decrease in the rate of formation. The effects observed are similar to that observed for D except they are pronounced due to the faster rate of formation of L compared to D. The rate of removal of S2 decreases close to equilibrium compared to the base case since this is when L forms in significant concentrations. Again, as for case 4, the other skeletal structures, D and S3, are now favoured over L.

5.5.3.3 Insights from Sensitivity Analysis

A combination of high rate constants and low diffusion coefficients lead to highly developed profiles inside the catalyst particle, since the Thiele modulus is large. The opposite is true for low rate constants and high diffusion coefficients (small Thiele modulus).

The sensitivity analysis showed that a reduction in all of the D_i's (or an increase in ϕ's) brought about unique changes in the product spectra. Since S2 forms all other isomers, a change in S3, L or D automatically leads to a change in S2 with regard to concentration profile and effectiveness factor and vice versa. S2 and S3 react rapidly and establish equilibrium between themselves early on in the reaction. Thus a reduction in either of their diffusion coefficients influences their rates at the beginning of the reaction in a similar manner. On the other hand, L and D form more slowly and only when their concentrations increase substantially towards the end of the reaction, does a reduction in their D's have any effect on the concentration profiles of the other species. Additionally, the slower the reaction rate, the more the diffusivities must be decreased in order to significantly alter the Thiele modulus and observe an effect in the product spectrum.

This sensitivity analysis shows if diffusivities are altered, changes are observed in the product spectrum at low conversions for S2 and S3, while changes are observed close to equilibrium for D and L. Thus, experimental data should be collected over as wide a conversion range as possible to observe the behaviour of all the products.

5.5.3.4 Model Parameter Estimation

Unfortunately, values for the diffusion coefficients of C_6 olefins were not available. As a first approximation values for the diffusion coefficients, obtained from Ruthven and Kärger (1992), for the alkanes with similar carbon skeletons were used. These values, adjusted to 250°C, are as follows :

Table 5.12 : Diffusion Coefficients for Model C	
Olefin Skeletal Group	Diffusion Coefficient (cm^2/s)
S2 - 2-methyl-Pentenes	5.192e-6
S3 - 3-methyl-Pentenes	5.192e-6
L - Hexenes	7.484e-5
D - 2,3-dimethyl-Butenes	9.122e-9

The average crystal size, R, of 2 micron was determined from photographs taken using a scanning electron microscope. The crystal density, ρ_p, was taken to be 1.75 g/cm^3.

The Turbo-Pascal program used to calculate the rate constants was similar to that for Model A, except the rate equations were integrated numerically using a stable, accurate method for non-linear systems by Calahan (1968). The software for Model C contained an additional routine that calculated effectiveness factors down the catalyst bed for each set of rate constants. Again, as for Model A, the values of the rate constants were judged to have converged when the sum of the relative squared error between the model and experimental concentrations were less than 10^{-5}. The relative error was defined the same as for Model A.

A wide range of starting guesses was used for the optimization procedure. Because the data

is not in the form concentration versus time no single, unique answer could be found. Table 5.13 shows the results obtained for two different starting guesses.

The fits obtained from both answers are good (Figures 5.30 and 5.32). It can be seen that depending on the magnitude of the diffusional effects the rate constants relative to one another vary considerably. For guess 1 the reaction is kinetically controlled while the reaction for guess 2 is controlled by diffusion. The fit obtained using guess 2 is slightly better than for that obtained for guess 1 namely, 7.8% compared to 12.8%. It therefore appears that inclusion of diffusion into the isomerisation model produces a marginal improvement in fit.

The model itself however, shows promise. If new data could be obtained in which deactivation was minimal then it is likely that valuable information could be obtained.

Figure 5.31 and 5.33 show how the effectiveness factors vary with increasing conversion or alternatively, down the length of the catalyst bed. Some interesting phenomena are observed. Firstly, the effectiveness factors for S3 and L show asymptotic behaviour close to equilibrium. Secondly, the effectiveness factors for S2 and D do not approach 1 as equilibrium is reached, instead they decrease steadily to a minimum. This behaviour is explained in the following paragraphs.

The effectiveness factor was defined as follows :

$$\eta = \frac{\textit{average reaction rate for catalyst crystal with diffusion}}{\textit{rate of reaction evaluated at the surface conditions}} \qquad (5.107)$$

As shown in the sensitivity analysis for Model A, when S2 is fed, S3 is the major product. S3 forms rapidly via the methyl-shift reaction until a maximum concentration exceeding its equilibrium concentration is reached. Since all the reactions in the model are reversible, S3 then isomerises, together with S2, to form D or L until all the compounds reach equilibrium. Thus, at the beginning of the reaction S3 has a positive rate (i.e. rate of formation). Once

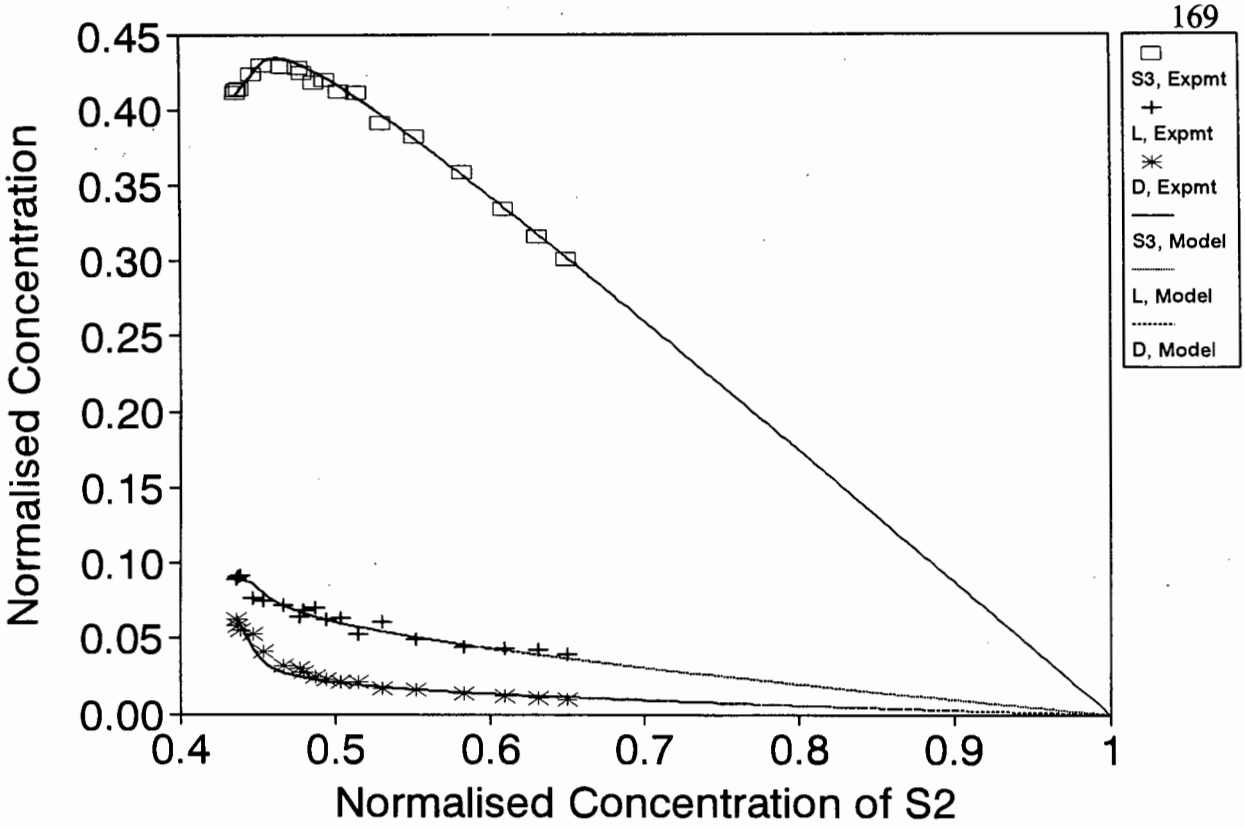

Figure 5.30 : Fit of Model C to 4-methyl-1-Pentene Data, Guess 1

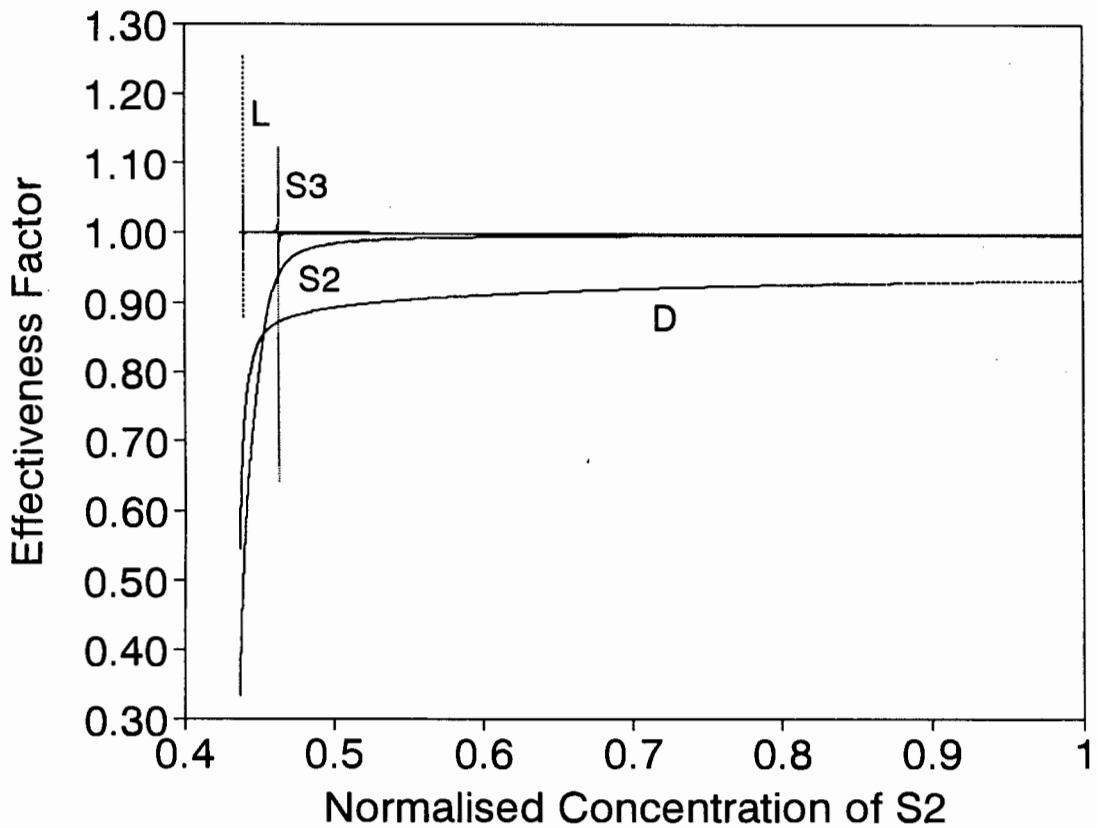

Figure 5.31 : Variation of Effectiveness Factors with Conversion, Model C, Guess 1

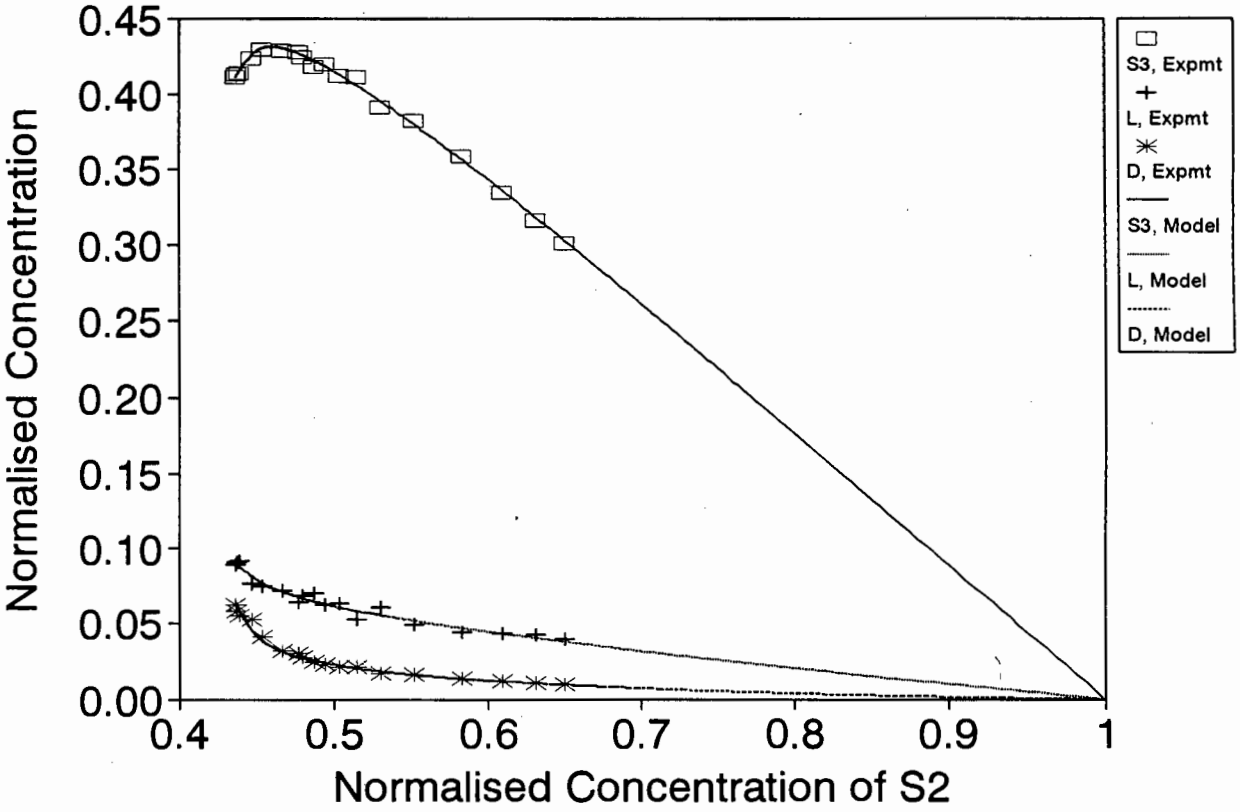

Figure 5.32 : Fit of Model C to 4-methyl-1-Pentene Data, Guess 2

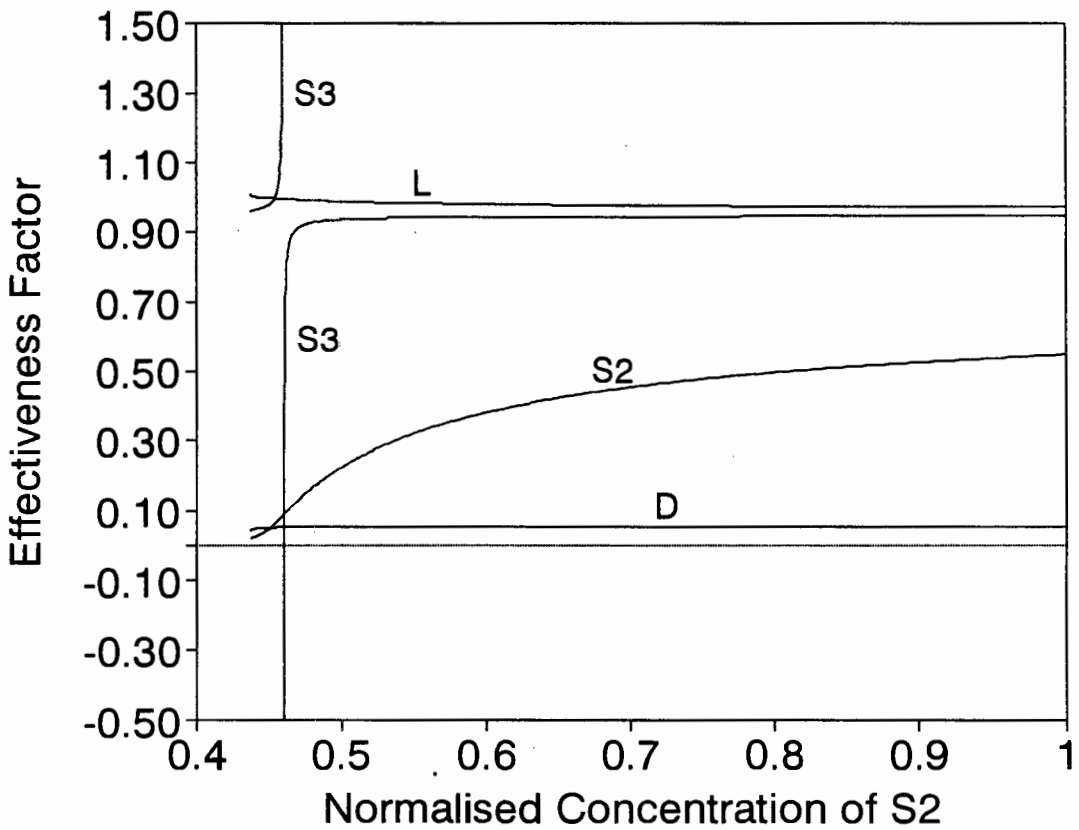

Figure 5.33 : Variation of Effectiveness Factors with Conversion, Model C, Guess 2

Table 5.13 : Model C - Effect of Starting Guesses				
	Guess 1 k2 = 0.1 k4 = 1.0 k6 = 0.1		Guess 2 k2 = 10 k4 = 100 k6 = 10	
Reaction	Forward	Reverse	Forward	Reverse
S2 ⇔ *L*	k1 = 0.092 $k1^*$ = 0.202	k2 = 0.445 $k2^*$ = 1.0	k1 = 3.22 $k1^*$ = 0.202	k2 = 15.95 $k2^*$ = 1.0
S2 ⇔ *S3*	k3 = 0.853 $k3^*$ = 1.87	k4 = 0.909 $k4^*$ = 2.04	k3 = 30.23 $k3^*$ = 1.90	k4 = 32.23 $k4^*$ = 2.02
S2 ⇔ *D*	k5 = 0.027 $k5^*$ = 0.061	k6 = 0.162 $k6^*$ = 0.364	k5 = 27.0 $k5^*$ = 1.69	k6 = 159.0 $k6^*$ = 9.97
Error	12.8%		7.8%	

Key : ki^* - rate constant normalised with respect to k2

the maximum concentration is reached, S3 reacts back so that L and D can now form in appreciable amounts and therefore its rate is now negative (i.e. rate of removal). In going from a positive to a negative reaction rate, the rate of S3 must pass through zero. Because of diffusional restrictions, the reaction on the surface of the catalyst lags behind the reaction inside the catalyst particle. The concentration of S3 inside the catalyst particle thus reaches its maximum and begins reacting back before the S3 on the surface. The reversal in sign for the reaction rate and the difference in rates between the surface and inside the catalyst lead to an asymptote at the point of maximum S3 concentration.

For guess 1, L also passes through a maximum concentration closer to equilibrium than S3, and for similar reasons described above for S3 displays asymptotic behaviour at this point of maximum concentration. Under conditions of diffusion control, guess 2, L no longer

passes through a maximum concentration close to equilibrium and so its effectiveness factor curve shows no asymptotic behaviour.

Additionally, close to equilibrium the reaction rates slow down. Due to diffusional restrictions, the concentration of D is higher inside the catalyst and therefore approaches equilibrium faster inside the catalyst than on the surface. This leads to a sharp drop in the effectiveness factor close to equilibrium because the numerator in equation 5.91 above is much closer to zero than the denominator. There is less difference between the rate inside and outside the catalyst for the other products because their diffusion coefficients are higher and thus η is close to 1. Since S2 is also affected by D, the effectiveness factor of this compound also drops as equilibrium is approached.

For guess 2 the reaction is diffusion controlled while for guess 1 it is rate controlled. For guess 2 the Thiele Modulus (rate of reaction versus rate of diffusion) for all isomers has increased. As D has the lowest diffusivity this compound is the most affected and there is a corresponding decrease in its effectiveness factor. D in turn affects S2 whose η is less than for guess 1.

5.6 Conclusions

In the absence of diffusional restrictions, the conclusions reached regarding the rate constants for hexene isomer skeletal isomerisation over superacid catalysts are similar those for H-ZSM5. That is, the 1,2-methyl-shift reactions are approximately one order of magnitude faster than reactions involving changes in degree of branching.

During the dimerisation of propene the primary products are the 2-methyl-pentenes. These undergo rapid methyl shift to form 3-methyl-pentenes. The formation of linear hexenes and 2,3-dimethyl-butenes is much slower. There is no 3,3-dimethyl-butene formed as suggested by the model for superacid catalysts. This is probably due to shape selective constraints imposed by H-ZSM-5.

The sensitivity analysis showed that no additional information could be obtained by applying the Langmuir-Henshilwood equation to this set of hexene isomerisation data. This is because it was shown that the equilibrium constants of adsorption have no influence on the normalised concentration versus feed concentration plots.

Although no unique solution could be found for Model C, the inclusion of diffusion into the isomerisation model produced a slight improvement it fit. Model C however, shows promise and could be useful in determining the extent of diffusional restrictions if it were possible to obtain data from which the effect of catalyst deactivation had been eliminated.

CHAPTER 6 - PROPENE TRIMERISATION

6.1 Introduction

The aim of this last section was to develop a model for propene oligomerisation that lumped the reaction products according to their skeletal structure. To this end, several experimental runs were carried out a different feed concentrations at low conversion. Operation at low conversion ensured firstly, that side reactions such as cracking, disproportionation and aromatisation were minimised. Secondly, since the skeletal structures were not at equilibrium, their interconversion could be modelled. Finally, the reactor could be treated as a differential one and this would make the modelling task easier.

It was intended that the information regarding the relative rates of isomerisation obtained from the hexene isomerisation study could be incorporated into this model.

The first section of this chapter covers the experimental details relevant to this section of the work. Next, a proposed reaction pathway for the formation of the trimers is presented. Following this the results of the oligomerisation at various feed concentrations is presented and discussed. Finally, conclusions are presented.

6.2 Experimental

The data for this chapter was obtained by conducting a number of propene oligomerisation reactions using several different feed concentrations. The propene feed concentration was varied by one order of magnitude by diluting with high purity nitrogen. Reaction conditions were kept constant at 250°C and 5MPa. The reactor was operated at less than 10% conversion and assumed to be differential for all runs. A summary of all the reactions is shown in Table 6.1. More details regarding each experimental run can be found in Appendix E.

Table 6.1 : Summary of Reaction Conditions for Propene Oligomerisation Runs		
Feed Composition (mol%)		WHSV (hr^{-1}) (Propene & N_2)
Propene	Nitrogen	
100	0	266
83	17	435
77	23	345
49	51	271
42	58	292
30	70	253
23	77	240
12	88	231

As mentioned in Chapter 2, the skeletal structure of the products was identified using a G.C. which included pre-column hydrogenation. Only partial separation was achieved for following structures, 4-methyl-octane/2-methyl-octane, 2,5-dimethyl-heptane/3,5-dimethyl-heptane and 2,6-dimethyl-heptane/2-methyl-4-ethyl-hexane, and these pairs were thus grouped together. The experimental apparatus and procedure have been discussed fully in Chapter 2.

Due to the low conversion, the peak areas for the reaction products in the G.C. spectra were small. Therefore, in order to obtain significant peak areas the quantity injected into the G.C. had to be increased. Unfortunately, this led to an overload in the signal for the propene peak and mass balances could not be calculated. As a compromise, one sample per run was used to calculate the mass balance while the others were used to calculate accurate product compositions. For the non-mass balance samples conversion was calculated based on the amount of reaction product, assuming 100% mass balance. Since it was established that no methane was produced during the reaction, it was used as an internal standard because its G.C. response factor was similar to the other reaction products.

Since the reaction mixture could not be regarded as ideal, compressibility factors, Z, were calculated for each run. This was used to calculate the molar density of the feed :

$$molar\ density = \frac{P}{ZRT}$$

Z was calculated using the Lee-Kesler method (see Reid et al. (1987)). For the purposes of this calculation it was assumed the reaction mixture consisted only of propene and nitrogen since the conversion for all runs was low.

6.3 Reaction Pathway for the Formation of Nonene Isomers

The proposed reaction pathway for the formation of the primary and secondary nonene isomers during propene oligomerisation is shown in Table 6.2. As the product structures were identified using a G.C. with pre-column hydrogenation, the hexene and nonene isomers are classified according to their alkane carbon skeletons. Those identified during product analysis are marked in bold.

The oligomerisation pathway shown in Table 6.2 is based on the following assumptions and principles:

1. Even at low conversion, all hexene and nonene isomers are at equilibrium with respect to their double bonds (see Chapter 4). Because of double-bond equilibrium, the isomers are grouped according to their skeletal structures and only skeletal isomerisation reactions are considered.

2. During the hexene isomerisation studies discussed in Chapter 5, four major hexene carbon skeletons were identified namely, 2-methyl-pentane, 3-methyl-pentane, hexane and 2,3-dimethyl-butane. These skeletons were present in the form of primary, secondary or tertiary carbenium ions. For the purposes of this study, primary carbenium ions were ignored since

these less stable ions isomerise readily to the more stable secondary or tertiary ions.

3. The formation of primary nonene isomers takes place via the Markownikov addition of a propene molecule to a hexyl carbenium ion. It was not possible to establish whether the reaction involved :

a) a Markownikov addition of an adsorbed propene molecule to an adsorbed, adjacent hexyl carbenium ion or

b) a Markownikov addition of a gas phase propene molecule to an adsorbed hexyl carbenium ion.

However, due to the structure of the reaction products from the non-shape selective catalysts studied it appears that the Markownikov addition of a gas phase hexene molecule to an adsorbed propyl ion does not predominate over the addition of a gas phase propene molecule to an adsorbed hexyl carbenium ion. The addition of the propene molecule to the dimers and the formation of the proposed primary products along with their structure is shown in Figure 6.1.

4. Once formed, the primary nonene isomers undergo Type A or Type B isomerisation to produce an array of secondary nonene isomers. In a manner similar to the hexene isomers, nonene isomers undergo isomerisation via protonated cyclopropane intermediates. An example of this isomerisation is shown for the 2,4-dimethyl-heptane skeleton in Figure 6.2. The 2,5-dimethyl-heptane skeleton is produced via Type A isomerisation and thus only involves a methyl shift reaction while the 2-methyl-octane skeleton is formed via Type B isomerisation.

5. This scheme covers reactions occurring during the initial stages of oligomerisation, i.e. under conditions of low conversion. For this reason, further nonene isomerisation, cracking and disproportionation reactions are not considered.

6. This reaction scheme does not include shape selective effects.

Table 6.2 : Formation of Nonene Carbon Skeletons - Non-Shape Selective

Hexene Skeletons	Nonene Primary Skeletons	Nonene Secondary Skeletons			
		Single Branch / Linear	Double Methyl Branch	Triple Methyl Branch	Double Methyl-Ethyl Branch
2-methyl-Pentane → + Propene	**4,4-dimethyl-Heptane →**	**4-methyl-Octane**	**3,4-dimethyl-Heptane**		**2-methyl-3-ethyl-Hexane** **2-methyl-4-ethyl-Hexane**
2-methyl-Pentane → + Propene	**2-methyl-3-ethyl-Hexane →**	**4-ethyl-Heptane** 3-propyl-Hexane	**2,3-dimethyl-Heptane** **2,4-dimethyl-Heptane**		2,4-dm-3-eth-Pentane 2,3-dm-3-eth-Pentane 2-methyl-2-ethyl-Hexane **3-methyl-3-ethyl-Hexane** **2-methyl-4-ethyl-Hexane** 2-meth-2-propyl-Pentane 3-meth-3-propyl-Pentane
2-methyl-Pentane → + Propene	**2,4-dimethyl-Heptane →**	**2-methyl-Octane** **4-methyl-Octane**	**2,3-dimethyl-Heptane** **2,5-dimethyl-Heptane** **3,4-dimethyl-Heptane**	2,2,3-trimethyl-Hexane 2,3,3-trimethyl-Hexane 2,4,4-trimethyl-Hexane 2,4,5-trimethyl-Hexane	**2-methyl-3-ethyl-Hexane** **2-methyl-4-ethyl-Hexane**
3-methyl-Pentane → + Propene	**3-methyl-3-ethyl-Hexane →**	3-ethyl-Heptane	**3,4-dimethyl-Heptane**		3-methyl-4-ethyl-Hexane
3-methyl-Pentane → + Propene	**3,4-dimethyl-Heptane →**	**3-methyl-Octane** **4-methyl-Octane**	**2,4-dimethyl-Heptane** **3,3-dimethyl-Heptane** **3,5-dimethyl-Heptane** **4,4-dimethyl-Heptane**	**2,3,4-trimethyl-Hexane** 3,3,4-trimethyl-Hexane	**3-methyl-3-ethyl-Hexane** 3-methyl-4-ethyl-Hexane
Hexane → + Propene	**4-methyl-Octane →**	**Nonane** **3-methyl-Octane** 3-ethyl-Heptane **4-ethyl-Heptane**	**2,3-dimethyl-Heptane** **2,4-dimethyl-Heptane** **3,3-dimethyl-Heptane** **3,4-dimethyl-Heptane** **4,4-dimethyl-Heptane**		
Hexane → + Propene	**4-ethyl-Heptane →**	**4-methyl-Octane** 3-ethyl-Heptane **4-ethyl-Heptane** 3-propyl-Hexane			**2-methyl-3-ethyl-Hexane** **3-methyl-3-ethyl-Hexane**
2,3-dimethyl-Butane → + Propene	2,3,3-trimethyl-Hexane →		**2,3-dimethyl-Heptane**	**2,3,4-trimethyl-Hexane**	2-meth-2-isoprop-Butane 2-meth-3-isoprop-Butane

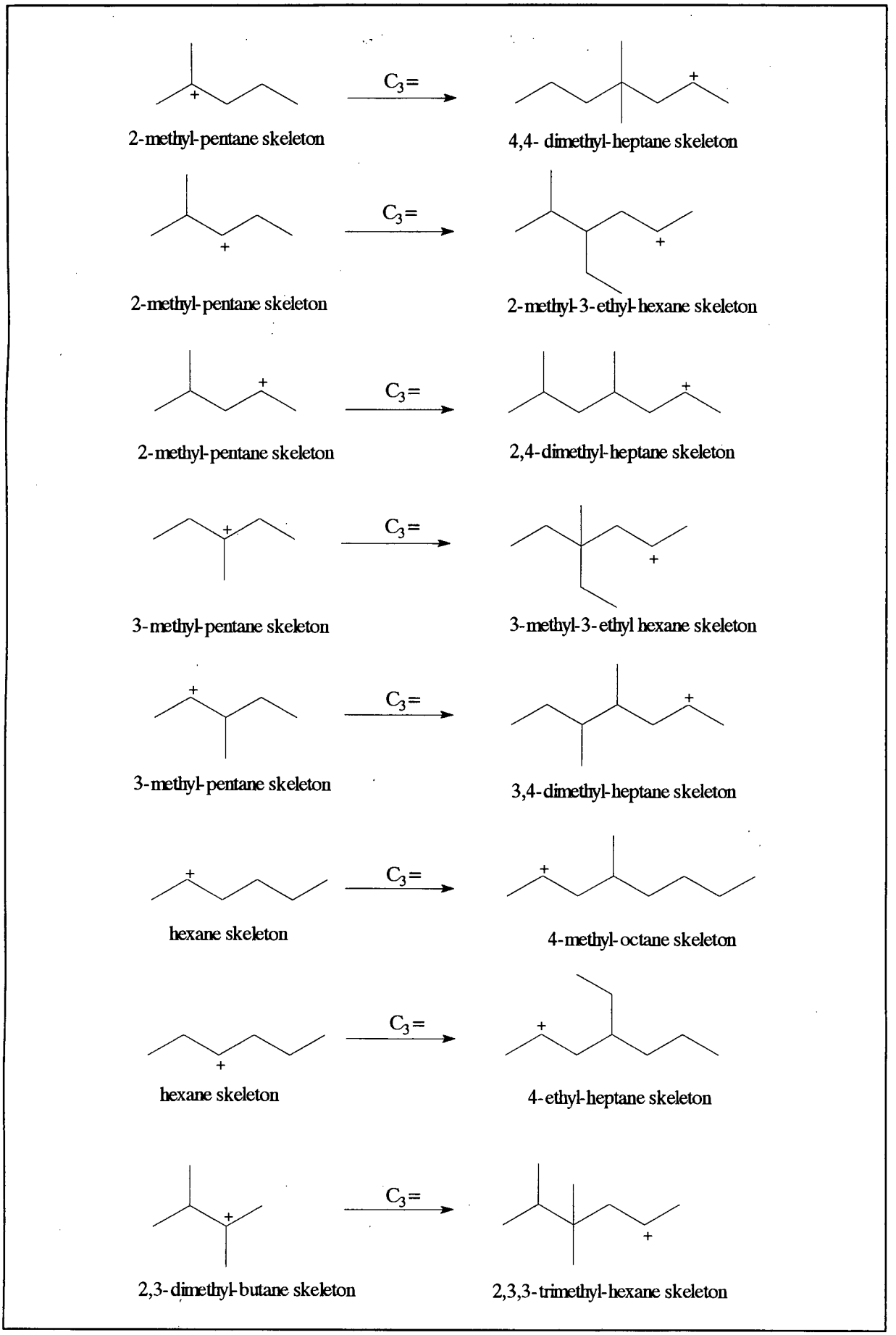

Figure 6.1 : Formation of Primary Nonene Isomers

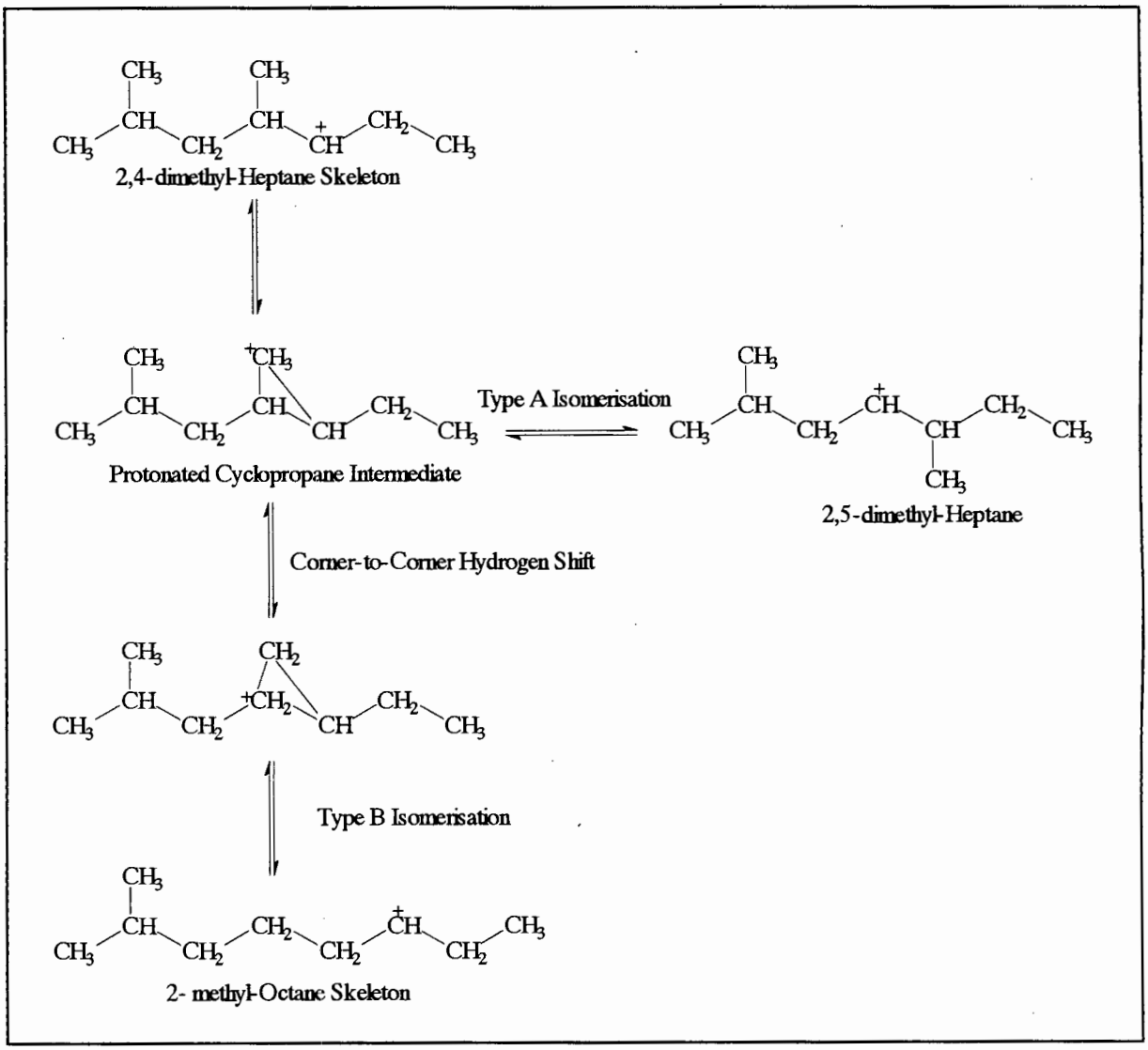

Figure 6.2 : Type A and Type B Isomerisation of the 2,4-dimethyl-Heptane Skeleton

Table 6.3 : Major Nonene Skeletons Ranked in Order of Decreasing Concentration			
H-ZSM-5	H-Beta	Silica Alumina	Sapo34
4-m-C8 / 2-m-C8 *	3,4-dm-C7 *	3,4-dm-C7 *	3,4-dm-C7 *
2,5-dm-C7/3,5-dm-C7 #	2,3-dm-C7 #	2-meth-3-eth-C6 *	2-meth-3-eth-C6 *
3,4-dm-C7 *	2,5-dm-C7/3,5-dm-C7 #	2,5-dm-C7/3,5-dm-C7 #	2,3-dm-C7 #
2,4-dm-C7 *	2-meth-3-eth-C6 *	2,3-dm-C7 #	2,5-dm-C7/3,5-dm-C7 #
3-m-C8 #	2,4-dm-C7 *	2,4-dm-C7 *	2,4-dm-C7 *
2,3-dm-C7 #	4,4-dm-C7 *	2,3,5-tm-C6	2,3,5-tm-C6
2-meth-3-eth-C6 *	4-m-C8 / 2-m-C8 *	2,3,4-trm-C6 #	2,3,4-trm-C6 #
linear C9	3-m-C8 #	4,4-dm-C7 *	4,4-dm-C7 *
2,6-dm-C7/2-m-4-e-C6#	2,3,4-trm-C6 #	2,6-dm-C7/2-m-4-e-C6#	2,6-dm-C7/2-m-4-e-C6#
2,2-dm-C7	2,3,5-trm-C6	4-m-C8 / 2-m-C8 *	3-meth-3-eth-C6 *
4,4-dm-C7 *	2,6-dm-C7/2-m-4-e-C6#	3-m-C8 #	4-m-C8 / 2-m-C8 *
2,3,4-trm-C6#	2,2-dm-C7	2,2-dm-C7	3-m-C8 #
2,3,5-trm-C6	3-meth-3-eth-C6 *	3-eth-3-meth-C6 *	2,2-dm-C7
3-meth-3-eth-C6 *			

Key : * = primary structures

\# = primary structures that have undergone rapid Type A isomerisation

A number of additional propene oligomerisation runs were performed on H-Beta, Silica-Alumina and SAPO-34, the results of which were discussed in detail in Chapter 3. The distribution of the nonene skeletal structures for these runs is shown again in Figure 6.3. The carbon skeletons of the C_9 olefins identified after hydrogenation of the reaction products are listed in Table 6.3 for each catalyst in order of decreasing concentration within the C_9 group. All these runs were carried out at approximately 5% conversion.

As discussed in Chapter 3, none of the reaction products from H-Beta, Silica-Alumina or SAPO-34 exhibit shape selective effects while those from H-ZSM-5 do. The following examples illustrate this. Figure 6.3 shows that the percentage of linear isomers in the product from H-ZSM-5 is much higher than that for the other catalysts studied. Additionally, while the major skeletons from H-ZSM-5 are 4-methyl-octane and 2-methyl-octane, 3,4-dimethyl-

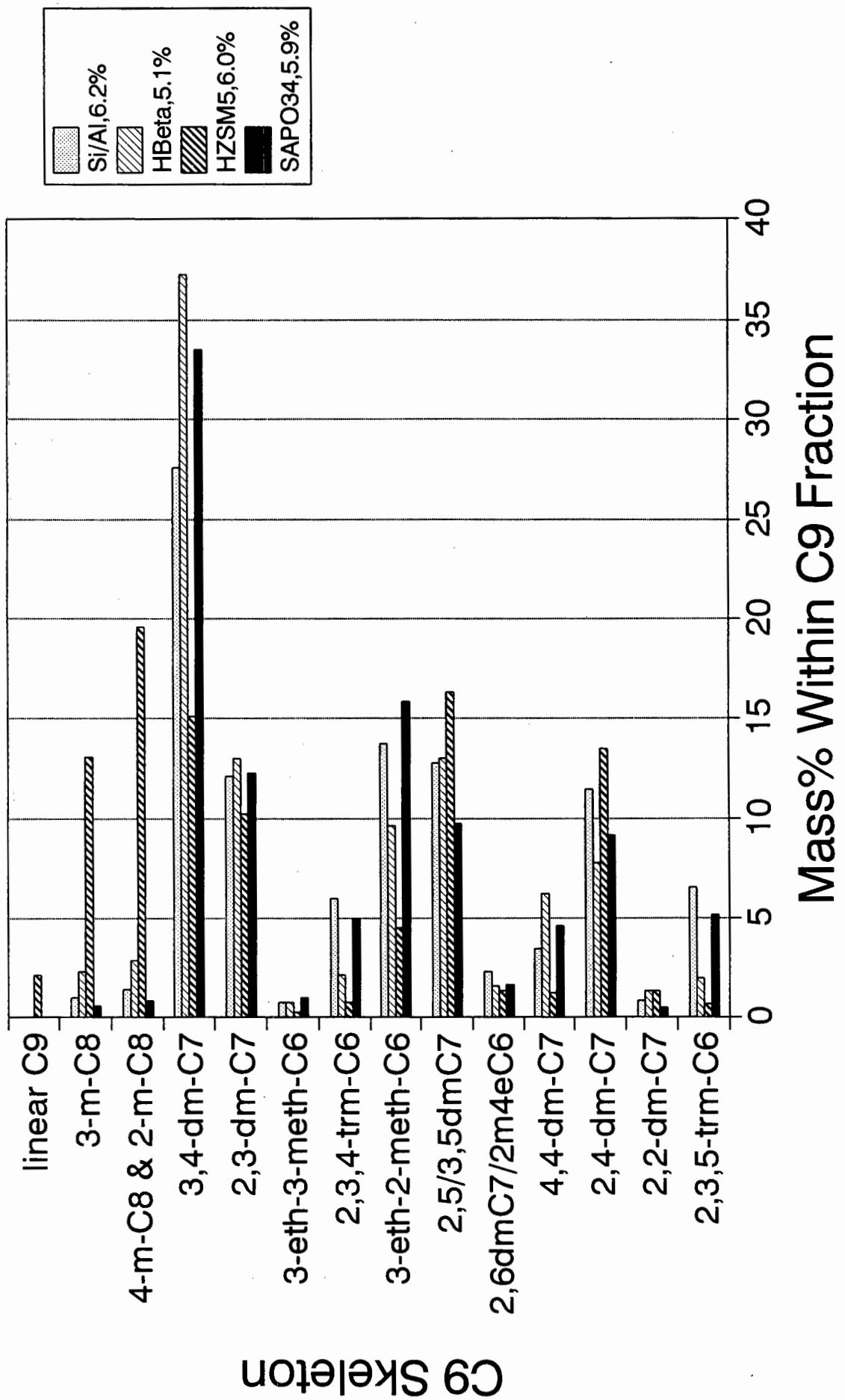

Figure 6.3 : Nonene Selectivity for Different Catalysts (Conversion Shown for Each Catalyst)

heptane is the major product from the non-shape selective catalysts. Also, the linear C_9 structure only appears in the H-ZSM-5 product spectrum. When the liquid product from the oligomerisation runs was analysed using the mass spectrometer, it was observed that when the non-shape selective catalysts were used, the 2,6-dimethyl-heptane/2-methyl-4-ethyl-hexane peak consisted mostly of 2-methyl-4-ethyl-hexane while for H-ZSM-5 it consisted mostly of 2,6-dimethyl-heptane.

The experimental data shown in Figure 6.3 and Table 6.3 confirm, in part, the validity of the oligomerisation reaction pathway shown in Table 6.2 :

1. All the non-shape selective catalysts have similar product spectra at 5% conversion. This points to a common reaction mechanism.

2. For the non-shape selective catalysts, the following major nonene skeletons are observed: 3,4-dimethyl-heptane, 2,3-dimethyl-heptane, 2-methyl-3-ethyl-hexane, 2,5 and 3,5-dimethyl-heptane and 2,4-dimethyl-heptane. These structures are, according to the proposed reaction scheme, primary products or primary products that have undergone rapid methyl-shift reactions. The major products observed for H-ZSM-5 can also be classified in this way, except that there is a shift towards the more linear primary products. For example, the concentration of 4-methyl/2-methyl-octane increases relative to 3,4-dimethyl-heptane.

3. For both the shape selective and non-shape selective catalysts studied, the majority of the less dominant structures are, according to Table 6.2, secondary isomerisation products.

It is interesting to note that those primary nonene skeletons formed from the most stable hexene structures (those classified as tertiary carbenium ions) i.e. 4,4-dimethyl-heptane, 3-methyl-3-ethyl-hexane and 2,3,3-trimethyl-hexane are not present in large amounts, even for non-shape selective catalysts (see Figure 6.1). Neckers and Doyle (1977) provide a possible explanation for this. They state that in general the more rapid the rate of formation of a carbenium ion, the less rapid the rate of reaction of that same carbenium ion with a nucleophile. The faster the rate of formation of the carbenium ion, the more stable the

carbenium ion, and the slower its subsequent reaction with a Lewis base (olefin).

In other words, a possible reason for the low concentration of these primary isomers is the stability of the reacting hexenes which inhibits them from oligomerising further with propene.

From the above discussion, it is evident that determining the reaction pathway for propene trimerisation is a non-trivial task. Furthermore, in order to determine the reaction pathway unequivocally, additional runs should be carried out by feeding various nonene isomers, of varying skeletal structures, as was done for the hexenes.

6.4 Propene Oligomerisation over H-ZSM-5 under Conditions of Low Conversion

The following reaction scheme involving elementary, homogeneous reactions was proposed for oligomerisation over H-ZSM-5. The alkanes in this scheme represent the skeletal structures of the nonene isomers. Only those compounds present in the H-ZSM-5 product spectrum are included here. :

$C_3= + C_3= \rightarrow$ 2-methyl-pentane	Formation of primary C_6 structure
2-methyl-pentane $\leftrightarrow$ 3-methyl-pentane	Hexene Skeletal Isomerisation
2-methyl-pentane $\leftrightarrow$ hexane	
2-methyl-pentane $\leftrightarrow$ 2,3-dimethyl-butane	
2-methyl-pentane + $C_3= \rightarrow$ 2,4-dimethyl-heptane	Formation of primary C_9 structures
2-methyl-pentane + $C_3= \rightarrow$ 2-methyl-3-ethyl-hexane	
2-methyl-pentane + $C_3= \rightarrow$ highly branched C_9's	
3-methyl-pentane + $C_3= \rightarrow$ 3,4-dimethyl-heptane	
3-methyl-pentane + $C_3= \rightarrow$ highly branched C_9's	
hexane + $C_3= \rightarrow$ 4-methyl-octane	

2,4-dimethyl-heptane ⇔ 2-methyl-octane	Nonene Skeletal Isomerisation
2,4-dimethyl-heptane ⇔ 4-methyl-octane	
2,4-dimethyl-heptane ⇔ 2,3-dimethyl-heptane	
2,4-dimethyl-heptane ⇔ 2,5-dimethyl-heptane	
2,4-dimethyl-heptane ⇔ 3,4-dimethyl-heptane	
2,4-dimethyl-heptane ⇔ 2-methyl-3-ethyl-hexane	
2-methyl-3-ethyl-hexane ⇔ 2,3-dimethyl-heptane	
3,4-dimethyl-heptane ⇔ 3-methyl-octane	
3,4-dimethyl-heptane ⇔ 4-methyl-octane	
3,4-dimethyl-heptane ⇔ 3,5-dimethyl-heptane	
4-methyl-octane ⇔ 3-methyl-octane	
4-methyl-octane ⇔ 2,3-dimethyl-heptane	
Total C_9's + C_3= → C_{12}'s	Formation of C_{12}'s

Using the above reaction scheme the following rate equations can be written :

Subscripts used in the model are :

2-methyl-pentane structure -	S2
3-methyl-pentane structure -	S3
hexane structure -	L
2,3-dimethyl-butane structure -	D
BranC9 -	those C_9's appearing in low concentration, mainly highly branched structures
totC9 -	total of all C_9's

The other subscripts used are self explanatory.

$$\frac{dC_{C3}}{dt} = -2k_{2C3\rightarrow S2}C_{C3}^2 - (k_{S2+C3\rightarrow 2AdmC7} + k_{S2+C3\rightarrow 2m3eC6} + k_{S2+C3\rightarrow BranC9})C_{C3}C_{S2} - (k_{S3+C3\rightarrow 34dmC7} + k_{S3+C3\rightarrow BranC9})C_{C3}C_{S3} - k_{L+C3\rightarrow 4mC8}C_{C3}C_L - k_{totC9+C3\rightarrow C12}C_{C3}C_{totC9} \quad (6.1)$$

$$\frac{dC_D}{dt} = -k_{D\rightarrow S2}C_D + k_{S2\rightarrow D}C_{S2} \tag{6.2}$$

$$\frac{dC_{S2}}{dt} = k_{2C3\rightarrow S2}C_{C3}^2 + k_{D\rightarrow S2}C_D - (k_{S2\rightarrow D} + k_{S2\rightarrow S3} + k_{S2\rightarrow L})C_{S2} + k_{S3\rightarrow S2}C_{S3} + k_{L\rightarrow S2}C_L - (k_{S2+C3\rightarrow 2AdmC7} + k_{S2+C3\rightarrow 2m3eC6} + k_{S2+C3\rightarrow BranC9})C_{C3}C_{S2} \tag{6.3}$$

$$\frac{dC_{S3}}{dt} = k_{S2\rightarrow S3}C_{S2} - k_{S3\rightarrow S2}C_{S3} - (k_{S3+C3\rightarrow 34dmC7} + k_{S3+C3\rightarrow BranC9})C_{C3}C_{S3} \tag{6.4}$$

$$\frac{dC_L}{dt} = k_{S2\rightarrow L}C_{S2} - k_{L\rightarrow S2}C_L - k_{L+C3\rightarrow 4mC8}C_{S3}C_L \tag{6.5}$$

$$\frac{dC_{2AdmC7}}{dt} = k_{S2+C3\rightarrow 2AdmC7}C_{C3}C_{S2} - (k_{2AdmC7\rightarrow 25dmC7} + k_{2AdmC7\rightarrow 2m3eC6} + k_{2AdmC7\rightarrow 23dmC7} + k_{2AdmC7\rightarrow 34dmC7} + k_{2AdmC7\rightarrow 4mC8} + k_{2AdmC7\rightarrow 2mC8})C_{2AdmC7} + k_{25dmC7\rightarrow 2AdmC7}C_{25dmC7} + k_{2m3eC6\rightarrow 2AdmC7}C_{2m3eC6} + k_{23dmC7\rightarrow 2AdmC7}C_{23dmC7} + k_{34dmC7\rightarrow 2AdmC7}C_{34dmC7} + k_{4mC8\rightarrow 2AdmC7}C_{4mC8} + k_{2mC8\rightarrow 2AdmC7}C_{2mC8} \tag{6.6}$$

$$\frac{dC_{25dmC7}}{dt} = k_{2AdmC7\rightarrow 25dmC7}C_{2AdmC7} - k_{25dmC7\rightarrow 2AdmC7}C_{25dmC7} \tag{6.7}$$

$$\frac{dC_{35dmC7}}{dt} = -k_{35dmC7\rightarrow 34dmC7}C_{35dmC7} + k_{34dmC7\rightarrow 35dmC7}C_{34dmC7} \tag{6.8}$$

$$\frac{dC_{2m3eC6}}{dt} = k_{S2+C3\rightarrow 2m3eC6}C_{C3}C_{S2} + k_{2AdmC7\rightarrow 2m3eC6}C_{2AdmC7} - (k_{2m3eC6\rightarrow 2AdmC7} + k_{2m3eC6\rightarrow 23dmC7})C_{2m3eC6} + k_{23dmC7\rightarrow 2m3eC6}C_{23dmC7} \tag{6.9}$$

$$\frac{dC_{23dmC7}}{dt} = k_{24dmC7\rightarrow 23dmC7}C_{24dmC7} + k_{2m3eC6\rightarrow 23dmC7}C_{2m3eC6} - (k_{23dmC7\rightarrow 24dmC7} + k_{23dmC7\rightarrow 2m3eC6} + k_{23dmC7\rightarrow 4mC8})C_{23dmC7} + k_{4mC8\rightarrow 23dmC7}C_{4mC8} \quad (6.10)$$

$$\frac{dC_{34dmC7}}{dt} = k_{S3+C3\rightarrow 34dmC7}C_{C3}C_{S3} + k_{24dmC7\rightarrow 34dmC7}C_{24dmC7} + k_{35dmC7\rightarrow 34dmC7}C_{35dmC7} - (k_{34dmC7\rightarrow 24dmC7} + k_{34dmC7\rightarrow 35dmC7} + k_{34dmC7\rightarrow 4mC8} + k_{34dmC7\rightarrow 3mC8})C_{34dmC7} + k_{4mC8\rightarrow 34dmC7}C_{4mC8} + k_{3mC8\rightarrow 34dmC7}C_{3mC8} \quad (6.11)$$

$$\frac{dC_{4mC8}}{dt} = k_{L+C3\rightarrow 4mC8}C_{C3}C_{L} + k_{24dmC7\rightarrow 4mC8}C_{24dmC7} + k_{23dmC7\rightarrow 4mC8}C_{23dmC7} + k_{34dmC7\rightarrow 4mC8}C_{34dmC7} - (k_{4mC8\rightarrow 24dmC7} + k_{4mC8\rightarrow 23dmC7} + k_{4mC8\rightarrow 34dmC7} + k_{4mC8\rightarrow 3mC8})C_{4mC8} + k_{3mC8\rightarrow 4mC8}C_{3mC8} \quad (6.12)$$

$$\frac{dC_{2mC8}}{dt} = k_{24dmC7\rightarrow 2mC8}C_{24dmC7} - k_{2mC8\rightarrow 24dmC7}C_{2mC8} \quad (6.13)$$

$$\frac{dC_{3mC8}}{dt} = k_{34dmC7\rightarrow 3mC8}C_{34dmC7} + k_{4mC8\rightarrow 3mC8}C_{4mC8} - (k_{3mC8\rightarrow 34dmC7} + k_{3mC8\rightarrow 4mC8})C_{3mC8} \quad (6.14)$$

$$\frac{dC_{12}}{dt} = k_{totC9+C3\rightarrow C12}C_{C3}C_{totC9} \quad (6.15)$$

$$\frac{dC_{totC9}}{dt} = -k_{totC9+C3\rightarrow C12}C_{C3}C_{totC9} \quad (6.16)$$

$$\frac{dC_{BranC9}}{dt} = k_{S2+C3\rightarrow BranC9}C_{C3}C_{S2} + k_{S3+C3\rightarrow BranC9}C_{C3}C_{S3} \quad (6.17)$$

Since the propene oligomerisation runs were carried out at less than 10% conversion, the

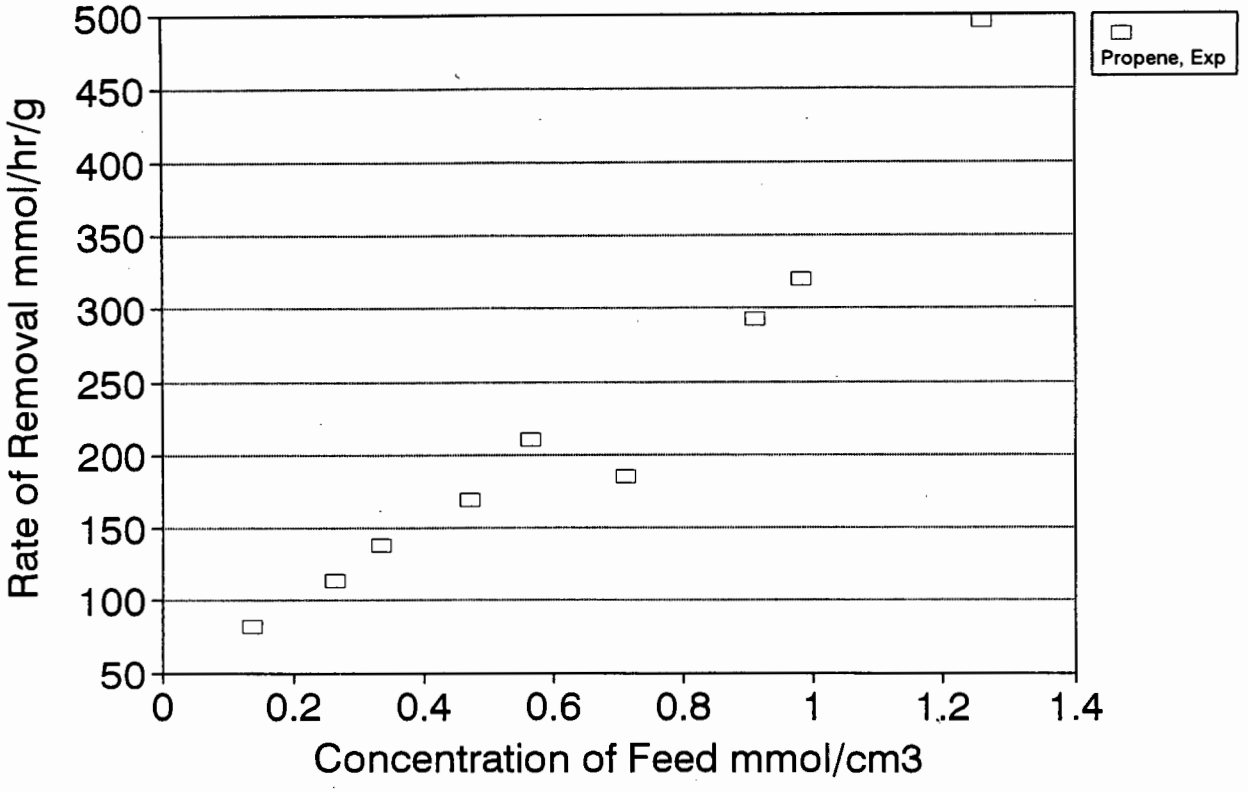

Figure 6.4 : Initial Rates for Propene During Propene Oligomerisation

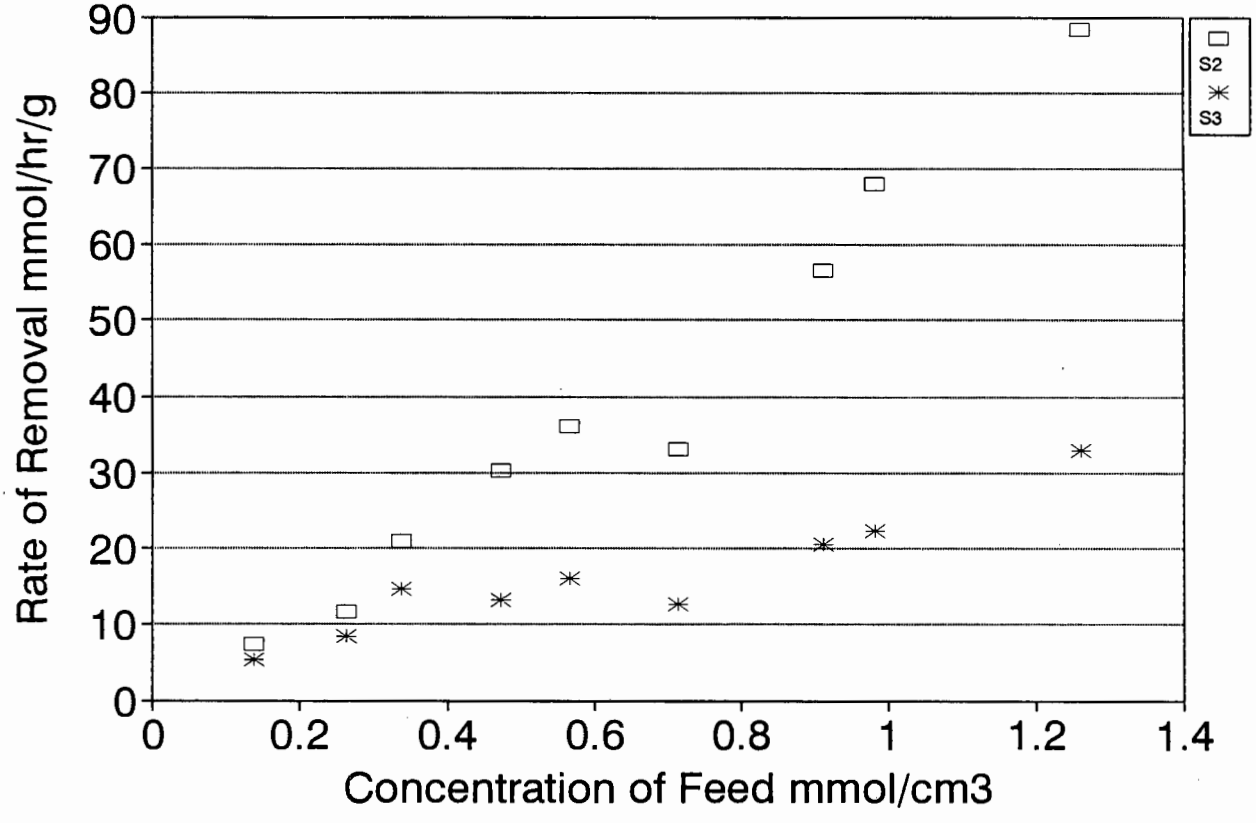

Figure 6.5a : Initial Rates for Hexene Skeletal Stuctures During Propene Oligomerisation

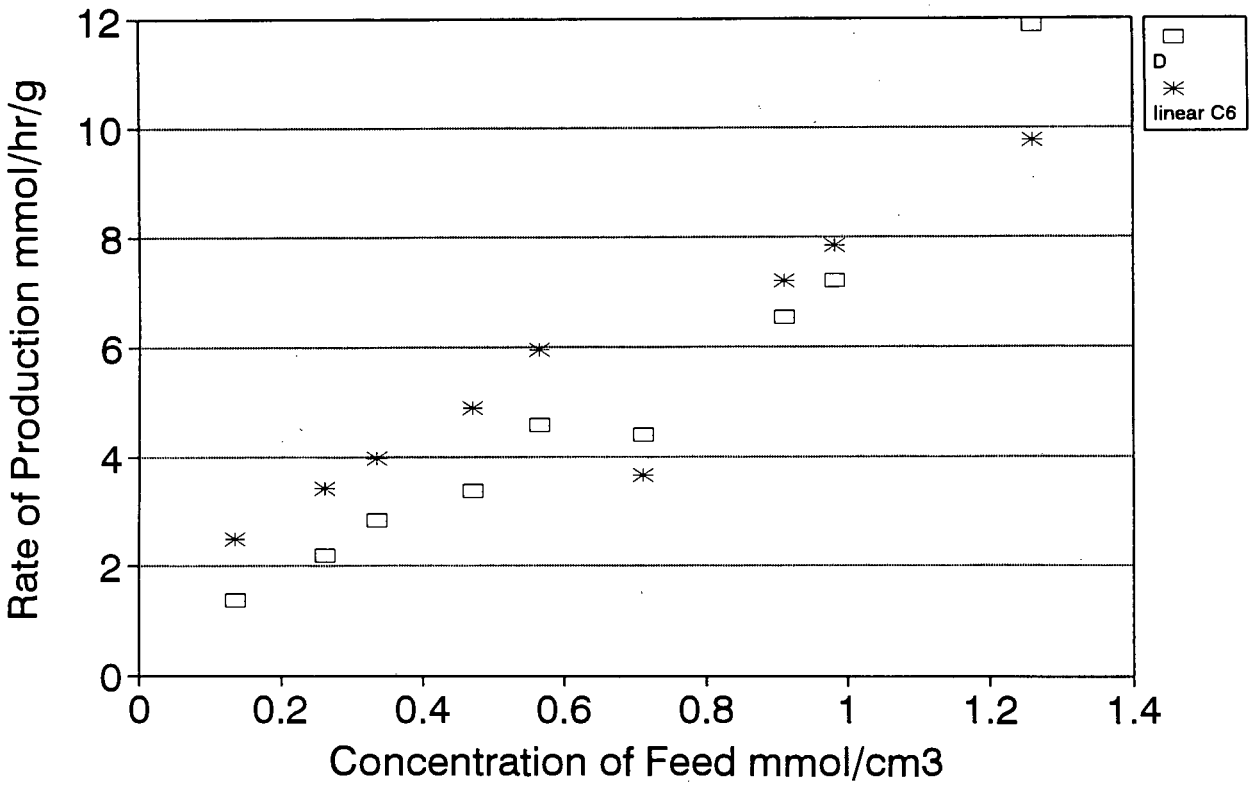

Figure 6.5b : Initial Rates for Hexene Skeletal Structures During Propene Oligomerisation

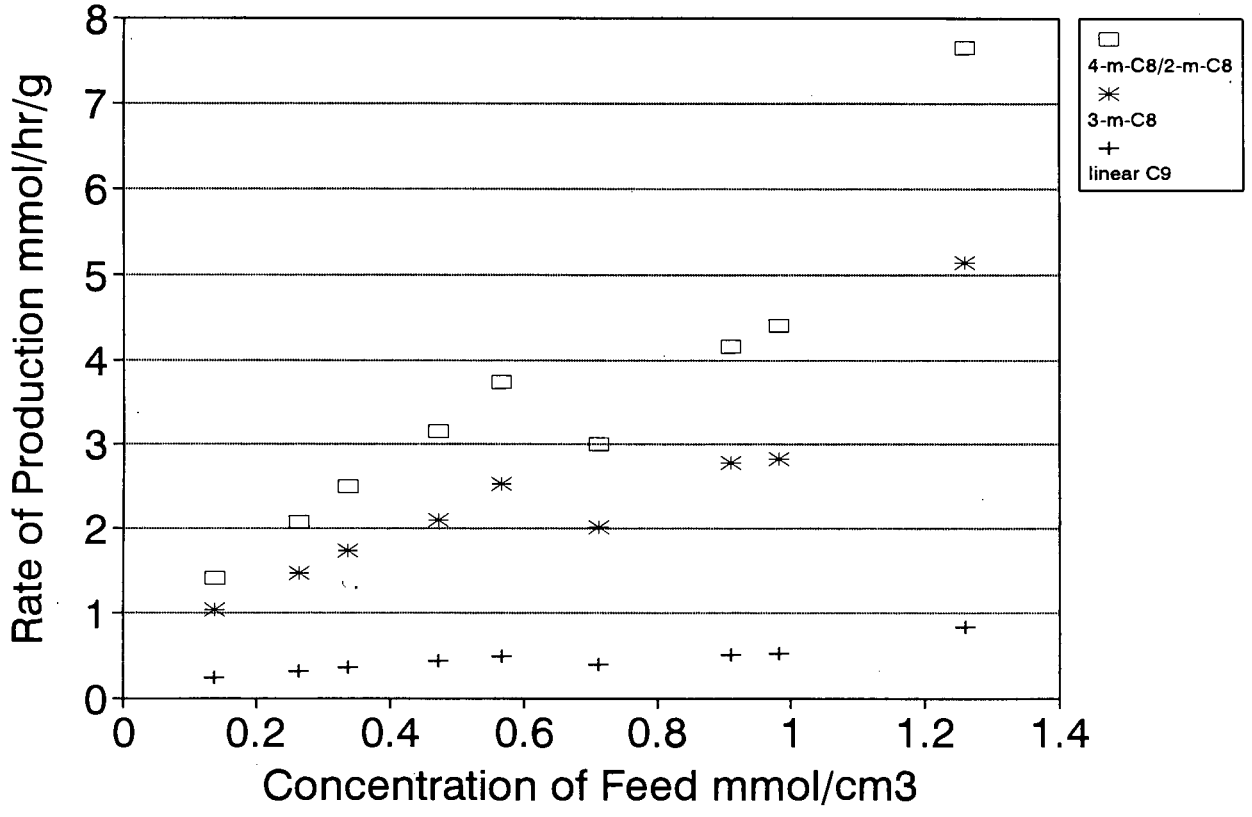

Figure 6.6a : Initial Rates for Nonene Skeletal Structures During Propene Oligomerisation

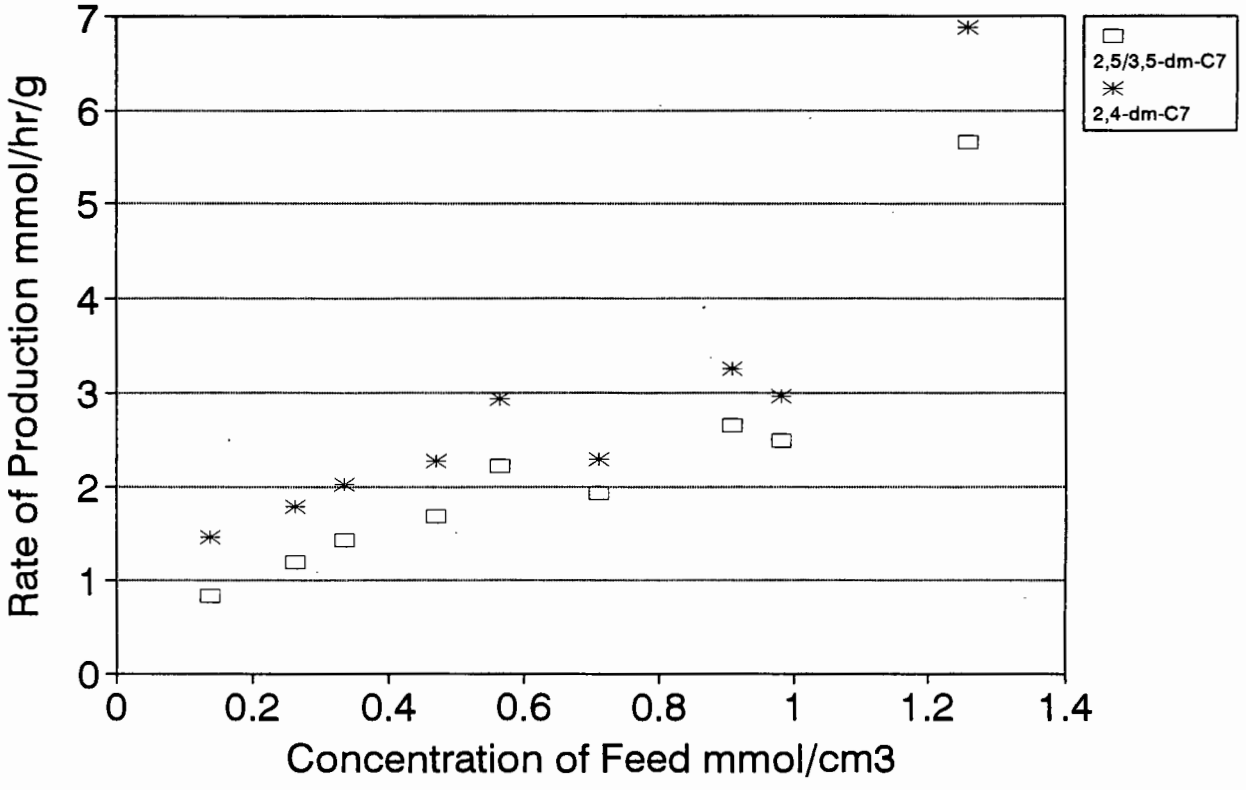

Figure 6.6b : Initial Rates for Nonene Skeletal Structures During Propene Oligomerisation

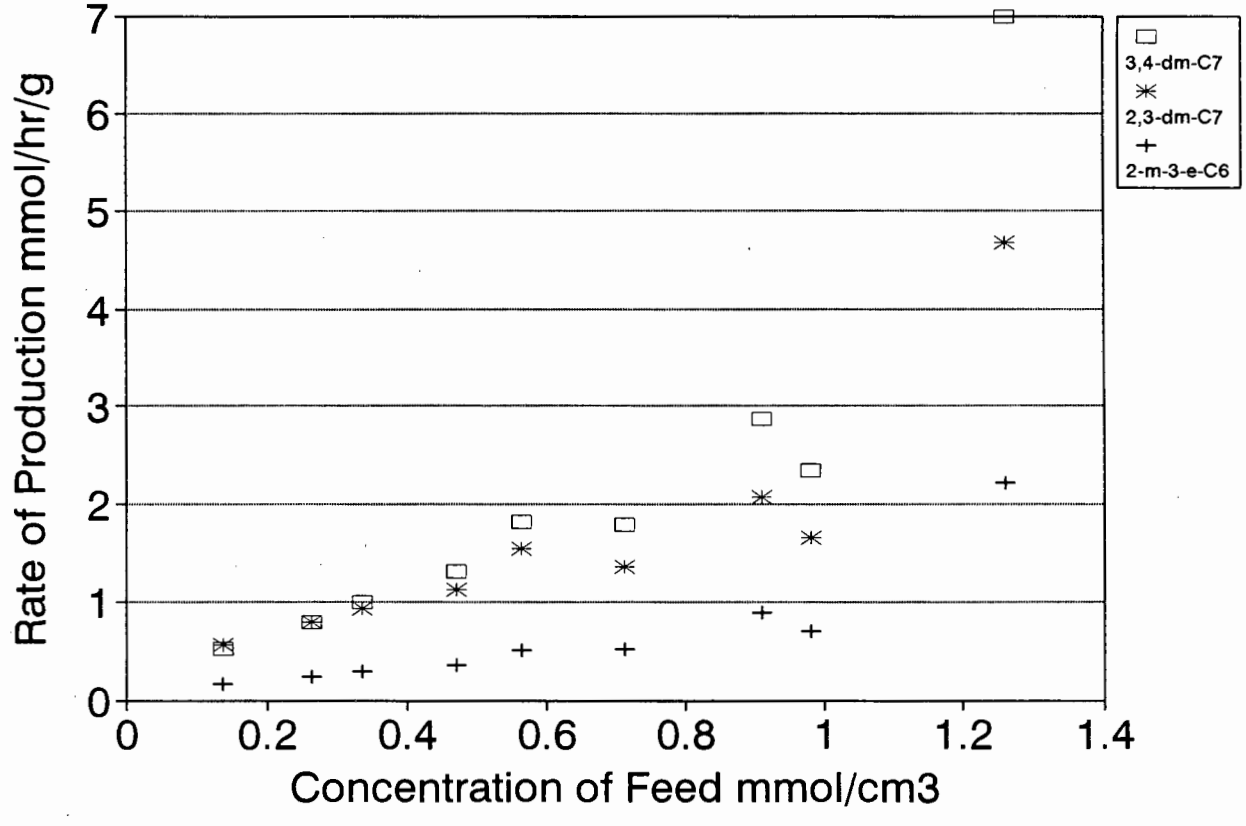

Figure 6.6c : Initial Rates for Nonene Skeletal Structures During Propene Oligomerisation

reactor was treated as differential and the reaction rate was taken as constant over the catalyst bed. Thus, for each run average rates of formation for each product could be plotted as a function of average feed concentration. This is shown in Figures 6.4 to 6.6.

According to the rate equations above, at low conversions the rate of removal of propene should be directly proportional to the square of the feed concentration (Equation 6.1). Similarly, the rate of formation of the primary 2-methyl-pentane structure should also be directly proportional to the square of the feed concentration (Equation 6.3). The rate of formation of the primary nonene structures namely, 2,4-dimethyl-heptane, 2-methyl-3-ethyl-hexane, 3,4-dimethyl-heptane and 4-methyl-octane should be proportional to $C_6.C_3$ (Equations 6.6, 6.9, 6.11 and 6.12).

When the experimental data plotted in Figures 6.4 to 6.6 was studied it was found that either a straight line (first order relationship) or a curve (second order relationship) could be fitted to most of the sets of data points. It should be noted that the last data point for all curves corresponds to the run conducted at pure feed concentration. This last point does not form part of the trend exhibited by the other data points corresponding to lower feed concentrations.

In order to clarify whether the rate of formation of each species was first or second order, the selectivity of each reaction product was plotted against the propene concentration in the feed (Figures 6.7 and 6.8). The selectivity for most of the carbon skeletons is either unvarying or exhibits only a weak trend for example, S3, linear C9, 2-methyl-3-ethyl-hexane, 2,3-dimethyl-heptane, 3,4-dimethyl-heptane and 2,4-dimethyl-heptane. Only a few structures exhibit obvious changes in selectivity with feed concentration for example, S2 and 2,5-/3,5-dimethyl-heptane.

Unvarying selectivity with feed concentration indicates a first order relationship between reaction rate and propene concentration as shown by the following example.

Consider the following first order series reaction :

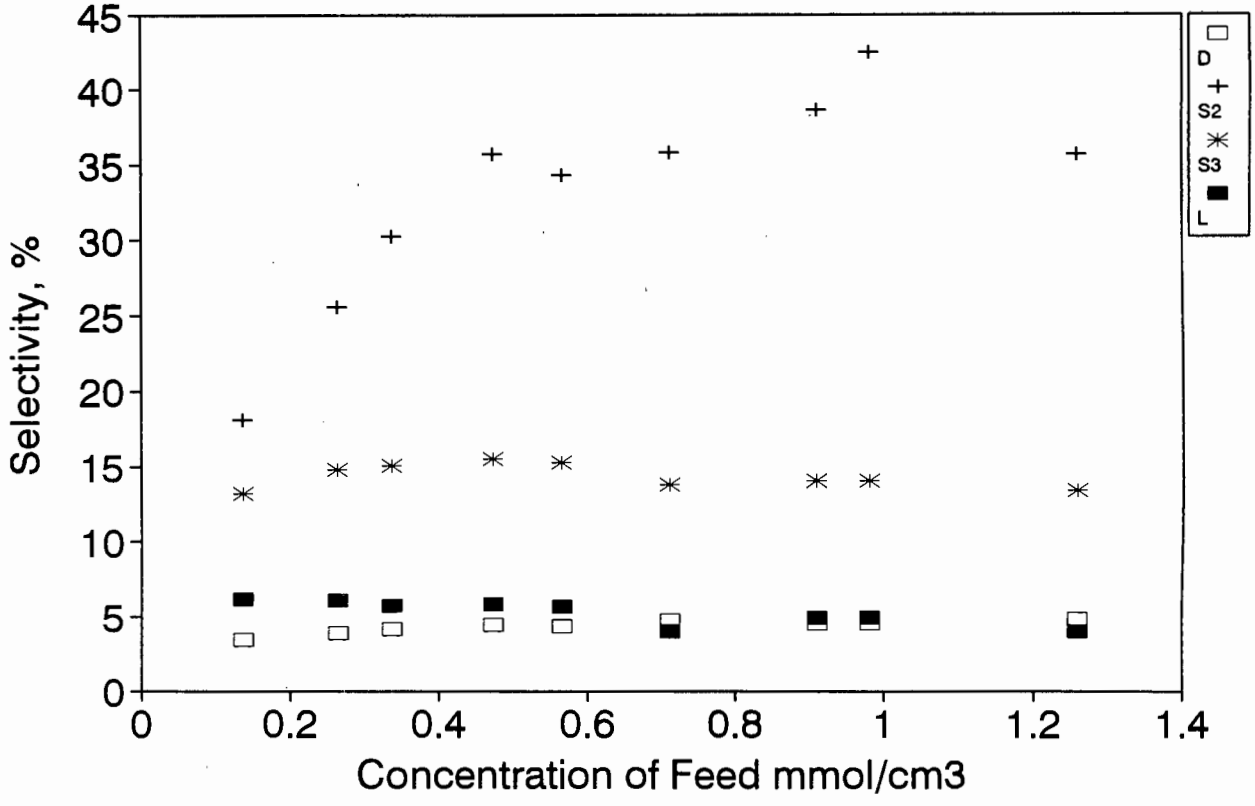

Figure 6.7 : Selectivity of Hexene Skeletal Structures at Low Conversions

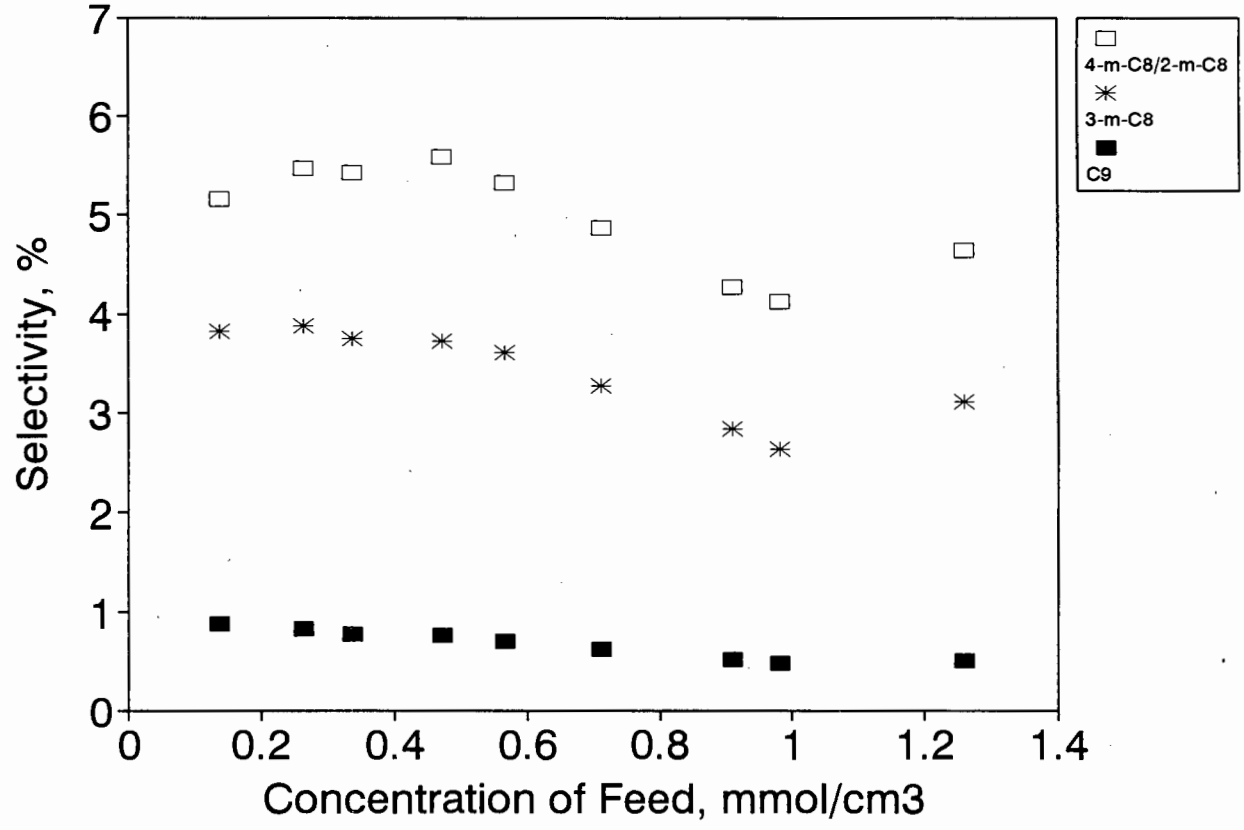

Figure 6.8a : Selectivity of Nonene Skeletal Structures at Low conversions

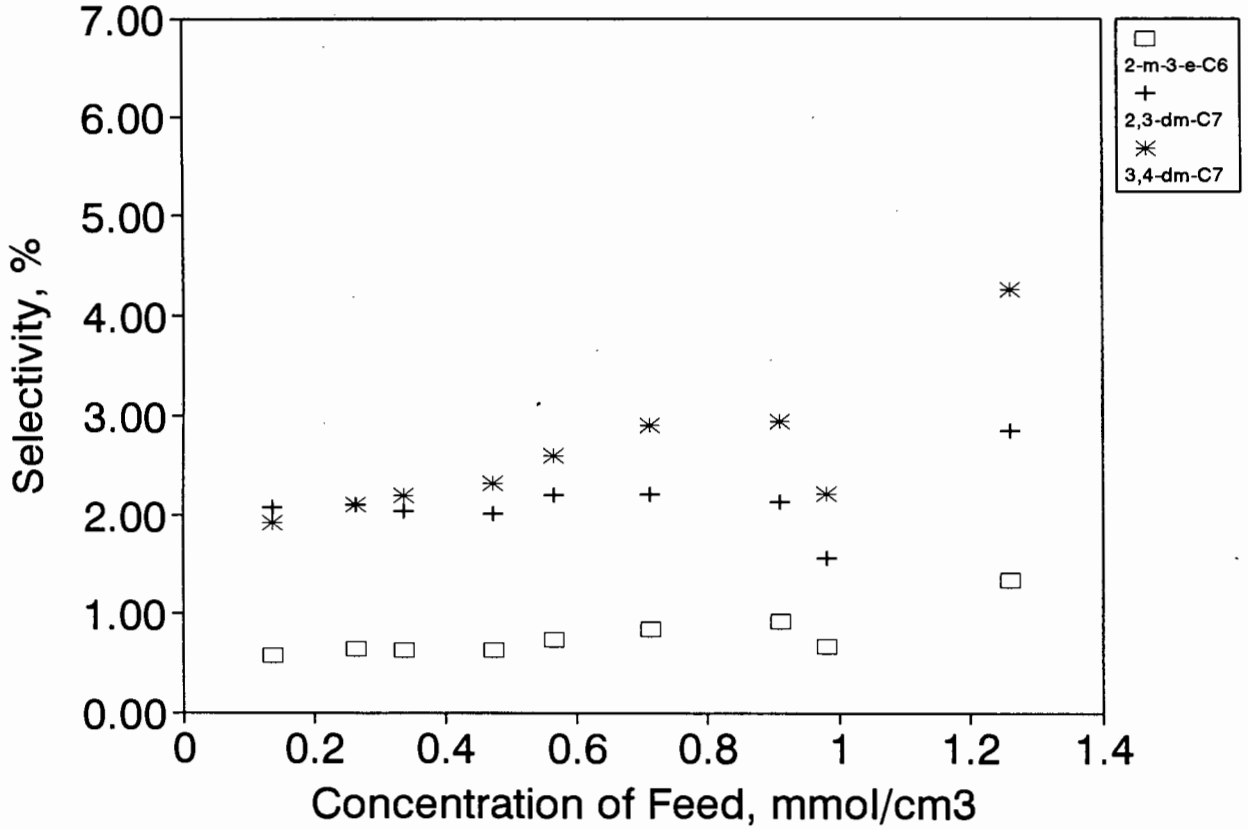

Figure 6.8b : Selectivity of Nonene Skeletal Structures at Low Conversions

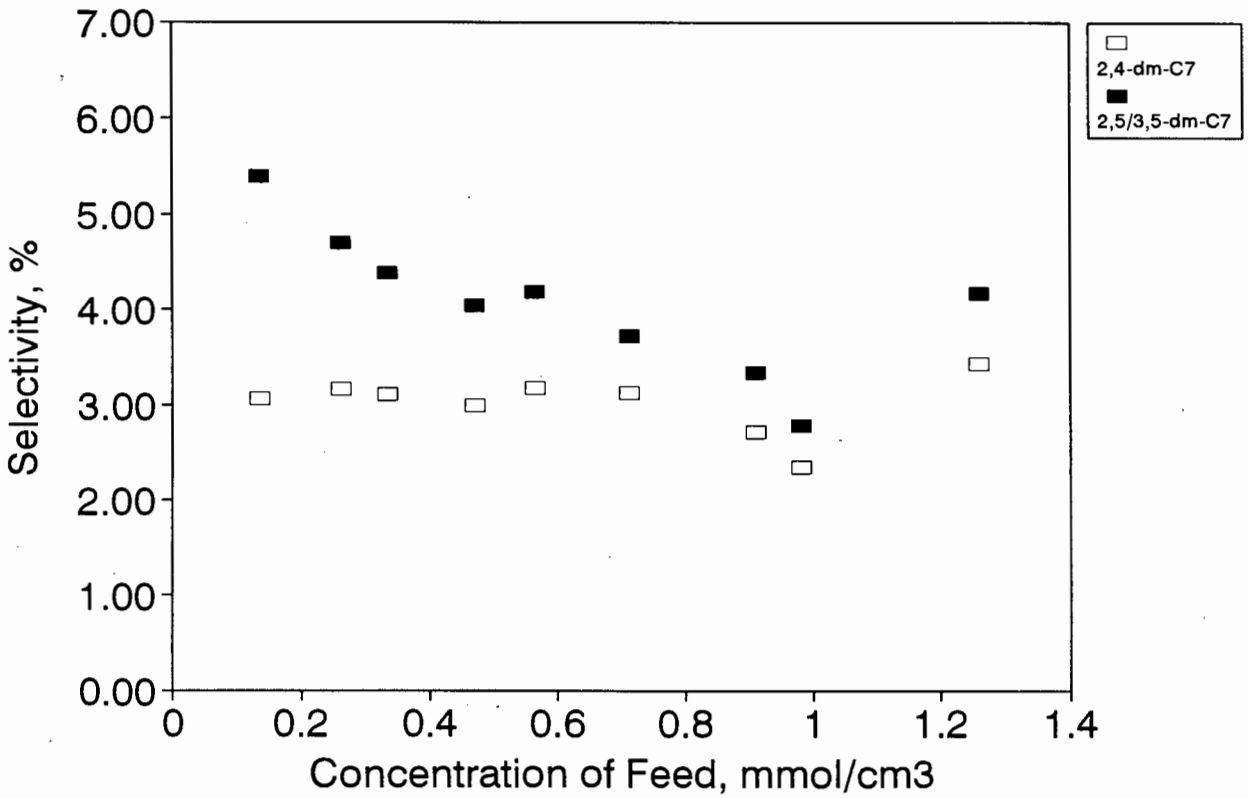

Figure 6.8c : Selectivity of Nonene Skeletal Structures at Low Conversions

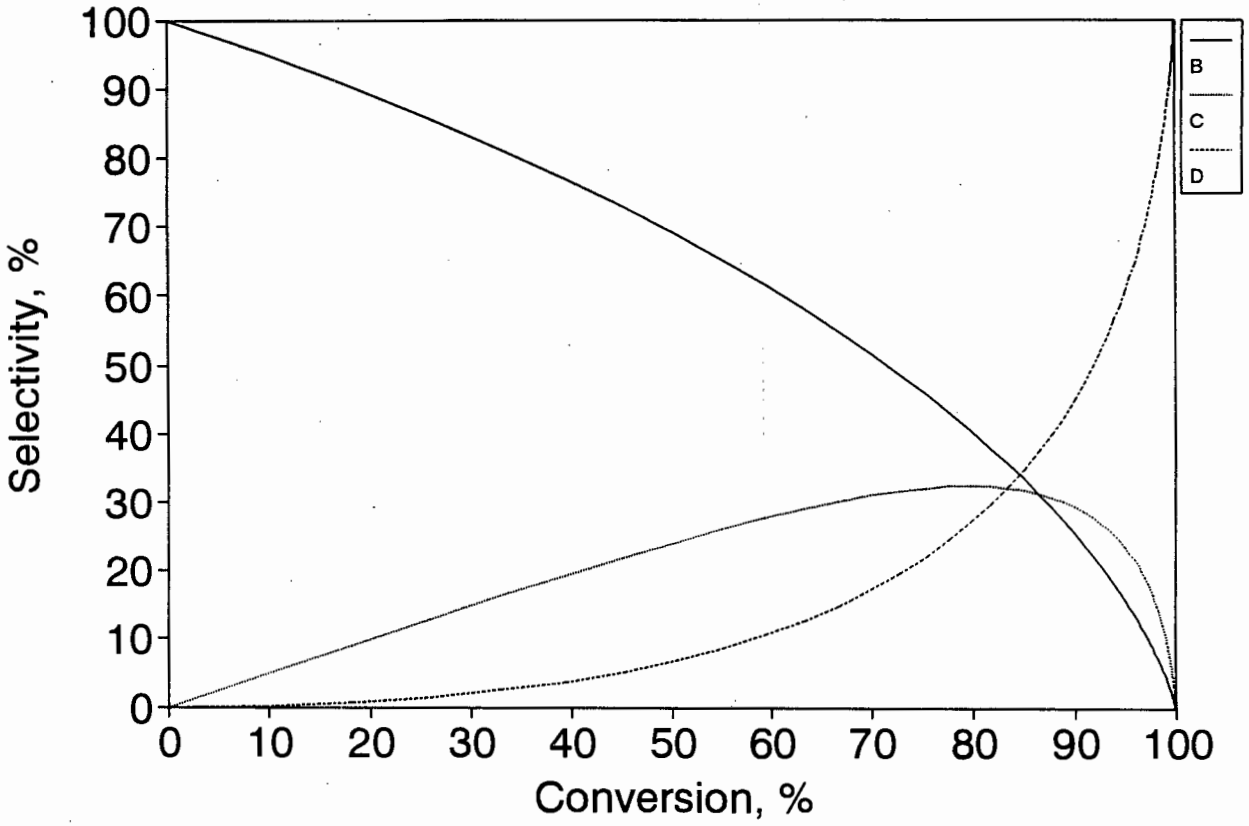

Figure 6.9a : First Order Series Reaction, Feed - 1 mol A

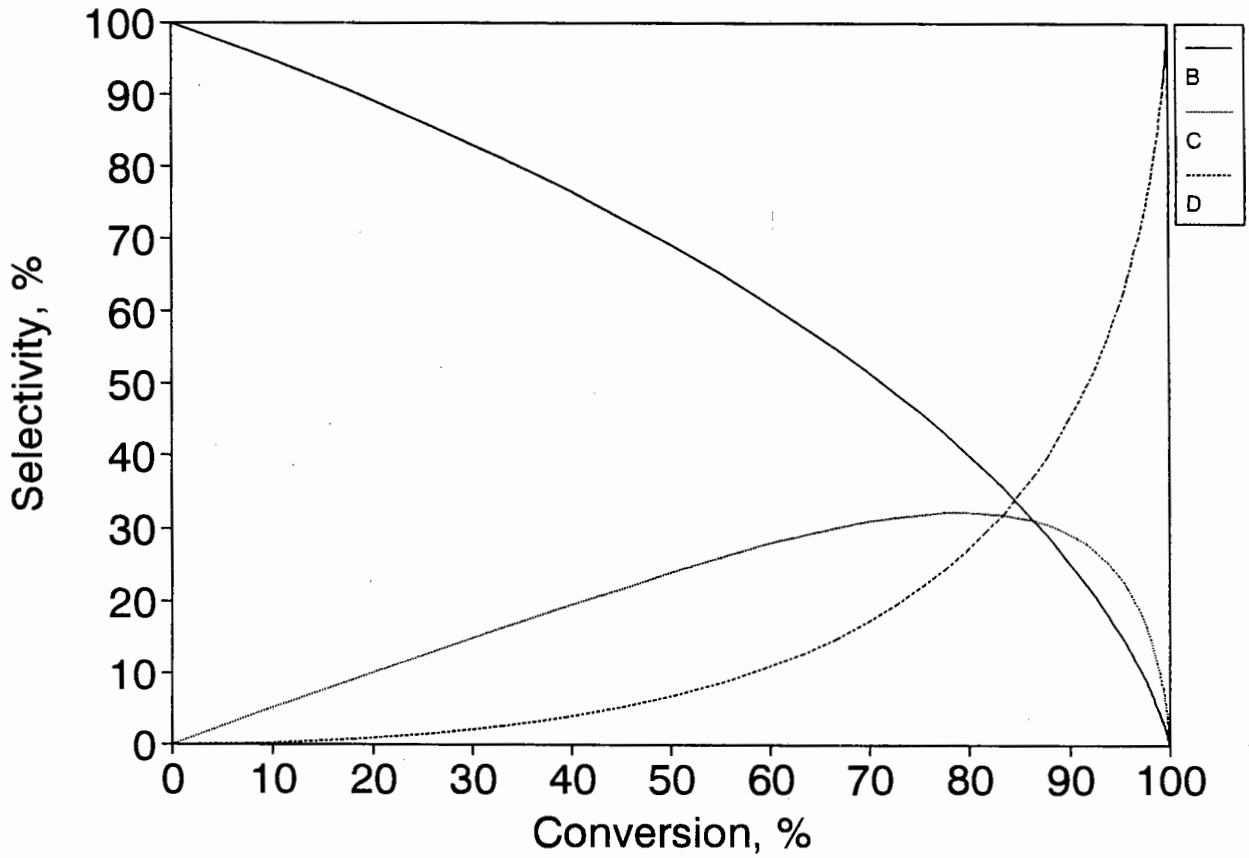

Figure 6.9b : First Order Series Reaction, Feed - 0.1 mol A

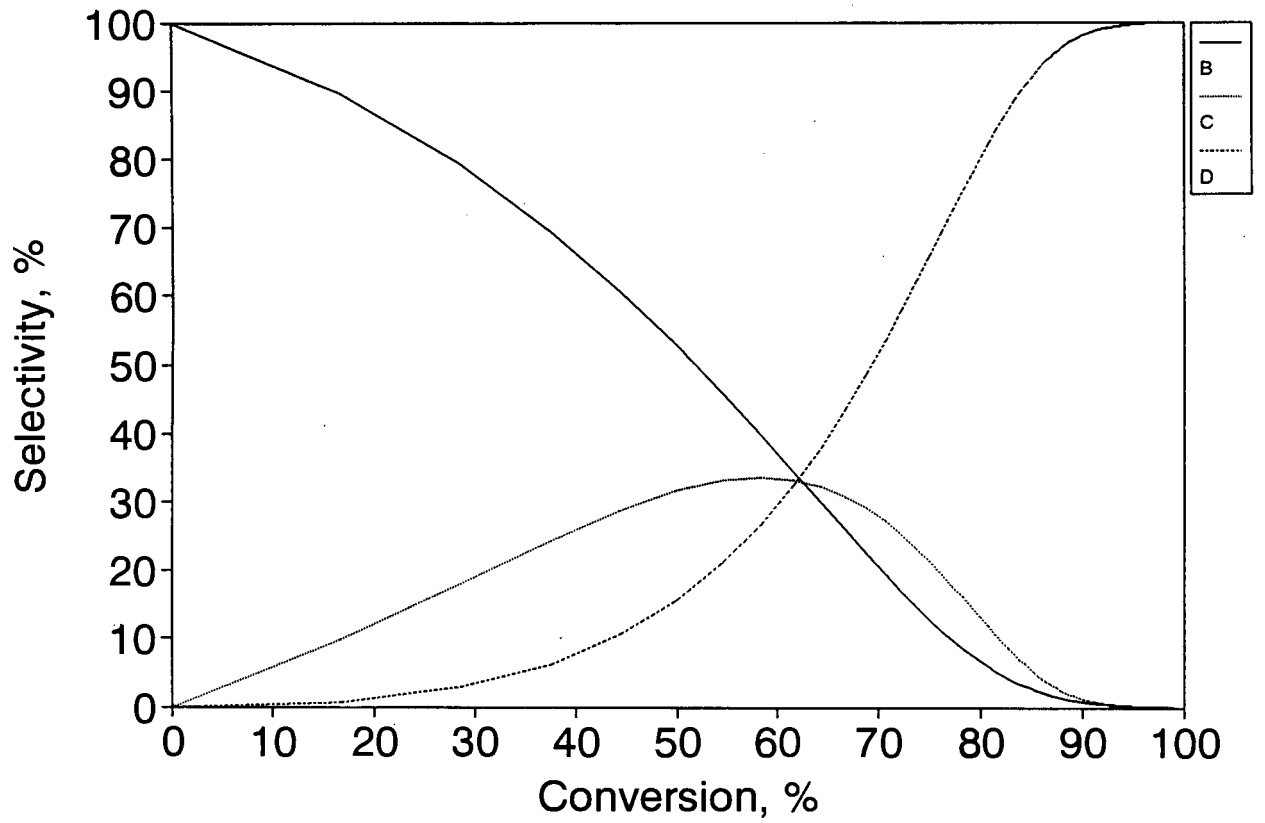

Figure 6.10a : Second Order Series Reaction, Feed - 1 mol A

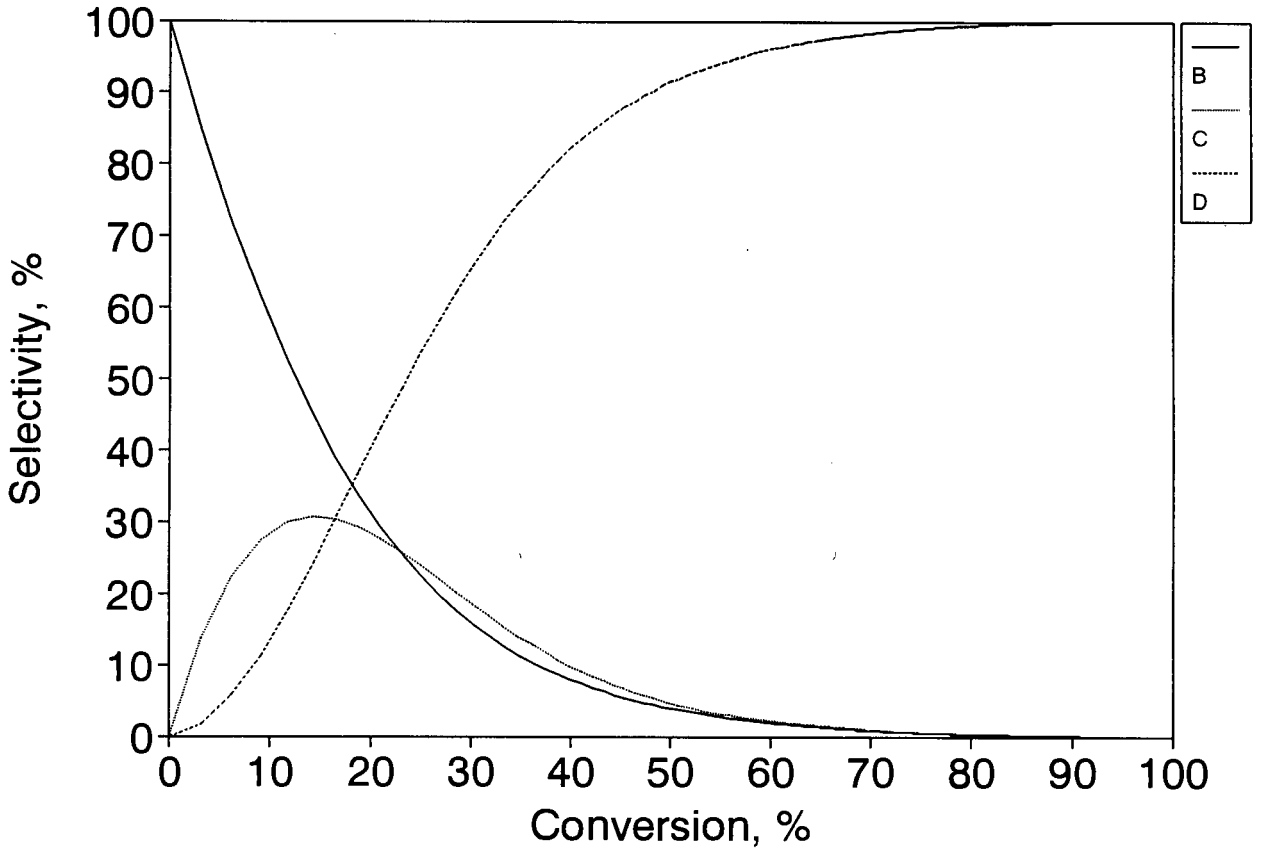

Figure 6.10b : Second Order Series Reaction, Feed - 0.1 mol A

$A \rightarrow B \rightarrow C \rightarrow D$, where all k's = 100

If the feed concentration is varied by one order of magnitude from A = 1 mols to A = 0.1 mols there is no change in the selectivity versus conversion curves. This is shown in Figures 6.9a and 6.9b. Therefore, for a fixed conversion, selectivity would not vary with feed concentration. On the other hand, if the following second order series reaction is chosen,

$2A \rightarrow B \rightarrow C \rightarrow D$, where all k's = 100,

and the feed concentration altered by one order of magnitude, Figures 6.10a and 6.10b show that different product selectivities are obtained for varying conversion. Now, at a fixed conversion, the product selectivities are no longer constant for varying feed concentration.

Other workers who have studied initial rates for liquid phase oligomerisation have observed first order behaviour for the removal of the monomer versus its concentration for two different catalyst types. Haag(1967) studied liquid phase isobutene oligomerisation over ion-exchange resins. It was observed that when the feed concentration was high, first order behaviour was not restricted to low conversion. On the contrary, at conversions as high as 80% first order behaviour resulted. When the feed concentration was dropped below 0.04 mol/litre, second order behaviour resulted. This behaviour was also observed for the dimerisation of di-isobutene to tetra-isobutene. Again, at high feed concentrations a first order relationship existed while at low feed concentrations the reaction reverted to second order.

Ngandjui and Thyrion (1992) studied liquid phase isobutene oligomerisation over H-Mordenite and also observed first order behaviour for the feed olefin. Both these authors explained this behaviour using the Langmuir-Rideal adsorption mechanism whereby reaction occurs between an adsorbed molecule and one in the gas phase.

Consider the following simple dimerisation reaction,

$$A + S \rightleftharpoons A^*$$

$$A^* + A \rightarrow B^*$$

$$B^* \rightleftharpoons B + S$$

where A = monomer (propene) , B = dimer (hexenes) and S = surface site. If the Langmuir-Rideal mechanism applies then the reaction rate is then given by:

$$r = k\frac{K_A C_A^2}{1 + K_A C_A + K_B C_B} \tag{6.18}$$

where K_i = equilibrium constant of adsorption and k = rate constant.

Ruthven and Kärger (1992) state that under conditions of elevated pressure the total adsorbed phase concentration will increase and the terms the denominator in Equation 6.18 become significant. This is especially so for zeolites and results in a decrease in reaction order. Where the terms in the denominator are small for example, under conditions of low feed concentration, the reaction is second order.

On the other hand, strong diffusion effects can also result in a reduction of reaction order. Ruthven and Kärger (1992) also show how for a simple irreversible reaction with reaction order of two, the apparent reaction order drops to 3/2 under conditions of strong pore diffusion limitations.

Based on the experimental data shown in this chapter, it is not possible to draw firm conclusions as to whether the rate of formation of each species is first or second order. However, for most of the species, the selectivity varies very little with feed concentration. The observed behaviour could be caused by saturation of the catalyst surface with feed and/or product molecules, or by diffusional effects, or both. (Further evidence for adsorption and diffusion effects was discussed in Chapter 3.)

Because the selectivities do not vary strongly with feed concentration, it is not possible to model the low conversion oligomerisation data, presented in Figures 6.4 to 6.9, using the proposed oligomerisation model. Operation under conditions of high conversion is also not preferred since firstly, there is an increase in side reactions such as cracking and secondly, at high conversions the isomers at each carbon number approach equilibrium.

6.5 Conclusions

Based on the previous discussions the following conclusions regarding the formation of the nonene isomers can be drawn:

1) For the non-shape selective catalysts studied there is agreement between the skeletal structure of the trimers observed and their relative concentrations and the reaction pathway proposed in Table 6.1.

2) The relative concentrations of the nonene skeletal structures is similar for the non-shape selective catalysts studied and thus points to a common reaction pathway, similar to that illustrated in Table 6.2.

3) If the reaction product from shape selective catalysts is to be modelled then some additional factor accounting for the shape selective effects needs to be superimposed on the non-shape selective mechanism to account for the shift in relative nonene concentrations to the linear products.

4) Under conditions of low conversion, the selectivities of the product molecules do not vary significantly with the concentration of the propene in the feed. This is possibly due to the saturation of the catalyst surface with feed and/or product molecules. It is also possible that strong diffusional restrictions are also affecting the reaction. These phenomena complicate the modelling procedure.

6) The reaction scheme for the formation of the nonene isomers is highly complex and further studies should be carried out to fully understand the reaction pathways involved. This could be achieved by feeding various nonene isomers and observing the isomerisation products that result.

CHAPTER 7 - CONCLUSIONS

Based on the results presented in Chapters 3 to 6, the following conclusions regarding the development of a model for high pressure propene oligomerisation over H-ZSM-5 can be drawn.

7.1 Process Conditions

The effect of catalyst structure and temperature on the reaction products from high pressure propene oligomerisation was investigated. Based on these studies it was concluded that the catalyst structure had a definite influence, namely that of shape selectivity, on the reaction product, especially the trimer. The structure of the products obtained from Silica-Aluimina, H-Beta and SAPO-34 was similar and was characterised by an abundance of branched structures. H-ZSM-5, however, gave rise to products that were more linear in structure. The most striking difference between catalyst types was observed for the dimethyl-heptenes. Those with methyl groups separated by a single carbon atom experienced an increase in concentration over H-ZSM-5. On the other hand, those with adjacent methyl groups decreased in concentration as the shape selectivity of the catalyst increased. It is therefore possible that those dimethyl-heptenes with their methyl-branches separated by at least one carbon can "twist" and diffuse out of the catalyst pores more easily than those with adjacent branches.

A change in reaction temperature from 200°C to 280°C over H-ZSM-5 resulted in a definite shift in the structure of the reaction products from branched to linear. For example, those dimethyl heptane structures which possessed adjacent methyl groups and highly branched nonene skeletons such as 2-methyl-3-ethyl-hexane decreased with increasing temperature. On the other hand, the methyl-octane and nonane skeletons underwent an increase.

It is possible that the clear shift in selectivity with temperature is caused by strong diffusion

and/or adsorption effects. In order to clarify this, Arrhenius plots were generated. Literature shows that if there is a transition from one controlling regime to another then there should be a change in slope in the Arrhenius plot. This was not observed and therefore the Arrhenius plots could not confirm the presence of diffusion or adsorption effects.

However, if a truly general model is to be developed that is to apply to all reaction conditions and catalysts, cognizance should be taken of the shape selective, diffusional and adsorption effects occurring in zeolites.

7.2 Equilibrium Studies

Oligomerisation runs were carried out at 250°C, 5MPa at 5 and 50% conversion. Equilibrium concentrations were simulated using the flowsheeting package PROCESS. Firstly, it was concluded that the accuracy of the predicted equilibrium concentrations were dependent on the source of the physical and thermodynamic data used. Secondly, as a result of these equilibrium studies, it was concluded that at 5% conversion the skeletal structures were not at equilibrium. However, there was equilibrium with respect to the double bonds within each skeletal structure, even at this low conversion. By comparing predicted equilibrium compositions and experimental compositions at 50% conversion it was concluded that at 50% conversion, the skeletal structures were close to equilibrium.

Therefore it can be concluded that firstly, double bond isomerisation is much faster than skeletal isomerisation and reaches equilibrium almost immediately the products are formed. This validates the use of a model for propene oligomerisation which lumps products according to the skeletal structures at each carbon number. Secondly, if the relative rates of interconversion of the different skeletal structures are to be studied then the reaction should be conducted under conditions of low conversion. That is, operation under equilibrium conditions provides no information about the isomerisation reactions occurring.

7.3 Hexene Isomerisation

Hexene isomerisation was carried out using two hexene isomers of different skeletal structures, namely 4-methyl-1-pentene and 1-hexene. This enabled the isomerisation pathway for the dimers to be established. Three models of increasing complexity were proposed to model hexene isomerisation. **Model A** was the simplest and considered only homogeneous, elementary, isomerisation reactions :

S2 ⇋ S3	methyl shift reaction
S2 ⇋ D	increase in branching
S3 ⇋ D	increase in branching
S2 ⇋ L	decrease in branching

The rate equations are as follows :

$$\frac{dC_{S2}}{dt} = (k_2 - k_6)C_L - (k_5 + k_3 + k_1 + k_6)C_{S2} + (k_4 - k_6)C_{S3} + k_6$$

$$\frac{dC_{S3}}{dt} = k_7C_L + k_3C_{S2} - (k_4 + k_8)C_{S3}$$

$$\frac{dC_L}{dt} = k_1C_{S2} - (k_2 + k_7)C_L + k_8C_{S3}$$

Model B was a Langmuir-Henshilwood model with surface reaction controlling. The last model, **Model C**, included intracrystalline diffusional effects during the isomerisation reaction.

Before modelling the reaction, sensitivity analyses were carried out on all the models. On the basis of the sensitivity studies the following conclusions could be drawn.

Model A - For a particular set of initial conditions and values of rate constants relative to one another, widely different concentration profiles can be obtained. Thus each rate constant could be determined uniquely. The rate constants for the interconversion of S3 and S2, however, had the greatest effect on the concentration profiles and thus could be determined with the greatest degree of accuracy. Data in the form of concentration versus time over the entire conversion range was found to be the most valuable for observing the influence of each rate constant.

By examining the slope of the concentration versus time curves as $t \rightarrow 0$ does not necessarily establish whether a product is primary or secondary. Large rate constants can cause a secondary product to mimic primary product behaviour if only the slope near zero time is considered.

Model B - The results of the sensitivity analyses lead to the conclusion that if the data is in the form of normalised product concentration versus normalised concentration of the feed no information can be extracted regarding the equilibrium constants of adsorption. It was therefore concluded that this model cannot be used to model hexene isomerisation where catalyst deactivation is occurring.

Model C - Each D_i had a unique influence on the product spectrum. The sensitivity analysis showed that if diffusivities altered, due to differences in reaction rates, changes are observed in the product spectrum at low conversions for S2 and S3, while changes are observed close to equilibrium for D and L. Thus experimental data should be collected over as wide a conversion range as possible to observe the behaviour of all the products.

Model A provided the best fit to the experimental data. Using both sets of experimental data, the rate constants that gave the best fit to the experimental data were obtained. Based on the results from Model A it was concluded, firstly that the primary product from propene dimerisation, namely the 2-methyl-pentane skeleton, undergoes a rapid Type A methyl-shift reaction to form the 3-methyl-pentane structure. The 2-methyl-pentane skeleton also undergoes simultaneous Type B isomerisation to increase or decrease the degree of

branching. These Type B reactions are one order of magnitude slower than Type A reactions. The 3,3-dimethyl-butane structure, which according to the hexene isomerisation mechanism from Martens and Jacobs (1990) is supposed to form with equal probability as the 2,3-dimethyl-butane structure, is not observed. It was concluded that this was probably due to shape selective constraints.

Finally, it was concluded that if the effect of internal diffusion on the hexene isomers is included in the model, then using the present form of the experimental data, it was not possible to obtain a unique set of rate constants. However, Model C shows promise and could be useful in determining the extent of diffusional restrictions if it is possible to obtain data in the form of concentration versus time, without the influence of catalyst deactivation.

7.4 Propene Trimerisation

The following conclusions regarding the formation of nonene isomers were drawn. For Silica-Alumina, H-Beta and SAPO-34 there is agreement between the skeletal structure of the trimers observed and their relative concentrations and the proposed reaction pathway for trimerisation. According to the model, at low levels of conversion, the major products should be primary products or those that have undergone rapid methyl shift reactions. This was indeed found to be the case. Thus it can be concluded that 3,4-dimethyl-heptenes, 2,4-dimethyl-heptenes and 2-methyl-3-ethyl-hexenes are primary products during non-shape selective trimerisation. Additionally, those products formed by the addition of propene to a stable tertiary carbenium ion do not appear to be formed in large amounts. This is in agreement with conventional organic chemistry theory. There is also agreement regarding structure and concentration of the dimers and trimers at low conversion between all three catalysts. This points to a common reaction pathway for non-shape selective propene oligomerisation.

Secondly, it was concluded that if the reaction product from shape selective catalysts is to be modelled then some additional factor accounting for the shape selective effects needs to

be superimposed on the non-shape selective mechanism to account for the shift in relative nonene concentrations to the linear products.

It was not possible to confirm either a first or second order relationship when the initial rates of propene removal and product formation were plotted against the concentration of propene in the feed. When the selectivity of each component was plotted against the feed concentration, the absence of a strong trend was observed for most species.

The possible existence of strong diffusion and adsorption effects during propene oligomerisation were presented and discussed in Chapter 3. Ruthven and Kärger (1992) show that both these phenomena can result in a reduction in reaction order. Saturation of the catalyst surface with feed and/or product molecules and strong diffusional resistances could therefore be responsible for the weak trend observed in the selectivity versus feed concentration plots.

It was therefore concluded that it was not possible to model this reaction using differential data since there is no change in selectivity with changing feed concentration. On the other hand, operation in integral reactor mode leads to an increase in side reactions. Operation at high conversion also results in equilibrium between the isomers at each carbon number and prevents the study of isomerisation reactions.

Thus, the reaction scheme for the formation of the nonene isomers is highly complex and further studies should be carried out to fully understand the reaction pathways involved. This could be achieved by feeding various nonene isomers and observing the isomerisation products that result.

7.5 Overall Conclusions

In summary, the main conclusions drawn regarding the development of an oligomerisation model are the following :

1) Apart from oligomerisation and isomerisation reactions occurring over H-ZSM-5, mass transport phenomena such as diffusion and adsorption occur simultaneously. These additional phenomena are not insignificant and should be accounted for in a model for oligomerisation that is to be widely applicable.

2) In order to model the interconversion of the skeletal structures the reaction should be operated away from equilibrium, i.e. under conditions of low conversion.

3) During the dimerisation step, the primary hexene skeletal structure, 2-methyl-pentane, undergoes rapid Type A, methyl-shift reaction to form the 3-methyl-pentane skeleton. According to the homogeneous model, this reaction is one order of magnitude faster than the slower, simultaneous Type B reactions that result in the formation of the 2,3-dimethyl-butane and hexane skeletons.

4) There appears to be a common reaction mechanism for the formation of the nonene skeletal structures over non-shape selective catalysts. The primary nonene isomers, formed during trimerisation reactions most probably are 3,4-dimethyl-heptenes, 2,4-dimethyl-heptenes and 2-methyl-3-ethyl-hexenes. These then undergo rapid Type A and slower Type B isomerisation reactions, similar to those at the C_6 level.

5) Differential reactor operation is not suitable for modelling propene oligomerisation over H-ZSM-5 because there is no significant change in selectivity with changing feed concentration. It is possible that this is caused by strong adsorption and diffusional effects.

REFERENCES

Alberty, R.A., *J. Phys. Chem.*, **87**, 4999-5002 (1983)

Alberty, R.A., *Chem. Eng. Sci.*, **42**, No.10, 2325-2330 (1987a)

Alberty, R.A., *J. Phys. Chem.*, **87**, No.6, 3660-3667 (1987b)

Al-Jarallah, A.M., Anabtawi, J.A., Siddiqui, M.A.B., Aitani, A.M. and Al-Sa'dour, A.W., *Catalysis Today*, **14**, No.1 (1992)

Anderson, J.R., Foger, K., Mole, T., Rajadhyaksha, R.A. and Sanders, J.V., *J. Catal.*, **58**, 114-130 (1979)

Argauer, R.J. and Landolt, G.R., United States Patent 3 702 886, 1972

Aris, R., "The Mathematical Theory of Diffusion and Reaction in Permeable Catalysis, Vol 1", Clarendon Press Oxford, 1975

Beltrame, P., Forni, L., Talamini, A. and Zuretti, G., *Applied Catalysis A : General,* **110**, 39-48 (1994)

Bessel, S. and Seddon, D., *J. Catal.*, **105**, 270-275 (1987)

Bibby, D.M., Howe, R.F. and McLellan, G.D., *Applied Catalysis A : General*, **93**, 1-34 (1992)

Calahan, D.A., *Proceedings of the IEEE*, 744 (April 1968)

Cao, G., Viola, A., Baratti, R. and Morbidelli, M., *Applied Catalysis*, **41**, 301-312 (1988)

Chen, N.Y., Garwood, W.E. and Dwyer, F.G., "Shape Selective Catalysis in Industrial Applications", Marcel Dekker Inc., 1989

Cheney, H., McAllister, S.H., Fountain, E.B., Anderson, J. and Peterson, W.H., *Ind. Eng. Chem.*, **42**(12), 2580-2586 (1950)

Chu, C.T.W. and Valyocsik, E.W., U.S. Patent 4,665,250, 1987

Csicsery, S.M., *Zeolites*, **4**, 202-213 (1984)

Derouane, E.G. and Gabelica, Z., *J. Catal*, **65**, 486-489 (1980)

Derouane,E.G., Dejaifve P. and Gabelica,Z., *J. Chem. Soc., Faraday Disc.*, **72**, 331-344, (1981)

Espinoza, R.L., Korf, C.J., Nicolaides, C.P. and Snel, R., *Appl. Catal.*, **29**, 175-184 (1987)

Fel'dblyum, V. Sh. and Baranova, T.I., *Journal of Organic Chemistry of the USSR*, **7**, No.11, 2257-2263 (November 1971)

Forni, L. and Invernizzi, R., *Ind. Eng. Chem. Process Des. Develop.*, **12**, No.4, 455-459 (1973)

Forni,L., Invernizzi, R and Van Mao, L., *Chimica E L'Industria*, **57**, No.9, 577-580 (1975)

Fletcher, J.C.Q, Kojima, M. and O'Connor, C.T., *Appl. Catal.*, **28**, 181-191 (1986)

Finlayson, B.A., "Nonlinear Analysis in Chemical Engineering", McGraw-Hill Inc., 1980

Frillette, V.J., Haag, W.O. and Lago, R.M., *J. Catal*, **67**, 218-222 (1981)

Froment, G.F., *Revue De L'Institut Fŕançais Du Pétrole*, **46**, No.4, 491-500 (1991)

Galtier, P.A., Forestière, A.A., Glaize, Y.H. and Wauquier, J.P., *Chemical Engineering Science*, **43**, No.8, 1855-1860 (1988)

Garwood, W.E., *in* "Intrazeolite Chemistry", (Stucky, G.D. and Dwyer, F.G., Eds), ACS Symposium Seies, No. 218, 383-396, Amer. Chem. Soc., Washington, D.C., 1983

Garwood, W.E., Caesar, P.D. and Brennan, J.A., U.S. Patent 4,150,062, 1972

Garwood, W.E., Krambeck, F.J., Kushnerick, J.D. and Tabak, S.A., U.S. Patent 4,740,645, 1988

Garwood, W.E. and Lee W., U.S. Patent 4,227,992, 1980

Haag, W.O. and Chen, N.Y.,*in* "Catalytst Design, Progress and Perspectives", (Hegedus, L.L. Ed.), Chap 6, John Wiley & Sons, 1987

Haag, W.O., *Chem. Eng. Prog. Sym. Ser.*, **63**, No.73, 140-147 (1967)

Haag, W.O., Lago, R.M. and Weisz, P.B., *Faraday Discussions of the Chemical Society*, No. 72, 317-330 (1982)

Harms, S.M., Kojima, M. and O'Connor, C.T., *Fuel Processing Technology*, **31**, 231-243 (1989)

Hassan, S.M., Panchenkov, G.M. and Kuznetsov, O.I., *Bulletin of the Chemical Society of Japan*, **50**(10), 2597-2601 (1977)

Haw, J.F., Richardson, B.R., Oshiro, I.S., Lazo, N.D. and Speed, J.A., *J. Am. Chem. Soc*, **111**, No. 6, 2052-2058 (1989)

Ho, T.C. and Aris, R., *AIChE Journal*, **33**, No.6, 1050-1051 (1987)

Hogan, J.P., Banks, R.L., Lanning, W.C. and Clark, A., *Ind. Eng. Chem.*, **47**, 752-757 (1955)

HYSIM, Hyprotech Ltd., ver. C1.50, April 1991

Imai, H. and Uchida, H, *Bull. Chem. Soc. Japan*, **38**, No. 6, 925-930 (1964)

Imai, H and Uchida, H, *Bull. Chem. Soc. Japan*, **40**, No.2, 321-326 (1966)

Imai, H, Hasegawa, T. and Uchida, H., *Bull. Chem. Soc. Japan*, **41**, 45-48, (1968)

Ipatieff, V.N., *Ind. Eng. Chem.*, 1067-1071 (1935)

Kärger, J., Ruthven, D.M., *Diffusion in Zeolites and other Microporous Materials*, Wiley: New York, 1992

Keim, W., *Angew. Chem. Int. Ed. Engl.*, **29**, 235-244 (1990)

Kilpatrik, J.E., Prosen, J.P., Pitzer, K.S., Rossini, F.D., *J. Research NBS*, **36**, 559-612, RP1722 (1946)

Krambeck, F.J., *in* "Chemical Reactions in Complex Mixtures, Mobil Symposium", (F.J. Krambeck. and A.V. Sapre, Eds.), pages 42-59 ,Van Nostrand, New York, 1991

Krambeck, F.J., *ChemTech*, 292-299 (May 1992)

Kreyszig, E., "Advanced Engineering Mathematics", John Wiley and Sons, 1979

Lee,H. and Thodos,G., *Ind. Eng. Chem. Fundam.*, **22** , 17 - 26 (1983)

Lok, B.M., Messina, C.A., Patten, R.L., Gajek, R.T.,Cannan, T.R., Flanigen, E.M., United States Patent, 4,440,871, April 3 1984

Long, G.N., Pellet, R.J. and Rabo, J.A., U.S. Patent 4,528,414, 1985

Lin, H. and Chao, K., *AIChE Journal*, **30**, No. 6, 981-983 (1984)

Martens, J.A., Jacobs, P.A., "Conceptual Background for the Conversion of Hydrocarbons on Heterogeneous Acid Catalysts" *in* "Theoretical Aspects of Heterogeneous Catalysis", (J.B. Moffat, Ed.), Chapter 2, 52-109, van Nostrand Reinhold Catalysis Series, 1990

McCoy, B., *AIChE Journal*, **39**, No.11, 1827-1833 (November 1993)

Meier, W.M. and Olson, D.H., "Atlas of Zeolite Structure Types", Butterworth and Heinemann, 1992

Meisel, S.L., McCullough, J.P., Lechthaler, C.H. and Weisz, P.B., *Chem. Tech*, **6**, 86 (1976)

Miale, J.N., Chen, N.Y.,Weisz, P.B., *J. Catal.*, **6**, 278-287 (1966)

Miller, S.J., U.S. Patent, 4,542,251, 1985

Miller, S.J., *in* "Catalysis 1987, Proceedings of the 10th North American Meeting of the Catalysis Society", Studies in Surface Science and Catalysis **38**, (Ward, J.W, Ed.), pages 187-197, Elsevier Scientific Publishing Company, (1988)

Nierlich, F., *Hydrocarbon Processing*, 45-46 (Feb. 1992)

Ngandjui, L.T. and Thyrion, F.C., *Chem. Eng. Proc.*, **31**, 1-6 (1992)

Neckers, D.C., Doyle, M.P., *Organic Chemistry*, John Wiley & Sons, 1977

Nelder, J.A. and Mead, R., *The Computer Journal*, **7**, 308-313 (1965)

Occelli, M.L., Hsu, J.T. and Galya, L.G., *J. Mol. Catal.*, **32,** 377-390 (1985)

O'Connor C.T. and Kojima M., *Catalysis Today*, **6**, No.3, 329-347 (1990)

Paynter, J.D. and Schuette, W.L., *Ind. Eng. Chem. Process Des. Develop.*, **10**, No.2, 250-257 (1971)

Physical Properties Data Service - jointly sponsored by the National Physical Laboratory, National Engineering Laboratory, and the Institute of Chemical Engineers in the UK

Pines, H., *The Chemistry of Catalytic Hydrocarbon Conversions*, pages 135-139, Academic Press, New York, 1981

PROCESS, Simulation Sciences Inc., September 1986, ver. 2.01

Quann, R.J., Green, L.A., Tabak, S.A., Krambeck, F.J., *I&EC Research*, **27**, 565-570 (1988)

Quann, R.J., Krambeck, F.J., *in* "Chemical Reactions in Complex Mixtures, Mobil Symposium", (F.J. Krambeck. and A.V. Sapre, Eds.), pages 143-161, Van Nostrand, New York, 1991

Reid, C.R., Prausnitz, J.M., Poling, B.E., "The Properties of Gases and Liquids", McGraw-Hill Book Company, 1987

Rossini, F.D.,Pitzer, K.S.,Arnett, R.L.,Braun, R.M. and Pimentel, G.C., "Selected Values of Physical and Thermodynamic Properties of Hydrocarbons and Related Compounds,Comprising the Tables of the American Petroleum Institute Research Project 44, Extant as of December 31, 1952", Carnegie Press, 1953

Ruthven, D. M., "Principles of Adsorption and Adsorption Proceses", John Wiley and Sons, 1984

Shepard, F.E., Rooney, J.J. and Kemball, C., *J. Catal.*, **1**, 379-388 (1962)

Smith, J.M., "Chemical Engineering Kinetics", MacGraw-Hill Book Company, 1981

Smith, J.M. and Van Ness, H.C., "Introduction to Chemical Engineering Thermodynamics", MacGraw-Hill Book Company, 1987

Sohn, J.R. and Kim, H.J., *J. Catal.*, **101**, 428-433 (1986)

Sohn, J.R., Kim, H.W. and Kim, J.T., *Korean J. Chem. Eng.*, **4**, No.1, 1-7 (1987a)

Sohn, J.R., Kim, H.W. and Kim, J.T., *J. Mol. Catal.*, 41, 375-378 (1987b)

Stepanov, A.G., Luzgin, M.V., Romannikov, V.N and Zamaraev, K.I., *Catalysis Letters*, **24**, 271-284 (1994)

Stull, D.R., Westrum, Jr., E.F. and Sinke, G.C., "The Chemical Thermodynamics of Organic Compounds", John Wiley and Sons, Inc., 1969

Szostak, R., "Handbook of Molecular Sieves", Van Nostrand Reinhold, New York, 1992

Tabak, S.A., U.S. Patent 4,254,295, 1981

Tabak, S.A., "Mobil Olefins to Gasoline and Distillate Process", Thailand-U.S. Natural Gas Untilization Symposium, Bangkok, Thailand, 7-11 February, 1984

Tabek, S.A., Krambeck, F.J. and Garwood, W.E., *AIChE Journal*, **32**, No. 9, 1526-1531 (1986)

Takahashi, K., Nishi, H., Yoneda, N. and Ohtsuka, H., *Sekiyu Gakkai Shi*, **15**, No.6, 482-486 (1972)

Tsuda, N., Mori, T., Kosaka, N. and Sakai, Y., *J. Mol. Catal.*, **28**, 183-190 (1985)

Uytterhoeven, J.B., Christner, L.G. and Hall, W.K., *J. Phys. Chem.*, **69**, No.6, 2117-2126 (1965)

Van Steen, E., PhD Thesis - "Elementarschritte der Fischer-Tropsch CO-Hydrierung mit Eisen- und Kobaltkatalysatoren", University of Karlsruhe, 32, 1993

Venuto, P.B., *Microporous Materials*, **2**, 297-411 (1994)

Wadlinger, R.L., G.T., Kerr, Rosinski, E.J., US Patent 3,308,069, 1967

Wakao, N. and Tanisho, S., *Chemical Engineering Science*, **29**, 1991-1994 (1974)

Wei J., *Ind. Eng. Chem. Res.*, **33**, 2467-2472 (1994)

Weisz,P.B., *Zeitschrift für Physikalische Chemie, Neue Folge*, **11**, 1 - 15 (1956)

Weisz,P.B., Haag,W.O and Derouane,E.G., *Faraday Discussions of the Chemical Society*, (General Discussion), **72**, 374-375 (1981)

Wilshier, K.G., Smart, P., Western, R., Mole, T. and Behrsing, T., *Appl. Catal*, **31**, 339-359 (1987)

APPENDIX A

Table A.1
X-Ray Diffraction Data for H-ZSM-5

UCT 2 Theta (degrees)	d space (Angstrom)	height	h/hmax	Szostak(1992) d space (Angstrom)	I/Io
7.88	11.2193	2932	64	11.1	strong
8.77	10.0827	1972	43	10	strong
				7.4	weak
13.18	6.7173	366	8	7.1	weak
13.88	6.38	594	13	6.3	weak
14.75	6.0056	830	18	6.04	weak
15.52	5.7094	491	11	5.97	weak
15.84	5.5947	644	14	5.56	weak
17.66	5.022	407	9	5.01	weak
19.2	4.6226	358	8	4.6	weak
20.33	4.3681	476	10		
20.81	4.2684	730	16	4.25	weak
22.12	4.0185	438	10		
23.06	3.8551	4597	100	3.85	v.strong
23.86	3.7293	2256	49	3.71	strong
24.33	3.6583	1489	32		
25.86	3.4452	582	13		
26.78	3.3289	685	15		
29.23	3.0552	736	16	3.04	weak
29.89	2.9892	912	20	2.99	weak
32.74	2.7352	419	9	2.94	weak
34.36	2.6099	455	10		
36.14	2.4853	438	10		
37.15	2.3977	440	10		
45.39	1.9981	939	20		

Table A.2
X-Ray Powder Diffraction for H-Beta

UCT 2 Theta (degrees)	d space (Angstrom)	height	h/hmax	Szostak (1992) d space (Angstrom)	I/Io
				14.30	m.weak
7.5	11.7869	1300	21	11.50	strong
				7.44	v.weak
				6.86	n.weak
				6.17	v.weak
				5.64	medium
16.7	5.3085	483	8	5.51	weak
18.1	4.9009	626	10	5.09	m.weak
				4.75	weak
				4.29	medium
21.3	4.1713	1315	21	4.17	medium
22.3	3.9865	6213	100	3.98	v.strong
25.2	3.5339	752	12	3.54	weak
25.8	3.4531	520	8	3.42	weak
26.8	3.3265	1246	20	3.33	m.weak
28.7	3.1104	739	12	3.12	weak
29.4	3.0379	1408	23	3.03	medium
30.4	2.9402	657	11	2.90	medium
				2.74	v.weak
33.2	2.6980	613	10	2.69	weak
				2.58	weak
				2.49	weak
				2.41	f.weak
				2.34	weak
				2.25	v.weak
43.4	2.0849	979	16	2.08	weak
44.6	2.0316	777	13	2.03	v.weak

Table A.3
X-Ray Powder Diffraction Data for SAPO-34

UCT 2 Theta (degrees)	d space (Angstrom)	height	h/hmax	Szostak (1992) d space (Angstrom)	I/Io
9.6	9.2127	2437	86	9.21	100
13	6.8099	471	17	6.81	17
14.1	6.281	458	16	6.3	23
16.1	5.505	1081	38	5.5	33
18.1	4.9009	618	22	4.97	75
				4.67	2
20.7	4.2909	2826	100	4.29	99
				4.03	4
				3.85	10
25.3	3.5202	962	34	3.57	76
26.1	3.4141	937	33	3.43	19
				3.22	3
				3.17	12
				3.038	4
30.7	2.9122	1592	56	2.912	67
31.3	2.8577	1331	47	2.88	28
				2.763	2
				2.683	6
				2.596	14
				2.495	11
				2.27	4
				2.085	3
				1.91	6
				1.866	7
				1.852	5
				1.802	8
				1.722	6
				1.691	4
				1.645	4

Table A.4 Reproducibility Between Different Analyses of the Same Sample

Run 57, sample 1												
Compound	Inj 1	x/mean	sq(x-mean)	Inj 2	x/mean	sq(x-mean)	Inj 3	x/mean	sq(x-mean)	std dev.	coeff. var	mean
2-eth-1-C4=	1.974	1.0003	4.139E-07	1.968	0.9977	2.108E-05	1.977	1.0020	1.558E-05	4.31E-03	0.2182	1.973
2,3-dm-2-C4=	11.911	0.9998	3.764E-06	11.901	0.9991	1.265E-04	11.926	1.0011	1.739E-04	1.23E-02	0.1035	11.913
2,3-dm-1-C4=	3.478	1.0126	1.878E-03	3.378	0.9835	3.226E-03	3.448	1.0039	1.818E-04	5.14E-02	1.4963	3.435
4-meth-2-C5=,t	6.790	0.9985	1.107E-04	6.822	1.0030	4.256E-04	6.791	0.9985	1.022E-04	1.79E-02	0.2627	6.801
4-meth-2-C5=,c	1.417	0.9794	8.886E-04	1.475	1.0193	7.812E-04	1.449	1.0013	3.462E-06	2.89E-02	1.9989	1.447
3-meth-2-C5=,t	18.640	1.0002	2.113E-05	18.629	0.9997	3.766E-05	18.637	1.0001	2.370E-06	5.53E-03	0.0297	18.635
3-meth-2-C5=,c	10.245	0.9988	1.450E-04	10.278	1.0020	4.327E-04	10.248	0.9991	7.675E-05	1.81E-02	0.1764	10.257
2-meth-2-C5=	24.334	0.9995	1.489E-04	24.423	1.0032	5.891E-03	24.282	0.9973	4.167E-03	7.14E-02	0.2934	24.346
4-meth-1-C5=	0.967	1.0131	1.553E-04	0.943	0.9886	1.180E-04	0.953	0.9983	2.564E-06	1.17E-02	1.2307	0.954
3-meth-1-C5=	0.861	0.9887	9.611E-05	0.876	1.0067	3.412E-05	0.875	1.0046	1.570E-05	8.54E-03	0.9811	0.871
2m1C5=/1C6=	8.644	0.9994	2.776E-05	8.656	1.0008	4.524E-05	8.648	0.9998	2.123E-06	6.13E-03	0.0709	8.649
3-C6=,c & t	2.946	1.0018	2.843E-05	2.927	0.9953	1.879E-04	2.949	1.0028	7.015E-05	1.20E-02	0.4071	2.940
2-C6=,t	5.324	1.0045	5.637E-04	5.239	0.9884	3.793E-03	5.338	1.0071	1.432E-03	5.38E-02	1.0150	5.300
2-C6=,c	2.469	0.9966	7.225E-05	2.483	1.0025	3.878E-05	2.480	1.0009	5.166E-06	7.62E-03	0.3077	2.477
Total	100.00			100.00			100.00					
Average										2.21E-02	0.6137	

Table A.5 Reproducibility Between Runs - Propene Oligomerisation

Conv	7.3			7.3			7.1					
Date	16/12/94			2/3/95			4/3/95					
WHSV	318			315			266					
Product	Run 78	x/mean	sq(x-mean)	Run 81	x/mean	sq(x-mean)	Run 82	x/mean	sq(x-mean)	std dev	coeff var	mean
C6	4.335	1.1070	1.755E-01	3.711	0.9475	4.220E-02	3.703	0.9455	4.558E-02	0.3628	9.2648	3.916
2-m-C5	36.121	1.0169	3.604E-01	35.158	0.9898	1.314E-01	35.283	0.9933	5.658E-02	0.5236	1.4742	35.521
3-m-C5	13.034	0.9998	9.643E-06	13.029	0.9994	6.989E-05	13.048	1.0009	1.315E-04	0.0103	0.0788	13.037
2,3-dm-C4	4.395	0.9417	7.401E-02	4.774	1.0230	1.154E-02	4.832	1.0353	2.709E-02	0.2373	5.0852	4.667
linear C9	0.451	0.8951	2.793E-03	0.535	1.0633	1.015E-03	0.525	1.0417	4.404E-04	0.0461	9.1514	0.504
3-m-C8	2.774	0.8948	1.064E-01	3.256	1.0501	2.416E-02	3.271	1.0551	2.916E-02	0.2826	9.1159	3.100
4-m-/2-m-C8	4.186	0.9080	1.600E-01	4.814	1.0441	4.131E-02	4.832	1.0479	4.884E-02	0.3675	7.9711	4.611
3,4-dm-C7	4.309	1.0096	1.682E-03	4.110	0.9630	2.491E-02	4.385	1.0274	1.370E-02	0.1419	3.3251	4.268
*4-e-C7	0.175	1.1027	2.659E-04	0.141	0.8914	2.974E-04	0.160	1.0059	8.774E-07	0.0168	10.5818	0.159
2,3-dm-C7	2.793	0.9853	1.744E-03	2.785	0.9823	2.527E-03	2.927	1.0325	8.470E-03	0.0798	2.8152	2.835
*3-e-3-m-C6	0.079	0.9975	4.007E-08	0.075	0.9482	1.687E-05	0.084	1.0543	1.855E-05	0.0042	5.3086	0.079
*2,3,4-trm-C6	0.249	1.0298	5.196E-05	0.217	0.8949	6.480E-04	0.260	1.0754	3.329E-04	0.0227	9.3849	0.242
*3-e-2-m-C6	1.350	1.0126	2.831E-04	1.275	0.9565	3.361E-03	1.374	1.0309	1.693E-03	0.0517	3.8750	1.333
2,5-/3,5-dm-C7	3.882	0.9412	5.875E-02	4.209	1.0204	7.108E-03	4.282	1.0383	2.499E-02	0.2131	5.1676	4.124
*2,6-dm-C7	0.369	1.0193	4.886E-05	0.356	0.9838	3.447E-05	0.361	0.9969	1.251E-06	0.0065	1.7951	0.362
*4,4-dm-C7	0.355	1.0445	2.284E-04	0.324	0.9541	2.433E-04	0.340	1.0014	2.337E-07	0.0154	4.5213	0.340
2,4-dm-C7	3.103	0.9281	5.776E-02	3.406	1.0189	4.000E-03	3.520	1.0530	3.138E-02	0.2158	6.4560	3.343
*2,2-dm-C7	0.444	1.0265	1.314E-04	0.414	0.9574	3.392E-04	0.439	1.0181	4.838E-05	0.0161	3.7281	0.432
*2,3,5-trm-C6	0.235	1.1020	4.727E-04	0.188	0.8819	6.346E-04	0.217	1.0182	1.190E-05	0.0237	11.0937	0.213
*C12	9.619	1.0298	7.743E-02	9.364	1.0025	5.382E-04	9.040	0.9677	9.088E-02	0.2906	3.1105	9.341
*cracked prod.	7.740	1.0221	2.792E-02	7.862	1.0382	8.368E-02	7.116	0.9397	2.083E-01	0.3999	5.2811	7.573
Total	100.00			100.00			100.00					
Average										0.1585	5.6469	

* - small peaks, subject to greater variability

Sample Calculation of Mass Balance, Conversion and Selectivity for a Low Conversion Run

Run 67 : 4-methyl-1-Pentene Isomerisation Date : 20 April 1994

Catalyst : H-ZSM-5
Catalyst Mass (g) : 0.30
Mass of Quartz Sand (g) : 15.06

Reaction Conditions

Temperature, C : 250
Pressure, MPa : 5
Feed Flow, mg/min : 87 WHSV /hr: 17
Internal Std, mg/min : 47 (const flow)

Total Flow In = (87 + 47) = 134 mg/min

Compound	C6 Skeleton	Mass% from G.C.	Mass mg/min	Mass% without D	Mass% Selec
C2-C1		0.0000	0.00	0.0000	0.00
C3=		0.1047	0.15	0.1575	0.31
DME, Int. Std.		33.5409	47.00		
C4-C5		0.6207	0.87	0.9340	1.85
4-m-1-C5=	2-m-C5	0.8167	1.14	1.2289	
3-m-1-C5=	3-m-C5	0.9137	1.28	1.3748	2.72
2,3-dm-1-C4=	2,3-dm-C4	0.4003	0.56	0.6023	1.19
4-m-2-C5=,cis	2-m-C5	1.2594	1.76	1.8950	
4-m-2-C5=,trans	2-m-C5	4.6932	6.58	7.0618	
2-m-1-C5=	2-m-C5	7.2881	10.21	10.9663	
1-C6=	linear C6	0.0000	0.00	0.0000	0.00
2-e-1-C4=	3-m-C5	1.8019	2.52	2.7113	5.37
3-C6=	linear C6	1.1708	1.64	1.7617	3.49
2-C6=,trans	linear C6	2.0047	2.81	3.0164	5.98
2-m-2-C5=	2-m-C5	18.8602	26.43	28.3787	
3-m-2-C5=,cis	3-m-C5	8.9727	12.57	13.5011	26.75
2-C6=,cis	linear C6	0.9550	1.34	1.4370	2.85
3-m-2-C5=,trans	3-m-C5	15.2301	21.34	22.9165	45.41
2,3-dm-2-C4=	2,3-dm-C4	0.9588	1.34	1.4427	2.86
C7=+		0.4080	0.57	0.6139	1.22
Total		99.9999	140.13	99.9998	100.00

Mass Flow of i =

(Mass % of i) / (Mass % of Int. Std.) x Mass Flow Int. Std.

Mass Balance =

100 - (Total Mass In - Total Mass Out)/(Total Mass In) x 100 =

100 - (134 - 140.13)/(134) x 100 = 95.4

Conversion (Based on 100% Mass Balance) =

(100 - Mass% of C6 skeletons (other than 2-methyl-pentane) in product) =

50.5

Selectivity to Component i =

(Mass % of i) / Conversion x 100

Sample Calculation of Mass Balance and Conversion for a High Conversion Run

Run 57 : Propene Oligomerisation

Date : 6 May 1993

Catalyst :	H-ZSM-5
Catalyst Mass (g) :	0.38
Mass of Quartz Sand :	19

Reaction Conditions

Temperature, C :	250
Pressure, MPa :	5
Feed Flow, g/min	0.23
Internal Std, g/min	0.0642

Sample 3 Sample Time, min: 375 - 435

Mass Balance

In	g	Out	g	Out (100% Mass Balance)	
Propene	13.2	Gas	10.57	Gas	11.06
DME	3.85	Liquid	5.72	Liquid	5.99
Total	17.05	Total	16.29	Total	17.05

Compound	Feed Sample Mass%	Gas Sample Mass%	Actual Mass,g	100% MB Mass,g
ethane	0.0281	0.0434	0.0046	0.0048
propene	78.1162	62.9322	6.6545	6.9623
dme	21.8215	31.6786	3.3497	3.5046
C4=	0.0342	0.5426	0.0574	0.0600
C5=		0.6431	0.0680	0.0711
C6=		3.9822	0.4211	0.4406
C7/C8=		0.1522	0.0161	0.0168
C9=		0.0258	0.0027	0.0029
Total	100.00	100.00	10.5741	11.0631

Liquid Sample

Compound	Mass%	Actual Mass,g	100% MB Mass,g
ethane	0.0000	0.0000	0.0000
propene	1.9839	0.1135	0.1188
dme	1.3769	0.0788	0.0824
C4=	0.0851	0.0049	0.0051
C5=	0.4577	0.0262	0.0274
4-m-1-C5=	0.1067	0.0061	0.0064
3-m-1-C5=	0.1136	0.0065	0.0068
23-dm-1-C4=	0.3405	0.0195	0.0204
4-m-2-C5=,c	0.1850	0.0106	0.0111
4-m-2-C5=,t	0.7972	0.0456	0.0477
2m1C5=/1-C6=	1.0675	0.0611	0.0639
2-e-1-C4=	0.2360	0.0135	0.0141
3-C6=,c & t	0.3887	0.0222	0.0233
2-C6=,t	0.7031	0.0402	0.0421
2-m-2-C5=	2.9790	0.1704	0.1783
3-m-2-C5=,c	1.2451	0.0712	0.0745
2-C6=,c	0.3303	0.0189	0.0198
3-m-2-C5=,t	2.2670	0.1297	0.1357
23-dm-2-C4=	1.2557	0.0718	0.0752
> C6=	84.081	4.8094	5.0338
	100.0	5.72	5.99

Total Stream

Compound	Mass,g	Mass %
ethane	0.0048	0.0282
propene	7.0810	41.5311
dme	3.5871	21.0386
C4=	0.0651	0.3820
C5=	0.0985	0.5780
C6=	1.1599	6.8029
> C6=	5.0535	29.6393
Total	17.05	100.00

Mass Balance =

100 - (Total Mass In - Total Mass Out)/(Total Mass In) x 100 =

100 - (17.05-16.29)/17.05 x 100 = 95.54

Conversion (Based on 100% Mass Balance) =

(Mass% C3= in Feed - Mass% of C3= in Product)/(Mass% C3= in Feed) x 100 =

46.8

Selectivities : as for low conversion runs

APPENDIX B

Calculation of Viscosity of Pure Propene Gas at High Pressures

Lucas Method - Reid, Sherwood and Poling (1987)

Reaction Temperature	: 523 K	P_r	: 1.087
Reaction Pressure	: 50 bar	T_r	: 1.433
M	: 42.081	ρ_r	: 0.233
T_c	: 364.9 K		
P_c	: 46 bar		
Z_c	: 0.274		
V_c	: 181 cm3/mol		
acentric factor, ω	: 0.144		
dipole moment, μ	: 0.4 debye		

Reduced inverse viscosity, $m^2/(N.s)$:

$$\xi = 0.176\left(\frac{T_c}{M^3 P_c^4}\right)^{1/6} = 0.005649$$

Reduced dipole moment :

$$\mu_r = 52.46\left(\frac{\mu^2 P_c}{T_c^2}\right) = 0.0029$$

F_P^o and F_Q^o , correction factors to account for polarity or quantum effects :

If $0 \leq \mu_r < 0.022$ then $F_P^o = 1$
$F_Q^o = 1$ (This is only used for quantum gases)

Parameter Z_1 :

$$Z_1 = [0.807 T_r^{0.618} - 0.357\exp(-0.449 T_r) + 0.340\exp(-4.058 T_r) + 0.018] F_P^o F_Q^o$$

$$Z_1 = 0.8395 = \eta^o \xi$$

Thus the low pressure viscosity, $\eta^o = 148.6\ \mu P$

If ($1 < T_r < 40$) and ($0 < P_r \leq 100$) then,

$$Z_2 = \eta^o \xi \left[1 + \frac{a P_r^e}{b P_r^f + (1 + c P_r^d)^{-1}}\right] = 0.9484$$

$$Y = \frac{Z_2}{Z_1}$$

Correction factors F_P and F_Q both = 1. Finally, the viscosity

$$\eta = \frac{Z_2 F_P F_Q}{\xi} = 1.68e\text{-}5 Pas$$

Calculation of Self-Diffusivity for Pure Propene Gas

Correlation by Huen Lee and George Thodos (1983)

The correlation used is as follows :

$$\frac{D\delta}{T_r} = \frac{0.77e\text{-}5}{\rho_r}$$

for reduced densities, $\rho_r \leq 1.0$.

The self diffusivity parameter is defined as follows :

$$\delta = \frac{M^{1/2}}{P_c^{1/2} V_c^{5/6}} = 0.01254$$

The compressibility factor, Z is calculated using the Lee-Kesler method, recommended by Reid et al (1987) for expanded ranges of temperature and pressure :

$$Z = Z^0 + \omega Z^1$$

Z^0 = 0.8827 and Z^1 = 0.0857 are both functions of T_r and P_r. Thus, Z = 0.895.

Using

$$PV = ZRT$$

ρ = 54.06 kg/m^3 and ρ_r = 0.233. Tr is given above.

The self diffusivity ,D, is therefore = 0.00377 cm^2/s

Table B.1 - Runs to Determine the Effect of Superficial Gas Velocity

Run No : 47 Date : 14 April 1993

Catalyst : H-ZSM-5

Mass Catalyst,g : 0.05

Mass Sand,g : 2.5

Pretreatment: calcined at 500C in air overnight

Reaction Conditions : 250C, 5 MPa

WHSV g feed/g cat/hr : 325

Internal Standard : Dimethyl Ether

Sample No.	Feed	1			2			3			4		
Bed Temp, C		251			250			251			252		
Time, min		127			164			210			241		
Compound	Mass%	Mass%	Selec. (mass%)	C6 Selec. (mass%)	Mass%	Selec. (mass%)	C6 Selec. (mass%)	Mass%	Selec. (mass%)	C6 Selec. (mass%)	Mass%	Selec. (mass%)	C6 Selec. (mass%)
C2	0.0352	0.0321			0.0337			0.0325			0.0334		
C3=	99.9580	94.7129			95.8987			95.4501			97.0804		
C4 & C4='s	0.0067	0.0866	1.523		0.0797	1.799		0.0679	1.365		0.0651	2.031	
C5='s		0.1169	2.228		0.0942	2.321		0.0939	2.081		0.0645	2.242	
4-m-1-C5=		0.0758	1.445	2.2424	0.0625	1.538	2.317	0.0717	1.590	2.258	0.0500	1.735	2.472
3-m-1-C5=		0.0500	0.953	1.4785	0.0407	1.003	1.511	0.0469	1.040	1.478	0.0327	1.136	1.619
23-dm-1-C4=		0.1017	1.937	3.0064	0.0759	1.869	2.815	0.0763	1.692	2.403	0.0507	1.762	2.511
4-m-2-C5=,c		0.0908	1.729	2.6837	0.0733	1.805	2.719	0.0803	1.781	2.529	0.0561	1.948	2.775
4-m-2-C5=,t		0.3159	6.019	9.3418	0.2592	6.383	9.616	0.2899	6.425	9.125	0.1993	6.922	9.862
2m1C5=/1-C6		0.4430	8.440	13.0989	0.3670	9.037	13.614	0.4313	9.561	13.579	0.2859	9.929	14.146
2-e-1-C4=		0.0561	1.069	1.6596	0.0440	1.083	1.632	0.0513	1.137	1.615	0.0310	1.078	1.536
3-C6=,c & t		0.0538	1.027	1.5938	0.0513	1.262	1.901	0.0639	1.415	2.009	0.0422	1.465	2.087
2-C6=,t		0.0929	1.770	2.7462	0.0857	2.111	3.180	0.1069	2.371	3.367	0.0700	2.431	3.464
2-m-2-C5=		1.1409	21.739	33.7384	0.9061	22.313	33.613	1.1031	24.453	34.728	0.6895	23.946	34.117
3-m-2-C5=,c		0.2550	4.859	7.5406	0.2013	4.958	7.469	0.2322	5.147	7.310	0.1426	4.951	7.054
2-C6=,c		0.0433	0.825	1.2809	0.0389	0.959	1.445	0.0514	1.139	1.618	0.0328	1.140	1.624
3-m-2-C5=,t		0.4347	8.283	12.8552	0.3326	8.191	12.339	0.3946	8.746	12.421	0.2376	8.251	11.756
23-dm-2-C4=		0.2277	4.339	6.7338	0.1571	3.869	5.829	0.1767	3.916	5.562	0.1006	3.494	4.978
C7= & C8=		0.0540	1.029		0.0157	0.386		0.0257	0.570		0.0000	0.000	
C9=		1.5828	30.158		1.0965	27.001		1.1535	25.570		0.7354	25.539	
C10= & C11=		0.0000	0.000		0.0000	0.000		0.0000	0.000		0.0000	0.000	
C12=		0.0075	0.142		0.0000	0.000		0.0000	0.000		0.0000	0.000	
>C12=		0.0255	0.486		0.0857	2.111		0.0000	0.000		0.0000	0.000	
Total	100.00	100.00	100.00	100.00	100.00	100.00	100.00	100.00	100.00	100.00	100.00	100.00	100.00
Conversion		5.2			4.1			4.5			2.9		
Mass Bal. %		106			102			103			107		

Table B.1 cont.

Sample No.	5			6		
Bed Temp, C	252			251		
Time, min	301			339		
Compound	Mass%	Selec. (mass%)	C6 Selec. (mass%)	Mass%	Selec. (mass%)	C6 Selec. (mass%)
C2	0.0328			0.0329		
C3=	96.1947			96.4827		
C4 & C4='s	0.0522	1.218		0.0536	1.349	
C5='s	0.0651	1.728		0.0607	1.746	
4-m-1-C5=	0.0644	1.710	2.297	0.0537	1.545	2.331
3-m-1-C5=	0.0411	1.092	1.467	0.0363	1.043	1.574
23-dm-1-C4	0.0615	1.632	2.193	0.0524	1.507	2.272
4-m-2-C5=,c	0.0702	1.865	2.505	0.0584	1.678	2.531
4-m-2-C5=,t	0.2568	6.819	9.159	0.2182	6.276	9.466
2m1C5=/1-C	0.3984	10.579	14.209	0.3306	9.506	14.338
2-e-1-C4=	0.0415	1.101	1.479	0.0352	1.011	1.525
3-C6=,c & t	0.0586	1.554	2.088	0.0503	1.447	2.183
2-C6=,t	0.1000	2.656	3.567	0.0845	2.43	3.665
2-m-2-C5=	1.0045	26.673	35.825	0.8158	23.457	35.382
3-m-2-C5=,c	0.1933	5.133	6.894	0.1601	4.604	6.944
2-C6=,c	0.0456	1.212	1.627	0.0395	1.137	1.715
3-m-2-C5=,t	0.3308	8.783	11.796	0.2634	7.575	11.426
23-dm-2-C4	0.1372	3.644	4.894	0.1072	3.081	4.648
C7= & C8=	0.0000	0.000		0.3278	9.425	
C9=	0.8511	22.600		0.7367	21.183	
C10= & C11	0.0000	0.000		0	0	
C12=	0.0000	0.000		0	0	
>C12=	0.0000	0.000		0	0	
Total	100.00	100.00	100.00	100.00	100.00	100.00
Conversion	3.8			3.5		
Mass Bal. %	98			96		

Table B.2 - Runs to Determine the Effect of Superficial Velocity

Run No : 59 Date : 18 May 1993

Catalyst : H-ZSM-5

Mass Catalyst,g : 0.093

Mass Sand,g : 5.0

Pretreatment: calcined at 500C in air overnight

Reaction Conditions : 250C, 5 MPa

WHSV g feed/g cat/hr : 340

Internal Standard : Dimethyl Ether

Sample No.	Feed	1			2			3			4			5		
Bed Temp, C		250			248			249			250			253		
Time, min		159			207			256			303			344		
Compound	Mass%	Mass%	Selec (mass%)	C6 Selec (mass%)	Mass%	Selec (mass%)	C6 Selec (mass%)	Mass%	Selec (mass%)	C6 Selec (mass%)	Mass%	Selec (mass%)	C6 Selec (mass%)	Mass%	Selec (mass%)	C6 Selec (mass%)
C2	0.0421	0.0326			0.0301			0.0294			0.0295			0.0301		
C3=	99.9411	95.0304			96.0501			96.1265			96.3370			96.3038		
C4 & C4='s	0.0168	0.1001	1.695		0.0700	1.364		0.0615	1.167		0.0596	1.184		0.0628	1.261	
C5='s		0.1228	2.495		0.0926	2.374		0.0804	2.101		0.0703	1.945		0.0786	2.154	
4-m-1-C5=		0.0879	1.786	2.4214	0.0859	2.200	2.435	0.0822	2.148	2.393	0.0778	2.151	2.398	0.0808	2.213	2.346
3-m-1-C5=		0.0540	1.097	1.4877	0.0540	1.384	1.531	0.0502	1.311	1.461	0.0490	1.355	1.510	0.0497	1.362	1.444
23-dm-1-C4=		0.1155	2.348	3.1839	0.0922	2.362	2.614	0.0847	2.213	2.465	0.0745	2.060	2.297	0.0785	2.151	2.280
4-m-2-C5=,c		0.1032	2.098	2.8447	0.0972	2.490	2.755	0.0942	2.460	2.741	0.0869	2.404	2.680	0.0905	2.480	2.629
4-m-2-C5=,t		0.3580	7.277	9.8662	0.3392	8.690	9.617	0.3261	8.521	9.492	0.3090	8.545	9.525	0.3232	8.857	9.390
2m1C5=/1-C6		0.4952	10.064	13.6446	0.4959	12.705	14.061	0.4865	12.710	14.159	0.4663	12.893	14.373	0.4986	13.662	14.484
2-e-1-C4=		0.0596	1.212	1.6433	0.0539	1.381	1.528	0.0491	1.282	1.428	0.0456	1.261	1.406	0.0518	1.418	1.504
3-C6=,c & t		0.0516	1.049	1.4223	0.0586	1.502	1.663	0.0594	1.553	1.730	0.0597	1.651	1.841	0.0656	1.797	1.905
2-C6=,t		0.0893	1.816	2.4619	0.1009	2.585	2.861	0.1044	2.728	3.039	0.1033	2.857	3.184	0.1136	3.113	3.300
2-m-2-C5=		1.2327	25.054	33.9683	1.2378	31.713	35.095	1.2287	32.103	35.762	1.1735	32.446	36.168	1.2363	33.878	35.916
3-m-2-C5=,c		0.2658	5.401	7.3234	0.2482	6.360	7.038	0.2351	6.143	6.843	0.2178	6.022	6.713	0.2340	6.412	6.798
2-C6=,c		0.0428	0.870	1.1796	0.0484	1.239	1.371	0.0480	1.255	1.398	0.0481	1.330	1.483	0.0521	1.428	1.514
3-m-2-C5=,t		0.4417	8.979	12.1724	0.4150	10.633	11.767	0.4006	10.468	11.661	0.3677	10.168	11.335	0.3966	10.869	11.522
23-dm-2-C4=		0.2315	4.706	6.3803	0.1998	5.118	5.664	0.1865	4.873	5.429	0.1651	4.564	5.088	0.1710	4.686	4.968
C7= & C8=		0.0040	0.080		0.0000	5.636		0.0064	0.168		0.0000	0.000		0.0000	0.000	
C9=		1.0734	21.817		0.2200	0.263		0.2601	6.798		0.2592	7.164		0.0825	2.259	
C10= & C11=		0.0000	0.000		0.0000	0.000		0.0000	0.000		0.0000	0.000		0.0000	0.000	
C12=		0.0077	0.156		0.0103	0.000		0.0000	0.000		0.0000	0.000		0.0000	0.000	
>C12=		0.0000	0.000		0.0000	0.000		0.0000	0.000		0.0000	0.000		0.0000	0.000	
Total	100.00	100.00	100.00	100.00	100.00	100.00	100.00	100.00	100.00	100.00	100.00	100.00	100.00	100.00	100.00	100.00
Conversion		4.9			3.9			3.8			3.6			3.6		
Mass Bal. %		99			99			100			99			97		

Table B.3 - Runs to Determine the Effect of Superficial Gas Velocity

Run No : 60 Date : 25 May 1993

Catalyst : H-ZSM-5

Mass Catalyst,g : 0.28

Mass Sand,g : 15.0

Pretreatment: calcined at 500C in air overnight

Reaction Conditions : 250C, 5 MPa

WHSV g feed/g cat/hr : 320

Internal Standard : Dimethyl Ether

Sample No.	Feed	1			2			3			4		
Bed Temp, C		249			252			251			249		
Time, min		346			392			433			557		
Compound	Mass%	Mass%	Selec (mass%)	C6 Selec (mass%)	Mass%	Selec (mass%)	C6 Selec (mass%)	Mass%	Selec (mass%)	C6 Selec (mass%)	Mass%	Selec (mass%)	C6 Selec (mass%)
C2	0.0317	0.0289			0.0281			0.0282			0.0282		
C3=	99.9629	93.7642			93.5549			96.0974			96.1504		
C4 & C4='s	0.0055	0.0771	1.154		0.0632	0.901		0.0539	1.251		0.0481	1.259	
C5='s		0.1030	1.661		0.0937	1.462		0.0794	2.053		0.0648	1.695	
4-m-1-C5=		0.0872	1.406	2.3803	0.0861	1.344	2.295	0.0830	2.145	2.384	0.0785	2.053	2.381
3-m-1-C5=		0.0535	0.863	1.4613	0.0535	0.834	1.425	0.0522	1.349	1.499	0.0479	1.254	1.454
23-dm-1-C4=		0.1047	1.688	2.8570	0.0953	1.486	2.539	0.0833	2.153	2.393	0.0696	1.822	2.113
4-m-2-C5=,c		0.1013	1.634	2.7656	0.0998	1.557	2.659	0.0927	2.396	2.663	0.0859	2.249	2.608
4-m-2-C5=,t		0.3537	5.704	9.6555	0.3535	5.514	9.418	0.3299	8.527	9.476	0.3087	8.079	9.368
2m1C5=/1-C6		0.5063	8.164	13.8197	0.5268	8.216	14.033	0.4947	12.787	14.210	0.4821	12.616	14.629
2-e-1-C4=		0.0546	0.880	1.4899	0.0563	0.878	1.500	0.0512	1.322	1.469	0.0457	1.196	1.387
3-C6=,c & t		0.0534	0.862	1.4585	0.0643	1.003	1.713	0.0643	1.662	1.847	0.0646	1.690	1.959
2-C6=,t		0.0921	1.485	2.5145	0.1106	1.725	2.947	0.1082	2.795	3.107	0.1119	2.927	3.394
2-m-2-C5=		1.2813	20.662	34.9773	1.3272	20.700	35.358	1.2504	32.320	35.917	1.2106	31.679	36.734
3-m-2-C5=,c		0.2599	4.191	7.0954	0.2633	4.106	7.014	0.2374	6.136	6.819	0.2169	5.675	6.581
2-C6=,c		0.0425	0.685	1.1588	0.0515	0.803	1.371	0.0543	1.403	1.559	0.0534	1.397	1.621
3-m-2-C5=,t		0.4396	7.088	11.9987	0.4478	6.984	11.929	0.3962	10.240	11.380	0.3659	9.576	11.104
23-dm-2-C4=		0.2333	3.761	6.3676	0.2177	3.395	5.799	0.1837	4.749	5.278	0.1538	4.024	4.667
C7= & C8=		0.0204	0.329		0.0126	0.197		0.0000	0.000		0.0000	0.000	
C9=		2.3071	37.202		2.4553	38.294		0.2596	6.711		0.4062	10.628	
C10= & C11=		0.0000	0.000		0.0000	0.000		0.0000	0.000		0.0000	0.000	
C12=		0.0063	0.101		0.0086	0.134		0.0000	0.000		0.0068	0.179	
>C12=		0.0298	0.481		0.0299	0.467		0.0000	0.000		0.0000	0.000	
Total	100.00	100.00	100.00	100.00	100.00	100.00	100.00	100.00	100.00	100.00	100.00	100.00	100.00
Conversion		6.2			6.4			3.9			3.8		
Mass Bal.%		106			95			110			91		

Table B.3 - Runs to Determine the Effect of Superficial Gas Velocity

Run No : 60 Date : 25 May 1993

Catalyst : H-ZSM-5

Mass Catalyst,g : 0.28

Mass Sand,g : 15.0

Pretreatment: calcined at 500C in air overnight

Reaction Conditions : 250C, 5 MPa

WHSV g feed/g cat/hr : 320

Internal Standard : Dimethyl Ether

Sample No.	Feed	1			2			3			4		
Bed Temp, C		249			252			251			249		
Time, min		346			392			433			557		
Compound	Mass%	Mass%	Selec (mass%)	C6 Selec (mass%)	Mass%	Selec (mass%)	C6 Selec (mass%)	Mass%	Selec (mass%)	C6 Selec (mass%)	Mass%	Selec (mass%)	C6 Selec (mass%)
C2	0.0317	0.0289			0.0281			0.0282			0.0282		
C3=	99.9629	93.7642			93.5549			96.0974			96.1504		
C4 & C4='s	0.0055	0.0771	1.154		0.0632	0.901		0.0539	1.251		0.0481	1.259	
C5='s		0.1030	1.661		0.0937	1.462		0.0794	2.053		0.0648	1.695	
4-m-1-C5=		0.0872	1.406	2.3803	0.0861	1.344	2.295	0.0830	2.145	2.384	0.0785	2.053	2.381
3-m-1-C5=		0.0535	0.863	1.4613	0.0535	0.834	1.425	0.0522	1.349	1.499	0.0479	1.254	1.454
23-dm-1-C4=		0.1047	1.688	2.8570	0.0953	1.486	2.539	0.0833	2.153	2.393	0.0696	1.822	2.113
4-m-2-C5=,c		0.1013	1.634	2.7656	0.0998	1.557	2.659	0.0927	2.396	2.663	0.0859	2.249	2.608
4-m-2-C5=,t		0.3537	5.704	9.6555	0.3535	5.514	9.418	0.3299	8.527	9.476	0.3087	8.079	9.368
2m1C5=/1-C6		0.5063	8.164	13.8197	0.5268	8.216	14.033	0.4947	12.787	14.210	0.4821	12.616	14.629
2-e-1-C4=		0.0546	0.880	1.4899	0.0563	0.878	1.500	0.0512	1.322	1.469	0.0457	1.196	1.387
3-C6=,c & t		0.0534	0.862	1.4585	0.0643	1.003	1.713	0.0643	1.662	1.847	0.0646	1.690	1.959
2-C6=,t		0.0921	1.485	2.5145	0.1106	1.725	2.947	0.1082	2.795	3.107	0.1119	2.927	3.394
2-m-2-C5=		1.2813	20.662	34.9773	1.3272	20.700	35.358	1.2504	32.320	35.917	1.2106	31.679	36.734
3-m-2-C5=,c		0.2599	4.191	7.0954	0.2633	4.106	7.014	0.2374	6.136	6.819	0.2169	5.675	6.581
2-C6=,c		0.0425	0.685	1.1588	0.0515	0.803	1.371	0.0543	1.403	1.559	0.0534	1.397	1.621
3-m-2-C5=,t		0.4396	7.088	11.9987	0.4478	6.984	11.929	0.3962	10.240	11.380	0.3659	9.576	11.104
23-dm-2-C4=		0.2333	3.761	6.3676	0.2177	3.395	5.799	0.1837	4.749	5.278	0.1538	4.024	4.667
C7= & C8=		0.0204	0.329		0.0126	0.197		0.0000	0.000		0.0000	0.000	
C9=		2.3071	37.202		2.4553	38.294		0.2596	6.711		0.4062	10.628	
C10= & C11=		0.0000	0.000		0.0000	0.000		0.0000	0.000		0.0000	0.000	
C12=		0.0063	0.101		0.0086	0.134		0.0000	0.000		0.0068	0.179	
>C12=		0.0298	0.481		0.0299	0.467		0.0000	0.000		0.0000	0.000	
Total	100.00	100.00	100.00	100.00	100.00	100.00	100.00	100.00	100.00	100.00	100.00	100.00	100.00
Conversion		6.2			6.4			3.9			3.8		
Mass Bal.%		106			95			110			91		

Table B.5 - Base Run for Shape Selectivity and Reaction Temperature Study

Run No : 81 Date : 2 March 1995

Catalyst : H-ZSM-5

Mass Catalyst,g : 0.06

Mass Sand,g : 3.0

Pretreatment: calcined at 500C in air overnight

Feed : Pure Propene

Z Factor : 0.896

Feed Concentration, mol/cm3 : 2.68e-3

Reaction Conditions : 250C, 5 MPa

WHSV g feed/g cat/hr : 315

Internal Standard : Methane

Mass Balance : 105%

Sample No.	1			2			3		
Bed Temp, C	251			251			251		
Time, min	149			202			210		
Product	Mass%	Avg Conc	Rate	Mass%	Avg Conc	Rate	Mass%	Avg Conc	Rate
(Hydrog)		mol/cm3	mol/hr/g		mol/cm3	mol/hr/g		mol/cm3	mol/hr/g
C3=		2.645E-03	-4.821E-01		2.652E-03	-3.911E-01		2.653E-03	-3.768E-01
C4	3.825	2.567E-06	1.383E-02	4.256	2.300E-06	1.248E-02	4.432	2.305E-06	1.253E-02
C5	1.866	1.002E-06	5.400E-03	1.787	7.725E-07	4.192E-03	1.676	6.973E-07	3.789E-03
2,3-dm-C4	4.774	2.136E-06	1.151E-02	4.682	1.688E-06	9.158E-03	4.609	1.598E-06	8.683E-03
2-m-C5	35.158	1.573E-05	8.474E-02	37.166	1.339E-05	7.268E-02	39.540	1.371E-05	7.450E-02
3-m-C5	13.029	5.830E-06	3.140E-02	13.160	4.742E-06	2.573E-02	13.462	4.668E-06	2.536E-02
C6	3.711	1.660E-06	8.943E-03	3.997	1.440E-06	7.816E-03	4.273	1.482E-06	8.051E-03
C7-C8	2.171	7.769E-07	4.185E-03	2.135	6.154E-07	3.339E-03	1.650	4.577E-07	2.487E-03
2,3,5-tm-C6	0.188	5.595E-08	3.014E-04	0.170	4.066E-08	2.206E-04	0.143	3.313E-08	1.800E-04
2,2-dm-C7	0.414	1.236E-07	6.659E-04	0.330	7.946E-08	4.312E-04	0.332	7.651E-08	4.158E-04
2,4-dm-C7	3.406	1.016E-06	5.472E-03	3.351	8.053E-07	4.370E-03	3.112	7.193E-07	3.908E-03
4,4-dm-C7	0.324	9.663E-08	5.205E-04	0.312	7.487E-08	4.063E-04	0.286	6.625E-08	3.600E-04
26dmC7/4e2mC6	0.356	1.065E-07	5.738E-04	0.330	7.946E-08	4.312E-04	0.306	7.058E-08	3.835E-04
2,5/3,5-dm-C7	4.208	8.315E-07	4.479E-03	4.061	6.487E-07	3.520E-03	3.687	6.473E-07	3.517E-03
3-e-2-m-C6	1.275	4.234E-07	2.281E-03	1.122	3.269E-07	1.774E-03	0.996	2.052E-07	1.115E-03
2,3,4-tm-C6	0.217	3.804E-07	2.049E-03	0.184	2.696E-07	1.463E-03	0.157	2.304E-07	1.252E-03
3-e-3-m-C6	0.075	6.450E-08	3.474E-04	0.067	4.425E-08	2.401E-04	0.060	3.646E-08	1.981E-04
2,3-dm-C6	2.785	2.223E-08	1.198E-04	2.542	1.599E-08	8.678E-05	2.319	1.409E-08	7.657E-05
3,4-dm-C7	4.110	8.308E-07	4.475E-03	3.774	6.105E-07	3.313E-03	3.408	5.363E-07	2.914E-03
4-e-C7	0.141	1.226E-06	6.603E-03	0.118	9.065E-07	4.919E-03	0.111	7.879E-07	4.281E-03
4-m-C8	4.814	4.202E-08	2.264E-04	3.142	2.863E-08	1.554E-04	3.019	2.559E-08	1.390E-04
2-m-C8	0.000	1.436E-06	7.737E-03	1.747	7.548E-07	4.096E-03	1.7522	6.979E-07	3.792E-03
3-m-C8	3.256	0.000E+00	0.000E+00	3.249	4.197E-07	2.278E-03	3.106	4.051E-07	2.201E-03
linear C9	0.535	9.712E-07	5.231E-03	0.529	7.802E-07	4.234E-03	0.513	7.179E-07	3.901E-03
> C9	9.364	1.598E-07	8.607E-04	7.787	1.269E-07	6.888E-04	7.051	1.185E-07	6.441E-04
Total	100.00	2.095E-06	1.129E-02	100.00	1.403E-06	7.614E-03	100.00	1.223E-06	6.643E-03
Conversion	6.4			5.2			5.0		

Table B.5 cont.

Sample No.	4			5			
Bed Temp, C	251			253			
Time, min	298			338			
Product	Mass%	Avg Conc	Rate	Mass%	Avg Conc	Rate	Avg Rate
(Hydrog)		mol/cm3	mol/hr/g		mol/cm3	mol/hr/g	mol/hr/g
C3=		2.655E-03	-3.535E-01		2.650E-03	-4.105E-01	-4.028E-01
C4	4.714	2.295E-06	1.250E-02	4.294	2.438E-06	1.322E-02	1.291E-02
C5	1.702	6.633E-07	3.612E-03	1.676	7.614E-07	4.127E-03	4.224E-03
2,3-dm-C4	4.614	1.498E-06	8.157E-03	4.544	1.720E-06	9.325E-03	9.366E-03
2-m-C5	41.813	1.357E-05	7.391E-02	40.601	1.537E-05	8.332E-02	7.783E-02
3-m-C5	13.776	4.472E-06	2.435E-02	13.948	5.280E-06	2.862E-02	2.709E-02
C6	4.620	1.500E-06	8.169E-03	4.699	1.779E-06	9.644E-03	8.524E-03
C7-C8	1.798	4.670E-07	2.543E-03	1.670	5.059E-07	2.742E-03	3.059E-03
2,3,5-tm-C6	0.148	3.182E-08	1.733E-04	0.123	3.104E-08	1.683E-04	2.087E-04
2,2-dm-C7	0.318	6.903E-08	3.759E-04	0.270	6.835E-08	3.705E-04	4.519E-04
2,4-dm-C7	2.933	6.346E-07	3.456E-03	2.947	7.437E-07	4.032E-03	4.248E-03
4,4-dm-C7	0.306	6.595E-08	3.591E-04	0.262	6.630E-08	3.594E-04	4.011E-04
26dmC7/4e2	0.310	6.698E-08	3.647E-04	0.307	7.716E-08	4.183E-04	4.343E-04
2,5/3,5-dm-C	3.469	7.508E-07	4.088E-03	3.501	8.838E-07	4.791E-03	4.079E-03
3-e-2-m-C6	0.904	0.000E+00	0.000E+00	0.849	0.000E+00	0.000E+00	1.034E-03
2,3,4-tm-C6	0.145	1.958E-07	1.066E-03	0.129	2.144E-07	1.162E-03	1.398E-03
3-e-3-m-C6	0.000	3.144E-08	1.712E-04	0.000	3.245E-08	1.759E-04	2.266E-04
2,3-dm-C6	2.101	0.000E+00	0.000E+00	2.083	0.000E+00	0.000E+00	5.662E-05
3,4-dm-C7	3.130	4.547E-07	2.476E-03	3.001	5.259E-07	2.851E-03	3.206E-03
4-e-C7	0.096	6.775E-07	3.689E-03	0.100	7.577E-07	4.107E-03	4.720E-03
4-m-C8	2.751	2.066E-08	1.125E-04	2.937	2.529E-08	1.371E-04	1.541E-04
2-m-C8	1.759	5.954E-07	3.242E-03	1.583	7.413E-07	4.019E-03	4.577E-03
3-m-C8	2.924	3.806E-07	2.072E-03	3.032	3.996E-07	2.166E-03	1.743E-03
linear C9	0.486	6.330E-07	3.447E-03	0.515	7.655E-07	4.150E-03	4.193E-03
> C9	5.179	1.053E-07	5.737E-04	6.925	1.298E-07	7.036E-04	6.942E-04
Total	100.00	8.407E-07	4.578E-03	100.00	1.311E-06	7.106E-03	7.445E-03
Conversion	4.7			5.5			

Table B.6 - Shape Selectivity Study

Run No : 106 Date : 2 May 1995

Catalyst : SAPO34

Mass Catalyst,g : 0.15

Mass Sand,g : 7.5

Pretreatment: calcined at 500C in air overnight

Feed : Pure Propene

Reaction Conditions : 250C, 5 MPa

WHSV g feed/g cat/hr : 144

Internal Standard : Methane

Mass Balance : 105%

Sample No.	1	2	3	4
Bed Temp, C	252	252	251	251
Time, min	95	142	185	226
Product (Hydrog.)	Mass%	Mass%	Mass%	Mass%
C4	5.810	7.669	8.697	9.617
C5	1.627	1.544	1.368	1.338
2,3-dm-C4	5.226	6.717	7.094	7.328
2-m-C5	39.272	51.627	53.244	54.981
3-m-C5	7.960	10.089	10.058	10.186
C6	0.777	0.896	0.963	0.936
C7-C8	0.829	0.340	0.369	0.000
2,3,5-tm-C6	1.479	1.201	1.015	0.901
2,2-dm-C7	0.143	0.000	0.000	0.000
2,4-dm-C7	2.627	2.079	1.797	1.663
4,4-dm-C7	1.318	1.156	1.131	1.063
26dmC7/4e2mC6	0.479	0.367	0.323	0.000
2,5/3,5-dm-C7	2.806	2.189	1.843	1.570
3-e-2-m-C6	4.563	3.434	3.056	2.761
2,3,4-tm-C6	1.438	1.213	1.005	0.936
3-e-3-m-C6	0.295	0.207	0.195	0.000
2,3-dm-C6	3.517	2.443	1.968	1.740
3,4-dm-C7	9.634	6.761	5.736	4.985
4-e-C7	0.000	0.000	0.000	0.000
4m/2m-C8	0.248	0.068	0.138	0.000
3-m-C8	0.182	0.000	0.000	0.000
linear C9	0.000	0.000	0.000	0.000
>C9	9.762	0.000	0.000	0.000
Total	99.99	100.00	100.00	100.00
Conversion	5.9	3.9	3.3	2.6

Table B.7 - Shape Selectivity Study

Run No : 104 Date : 28 April 1995

Catalyst : H-Beta

Mass Catalyst,g : 0.153

Mass Sand,g : 7.5

Pretreatment: calcined at 500C in air overnight

Feed : Pure Propene

Reaction Conditions : 250C, 5 MPa

WHSV g feed/g cat/hr : 134

Internal Standard : Methane

Mass Balance : 108%

Sample No.	1	2	3	4	5
Bed Temp, C	250	249	249	249	249
Time, min	105	163	206	249	287
Product (Hydrog.)	Mass%	Mass%	Mass%	Mass%	Mass%
C4	2.347	3.926	5.794	7.321	8.834
C5	1.516	1.315	1.368	1.350	1.407
2,3-dm-C4	3.890	5.237	5.945	6.210	6.317
2-m-C5	25.467	38.660	46.529	49.365	51.090
3-m-C5	10.017	12.076	13.089	13.080	13.072
C6	0.948	1.093	1.220	1.272	1.334
C7-C8	5.509	2.950	1.345	1.683	0.966
2,3,5-tm-C6	0.890	0.629	0.495	0.408	0.371
2,2-dm-C7	0.826	0.487	0.332	0.295	0.254
2,4-dm-C7	3.244	2.377	1.899	1.605	1.474
4,4-dm-C7	1.560	1.663	1.511	1.376	1.257
26dmC7/4e2mC6	0.747	0.506	0.385	0.396	0.361
2,5-dm-C7	2.621	1.881	1.585	1.489	1.207
3,5-dm-C7	3.235	2.223	1.570	1.090	0.959
3-e-2-m-C6	4.015	2.981	2.353	1.827	1.564
2,3,4-tm-C6	0.901	0.674	0.533	0.376	0.381
3-e-3-m-C6	0.363	0.239	0.181	0.145	0.000
2,3-dm-C6	6.810	4.358	3.162	2.353	1.999
3,4-dm-C7	14.661	11.503	9.066	7.153	6.106
4-e-C7	0.000	0.000	0.000	0.000	0.000
4m/2m-C8	0.922	0.830	0.712	0.694	0.608
3-m-C8	0.756	0.655	0.559	0.509	0.438
linear C9	0.117	0.104	0.000	0.000	0.000
>C9	8.643	3.636	0.365	0.000	0.000
Total	100.00	100.00	100.00	100.00	100.00
Conversion	13.0	8.5	5.1	4.2	3.4

Table B.8 - Shape Selectivity Study

Run No : 105 Date : 30 April 1995

Catalyst : Amorphous Silica Alumina, 9% Alumina

Mass Catalyst,g : 0.153

Mass Sand,g : 7.5

Pretreatment: calcined at 500C in air overnight

Feed : Pure Propene

Reaction Conditions : 250C, 5 MPa

WHSV g feed/g cat/hr : 142

Internal Standard : Methane

Mass Balance : 107%

Sample No.	1	2	3	4	5
Bed Temp, C	248	250	250	250	250
Time, min	101	144	189	227	264
Product (Hydrog.)	Mass%	Mass%	Mass%	Mass%	Mass%
C4	2.912	3.347	4.066	4.577	4.711
C5	1.964	1.699	1.638	1.592	1.505
2,3-dm-C4	5.818	6.521	7.065	7.145	7.189
2-m-C5	35.373	40.028	43.684	45.020	45.537
3-m-C5	10.568	11.914	12.611	12.633	12.619
C6	1.017	1.191	1.299	1.348	1.348
C7-C8	5.051	3.518	2.779	2.541	2.317
2,3,5-tm-C6	1.992	1.858	1.642	1.550	1.494
2,2-dm-C7	0.281	0.237	0.230	0.221	0.191
2,4-dm-C7	3.194	3.068	2.811	2.692	2.605
4,4-dm-C7	0.863	0.829	0.811	0.790	0.791
26dmC7/4e2mC6	0.631	0.613	0.547	0.516	0.519
2,5/3,5-dm-C7	3.456	3.323	3.051	2.929	2.891
3-e-2-m-C6	4.087	3.764	3.435	3.271	3.124
2,3,4-tm-C6	1.816	1.714	1.572	1.488	1.357
3-e-3-m-C6	0.242	0.234	0.218	0.206	0.177
2,3-dm-C6	3.888	3.523	3.115	2.923	2.745
3,4-dm-C7	8.432	7.612	6.819	6.508	6.256
4-e-C7	0.000	0.101	0.088	0.081	0.000
4m/2m-C8	0.294	0.349	0.348	0.329	0.328
3-m-C8	0.195	0.227	0.222	0.227	0.235
linear C9	0.000	0.000	0.000	0.000	0.000
>C9	7.930	4.330	1.954	1.414	2.062
Total	100.00	100.00	100.00	100.00	100.00
Conversion	12.8	10.1	7.5	6.7	6.2

Table B.9 - Reaction Temperature Study

Run No : 109 Date : 5 May 1995

Catalyst : H-ZSM-5

Mass Catalyst,g : 0.152

Mass Sand,g : 7.5

Pretreatment: calcined at 500C in air overnight

Feed : Pure Propene

Z Factor : 0.861

Feed Concentration, mol/cm3 : 3.04e-3

Reaction Conditions : 230C, 5 MPa

WHSV g feed/g cat/hr : 116

Internal Standard : Methane

Mass Balance : 93%

Sample No.	1			2			3			4		
Bed Temp, C	235			234			235			235		
Time, min	57			103			144			234		
Product	Mass%	Avg Conc	Rate	Mass%	Avg Conc	Rate	Mass%	Avg Conc	Rate	Mass%	Avg Conc	Rate
(Hydrog.)		mol/cm3	mol/hr/g		mol/cm3	mol/hr/g		mol/cm3	mol/hr/g		mol/cm3	mol/hr/g
C3=		2.99E-03	-1.986E-01		2.98E-03	-2.369E-01		2.99E-03	-2.028E-01		3.00E-03	-1.490E-01
C4	3.987	3.39E-06	5.939E-03	3.778	3.86E-06	6.714E-03	4.667	4.05E-06	7.100E-03	4.960	3.13E-06	5.543E-03
C5	2.027	1.38E-06	2.417E-03	1.447	1.18E-06	2.057E-03	1.450	1.01E-06	1.765E-03	1.396	7.04E-07	1.249E-03
2,3-dm-C4	5.999	3.40E-06	5.958E-03	4.807	3.28E-06	5.695E-03	4.764	2.76E-06	4.830E-03	4.535	1.91E-06	3.379E-03
2-m-C5	31.486	1.78E-05	3.127E-02	29.567	2.02E-05	3.502E-02	33.836	1.96E-05	3.431E-02	39.465	1.66E-05	2.941E-02
3-m-C5	12.434	7.04E-06	1.235E-02	11.313	7.71E-06	1.340E-02	12.126	7.02E-06	1.230E-02	13.073	5.49E-06	9.742E-03
C6	2.876	1.63E-06	2.857E-03	3.046	2.08E-06	3.607E-03	3.653	2.11E-06	3.703E-03	4.527	1.90E-06	3.374E-03
C7-C8	2.478	1.12E-06	1.969E-03	2.328	1.27E-06	2.207E-03	1.797	8.32E-07	1.458E-03	1.324	4.45E-07	7.894E-04
2,3,5-tm-C6	0.517	1.95E-07	3.426E-04	0.459	2.09E-07	3.624E-04	0.341	1.31E-07	2.299E-04	0.225	6.34E-08	1.125E-04
2,2-dm-C7	0.785	2.96E-07	5.197E-04	0.788	3.58E-07	6.220E-04	0.642	2.48E-07	4.338E-04	0.468	1.31E-07	2.322E-04
2,4-dm-C7	3.763	1.42E-06	2.492E-03	4.001	1.82E-06	3.161E-03	3.722	1.44E-06	2.517E-03	3.301	9.25E-07	1.640E-03
4,4-dm-C7	0.551	2.08E-07	3.655E-04	0.541	2.46E-07	4.271E-04	0.469	1.81E-07	3.172E-04	0.425	1.19E-07	2.109E-04
2,6-dm-C7	0.430	1.62E-07	2.846E-04	0.467	2.12E-07	3.685E-04	0.379	1.47E-07	2.567E-04	0.318	8.90E-08	1.579E-04
2,5-dm-C7	2.457	9.28E-07	1.627E-03	2.710	1.23E-06	2.140E-03	2.594	1.00E-06	1.754E-03	2.392	6.70E-07	1.188E-03
3,5-dm-C7	2.406	9.09E-07	1.593E-03	2.371	1.08E-06	1.872E-03	2.079	8.02E-07	1.406E-03	1.584	4.44E-07	7.875E-04
3-e-2-m-C6	2.936	1.11E-06	1.944E-03	2.733	1.24E-06	2.159E-03	2.348	9.06E-07	1.588E-03	1.794	5.03E-07	8.916E-04
2,3,4-tm-C6	0.789	2.98E-07	5.226E-04	0.657	2.99E-07	5.194E-04	0.511	1.98E-07	3.462E-04	0.355	9.98E-08	1.769E-04
3-e-3-m-C6	0.189	7.15E-08	1.254E-04	0.173	7.84E-08	1.362E-04	0.151	5.88E-08	1.031E-04	0.108	2.99E-08	5.301E-05
2,3-dm-C6	4.967	1.88E-06	3.289E-03	5.100	2.32E-06	4.028E-03	4.347	1.68E-06	2.939E-03	3.358	9.41E-07	1.669E-03
3,4-dm-C7	8.271	3.12E-06	5.477E-03	8.137	3.70E-06	6.425E-03	7.206	2.78E-06	4.872E-03	5.673	1.59E-06	2.818E-03
4-e-C7	0.211	7.95E-08	1.393E-04	0.228	1.03E-07	1.793E-04	0.196	7.59E-08	1.329E-04	0.133	3.74E-08	6.636E-05
4m/2m-C8	2.746	1.04E-06	1.818E-03	3.359	1.53E-06	2.653E-03	3.680	1.42E-06	2.489E-03	3.679	1.03E-06	1.827E-03
3-m-C8	1.921	7.26E-07	1.272E-03	2.363	1.07E-06	1.867E-03	2.519	9.72E-07	1.702E-03	2.435	6.82E-07	1.210E-03
linear C9	0.368	1.39E-07	2.435E-04	0.350	1.59E-07	2.758E-04	0.366	1.41E-07	2.469E-04	0.355	9.96E-08	1.766E-04
>C9	5.403	1.53E-06	2.683E-03	9.273	3.16E-06	5.492E-03	6.154	1.78E-06	3.121E-03	4.112	8.64E-07	1.532E-03
Total	100.00			100.00			100.00			100.00		
Conversion	7.2			8.5			7.3			5.4		

Table B.9 cont.

Sample No.	5			6			
Bed Temp, C	235			235			
Time, min	275			317			
Product	Mass%	Avg Conc	Rate	Mass%	Avg Conc	Rate	Avg Rate
(Hydrog.)		mol/cm3	mol/hr/g		mol/cm3	mol/hr/g	mol/hr/g
C3=		2.999E-03	-1.469E-01		3.000E-03	-1.415E-01	-1.793E-01
C4	5.094	3.164E-06	5.614E-03	5.308	3.171E-06	5.633E-03	6.090E-03
C5	1.305	6.487E-07	1.151E-03	1.335	6.380E-07	1.134E-03	1.629E-03
2,3-dm-C4	4.380	1.813E-06	3.217E-03	4.277	1.703E-06	3.026E-03	4.351E-03
2-m-C5	40.322	1.669E-05	2.962E-02	41.632	1.658E-05	2.945E-02	3.151E-02
3-m-C5	13.164	5.450E-06	9.670E-03	13.318	5.302E-06	9.420E-03	1.115E-02
C6	4.713	1.951E-06	3.461E-03	4.964	1.976E-06	3.511E-03	3.419E-03
C7-C8	1.282	4.247E-07	7.535E-04	1.289	4.105E-07	7.292E-04	1.318E-03
2,3,5-tm-C6	0.217	6.018E-08	1.068E-04	0.209	5.542E-08	9.846E-05	2.088E-04
2,2-dm-C7	0.454	1.253E-07	2.224E-04	0.439	1.166E-07	2.072E-04	3.729E-04
2,4-dm-C7	3.228	8.914E-07	1.582E-03	3.076	8.166E-07	1.451E-03	2.140E-03
4,4-dm-C7	0.411	1.139E-07	2.020E-04	0.418	1.111E-07	1.973E-04	2.867E-04
2,6-dm-C7	0.283	7.836E-08	1.390E-04	0.276	7.360E-08	1.307E-04	2.229E-04
2,5-dm-C7	2.380	6.572E-07	1.166E-03	2.139	5.677E-07	1.009E-03	1.481E-03
3,5-dm-C7	1.484	4.096E-07	7.267E-04	1.475	3.913E-07	6.951E-04	1.180E-03
3-e-2-m-C6	1.661	4.587E-07	8.138E-04	1.516	4.023E-07	7.148E-04	1.352E-03
2,3,4-tm-C6	0.316	8.680E-08	1.540E-04	0.274	7.249E-08	1.288E-04	3.080E-04
3-e-3-m-C6	0.101	2.814E-08	4.993E-05	0.096	2.549E-08	4.529E-05	8.548E-05
2,3-dm-C6	3.125	8.626E-07	1.531E-03	2.880	7.646E-07	1.358E-03	2.469E-03
3,4-dm-C7	5.414	1.494E-06	2.651E-03	4.977	1.321E-06	2.347E-03	4.098E-03
4-e-C7	0.000	0.000E+00	0.000E+00	0.000	0.000E+00	0.000E+00	8.632E-05
4m/2m-C8	3.794	1.047E-06	1.858E-03	3.732	9.904E-07	1.760E-03	2.067E-03
3-m-C8	2.499	6.894E-07	1.223E-03	2.451	6.506E-07	1.156E-03	1.405E-03
linear C9	0.351	9.654E-08	1.713E-04	0.341	9.022E-08	1.603E-04	2.124E-04
>C9	4.016	8.315E-07	1.475E-03	3.575	7.116E-07	1.264E-03	2.595E-03
Total	99.99			100.00			
Conversion	5.3			5.1			

Table B.10 - Reaction Temperature Study

Run No : 101 Date : 25 April 1995

Catalyst : H-ZSM-5

Mass Catalyst,g : 0.052

Mass Sand,g : 3.51

Pretreatment: calcined at 500C in air overnight

Feed : Pure Propene

Z Factor : 0.914

Feed Concentration, mol/cm3 : 2.36e-3

Reaction Conditions : 280C, 5 MPa

WHSV g feed/g cat/hr : 829

Internal Standard : Methane

Mass Balance : 95%

Sample No.	1			2			3			
Bed Temp, C	283			282			282			
Time, min	134			181			228			
Product	Mass%	Avg Conc	Rate	Mass%	Avg Conc	Rate	Mass%	Avg Conc	Rate	Avg Rate
(Hydrog.)		mol/cm3	mol/hr/g		mol/cm3	mol/hr/g		mol/cm3	mol/hr/g	mol/hr/g
C4	3.815	2.31E-03	-1.612E+00	3.695	2.32E-03	-1.356E+00	4.290	2.33E-03	-1.082E+00	-1E+00
C5	2.797	2.88E-06	4.612E-02	2.311	2.33E-06	3.759E-02	2.149	2.14E-06	3.481E-02	4.0E-02
2,3-dm-C4	4.362	1.69E-06	2.704E-02	4.224	1.17E-06	1.881E-02	4.452	8.59E-07	1.396E-02	2.0E-02
2-m-C5	32.806	2.20E-06	3.515E-02	36.629	1.78E-06	2.864E-02	42.029	1.48E-06	2.409E-02	2.9E-02
3-m-C5	14.947	1.65E-05	2.644E-01	15.086	1.54E-05	2.484E-01	15.914	1.40E-05	2.274E-01	2.5E-01
C6	4.580	7.54E-06	1.205E-01	4.866	6.35E-06	1.023E-01	5.290	5.30E-06	8.610E-02	1.0E-01
C7-C8	3.356	2.31E-06	3.690E-02	2.417	2.05E-06	3.299E-02	2.191	1.76E-06	2.862E-02	3.3E-02
2,3,5-tm-C6	0.156	1.35E-06	2.164E-02	0.128	8.14E-07	1.311E-02	0.119	5.83E-07	9.480E-03	1.5E-02
2,2-dm-C7	0.326	5.25E-08	8.387E-04	0.255	3.59E-08	5.780E-04	0.246	2.62E-08	4.264E-04	6.1E-04
2,4-dm-C7	3.654	1.10E-07	1.752E-03	3.102	7.16E-08	1.153E-03	2.878	5.43E-08	8.831E-04	1.3E-03
4,4-dm-C7	0.186	1.23E-06	1.963E-02	0.166	8.70E-07	1.402E-02	0.191	6.39E-07	1.038E-02	1.5E-02
2,6-dm-C7	0.464	6.22E-08	9.940E-04	0.363	4.68E-08	7.534E-04	0.353	4.22E-08	6.863E-04	8.1E-04
2,5-dm-C7	3.349	1.56E-07	2.493E-03	2.779	1.02E-07	1.641E-03	2.557	7.82E-08	1.272E-03	1.8E-03
3,5-dm-C7	1.341	1.13E-06	1.800E-02	1.084	7.80E-07	1.256E-02	0.908	5.67E-07	9.219E-03	1.3E-02
3-e-2-m-C6	0.862	4.51E-07	7.209E-03	0.676	3.04E-07	4.900E-03	0.557	2.01E-07	3.275E-03	5.1E-03
2,3,4-tm-C6	0.159	2.90E-07	4.633E-03	0.128	1.90E-07	3.055E-03	0.077	1.24E-07	2.011E-03	3.2E-03
3-e-3-m-C6	0.055	5.36E-08	8.568E-04	0.046	3.59E-08	5.780E-04	0.000	1.71E-08	2.775E-04	5.7E-04
2,3-dm-C6	2.239	1.86E-08	2.977E-04	1.812	1.30E-08	2.090E-04	1.574	0.00E+00	0.000E+00	1.7E-04
3,4-dm-C7	2.705	7.52E-07	1.203E-02	2.277	5.08E-07	8.190E-03	2.021	3.49E-07	5.677E-03	8.6E-03
4-e-C7	0.169	9.09E-07	1.453E-02	0.126	6.39E-07	1.029E-02	0.108	4.48E-07	7.289E-03	1.1E-02
4-m-C8	3.569	5.68E-08	9.085E-04	3.094	3.56E-08	5.728E-04	2.916	2.37E-08	3.860E-04	6.2E-04
2-m-C8	2.105	1.20E-06	1.917E-02	1.973	8.68E-07	1.399E-02	1.828	6.47E-07	1.052E-02	1.5E-02
3-m-C8	3.836	7.07E-07	1.131E-02	3.354	5.54E-07	8.923E-03	3.085	4.06E-07	6.595E-03	8.9E-03
linear C9	0.688	1.29E-06	2.061E-02	0.581	9.41E-07	1.516E-02	0.533	6.85E-07	1.113E-02	1.6E-02
>C9	7.475	2.31E-07	3.694E-03	8.826	1.63E-07	2.624E-03	3.741	1.18E-07	1.920E-03	2.7E-03
Total	100.00	1.88E-06	3.012E-02	100.00	1.86E-06	2.992E-02	100.00	6.23E-07	1.012E-02	2.3E-02
Conversion	8.2			6.9			5.5			

Table B.11 - Reaction Temperature Study

Run No : 108 Date : 4 May 1995

Catalyst : H-ZSM-5

Mass Catalyst,g : 0.152

Mass Sand,g : 7.5

Pretreatment: calcined at 500C in air overnight

Feed : Pure Propene

Z Factor : 0.861

Feed Conc, mol/cm3 : 3.49E-03

Reaction Conditions : 200C, 5 MPa

WHSV g feed/g cat/hr : 100

Internal Standard : Methane

Mass Balance : 95%

Sample No.	1			2			3			4			5			
Bed Temp, C	198			203			205			204			204			
Time, min	53			105			151			196			251			
Product	Mass%	Avg Conc	Rate	Mass%	Avg Conc	Rate	Mass%	Avg Conc	Rate	Mass%	Avg Conc	Rate	Mass%	Avg Conc	Rate	Avg Rate
(Hydrog.)		mol/cm3	mol/hr/g		mol/cm3	mol/hr/g		mol/cm3	mol/hr/g		mol/cm3	mol/hr/g		mol/cm3	mol/hr/g	mol/hr/g
C3=		3.46E-03	-9.723E-02		3.45E-03	-1.130E-01		3.46E-03	-9.595E-02		3.47E-03	-7.319E-02		3.47E-03	-6.5E-02	-9E-02
C4	7.761	4.25E-06	5.660E-03	7.368	4.70E-06	6.240E-03	7.339	3.96E-06	5.281E-03	8.573	3.51E-06	4.705E-03	10.176	3.70E-06	4.96E-03	5.4E-03
C5	0.840	3.68E-07	4.904E-04	0.714	3.65E-07	4.836E-04	1.086	4.70E-07	6.254E-04	0.938	3.08E-07	4.126E-04	0.940	2.73E-07	3.66E-04	4.8E-04
2,3-dm-C4	6.689	2.44E-06	3.253E-03	6.608	2.81E-06	3.732E-03	6.529	2.35E-06	3.132E-03	6.471	1.77E-06	2.368E-03	6.257	1.51E-06	2.03E-03	2.9E-03
2-m-C5	36.516	1.33E-05	1.775E-02	38.587	1.64E-05	2.179E-02	41.062	1.48E-05	1.970E-02	43.402	1.19E-05	1.588E-02	44.727	1.08E-05	1.45E-02	1.8E-02
3-m-C5	10.558	3.86E-06	5.133E-03	11.252	4.79E-06	6.355E-03	11.626	4.19E-06	5.577E-03	11.715	3.20E-06	4.286E-03	11.661	2.82E-06	3.79E-03	5.0E-03
C6	2.242	8.19E-07	1.090E-03	2.321	9.88E-07	1.310E-03	2.466	8.88E-07	1.183E-03	2.690	7.35E-07	9.841E-04	2.906	7.03E-07	9.44E-04	1.1E-03
C7-C8	1.130	3.30E-07	4.398E-04	1.018	3.47E-07	4.603E-04	0.754	2.17E-07	2.892E-04	0.204	4.43E-08	5.929E-05	0.000	0.00E+00	0.00E+00	2.5E-04
2,3,5-tm-C6	0.441	1.08E-07	1.432E-04	0.473	1.34E-07	1.781E-04	0.415	1.00E-07	1.331E-04	0.324	5.90E-08	7.898E-05	0.301	4.86E-08	6.52E-05	1.2E-04
2,2-dm-C7	0.650	1.58E-07	2.102E-04	0.649	1.84E-07	2.444E-04	0.538	1.29E-07	1.717E-04	0.391	7.13E-08	9.545E-05	0.335	5.43E-08	7.28E-05	1.6E-04
2,4-dm-C7	2.918	7.11E-07	9.459E-04	2.847	8.08E-07	1.072E-03	2.580	6.20E-07	8.252E-04	2.410	4.39E-07	5.878E-04	2.242	3.62E-07	4.86E-04	7.8E-04
4,4-dm-C7	0.834	2.03E-07	2.707E-04	0.825	2.35E-07	3.111E-04	0.754	1.81E-07	2.410E-04	0.735	1.34E-07	1.795E-04	0.753	1.21E-07	1.63E-04	2.3E-04
2,6-dm-C7	0.000	0.00E+00	0.000E+00	0.277	7.85E-08	1.041E-04	0.229	5.50E-08	7.324E-05	0.000	0.00E+00	0.000E+00	0.000	0.00E+00	0.00E+00	3.5E-05
2,5-dm-C7	1.608	3.92E-07	5.213E-04	1.551	4.40E-07	5.836E-04	1.459	3.50E-07	4.665E-04	1.345	2.45E-07	3.284E-04	1.296	2.09E-07	2.81E-04	4.4E-04
3,5-dm-C7	2.353	5.73E-07	7.623E-04	2.236	6.35E-07	8.419E-04	1.923	4.61E-07	6.145E-04	1.854	3.38E-07	4.524E-04	1.617	2.61E-07	3.50E-04	6.0E-04
3-e-2-m-C6	3.459	8.42E-07	1.121E-03	3.271	9.29E-07	1.232E-03	3.001	7.21E-07	9.598E-04	2.878	5.24E-07	7.021E-04	2.526	4.08E-07	5.47E-04	9.1E-04
2,3,4-tm-C6	0.771	1.88E-07	2.502E-04	0.745	2.12E-07	2.806E-04	0.652	1.57E-07	2.085E-04	0.598	1.09E-07	1.459E-04	0.432	6.95E-08	9.32E-05	2.0E-04
3-e-3-m-C6	0.224	5.44E-08	7.247E-05	0.183	5.20E-08	6.900E-05	0.186	4.50E-08	5.989E-05	0.188	3.41E-08	4.571E-05	0.000	0.00E+00	0.00E+00	4.9E-05
2,3-dm-C6	4.619	1.12E-06	1.497E-03	4.354	1.24E-06	1.639E-03	3.861	9.27E-07	1.235E-03	3.600	6.55E-07	8.779E-04	3.051	4.92E-07	6.61E-04	1.2E-03
3,4-dm-C7	10.468	2.55E-06	3.393E-03	9.712	2.76E-06	3.657E-03	8.942	2.15E-06	2.860E-03	8.433	1.54E-06	2.057E-03	7.398	1.19E-06	1.60E-03	2.7E-03
4-e-C7	0.000	0.00E+00	0.000E+00	0.000	0.00E+00	0.000E+00	0.000	0.00E+00	0.000E+00	0.000	0.00E+00	0.000E+00	0.000	0.00E+00	0.00E+00	0.0E+00
4-m-C8/2mC8	1.68	4.09E-07	5.442E-04	1.703	4.84E-07	6.414E-04	1.686	4.05E-07	5.391E-04	1.698	3.09E-07	4.144E-04	1.762	2.84E-07	3.82E-04	5.0E-04
3-m-C8	1.125	2.74E-07	3.648E-04	1.170	3.32E-07	4.406E-04	1.105	2.65E-07	3.536E-04	1.122	2.05E-07	2.739E-04	1.119	1.81E-07	2.43E-04	3.4E-04
linear C9	0.298	7.29E-08	9.709E-05	0.195	5.55E-08	7.363E-05	0.184	4.44E-08	5.917E-05	0.181	3.31E-08	4.437E-05	0.166	2.69E-08	3.61E-05	6.2E-05
>C9	2.810	5.13E-07	6.830E-04	1.937	4.13E-07	5.473E-04	1.622	2.92E-07	3.891E-04	0.254	3.46E-08	4.638E-05	0.332	4.01E-08	5.38E-05	3.4E-04
Total	100.00			100.00			100.00			100.00			100.00			
Conversion	4.1			4.8			4.0			3.1			2.7			

APPENDIX C

Table C.1 **Thermodynamic and Physical Properties of Hexene Isomers**
Data Required for Equilibrium Calculations

	Physical Properties				Critical Properties					
	Rossini et al(1953)		PROCESS		Correlation Lin/Chao(1984)			PROCESS		
Hexene Isomer	SG	NBP (K)	SG	NBP (K)	Tc (K)	Pc (MPa)	omega	Tc (K)	Pc (MPa)	omega
1-hexene	0.6685	336.64	0.678	336.64	507.51	3.184	0.26353	503.95	3.1107	0.296
2-hexene,cis	0.6823	341.99	0.6916	342	511.48	3.223	0.28987	518.00	3.2829	0.256
2-hexene,trans	0.6738	341.02	0.6826	341	507.43	3.153	0.29814	516.00	3.2728	0.242
3-hexene,cis	0.6749	339.59	0.6846	339.6	509.05	3.194	0.28097	517.00	3.2829	0.225
3-hexene,trans	0.6725	340.23	0.6815	340.3	507.28	3.156	0.29270	519.90	3.2525	0.227
2-methyl-1-pentene	0.6769	333.85	0.6892	335.25	512.72	3.300	0.22117	505.00	3.2880	0.274
3-methyl-1-pentene	0.6628	327.29	0.6726	327.31	508.66	3.247	0.17920	495.00	3.1180	0.240
4-methyl-1-pentene	0.6594	327.03	0.6686	327.02	507.39	3.223	0.18137	493.15	3.0904	0.207
2-methyl-2-pentene	0.6815	340.44	0.692	340.5	512.01	3.244	0.27620	518.00	3.2829	0.229
3-methyl-2-pentene,cis	0.6942	343.60	0.6987	340.9	516.79	3.313	0.28177	518.00	3.2829	0.269
3-methyl-2-pentene,trans	0.6898	340.78			515.98	3.320	0.26395			
4-methyl-2-pentene,cis	0.6642	329.45	0.674	329.54	508.69	3.240	0.19831	496.15	3.1917	0.185
4-methyl-2-pentene,trans	0.6638	331.70	0.674	331.76	507.73	3.213	0.22147	500.15	3.2931	0.211
2-ethyl-1-butene	0.6847	337.81	0.6947	337.82	514.82	3.318	0.24541	511.00	3.5280	0.283
2,3-dimethyl-1-butene	0.6731	328.82	0.6828	328.8	512.26	3.315	0.18011	501.00	3.2424	0.221
3,3-dimethyl-1-butene	0.6479	314.39	0.6578	314.4	504.22	3.178	0.07123	490.00	3.2525	0.121
2,3-dimethyl-2-butene	0.7034	346.36	0.7127	346.4	520.05	3.353	0.28935	524.00	3.3640	0.239

Thermodynamic Properties

	Heat of Formation (kJ/mol) at 298K			Gibbs Energy of Formation (kJ/mol) at 298K		
Hexene Isomer	NBS	Stull	PROCESS	NBS	Stull	PROCESS
1-hexene	-41.67	-41.67	-41.66	87.03	87.45	87.47
2-hexene,cis	-48.37	-52.34	-52.38	80.25	76.23	76.28
2-hexene,trans	-52.55	-53.89	-53.93	77.24	76.44	76.49
3-hexene,cis	-48.37	-47.61	-47.65	82.26	83.01	83.07
3-hexene,trans	-52.55	-54.43	-54.47	78.91	77.61	77.67
2-methyl-1-pentene	-56.74	-52.26	-56.73	73.14	77.61	73.12
3-methyl-1-pentene	-46.11	-45.02	-46.12	84.85	86.44	85.33
4-methyl-1-pentene	-48.79	-44.10	-48.81	83.26	90.04	85.35
2-methyl-2-pentene	-62.59	-59.75	-59.79	68.37	71.21	71.26
3-methyl-2-pentene,cis	-59.91	-57.74	-57.78	71.04	73.22	73.27
3-methyl-2-pentene,trans	-59.91	-58.66	-63.14	70.04	71.30	
4-methyl-2-pentene,cis	-55.48	-50.33	-55.46	76.99	82.13	77.03
4-methyl-2-pentene,trans	-59.66	-54.35	-59.67	74.35	79.62	74.31
2-ethyl-1-butene	-54.06	-51.55	-54.03	77.45	79.96	77.48
2,3-dimethyl-1-butene	-61.84	-55.73	-55.77	72.93	79.04	79.09
3,3-dimethyl-1-butene	-59.62	-43.14	-43.17	79.66	98.16	98.22
2,3-dimethyl-2-butene	-66.57	-59.20	-59.24	69.12	75.86	75.91

Table C.1 cont. Thermodynamic and Physical Properties of Hexene Isomers
Data Required for Equilibrium Calculations

	Enthalpy (kJ/kg) - NBS					Enthalpy (kJ/kg) - Stull				
Hexene Isomer	300 K	400 K	500 K	600 K	700 K	300 K	400 K	500 K	600 K	700 K
1-hexene	-493.26	-306.88	-82.73	177.27	461.19	-493.13	-313.80	-95.63	157.40	439.82
2-hexene,cis	-573.06	-399.87	-186.19	62.86	341.79	-620.11	-448.27	-56.43	11.46	289.89
2-hexene,trans	-622.77	-438.92	-217.27	37.76	321.67	-638.56	-460.24	-243.57	6.97	286.90
3-hexene,cis	-573.01	-403.06	-190.37	59.17	338.11	-563.84	-393.50	-181.80	66.74	345.68
3-hexene,trans	-622.82	-439.07	-214.93	41.09	325.01	-645.05	-464.72	-245.56	7.47	289.39
2-methyl-1-pentene	-672.63	-488.28	-265.63	-9.61	274.30	-618.65	-435.85	-214.18	41.84	326.25
3-methyl-1-pentene	-545.86	-354.24	-124.13	138.37	427.27	-532.46	-341.20	-111.08	150.92	440.83
4-methyl-1-pentene	-577.94	-393.15	-167.01	93.99	382.89	-522.00	-348.67	-135.98	111.57	389.01
2-methyl-2-pentene	-742.51	-569.32	-355.64	-106.59	172.34	-708.31	-534.97	-321.27	-72.22	206.21
3-methyl-2-pentene,cis	-710.63	-537.44	-323.76	-74.71	204.22	-684.38	-511.03	-297.36	-48.32	230.12
3-methyl-2-pentene,trans	-710.63	-537.44	-323.76	-74.71	204.22	-695.34	-522.00	-308.32	-59.27	219.16
4-methyl-2-pentene,cis	-657.63	-476.53	-255.37	-1.34	280.08	-596.22	-416.41	-196.75	57.28	340.20
4-methyl-2-pentene,trans	-707.39	-518.62	-291.98	-30.98	252.93	-643.54	-454.26	-228.13	30.38	316.29
2-ethyl-1-butene	-640.85	-459.09	-236.94	18.58	302.49	-610.65	-428.86	-206.71	49.24	335.02
2,3-dimethyl-1-butene	-733.29	-541.03	-310.41	-47.42	241.48	-659.98	-467.73	-238.09	23.91	312.80
3,3-dimethyl-1-butene	-707.49	-524.44	-300.8	-41.29	252.58	-510.53	-337.71	-124.03	126.02	405.95
2,3-dimethyl-2-butene	-789.98	-617.54	-406.35	-159.79	114.16	-701.82	-534.46	-328.74	-87.17	185.79

Table C.2 : Predicted Equilibrium at 250C, 5MPa

	PROCESS	HYSIM
Isomer	Mass%	Mass%
1 hexene	0.535	0.541
2 hexene,cis	2.230	2.391
2 hexene,trans	4.089	4.350
3 hexene, cis	0.945	0.968
3 hexene, trans	2.093	2.263
2 methyl 1 pentene	10.579	9.825
3 methyl 1 pentene	0.642	0.609
4 methyl 1 pentene	0.704	0.700
2 methyl 2 pentene	22.848	22.755
3 methyl 2 pentene,cis	12.611	12.444
3 methyl 2 pentene,trans	18.785	18.565
4 methyl 2 pentene,cis	2.639	2.499
4 methyl 2 pentene,trans	4.057	4.677
2,3 dimethyl 1 butene	5.254	5.445
2,3 dimethyl 2 butene	8.638	8.599
3,3 dimethyl 1 butene	0.445	0.494
2 ethyl 1 butene	2.906	2.877

Table C.3 : Isomerisation during 1-Hexene Oligomerisation

Data taken from Quann et al (1988)

Reaction Conditions : 227C, 4.2MPa

	Equilib	3 % Conv.	82 % Conv.
Isomer	Mass%	Mass%	Mass%
1 hexene	0.7	1.8	2.1
2 hexene,cis	2.9	12.1	5.4
2 hexene,trans	1.8	15.4	5.7
3 hexene,trans	1.8	11.4	3.6
2 methyl 1 pentene	8.2	7.9	7.5
3 methyl 1 pentene	1.8	0.5	0.5
2 methyl 2 pentene	30.9	22.1	22.7
3 methyl 2 pentene,cis	9.6	7.9	12.1
3 methyl 2 pentene,trans	20.7	15.0	22.1
4 methyl 2 pentene,trans	3.6	5.0	4.1
2,3 dimethyl 1 butene	6.8	1.1	5.4
2,3 dimethyl 2 butene	11.1	1.1	8.2
Total	99.82	101.25	99.46

Table C.4 : Hexene isomer equilibrium concentrations

Reaction conditions 573 K, 1 bar (concentrations in mol %)

Ratio	EXP NBS	PROCESS NBS	PROCESS STULL	PROCESS PPDS
N(2,3 dm 2-C4=)/N(3,3 dm 1-C4=)	18.6	15.1	63.1	357.2
N(2,3 dm 1-C4=)/N(3,3 dm 1-C4=)	9.8	11.4	52.6	269.7

Table C.5 : High Conversion Propene Oligomerisation Run

Run No : 57 Date : 6 May 1993

Catalyst : H-ZSM-5

Mass Catalyst, g : 0.38

Mass Sand,g : 19

Pretreatment : calcined at 500C in air overnight

Reaction Conditions : 250C, 5MPa

WHSV gfeed/gcat/hr : 35

Internal Standard : DME

Sample No (Every Hour)	Feed	1		1			1		2		2			2	
Bed Temp,C		251							255						
Time, Min		253-313							314-374						
Compound	Gas	Gas		Liquid			Total		Gas		Liquid			Total	
	Mass%	Mass%	100% MB Mass,g	Mass%	C6 only Mass%	100% MB Mass,g	Mass,g	Mass%	Mass%	100% MB Mass,g	Liquid Mass%	C6 only Mass%	100% MB Mass,g	Mass,g	Mass%
C2	0.0281	0.0316	0.0035	0		0.0000	0.0035	0.0205	0.0417	0.0045	0		0.0000	0.0045	0.0267
C3=	78.1162	60.3315	6.6666	2.037		0.1222	6.7888	39.8196	63.5823	6.9368	1.8469		0.1134	7.0502	41.3503
DME	21.8215	35.6567	3.9401	1.7374		0.1042	4.0443	23.7216	30.7979	3.3601	1.5108		0.0928	3.4528	20.2511
C4=	0.0342	0.4146	0.0458	0.0994		0.0060	0.0518	0.3037	0.5679	0.0620	0.1032		0.0063	0.0683	0.4006
C5=		0.5064	0.0560	0.5157		0.0309	0.0869	0.5097	0.6794	0.0741	0.5677		0.0349	0.1090	0.6392
C6=		2.9721	0.3284				1.0142	5.9485	3.9995	0.4363				1.2368	7.2541
C7/C8=		0.0867	0.0096						0.1795	0.0196					
C9=									0.1518	0.0166					
4-m-1-C5=				0.1105	0.9667	0.0066					0.117	0.8974	0.0072		
3-m-1-C5=				0.0984	0.8608	0.0059					0.123	0.9435	0.0076		
23-dm-1-C4=				0.3976	3.4783	0.0239					0.4051	3.1073	0.0249		
4-m-2-C5=,c				0.162	1.4172	0.0097					0.1924	1.4758	0.0118		
4-m-2-C5=,t				0.7762	6.7904	0.0466					0.8837	6.7784	0.0543		
2m1C5=/1-C6				0.9881	8.6442	0.0593					1.1442	8.7766	0.0703		
2-e-1-C4=				0.2256	1.9736	0.0135					0.2557	1.9613	0.0157		
3-C6=,c & t				0.3367	2.9456	0.0202					0.4111	3.1533	0.0252		
2-C6=,t				0.6086	5.3242	0.0365					0.7411	5.6846	0.0455		
2-m-2-C5=				2.7816	24.3343	0.1669					3.1834	24.4182	0.1955		
3-m-2-C5=,c				1.1711	10.2451	0.0703					1.3496	10.3521	0.0829		
2-C6=,c				0.2822	2.4688	0.0169					0.3509	2.6916	0.0215		
3-m-2-C5=,t				2.1307	18.6400	0.1278					2.4442	18.7482	0.1501		
23-dm-2-C4=				1.3615	11.9108	0.0817					1.4356	11.0117	0.0881		
> C6=				84.1798		5.0499	5.0595	29.6764			82.9346		5.0922	5.1283	30.0782
Total	100.00	100.00		100.00	100.00				100.00		100.00	100.00			100.00
Mass,g	17.05	9.80	11.05	5.32		6.00	17.05	100.00	10.21	10.91	5.75		6.14	17.05	
Mass Balance		88.7							93.6						
Conversion,%								49.03							47.07

Key : 100% MB : Assuming 100% Mass Balance applies

Note : Low Conversion Run, Run 47 is shown in Table B.1

Table C.5 cont.

Sample No (Every Hour)	3		3			3		4		4			4	
Bed Temp,C	252							255						
Time, Min	375-435							436-496						
Compound	Gas		Liquid			Total		Gas		Liquid			Total	
	Mass%	100% MB Mass,g	Mass%	C6 only Mass%	100% MB Mass,g	Mass,g	Mass%	Mass%	100% MB Mass,g	Liquid Mass%	C6 only Mass%	100% MB Mass,g	Mass,g	Mass%
C2	0.0434	0.0048	0		0.0000	0.0048	0.0281	0.041	0.0047	0		0.0000	0.0047	0.0275
C3=	62.9322	6.9603	1.9839		0.1190	7.0793	41.5059	62.3177	7.1229	1.3707		0.0769	7.1998	42.2525
DME	31.6786	3.5037	1.3769		0.0826	3.5863	21.0262	32.6853	3.7359	1.1313		0.0635	3.7994	22.2970
C4=	0.5426	0.0600	0.0851		0.0051	0.0651	0.3818	0.4895	0.0559	0.0731		0.0041	0.0601	0.3524
C5=	0.6431	0.0711	0.4577		0.0275	0.0986	0.5780	0.5752	0.0657	0.4286		0.0240	0.0898	0.5269
C6=	3.9822	0.4404				1.1612	6.8083	3.7859	0.4327				1.1594	6.8042
C7/C8=	0.1522	0.0168						0.0977	0.0112					
C9=	0.0258							0.0075	0.0009					
4-m-1-C5=			0.1067	0.8880	0.0064					0.1163	0.8978	0.0065		
3-m-1-C5=			0.1136	0.9455	0.0068					0.1185	0.9148	0.0066		
23-dm-1-C4=			0.3405	2.8339	0.0204					0.3491	2.6949	0.0196		
4-m-2-C5=,c			0.185	1.5397	0.0111					0.1935	1.4938	0.0109		
4-m-2-C5=,t			0.7972	6.6348	0.0478					0.832	6.4228	0.0467		
2m1C5=/1-C6			1.0675	8.8844	0.0640					1.1647	8.9911	0.0653		
2-e-1-C4=			0.236	1.9641	0.0142					0.2543	1.9631	0.0143		
3-C6=,c & t			0.3887	3.2350	0.0233					0.4197	3.2400	0.0235		
2-C6=,t			0.7031	5.8517	0.0422					0.7601	5.8677	0.0426		
2-m-2-C5=			2.979	24.7932	0.1787					3.2715	25.2549	0.1835		
3-m-2-C5=,c			1.2451	10.3625	0.0747					1.3504	10.4247	0.0758		
2-C6=,c			0.3303	2.7490	0.0198					0.3582	2.7652	0.0201		
3-m-2-C5=,t			2.267	18.8675	0.1360					2.4664	19.0398	0.1384		
23-dm-2-C4=			1.2557	10.4508	0.0753					1.2992	10.0294	0.0729		
> C6=			84.081		5.0440	5.0609	29.6717			84.0424		4.7148	4.7268	27.7395
Total	100.00		100.00	100.00				100.00		100.00	100.00			100.00
Mass,g	10.57	11.06	5.72		6.00	17.06	100.00	10.93	11.43	5.36		5.61	17.04	
Mass Balance	95.5							95.5						
Conversion,%							46.87							45.91

Table C.5 cont.							
Sample No (Every Hour)	5		5			5	
Bed Temp,C	254						
Time, Min	497-557						
Compound	Gas		Liquid			Total	
	Mass%	100% MB Mass,g	Mass%	C6 only Mass%	100% MB Mass,g	Mass,g	Mass%
C2	0.0416	0.0048	0		0.0000	0.0048	0.0281
C3=	64.6568	7.4485	2.2498		0.1244	7.5729	44.4151
DME	30.6253	3.5280	1.6484		0.0912	3.6192	21.2266
C4=	0.4835	0.0557	0.1426		0.0079	0.0636	0.3729
C5=	0.5427	0.0625	0.4291		0.0237	0.0862	0.5058
C6=	3.5646	0.4106				1.1468	6.7260
C7/C8=	0.0824	0.0095					
C9=	0.0033						
4-m-1-C5=			0.1205	0.9052	0.0067		
3-m-1-C5=			0.1241	0.9322	0.0069		
23-dm-1-C4=			0.3499	2.6285	0.0193		
4-m-2-C5=,c			0.2001	1.5032	0.0111		
4-m-2-C5=,t			0.8478	6.3687	0.0469		
2m1C5=/1-C6=			1.2124	9.1076	0.0670		
2-e-1-C4=			0.2613	1.9629	0.0144		
3-C6=,c & t			0.4307	3.2354	0.0238		
2-C6=,t			0.7988	6.0006	0.0442		
2-m-2-C5=			3.3903	25.4680	0.1875		
3-m-2-C5=,c			1.3866	10.4162	0.0767		
2-C6=,c			0.37	2.7794	0.0205		
3-m-2-C5=,t			2.5348	19.0415	0.1402		
23-dm-2-C4=			1.2847	9.6507	0.0710		
> C6=			82.2288		4.5473	4.5567	26.7254
Total	100.00		100.01	100.00			100.00
Mass,g	10.71	11.52	5.14		5.53	17.05	
Mass Balance	92.9						
Conversion,%							43.14

APPENDIX D

Table D.1 1-Hexene Isomerisation

Run No : 67 Date : 20 April 1994

Catalyst : H-ZSM-5

Mass Catalyst,g: 0.31

Mass Sand,g: 14.99

Pretreatment : calcined at 500C in air overnight

Feed : Pure 1-Hexene

Reaction Conditions : 250C, 5MPa

WHSV, g feed/g cat/hr: 10

Internal Standard : Propene

Sample No.	1	2	3	4
Time,min	174	223	276	331
Compound	Mass%	Mass%	Mass%	Mass%
cracked prods	0.3492	0.2256	0.0628	0.0000
2-methyl-Pentenes				
4m1C5=	0.3784	0.3602	0.1801	0.0000
4m2C5=,cis	0.5864	0.6016	0.5278	0.0000
4m2C5=,trans	1.9554	1.9554	1.6390	1.5113
2m1C5=	2.8891	2.7124	2.3036	2.1205
2m2C5=	8.4188	8.0778	7.0972	6.5118
3-methyl-Pentenes				
3m1C5=	0.3852	0.3381	0.0000	0.0000
2e1C4=	0.7218	0.6784	0.4970	0.4858
3m2C5=,cis	3.0420	2.7705	2.3562	2.0594
3m2C5=,trans	4.9754	4.5073	3.8018	3.2962
Hexenes				
1C6=	4.4315	4.9194	5.0970	5.3361
3C6=	18.3113	20.4393	21.4068	22.0937
2C6,trans	31.9455	35.5794	37.3400	38.6603
2C6=,cis	14.5572	16.2693	16.9868	17.5373
>C6=	7.0530	0.5657	0.7038	0.3879
Total	100.00	100.00	100.00	100.00
Conversion	30.8	22.8	19.2	16.4
Conv. to C6's	23.7	22.2	18.5	16.0
Mass Bal.%	98	95	97	94

Table D.2 1-Hexene Isomerisation

Run No : 68 Date : 21 April 1994

Catalyst : H-ZSM-5

Mass Catalyst,g: 0.31

Mass Sand,g: 14.99

Pretreatment : calcined at 500C in air overnight

Feed : Pure 1-Hexene

Reaction Conditions : 250C, 5MPa

WHSV, g feed/g cat/hr: 17

Internal Standard : Propene

Sample No.	1	2	3	4	5
Time,min	60	174	223	276	331
Compound	Mass%	Mass%	Mass%	Mass%	Mass%
cracked prods	1.0444	0.3028	0.1726	0.2294	0.2346
2-methyl-Pentenes					
4m1C5=	0.3828	0.1812	0.1102	0.0000	0.0000
4m2C5=,cis	0.6252	0.4244	0.3337	0.2847	0.2615
4m2C5=,trans	2.2208	1.2662	1.0008	0.8463	0.7268
2m1C5=	3.0623	1.6369	1.3069	1.0740	0.8683
2m2C5=	9.0565	5.4915	4.4113	3.8974	3.4562
3-methyl-Pentenes					
3m1C5=	0.4183	0.2303	0.0000	0.0000	0.0000
2e1C4=	0.8820	0.3422	0.2980	0.1760	0.0000
3m2C5=,cis	3.3610	1.6931	1.3012	1.1104	0.9432
3m2C5=,trans	5.5718	2.7477	2.0469	1.6330	1.3379
Hexenes					
1C6=	4.9906	5.6249	5.7975	5.9190	5.9661
3C6=	19.1274	22.4763	23.3176	23.8688	24.2129
2C6,trans	33.3736	39.1769	40.7903	41.6875	42.3224
2C6=,cis	15.1701	17.8568	18.6158	18.8131	19.2489
>C6=	0.7135	0.5487	0.4969	0.4602	0.4213
Total	100.00	100.00	100.00	100.00	100.00
Conversion	27.3	14.9	11.5	9.7	8.2
Conv. to C6's	26.6	14.3	11.0	9.3	7.8
Mass Bal.%	90	96	-	102	95

Table D.3 1-Hexene Isomerisation

Run No : 69 Date : 26 April 1994

Catalyst : H-ZSM-5

Mass Catalyst,g: 0.31

Mass Sand,g: 14.99

Pretreatment : calcined at 500C in air overnight

Feed : Pure 1-Hexene

Reaction Conditions : 250C, 5MPa

WHSV, g feed/g cat/hr: 8

Internal Standard : Propene

Sample No.	1	2	3	4
Time,min	68	130	206	353
Compound	Mass%	Mass%	Mass%	Mass%
cracked prods	1.0549	0.0000	0.0000	0.0376
2-methyl-Pentenes				
4m1C5=	0.4530	0.0000	0.2215	0.2862
4m2C5=,cis	0.7463	0.0000	0.5430	0.5044
4m2C5=,trans	2.8295	2.2569	1.7652	1.3667
2m1C5=	3.9186	3.3697	2.5297	1.8873
2m2C5=	11.0238	9.6037	7.4962	5.8061
3-methyl-Pentenes				
3m1C5=	0.4893	0.0000	0.0000	0.2638
2e1C4=	1.1133	0.5448	0.3833	0.3470
3m2C5=,cis	4.4389	3.4276	2.4243	1.8457
3m2C5=,trans	7.4966	5.9072	4.2352	2.9214
Hexenes				
1C6=	3.6717	4.7664	5.0966	5.4429
3C6=	14.9094	19.6653	21.1877	22.3416
2C6,trans	26.1306	34.3728	36.9233	38.8993
2C6=,cis	11.7602	15.6279	16.7599	17.6201
>C6=	9.9638	0.4579	0.4344	0.4303
Total	100.00	100.00	100.00	100.00
Conversion	43.5	25.6	20.0	15.7
Conv. to C6's	33.6	25.1	19.6	15.3
Mass Bal.%	91	104	98	90

Table D.4 4-methyl-1-Pentene Isomerisation

Run No : 71 Date : 5 April 1994

Catalyst : H-ZSM-5

Mass Catalyst,g: 0.3

Mass Sand,g: 15.06

Pretreatment : calcined at 500C in air overnight

Feed : Pure 4-methyl-1-Pentene

Reaction Conditions : 250C, 5MPa

WHSV, g feed/g cat/hr: 9

Internal Standard : Dimethyl Ether

Sample No.	1	2	3	4	5
Time,min	69	124	193	255	319
Compound	Mass%	Mass%	Mass%	Mass%	Mass%
cracked prods	4.3872	3.2272	2.2213	1.8600	1.6324
2-methyl-Pentenes					
4m1C5=	1.1779	1.1607	1.1431	1.2151	1.2568
4m2C5=,cis	1.6927	1.7052	1.7864	1.8470	1.8709
4m2C5=,trans	6.0014	6.1037	6.3090	6.6116	6.7383
2m1C5=	9.2534	9.7124	9.9179	10.4800	10.7069
2m2C5=	23.6145	24.4011	25.1254	26.3323	26.9078
3-methyl-Pentenes					
3m1C5=	1.3933	1.3696	1.3399	1.4187	1.3927
2e1C4=	2.8061	2.7774	2.7776	2.8372	2.8560
3m2C5=,cis	13.1579	13.5610	13.5772	13.7000	13.6060
3m2C5=,trans	22.1925	23.0486	23.0104	23.1814	22.8703
Hexenes					
1C6=	0.0000	0.0000	0.0000	0.0000	0.0000
3C6=	2.0795	2.0409	1.9571	1.9068	1.9494
2C6,trans	3.4718	3.4755	3.3086	3.2274	3.3028
2C6=,cis	1.5948	1.6435	1.5433	1.4681	1.5496
2,3-dm-Butenes					
2,3-dm-1-C4=	1.5085	1.1638	0.9389	0.8149	0.7490
2,3-dm-2-C4=	3.4026	2.7188	2.1236	1.848	1.6452
>C6=	2.2661	1.8907	2.9201	1.2514	0.9662
Total	100.00	100.00	100.00	100.00	100.00
Conversion	58.3	56.9	55.7	53.5	52.5
Conv. to C6's	51.6	51.8	50.6	50.4	49.9
Mass Bal.%	97	99	103	104	105

Table D.5 4-methyl-1-Pentene Isomerisation

Run No : 72 Date : 11 April 1994

Catalyst : H-ZSM-5

Mass Catalyst,g: 0.3

Mass Sand,g: 15.06

Pretreatment : calcined at 500C in air overnight

Feed : Pure 4-methyl-1-Pentene

Reaction Conditions : 250C, 5MPa

WHSV, g feed/g cat/hr: 17

Internal Standard : Dimethyl Ether

Sample No.	1	2	3	4
Time,min	80	138	198	311
Compound	Mass%	Mass%	Mass%	Mass%
cracked prods	2.1786	1.4780	1.0915	0.9318
2-methyl-Pentenes				
4m1C5=	1.2368	1.2408	1.2289	1.3082
4m2C5=,cis	1.8490	1.8899	1.8950	1.9963
4m2C5=,trans	6.6895	6.8791	7.0618	7.4743
2m1C5=	10.3604	10.7272	10.9663	11.6557
2m2C5=	26.1020	27.4965	28.3787	29.8889
3-methyl-Pentenes				
3m1C5=	1.4184	1.3924	1.3748	1.3612
2e1C4=	2.8302	2.7578	2.7113	2.6034
3m2C5=,cis	13.9684	13.6862	13.5011	12.8851
3m2C5=,trans	23.2630	23.1110	22.9165	21.7969
Hexenes				
1C6=	0.0000	0.0000	0.0000	0.0000
3C6=	1.7676	1.7245	1.7617	1.7195
2C6,trans	3.0153	2.9632	3.0164	2.9345
2C6=,cis	1.4558	1.3944	1.4370	1.4078
2,3-dm-Butenes				
2,3-dm-1-C4=	0.9065	0.6892	0.6023	0.4947
2,3-dm-2-C4=	2.0077	1.5696	1.4427	1.163
>C6=	0.9509	1.0000	0.6139	0.3787
Total	100.00	100.00	100.00	100.00
Conversion	53.8	51.8	50.5	47.7
Conv. to C6's	50.6	49.3	48.8	46.4
Mass Bal,%	94	93	106	101

Table D.6 4-methyl-1-Pentene Isomerisation

Run No : 75 Date : 27 April 1994

Catalyst : H-ZSM-5

Mass Catalyst,g: 0.5

Mass Sand,g: 15.06

Pretreatment : calcined at 500C in air overnight

Feed : Pure 4-methyl-1-Pentene

Reaction Conditions : 250C, 5MPa

WHSV, g feed/g cat/hr: 8

Internal Standard : Dimethyl Ether

Sample No	1	2	3	4	5
Time,min	63	130	192	250	306
Compound	Mass%	Mass%	Mass%	Mass%	Mass%
cracked pr	8.2829	5.5532	4.5209	4.3093	3.9831
2-methyl-P					
4m1C5=	1.1136	1.0462	1.0357	1.0310	1.0478
4m2C5=,ci	1.4363	1.5237	1.5779	1.6055	1.5890
4m2C5=,tr	5.1925	5.4881	5.6826	5.7180	5.6856
2m1C5=	8.3362	8.7727	9.1396	9.1584	9.2697
2m2C5=	20.5630	21.4073	22.2649	22.5395	22.7118
3-methyl-P					
3m1C5=	1.1558	1.2608	1.2413	1.3177	1.2680
2e1C4=	2.6347	2.5867	2.6172	2.6652	2.7138
3m2C5=,ci	11.3422	11.8077	12.3211	12.5852	12.5838
3m2C5=,tr	19.2709	20.2165	21.2220	21.2413	21.4354
Hexenes					
1C6=	0.0000	0.0000	0.0000	0.0000	0.0000
3C6=	2.2258	2.1974	2.2646	2.3624	2.3562
2C6,trans	3.7005	3.8053	3.9711	4.0919	4.1358
2C6=,cis	1.6820	1.7249	1.8436	1.9128	1.9028
2,3-dm-But					
2,3-dm-1-C	2.468015	1.978	1.7419	1.6559	1.5511
2,3-dm-2-C	5.50439	4.5128	3.9761	3.7156	3.4929
>C6=	5.0912	6.1198	4.5797	4.0895	4.2730
Total	100.00	100.00	100.00	100.00	100.00
Conversion	63.4	61.8	60.3	59.9	59.7
Conv. to C	50.0	50.1	51.2	51.5	51.4
Mass Bal.%	90	95	92	95	94

Table D.7 4-methyl-1-Pentene Isomerisation

Run No : 76 Date : 8 June 1994

Catalyst : H-ZSM-5

Mass Catalyst,g: 0.1

Mass Sand,g: 5

Pretreatment : calcined at 500C in air overnight

Feed : Pure 4-methyl-1-Pentene

Reaction Conditions : 250C, 5MPa

WHSV, g feed/g cat/hr: 56

Internal Standard : Dimethyl Ether

Sample No.	1	2	3	4	5	6
Time,min	66	114	165	212	259	311
Compound	Mass%	Mass%	Mass%	Mass%	Mass%	Mass%
cracked prods	0.9228	0.4720	0.3235	0.2831	0.1855	0.1727
2-methyl-Pentenes						
4m1C5=	1.4230	1.4622	1.5564	1.6494	1.7948	1.9281
4m2C5=,cis	1.9873	2.0980	2.2476	2.3617	2.4665	2.5990
4m2C5=,trans	7.4152	7.8610	8.3040	8.6163	8.9253	9.2359
2m1C5=	11.1688	12.1274	12.8689	13.5253	13.8912	14.3198
2m2C5=	28.8830	31.2715	33.1545	34.6706	35.9250	36.7557
3-methyl-Pentenes						
3m1C5=	1.4475	1.3841	1.3885	1.3287	1.2911	1.2987
2e1C4=	2.7541	2.5844	2.3990	2.2759	2.1327	2.0268
3m2C5=,cis	13.5955	12.6446	11.7979	11.1155	10.4644	9.7863
3m2C5=,trans	22.8394	21.3958	20.1133	18.6359	17.5987	16.8729
Hexenes						
1C6=	0.0000	0.0000	0.0000	0.0000	0.0000	0.0000
3C6=	1.5107	1.4125	1.2767	1.2547	1.2232	1.0790
2C6,trans	2.5330	2.3583	2.2076	2.1268	2.0475	1.9252
2C6=,cis	1.1725	1.1454	0.9824	0.9606	1.0170	0.9429
2,3-dm-Butenes						
2,3-dm-1-C4=	0.6605	0.4766	0.4107	0.354	0.3015	0.2763
2,3-dm-2-C4=	1.4602	1.1236	0.9688	0.8416	0.7090	0.6723
>C6=	0.2269	0.1824	0.0000	0.0000	0.0000	0.1086
Total	100.00	100.00	100.00	100.00	99.97	100.00
Conversion	49.1	45.2	41.9	39.2	37.0	35.2
Conv. to C6's	48.0	44.5	41.5	38.9	36.8	34.9
Mass Bal.%	84	117	98	99	95	97

Method of Eigenvectors and Eigenvalues (Kreyszig (1979))

Consider the following relationship, where **A** is a square matrix and λ a number :

$$\boldsymbol{Ax} = \lambda \boldsymbol{x} \tag{A.1}$$

The value of λ for which $(\mathbf{A} - \lambda\mathbf{I})\mathbf{x} = 0$ is called an eigenvalue of the matrix **A**. The solution vector x (non-zero), which corresponds to a particular λ, is called the eigenvector of **A**. By Cramer's theorem the set of differential equations has a solution if and only if :

$$\det(\boldsymbol{A}-\lambda\boldsymbol{I}) = 0 \tag{A.2}$$

By evaluating det $(\mathbf{A} - \lambda\mathbf{I})$ the characteristic polynomial is obtained. The roots of this polynomial are the eigenvalues of **A**.

A set of first order, linear, differential equations can be written as :

$$\boldsymbol{y'} = \boldsymbol{Ay} + \boldsymbol{h} \tag{A.3}$$

If λ_i is an eigenvalue with its corresponding eigenvector $\mathbf{x}_i$ then the following can be written

$$(\boldsymbol{Ax_1}\ \boldsymbol{Ax_2}\ \ldots\ \boldsymbol{Ax_n}) = (\lambda_1 x_1\ \lambda_2 x_2\ \ldots\ \lambda_n x_n). \tag{A.4}$$

Let

$$\boldsymbol{X} = (x_1\ \ldots\ x_n) \tag{A.5}$$

(A.5) can then be rewritten as :

$$\boldsymbol{AX} = \boldsymbol{DX} \tag{A.6}$$

Now set

$$\boldsymbol{y} = \boldsymbol{X}\boldsymbol{z} \tag{A.7}$$

and thus

$$\boldsymbol{y}' = \boldsymbol{X}\boldsymbol{z}' \tag{A.8}$$

Substituting into (A.3) above :

$$\boldsymbol{X}\boldsymbol{z}' = \boldsymbol{A}\boldsymbol{X}\boldsymbol{z} + \boldsymbol{h} \tag{A.9}$$

Solving for z′ :

$$\boldsymbol{z}' = \boldsymbol{X}^{-1}\boldsymbol{A}\boldsymbol{X}\boldsymbol{z} + \boldsymbol{X}^{-1}\boldsymbol{h} \tag{A.10}$$

which is the same as

$$\boldsymbol{z}' = \boldsymbol{D}\boldsymbol{z} + \boldsymbol{X}^{-1}\boldsymbol{h} \tag{A.11}$$

or for each component :

$$z_i' - \lambda_i z_i = r_i(t) \tag{A.12}$$

The solution of (A.12) is given by :

$$z_i(t) = e^{\lambda_i t}\left(\int e^{-\lambda_i t} r_i(t)\,dt + c_i\right) \tag{A.13}$$

Therefore, since both **z** and **X** are known **y** can be determined from (A.7). The constant of integration, c_i, is solved for using initial conditions.

APPENDIX E

Table E.1 - Propene Oligomerisation

Run No : 90
Catalyst : H-ZSM-5
Mass Catalyst,g : 0.182
Mass Sand,g : 9.1
Pretreatment : calcined at 500C in air overnight
Feed : 88 mol% N2, 12 mol% C3=
N2 flow, g/min : 0.583
C3= flow, g/min : 0.119
Molar density of feed mol/cm3 : 0.00120
Z Factor, feed : 1
Conc C3=, feed, mol/cm3 : 1.432e-4
Reaction Conditions : 250C, 5MPa
Internal Standard : Methane

Sample No.	1 (Mass Balance Sample)			2			3			4			5		
Bed Temp,C	251			252			252			252			252		
Time,min	95			142			185			231			278		
Compound (Hydrogenated)	Mass%	Avg Conc mol/cm3	Rate mol/hr/g	Mass%	Avg Conc mol/cm3	Rate mol/hr/g	Mass%	Avg Conc mol/cm3	Rate mol/hr/g	Mass%	Avg Conc mol/cm3	Rate mol/hr/g	Mass%	Avg Conc mol/cm3	Rate mol/hr/g
CH4	7.1272			43.2635			44.9873			47.5812			46.9778		
C3	81.8902	1.35E-04	-1.13E-01		1.37E-04	-9.01E-02		1.37E-04	-8.40E-02		1.38E-04	-7.57E-02		1.38E-04	-7.75E-02
C4	1.1146	6.48E-07	8.38E-03	4.9876	4.58E-07	5.94E-03	4.8743	4.30E-07	5.58E-03	5.4610	4.56E-07	5.91E-03	4.6717	3.95E-07	5.12E-03
C5	0.4215	1.98E-07	2.53E-03	2.9373	2.16E-07	2.80E-03	2.8013	1.98E-07	2.57E-03	1.7192	1.15E-07	1.49E-03	2.5445	1.72E-07	2.23E-03
2,3-dm-C4	0.3969	1.54E-07	1.99E-03	1.8699	1.15E-07	1.48E-03	1.9002	1.12E-07	1.45E-03	1.8759	1.04E-07	1.35E-03	1.7589	9.91E-08	1.29E-03
2-m-C5	1.6051	6.22E-07	8.04E-03	9.4539	5.79E-07	7.50E-03	10.1213	5.98E-07	7.73E-03	9.8871	5.50E-07	7.14E-03	9.9810	5.62E-07	7.30E-03
3-m-C5	1.2574	4.87E-07	6.30E-03	6.9671	4.27E-07	5.53E-03	7.2783	4.28E-07	5.56E-03	7.2250	4.02E-07	5.21E-03	7.1434	4.03E-07	5.22E-03
C6	0.5903	2.29E-07	2.96E-03	3.2428	1.99E-07	2.57E-03	3.3729	1.99E-07	2.57E-03	3.3166	1.84E-07	2.39E-03	3.2955	1.86E-07	2.41E-03
C7-C8	0.9431	2.92E-07	3.78E-03	4.1434	2.03E-07	2.63E-03	3.7697	1.78E-07	2.30E-03	3.5164	1.58E-07	2.03E-03	3.6151	1.63E-07	2.11E-03
2,3,5-tm-C6	0.0253	6.54E-09	8.46E-05	0.1017	4.15E-09	5.38E-05	0.0789	3.09E-09	4.01E-05	0.0786	2.92E-09	3.78E-05	0.0781	2.93E-09	3.81E-05
2,2-dm-C7	0.0602	1.55E-08	2.01E-04	0.2660	1.09E-08	1.41E-04	0.2692	1.08E-08	1.37E-04	0.2281	8.46E-09	1.10E-04	0.2352	8.84E-09	1.15E-04
2,4-dm-C7	0.3492	9.02E-08	1.17E-03	1.6892	6.90E-08	8.94E-04	1.7133	6.72E-08	8.72E-04	1.5913	5.90E-08	7.66E-04	1.6461	6.18E-08	8.02E-04
4,4-dm-C7	0.0162	4.18E-09	5.40E-05	0.0725	2.96E-09	3.84E-05	0.0758	2.98E-09	3.86E-05	0.0714	2.65E-09	3.44E-05	0.0656	2.48E-09	3.19E-05
2,6-dm-C7	0.1343	3.47E-08	4.49E-04	0.5464	2.23E-08	2.89E-04	0.5324	2.09E-08	2.71E-04	0.4751	1.76E-08	2.29E-04	0.4863	1.83E-08	2.37E-04
2,5-dm-C7	0.5266	1.36E-07	1.76E-03	3.0650	1.25E-07	1.62E-03	2.9731	1.17E-07	1.51E-03	2.8011	1.04E-07	1.35E-03	2.8844	1.08E-07	1.41E-03
3,5-dm-C7	0.1377	3.56E-08	4.60E-04	0.0000	0.00E+00	0.00E+00	0.0000	0.00E+00	0.00E+00	0.0000	0.00E+00	0.00E+00	0.0000	0.00E+00	0.00E+00
3-e-2-m-C6	0.0849	2.19E-08	2.84E-04	0.3686	1.50E-08	1.95E-04	0.3531	1.39E-08	1.80E-04	0.2597	9.63E-09	1.25E-04	0.2617	9.83E-09	1.28E-04
2,3,4-tm-C6	0.0138	3.57E-09	4.62E-05	0.0511	2.08E-09	2.70E-05	0.0462	1.81E-09	2.35E-05	0.0000	0.00E+00	0.00E+00	0.0000	0.00E+00	0.00E+00
3-e-3-m-C6	0.0000	0.00E+00	0.00E+00	0.0000	0.00E+00	0.00E+00	0.0000	0.00E+00	0.00E+00	0.0000	0.00E+00	0.00E+00	0.0000	0.00E+00	0.00E+00
2,3-dm-C7	0.2676	6.91E-08	8.94E-04	1.1987	4.89E-08	6.34E-04	1.1568	4.54E-08	5.89E-04	1.0719	3.97E-08	5.16E-04	1.0638	4.00E-08	5.18E-04
3,4-dm-C7	0.2527	6.53E-08	8.44E-04	1.1110	4.54E-08	5.88E-04	1.0779	4.23E-08	5.49E-04	1.0049	3.73E-08	4.84E-04	0.9819	3.69E-08	4.78E-04
4-e-C7	0.0575	1.48E-08	1.92E-04	0.2574	1.05E-08	1.36E-04	0.2290	8.99E-09	1.17E-04	0.2420	8.97E-09	1.16E-04	0.2217	8.33E-09	1.08E-04
4-m-C8	0.3009	7.77E-08	1.01E-03	2.7627	1.13E-07	1.46E-03	1.6922	6.64E-08	8.61E-04	1.6317	6.05E-08	7.85E-04	1.8509	6.95E-08	9.02E-04
2-m-C8	0.2153	5.56E-08	7.19E-04	0.0000	0.00E+00	0.00E+00	1.1025	4.33E-08	5.61E-04	1.1810	4.38E-08	5.68E-04	1.0079	3.79E-08	4.91E-04
3-m-C8	0.3884	1.00E-07	1.30E-03	2.0897	8.45E-08	1.10E-03	2.0775	8.15E-08	1.06E-03	2.0813	7.72E-08	1.00E-03	2.1011	7.89E-08	1.02E-03
C9	0.0912	2.35E-08	3.05E-04	0.4867	1.99E-08	2.58E-04	0.4757	1.87E-08	2.42E-04	0.4767	1.77E-08	2.29E-04	0.4912	1.85E-08	2.39E-04
C12	1.7319	3.355E-07	4.340E-03	9.0878	2.783E-07	3.607E-03	7.0407	2.072E-07	2.687E-03	6.2228	1.731E-07	2.246E-03	6.6363	1.870E-07	2.426E-03
Total	100.00			100.00			100.00			100.00			100.00		
Conversion	12.1			9.6			9.0			8.1			8.3		
	Mass Balance: 96%														

Table E.2 - Propene Oligomerisation

Run No : 91

Catalyst : H-ZSM-5

Mass Catalyst,g : 0.182

Mass Sand,g : 9.1

Pretreatment : calcined at 500C in air overnight

Feed : 77 mol% N2, 23 mol% C3=

N2 flow, g/min : 0.505

C3= flow, g/min : 0.222

Molar density of feed mol/cm3 : 0.00120

Z Factor, feed : 1

Conc C3=, feed, mol/cm3 : 2.710e-4

Reaction Conditions : 250C, 5MPa

Internal Standard : Methane

Sample No.	1 (Mass Balance Sample)			2			3			4			5		
Bed Temp,C	250			250			250			250			250		
Time,min	95			135			177			219			263		
Compound	Mass%	Avg Conc	Rate	Mass%	Avg Conc	Rate	Mass%	Avg Conc	Rate	Mass%	Avg Conc	Rate	Mass%	Avg Conc	Rate
(Hydrogenated		mol/cm3	mol/hr/g		mol/cm3	mol/hr/g		mol/cm3	mol/hr/g		mol/cm3	mol/hr/g		mol/cm3	mol/hr/g
CH4	3.5502			36.5005			36.2587			38.6593			39.2842		
C3	88.4039	2.61E-04	-1.41E-01		2.63E-04	-1.19E-01		2.63E-04	-1.21E-01		2.63E-04	-1.09E-01		2.64E-04	-1.06E-01
C4	0.3452	3.68E-07	4.69E-03	3.9647	4.39E-07	5.60E-03	4.9422	5.51E-07	7.02E-03	5.0336	5.26E-07	6.71E-03	5.4182	5.57E-07	7.10E-03
C5	0.3696	3.16E-07	4.02E-03	2.5591	2.27E-07	2.89E-03	2.4179	2.16E-07	2.75E-03	2.2304	1.86E-07	2.38E-03	2.1166	1.74E-07	2.22E-03
2,3-dm-C4	0.3745	2.66E-07	3.39E-03	2.5919	1.91E-07	2.44E-03	2.4779	1.84E-07	2.35E-03	2.3301	1.62E-07	2.07E-03	2.2742	1.56E-07	1.99E-03
2-m-C5	1.7891	1.27E-06	1.62E-02	15.0200	1.11E-06	1.41E-02	15.9231	1.18E-06	1.51E-02	16.1742	1.13E-06	1.44E-02	16.7177	1.14E-06	1.46E-02
3-m-C5	1.1907	8.47E-07	1.08E-02	9.2774	6.85E-07	8.73E-03	9.2902	6.90E-07	8.80E-03	9.1256	6.35E-07	8.11E-03	9.1010	6.23E-07	7.96E-03
C6	0.4402	3.13E-07	3.99E-03	3.6581	2.70E-07	3.44E-03	3.7577	2.79E-07	3.56E-03	3.7768	2.63E-07	3.35E-03	3.8050	2.61E-07	3.33E-03
C7-C8	0.4462	2.54E-07	3.23E-03	3.1482	1.86E-07	2.37E-03	2.7217	1.62E-07	2.06E-03	2.4548	1.37E-07	1.74E-03	2.2870	1.25E-07	1.60E-03
2,3,5-tm-C6	0.0164	7.78E-09	9.91E-05	0.0969	4.76E-09	6.08E-05	0.0848	4.20E-09	5.35E-05	0.0690	3.20E-09	4.09E-05	0.0495	2.26E-09	2.88E-05
2,2-dm-C7	0.0460	2.18E-08	2.78E-04	0.2826	1.39E-08	1.77E-04	0.2599	1.29E-08	1.64E-04	0.2180	1.01E-08	1.29E-04	0.1942	8.87E-09	1.13E-04
2,4-dm-C7	0.2610	1.24E-07	1.58E-03	2.1573	1.06E-07	1.35E-03	2.0391	1.01E-07	1.29E-03	1.9095	8.86E-08	1.13E-03	1.7641	8.05E-08	1.03E-03
4,4-dm-C7	0.0000	0.00E+00	0.00E+00	0.0857	4.21E-09	5.37E-05	0.0842	4.17E-09	5.31E-05	0.0626	2.91E-09	3.71E-05	0.0715	3.26E-09	4.17E-05
2,6-dm-C7	0.0691	3.28E-08	4.17E-04	0.4435	2.18E-08	2.78E-04	0.4053	2.01E-08	2.56E-04	0.3586	1.66E-08	2.12E-04	0.3170	1.45E-08	1.85E-04
2,5-dm-C7	0.3242	1.54E-07	1.96E-03	2.4766	1.22E-07	1.55E-03	2.3201	1.15E-07	1.46E-03	2.1933	1.02E-07	1.30E-03	1.9462	8.88E-08	1.13E-03
3,5-dm-C7	0.1252	5.94E-08	7.56E-04	0.7893	3.88E-08	4.95E-04	0.7432	3.66E-08	4.69E-04	0.5964	2.77E-08	3.53E-04	0.6341	2.89E-08	3.70E-04
3-e-2-m-C6	0.0760	3.60E-08	4.59E-04	0.4715	2.32E-08	2.96E-04	0.4122	2.04E-08	2.60E-04	0.3644	1.69E-08	2.16E-04	0.3286	1.50E-08	1.92E-04
2,3,4-tm-C6	0.0129	6.14E-09	7.82E-05	0.0616	3.03E-09	3.87E-05	0.0477	2.36E-09	3.01E-05	0.0626	2.91E-09	3.71E-05	0.0519	2.37E-09	3.03E-05
3-e-3-m-C6	0.0000	0.00E+00	0.00E+00	0.0000	0.00E+00	0.00E+00	0.0000	0.00E+00	0.00E+00	0.0000	0.00E+00	0.00E+00	0.0000	0.00E+00	0.00E+00
2,3-dm-C7	0.2271	1.08E-07	1.37E-03	1.5129	7.44E-08	9.49E-04	1.3602	6.74E-08	8.59E-04	1.2133	5.63E-08	7.19E-04	1.1362	5.19E-08	6.62E-04
3,4-dm-C7	0.2291	1.09E-07	1.38E-03	1.5153	7.45E-08	9.50E-04	1.3809	6.74E-08	8.59E-04	1.2261	5.69E-08	7.26E-04	1.1172	5.10E-08	6.51E-04
4-e-C7	0.0381	1.81E-08	2.30E-04	0.2401	1.18E-08	1.51E-04	0.1974	9.78E-09	1.25E-04	0.1681	7.80E-09	9.96E-05	0.1381	6.30E-09	8.05E-05
4-m-C8	0.2581	1.22E-07	1.56E-03	2.1396	1.05E-07	1.34E-03	2.2192	1.10E-07	1.40E-03	3.3159	1.54E-07	1.96E-03	3.2998	1.51E-07	1.92E-03
2-m-C8	0.1613	7.65E-08	9.74E-04	1.3632	6.71E-08	8.55E-04	1.2977	6.43E-08	8.19E-04	0.0000	0.00E+00	0.00E+00	0.0000	0.00E+00	0.00E+00
3-m-C8	0.3096	1.47E-07	1.87E-03	2.5567	1.26E-07	1.60E-03	2.4952	1.24E-07	1.58E-03	2.3269	1.08E-07	1.38E-03	2.2730	1.04E-07	1.32E-03
C9	0.0747	3.54E-08	4.51E-04	0.5379	2.65E-08	3.37E-04	0.5520	2.73E-08	3.49E-04	0.5057	2.35E-08	2.99E-04	0.4930	2.25E-08	2.87E-04
C12	0.8616	3.065E-07	3.903E-03	6.54942486	2.416E-07	3.081E-03	6.33149534	2.351E-07	2.998E-03	5.62431278	1.957E-07	2.498E-03	5.18181874	1.774E-07	2.265E-03
Total	100.00			100.00			100.00			100.00			100.00		
Conversion	8.1			6.9			6.9			6.3			6.1		
	Mass Balance: 107%														

Table E.3 - Propene Oligomerisation

Run No : 93

Catalyst : H-ZSM-5

Mass Catalyst,g : 0.131

Mass Sand,g : 6.5

Pretreatment : calcined at 500C in air overnight

Feed : 70 mol% N2, 30 mol% C3=

N2 flow, g/min : 0.337

C3= flow, g/min : 0.216

Molar density of feed mol/cm3 : 0.00115

Z Factor, feed : 1

Conc C3=, feed, mol/cm3 : 3.448e-4

Reaction Conditions : 250C, 5MPa

Internal Standard : Methane

Sample No.	1			2			3			4			5			6 (Mass Balance Sample)		
Bed Temp,C	250			250			250			251			251			251		
Time,min	95			139			181			222			268			310		
Compound (Hydrog.)	Mass%	Avg Conc mol/cm3	Rate mol/hr/g	Mass%	Avg Conc mol/cm3	Rate mol/hr/g	Mass%	Avg Conc mol/cm3	Rate mol/hr/g	Mass%	Avg Conc mol/cm3	Rate mol/hr/g	Mass%	Avg Conc mol/cm3	Rate mol/hr/g	Mass%	Avg Conc mol/cm3	Rate mol/hr/g
CH4	51.8539			57.1564			60.1003			60.3385			61.4858			7.2237		
C3		3.337E-04	-1.772E-01		3.359E-04	-1.431E-01		3.369E-04	-1.267E-01		3.370E-04	-1.254E-01		3.373E-04	-1.195E-01	88.8593	3.390E-04	-9.197E-02
C4	5.7893	1.184E-06	1.598E-02	2.8885	5.346E-07	7.233E-03	2.8157	4.950E-07	6.706E-03	2.8069	4.914E-07	6.658E-03	2.8515	4.897E-07	6.638E-03	0.1379	1.939E-07	2.635E-03
C5	1.6494	2.698E-07	3.642E-03	1.4368	2.127E-07	2.878E-03	1.2326	1.734E-07	2.348E-03	1.1937	1.672E-07	2.265E-03	1.1008	1.512E-07	2.050E-03	0.1131	1.272E-07	1.729E-03
2,3-dm-C4	2.0641	2.813E-07	3.798E-03	1.8007	2.222E-07	3.006E-03	1.6094	1.886E-07	2.555E-03	1.5841	1.849E-07	2.505E-03	1.5124	1.732E-07	2.347E-03	0.1650	1.546E-07	2.101E-03
2-m-C5	11.7893	1.607E-06	2.169E-02	12.6713	1.563E-06	2.115E-02	12.8355	1.504E-06	2.038E-02	13.0846	1.527E-06	2.069E-02	13.3825	1.532E-06	2.077E-02	1.5394	1.443E-06	1.961E-02
3-m-C5	6.7200	9.159E-07	1.237E-02	6.4295	7.933E-07	1.073E-02	6.1193	7.172E-07	9.716E-03	6.2088	7.247E-07	9.819E-03	6.1129	6.999E-07	9.487E-03	0.6798	6.373E-07	8.659E-03
C6	2.2085	3.010E-07	4.064E-03	2.4160	2.981E-07	4.033E-03	2.4395	2.859E-07	3.873E-03	2.5112	2.931E-07	3.971E-03	2.5318	2.899E-07	3.929E-03	0.2928	2.745E-07	3.729E-03
C7-C8	2.2588	2.463E-07	3.325E-03	1.5159	1.496E-07	2.025E-03	1.0760	1.009E-07	1.367E-03	1.1461	1.070E-07	1.450E-03	0.9281	8.500E-08	1.152E-03	0.0620	4.646E-06	6.313E-04
2,3,5-tm-C6	0.0908	8.250E-09	1.114E-04	0.0000	0.000E+00	0.000E+00	0.0000	0.000E+00	0.000E+00	0.0000	0.000E+00	0.000E+00	0.0000	0.000E+00	0.000E+00			
2,2-dm-C7	0.2341	2.127E-08	2.872E-04	0.1825	1.501E-08	2.031E-04	0.1446	1.130E-08	1.530E-04	0.1365	1.062E-08	1.439E-04	0.1192	9.095E-09	1.233E-04			
2,4-dm-C7	1.5847	1.440E-07	1.944E-03	1.3990	1.151E-07	1.557E-03	1.2250	9.571E-08	1.297E-03	1.1758	9.149E-08	1.240E-03	1.0888	8.310E-08	1.126E-03			
4,4-dm-C7	0.0894	8.127E-09	1.097E-04	0.0000	0.000E+00	0.000E+00	0.0000	0.000E+00	0.000E+00	0.0000	0.000E+00	0.000E+00	0.0000	0.000E+00	0.000E+00			
2,6-dm-C7	0.3003	2.729E-08	3.684E-04	0.2249	1.850E-08	2.503E-04	0.1982	1.549E-08	2.098E-04	0.1708	1.329E-08	1.801E-04	0.1454	1.110E-08	1.504E-04			
2,5-dm-C7	2.3176	2.106E-07	2.843E-03	1.4523	1.195E-07	1.616E-03	1.2814	1.001E-07	1.356E-03	1.2138	9.445E-08	1.280E-03	1.1183	8.535E-08	1.157E-03			
3,5-dm-C7	0.0000	0.000E+00	0.000E+00	0.5217	4.291E-08	5.806E-04	0.4425	3.457E-08	4.683E-04	0.4136	3.218E-08	4.361E-04	0.3711	2.833E-08	3.840E-04			
3-e-2-m-C6	0.4328	3.932E-08	5.309E-04	0.2606	2.143E-08	2.900E-04	0.2103	1.643E-08	2.226E-04	0.1952	1.519E-08	2.058E-04	0.1755	1.339E-08	1.815E-04			
2,3,4-tm-C6	0.0840	7.636E-09	1.031E-04	0.0000	0.000E+00	0.000E+00	0.0000	0.000E+00	0.000E+00	0.0000	0.000E+00	0.000E+00	0.0000	0.000E+00	0.000E+00			
3-e-3-m-C6	0.0293	2.661E-09	3.593E-05	0.0000	0.000E+00	0.000E+00	0.0000	0.000E+00	0.000E+00	0.0000	0.000E+00	0.000E+00	0.0000	0.000E+00	0.000E+00			
2,3-dm-C7	1.1898	1.081E-07	1.460E-03	0.9177	7.549E-08	1.021E-03	0.7661	5.986E-08	8.109E-04	0.7071	5.503E-08	7.455E-04	0.6444	4.919E-08	6.667E-04			
3,4-dm-C7	1.3339	1.212E-07	1.636E-03	0.9658	7.944E-08	1.075E-03	0.8028	6.272E-08	8.497E-04	0.7352	5.721E-08	7.751E-04	0.6772	5.169E-08	7.006E-04			
4-e-C7	0.1602	1.455E-08	1.965E-04	0.1075	8.846E-09	1.197E-04	0.0827	6.461E-09	8.752E-05	0.0714	5.556E-09	7.528E-05	0.0656	5.006E-09	6.786E-05			
4-m-C8	2.3775	2.160E-07	2.917E-03	1.5226	1.252E-07	1.695E-03	1.4637	1.144E-07	1.549E-03	1.4138	1.100E-07	1.490E-03	1.3927	1.063E-07	1.441E-03			
2-m-C8	0.0000	0.000E+00	0.000E+00	0.8763	7.209E-08	9.753E-04	0.8039	6.281E-08	8.509E-04	0.8039	6.256E-08	8.476E-04	0.7455	5.690E-08	7.713E-04			
3-m-C8	1.7149	1.558E-07	2.104E-03	1.6596	1.365E-07	1.847E-03	1.5278	1.194E-07	1.617E-03	1.5079	1.173E-07	1.590E-03	1.4386	1.098E-07	1.488E-03			
C9	0.3740	3.398E-08	4.588E-04	0.3459	2.845E-08	3.849E-04	0.3149	2.460E-08	3.333E-04	0.3247	2.527E-08	3.424E-04	0.2864	2.186E-08	2.963E-04			
Total C9																0.9270	5.793E-07	7.871E-03
C12	3.3535	2.285E-07	3.085E-03	3.2489	2.004E-07	2.712E-03	2.5080	1.470E-07	1.991E-03	2.2563	1.317E-07	1.784E-03	1.8256	1.045E-07	1.417E-03	0	0.000E+00	0.000E+00
Total	100.00			100.00			100.00			100.00			100.00			100		
Conversion	7.5			6.1			5.4			5.3			5.1			3.9		
																Mass Balance: 104%		

Table E.4 - Propene Oligomerisation

Run No : 97

Catalyst : H-ZSM-5

Mass Catalyst,g : 0.071

Mass Sand,g : 3.5

Pretreatment : calcined at 500C in air overnight

Feed : 58 mol% N2, 42 mol% C3=

N2 flow, g/min : 0.168

C3= flow, g/min : 0.178

Molar density of feed mol/cm3 : 0.00116

Z Factor, feed : 0.992

Conc C3=, feed, mol/cm3 : 4.811e-4

Reaction Conditions : 250C, 5MPa

Internal Standard : Methane

Sample No.	1			2			3			4			5			6 (Mass Balance Sample)		
Bed Temp,C	252			254			254			256			256			256		
Time,min	95			146			199			243			289			339		
Compound (Hydrog.)	Mass%	Avg Conc mol/cm3	Rate mol/hr/g	Mass%	Avg Conc mol/cm3	Rate mol/hr/g	Mass%	Avg Conc mol/cm3	Rate mol/hr/g	Mass%	Avg Conc mol/cm3	Rate mol/hr/g	Mass%	Avg Conc mol/cm3	Rate mol/hr/g	Mass%	Avg Conc mol/cm3	Rate mol/hr/g
CH4	72.0094			73.7712			74.6250			73.9596			75.2338			11.6711		
C3		4.71E-04	-1.9E-01		4.72E-04	-1.704E-01		4.73E-04	-1.6E-01		4.72E-04	-1.7E-01		4.73E-04	-1.6E-01	85.1495	4.74E-04	-1.2E-01
C4	1.4422	4.88E-07	7.20E-03	1.2903	4.26E-07	6.289E-03	2.0560	6.71E-07	9.91E-03	2.0356	6.70E-07	9.90E-03	2.0691	6.69E-07	9.89E-03	0.0993	2.05E-07	3.03E-03
C5	0.9483	2.57E-07	3.79E-03	0.7940	2.10E-07	3.096E-03	0.6313	1.65E-07	2.43E-03	0.6837	1.80E-07	2.66E-03	0.6294	1.83E-07	2.41E-03	0.0801	1.32E-07	1.96E-03
2,3-dm-C4	1.4199	3.20E-07	4.73E-03	1.1799	2.60E-07	3.834E-03	1.0203	2.22E-07	3.28E-03	1.0713	2.35E-07	3.47E-03	0.9790	2.11E-07	3.12E-03	0.1487	2.04E-07	3.03E-03
2-m-C5	9.1358	2.06E-06	3.04E-02	9.4927	2.09E-06	3.084E-02	9.0181	1.96E-06	2.90E-02	9.6175	2.11E-06	3.12E-02	9.4453	2.04E-06	3.01E-02	1.4773	2.03E-06	3.01E-02
3-m-C5	4.3745	9.87E-07	1.46E-02	4.1080	9.04E-07	1.335E-02	3.7792	8.22E-07	1.21E-02	4.1170	9.03E-07	1.33E-02	3.8379	8.27E-07	1.22E-02	0.5707	7.84E-07	1.16E-02
C6	1.3308	3.00E-07	4.43E-03	1.5243	3.35E-07	4.953E-03	1.4967	3.25E-07	4.81E-03	1.6309	3.58E-07	5.29E-03	1.5653	3.37E-07	4.99E-03	0.2461	3.38E-07	5.01E-03
C7-C8	1.0708	1.93E-07	2.85E-03	0.7267	1.28E-07	1.889E-03	0.4510	7.85E-08	1.16E-03	0.5442	9.55E-08	1.41E-03	0.4326	7.46E-08	1.10E-03	0.0392	4.30E-08	6.38E-04
2,3,5-tm-C6	0.0568	8.55E-09	1.26E-04	0.0000	0.00E+00	0.000E+00	0.0000	0.00E+00	0.00E+00	0.0000	0.00E+00	0.00E+00	0.0000	0.00E+00	0.00E+00			
2,2-dm-C7	0.1529	2.30E-08	3.39E-04	0.0973	1.43E-08	2.107E-04	0.0763	1.11E-08	1.63E-04	0.0758	1.11E-08	1.64E-04	0.0708	1.02E-08	1.50E-04			
2,4-dm-C7	0.9490	1.43E-07	2.11E-03	0.8056	1.18E-07	1.745E-03	0.7333	1.06E-07	1.57E-03	0.7353	1.08E-07	1.59E-03	0.6712	9.65E-08	1.43E-03			
4,4-dm-C7	0.0622	9.36E-09	1.38E-04	0.0000	0.00E+00	0.000E+00	0.0000	0.00E+00	0.00E+00	0.0000	0.00E+00	0.00E+00	0.0000	0.00E+00	0.00E+00			
2,6-dm-C7	0.1621	2.44E-08	3.60E-04	0.1200	1.76E-08	2.599E-04	0.0000	0.00E+00	0.00E+00	0.0928	1.36E-08	2.01E-04	0.0804	1.16E-08	1.71E-04			
2,5-dm-C7	0.9279	1.40E-07	2.06E-03	1.1312	1.66E-07	2.450E-03	0.7399	1.07E-07	1.58E-03	0.7286	1.07E-07	1.57E-03	0.8846	1.27E-07	1.88E-03			
3,5-dm-C7	0.3480	5.24E-08	7.72E-04	0.0000	0.00E+00	0.000E+00	0.2511	3.64E-08	5.38E-04	0.2519	3.69E-08	5.44E-04	0.0000	0.00E+00	0.00E+00			
3-e-2-m-C6	0.2796	4.21E-08	6.20E-04	0.1610	2.36E-08	3.488E-04	0.1356	1.97E-08	2.90E-04	0.1237	1.81E-08	2.67E-04	0.1123	1.81E-08	2.38E-04			
2,3,4-tm-C6	0.0565	8.50E-09	1.25E-04	0.0000	0.00E+00	0.000E+00	0.0000	0.00E+00	0.00E+00	0.0000	0.00E+00	0.00E+00	0.0000	0.00E+00	0.00E+00			
3-e-3-m-C6	0.0000	0.00E+00	0.00E+00	0.0000	0.00E+00	0.000E+00	0.0000	0.00E+00	0.00E+00	0.0000	0.00E+00	0.00E+00	0.0000	0.00E+00	0.00E+00			
2,3-dm-C7	0.7259	1.09E-07	1.61E-03	0.5489	8.05E-08	1.189E-03	0.4776	6.92E-08	1.02E-03	0.4559	6.67E-08	9.85E-04	0.4048	5.82E-08	8.60E-04			
3,4-dm-C7	0.8615	1.30E-07	1.91E-03	0.6322	9.28E-08	1.369E-03	0.5716	8.29E-08	1.22E-03	0.5109	7.47E-08	1.10E-03	0.4437	6.38E-08	9.43E-04			
4-e-C7	0.0757	1.14E-08	1.68E-04	0.0482	7.08E-09	1.045E-04	0.0481	6.98E-09	1.03E-04	0.0000	0.00E+00	0.00E+00	0.0000	0.00E+00	0.00E+00			
4-m-C8	0.9586	1.44E-07	2.13E-03	0.9794	1.44E-07	2.121E-03	0.9702	1.41E-07	2.08E-03	0.9381	1.37E-07	2.03E-03	0.8262	1.19E-07	1.75E-03			
2-m-C8	0.5189	7.81E-08	1.15E-03	0.5309	7.79E-08	1.150E-03	0.5365	7.78E-08	1.15E-03	0.5038	7.37E-08	1.09E-03	0.5266	7.57E-08	1.12E-03			
3-m-C8	1.0305	1.55E-07	2.29E-03	1.0053	1.47E-07	2.178E-03	1.0160	1.47E-07	2.18E-03	0.9339	1.37E-07	2.02E-03	0.8780	1.26E-07	1.86E-03			
C9	0.2047	3.08E-08	4.54E-04	0.2013	2.95E-08	4.360E-04	0.2188	3.17E-08	4.68E-04	0.1903	2.78E-08	4.11E-04	0.1806	2.60E-08	3.84E-04			
Total C9																0.5179	4.74E-07	7.03E-03
C12	0.8976	1.01E-07	1.49E-03	0.8518	9.37E-08	1.384E-03	1.1474	1.25E-07	1.84E-03	0.7994	8.77E-08	1.30E-03	0.7284	7.85E-08	1.16E-03	0.0000	0.00E+00	0.00E+00
Total	100.00			100.00			100.00			100.00			100.00			100.00		
Conversion	5.2			4.7			4.5			4.7			4.4			3.5		
																Mass Balance: 101%		

Table E.5 - Propene Oligomerisation

Run No : 92

Catalyst : H-ZSM-5

Mass Catalyst,g : 0.131

Mass Sand,g : 6.5

Pretreatment : calcined at 500C in air overnight

Feed : 51 mol% N2, 49 mol% C3=

N2 flow, g/min : 0.241

C3= flow, g/min : 0.388

Molar density of feed mol/cm3 : 0.00117

Z Factor, feed : 0.982

Conc C3=, feed, mol/cm3 : 5.772e-4

Reaction Conditions : 250C, 5MPa

Internal Standard : Methane

Sample No.	1			2			3			4			5			6 (Mass Balance Sample)		
Bed Temp,C	252			252			252			252			252			252		
Time,min	95			137			181			234			297			392		
Compound (Hydrog.)	Mass%	Avg Conc mol/cm3	Rate mol/hr/g	Mass%	Avg Conc mol/cm3	Rate mol/hr/g	Mass%	Avg Conc mol/cm3	Rate mol/hr/g	Mass%	Avg Conc mol/cm3	Rate mol/hr/g	Mass%	Avg Conc mol/cm3	Rate mol/hr/g	Mass%	Avg Conc mol/cm3	Rate mol/hr/g
CH4	41.4124			47.4013			48.0821			51.0260			51.1835			5.2259		
C3		5.621E-04	-2.700E-01		5.653E-04	-2.118E-01		5.656E-04	-2.062E-01		5.669E-04	-1.832E-01		5.669E-04	-1.820E-01	91.0944	5.680E-04	-1.695E-01
C4	3.0960	8.225E-07	1.070E-02	2.9705	8.865E-07	8.970E-03	3.0985	7.058E-07	9.227E-03	3.0037	6.433E-07	8.425E-03	3.1320	6.686E-07	8.758E-03	0.1023	2.352E-07	3.080E-03
C5	1.7898	3.804E-07	4.949E-03	1.4466	2.674E-07	3.494E-03	1.3450	2.451E-07	3.204E-03	1.1611	1.989E-07	2.606E-03	1.1280	1.926E-07	2.524E-03	0.0831	1.530E-07	2.003E-03
2,3-dm-C4	2.8095	4.976E-07	6.474E-03	2.2802	3.513E-07	4.590E-03	2.1822	3.314E-07	4.332E-03	2.0018	2.858E-07	3.743E-03	1.9885	2.830E-07	3.707E-03	0.1628	2.497E-07	3.270E-03
2-m-C5	17.2309	3.052E-06	3.970E-02	17.1980	2.650E-06	3.462E-02	18.3082	2.780E-06	3.635E-02	18.3585	2.621E-06	3.433E-02	19.2803	2.744E-06	3.594E-02	1.7442	2.674E-06	3.502E-02
3-m-C5	8.6330	1.529E-06	1.989E-02	7.8530	1.210E-06	1.581E-02	7.9936	1.214E-06	1.587E-02	7.6059	1.086E-06	1.422E-02	7.7963	1.109E-06	1.453E-02	0.6612	1.014E-06	1.328E-02
C6	2.6907	4.766E-07	6.200E-03	2.8217	4.347E-07	5.680E-03	3.0636	4.652E-07	6.082E-03	3.0762	4.392E-07	5.753E-03	3.2516	4.627E-07	6.062E-03	0.2936	4.502E-07	5.896E-03
C7-C8	2.1490	3.045E-07	3.961E-03	1.5441	1.903E-07	2.487E-03	1.2272	1.491E-07	1.949E-03	0.9744	1.113E-07	1.458E-03	0.9105	1.037E-07	1.358E-03	0.0725	8.899E-08	1.165E-03
2,3,5-tm-C6	0.1115	1.317E-08	1.713E-04	0.0000	0.000E+00	0.000E+00	0.0000	0.000E+00	0.000E+00	0.0000	0.000E+00	0.000E+00	0.0000	0.000E+00	0.000E+00			
2,2-dm-C7	0.2739	3.234E-08	4.208E-04	0.2199	2.258E-08	2.951E-04	0.1936	1.960E-08	2.563E-04	0.1583	1.507E-08	1.973E-04	0.1346	1.277E-08	1.672E-04			
2,4-dm-C7	2.1069	2.488E-07	3.236E-03	1.7539	1.801E-07	2.354E-03	1.6183	1.638E-07	2.142E-03	1.4222	1.354E-07	1.773E-03	1.3270	1.259E-07	1.649E-03			
4,4-dm-C7	0.1204	1.422E-08	1.849E-04	0.0870	8.938E-09	1.168E-04	0.0000	0.000E+00	0.000E+00	0.0000	0.000E+00	0.000E+00	0.0000	0.000E+00	0.000E+00			
2,6-dm-C7	0.3317	3.917E-08	5.095E-04	0.2342	2.405E-08	3.142E-04	0.2096	2.122E-08	2.775E-04	0.1711	1.629E-08	2.133E-04	0.1557	1.477E-08	1.935E-04			
2,5-dm-C7	2.0164	2.381E-07	3.097E-03	1.6290	1.673E-07	2.186E-03	1.5287	1.548E-07	2.023E-03	1.3246	1.261E-07	1.651E-03	1.2291	1.166E-07	1.528E-03			
3,5-dm-C7	0.8606	1.016E-07	1.322E-03	0.6478	6.654E-08	8.694E-04	0.6007	6.081E-08	7.950E-04	0.5076	4.832E-08	6.328E-04	0.4692	4.451E-08	5.831E-04			
3-e-2-m-C6	0.6418	7.576E-08	9.855E-04	0.4078	4.188E-08	5.473E-04	0.3186	3.205E-08	4.190E-04	0.2630	2.504E-08	3.279E-04	0.2294	2.177E-08	2.851E-04			
2,3,4-tm-C6	0.1265	1.493E-08	1.942E-04	0.0664	6.822E-09	8.914E-05	0.0000	0.000E+00	0.000E+00	0.0000	0.000E+00	0.000E+00	0.0000	0.000E+00	0.000E+00			
3-e-3-m-C6	0.0000	0.000E+00	0.000E+00	0.0000	0.000E+00	0.000E+00	0.0000	0.000E+00	0.000E+00	0.0000	0.000E+00	0.000E+00	0.0000	0.000E+00	0.000E+00			
2,3-dm-C7	1.6629	1.964E-07	2.554E-03	1.1931	1.225E-07	1.601E-03	1.0642	1.077E-07	1.409E-03	0.9004	8.571E-08	1.123E-03	0.8192	7.772E-08	1.018E-03			
3,4-dm-C7	1.9706	2.327E-07	3.027E-03	1.4003	1.438E-07	1.879E-03	1.2484	1.264E-07	1.652E-03	1.0663	1.015E-07	1.329E-03	0.9692	9.196E-08	1.205E-03			
4-e-C7	0.1681	1.985E-08	2.582E-04	0.0980	1.006E-08	1.315E-04	0.0895	9.062E-09	1.185E-04	0.0782	7.444E-09	9.749E-05	0.0614	5.821E-09	7.625E-05			
4-m-C8	1.9649	2.344E-07	3.049E-03	2.8827	2.961E-07	3.869E-03	2.8436	2.879E-07	3.764E-03	1.6369	1.558E-07	2.041E-03	1.6245	1.541E-07	2.019E-03			
2-m-C8	1.0731	1.267E-07	1.648E-03	0.0000	0.000E+00	0.000E+00	0.0000	0.000E+00	0.000E+00	0.9625	9.162E-08	1.200E-03	0.8945	8.486E-08	1.112E-03			
3-m-C8	2.1756	2.569E-07	3.342E-03	1.9885	2.042E-07	2.669E-03	1.8967	1.920E-07	2.510E-03	1.7142	1.632E-07	2.137E-03	1.6353	1.552E-07	2.032E-03			
C9	0.4283	5.057E-08	6.578E-04	0.3792	3.895E-08	5.089E-04	0.3693	3.739E-08	4.889E-04	0.3426	3.262E-08	4.272E-04	0.3253	3.086E-08	4.043E-04			
Total C9																0.5599	5.723E-07	7.495E-03
C12	4.1355	3.662E-07	4.764E-03	3.4969	2.694E-07	3.520E-03	2.7400	2.080E-07	2.720E-03	2.2445	1.602E-07	2.099E-03	1.4549	1.035E-07	1.356E-03	0.0000	0.000E+00	0.000E+00
Total	100.00			100.00			100.00			100.00			100.00			100.00		
Conversion	7.1			5.5			5.4			4.8			4.8			4.4		
																Mass Balance: 91%		

Table E.6 - Propene Oligomerisation

Run No : 110

Catalyst : H-ZSM-5

Mass Catalyst,g : 0.077

Mass Sand,g : 3.75

Pretreatment : calcined at 500C in air overnight

Feed : 38 mol% N2, 62 mol% C3=

N2 flow, g/min : 0.092

C3= flow, g/min : 0.231

Molar density of feed mol/cm3 : 0.00116

Z Factor, feed : 0.994

Conc C3=, feed, mol/cm3 : 7.219e-4

Reaction Conditions : 250C, 5MPa

Internal Standard : Methane

Sample No.	1			2			3			4			5			6 (Mass Balance Sample)		
Bed Temp,C	250			251			252			251			249			252		
Time,min	95			137			179			220			289			308		
Compound (Hydrog.)	Mass%	Avg Conc mol/cm3	Rate mol/hr/g	Mass%	Avg Conc mol/cm3	Rate mol/hr/g	Mass%	Avg Conc mol/cm3	Rate mol/hr/g	Mass%	Avg Conc mol/cm3	Rate mol/hr/g	Mass%	Avg Conc mol/cm3	Rate mol/hr/g	Mass%	Avg Conc mol/cm3	Rate mol/hr/g
CH4	57.9845			60.4419			62.4947			65.3811			70.1887			8.9315		
C3		7.103E-04	-2.282E-01		7.116E-04	-2.061E-01		7.125E-04	-1.890E-01		7.137E-04	-1.668E-01		7.16E-04	-1.338E-01	90.4715	7.16E-04	-1.236E-01
C4	2.4800	8.707E-07	1.010E-02	2.4795	8.336E-07	9.690E-03	2.5390	8.243E-07	9.596E-03	2.5235	7.815E-07	9.117E-03	2.4919	7.17E-07	8.386E-03	0.0690	2.03E-07	2.379E-03
C5	1.1457	3.218E-07	3.734E-03	0.9746	2.621E-07	3.047E-03	0.8808	2.288E-07	2.663E-03	0.8020	1.987E-07	2.318E-03	0.6239	1.44E-07	1.680E-03	0.0620	1.46E-07	1.711E-03
2,3-dm-C4	2.1714	5.082E-07	5.897E-03	1.8547	4.157E-07	4.832E-03	1.7218	3.727E-07	4.338E-03	1.6017	3.307E-07	3.858E-03	1.3433	2.58E-07	3.014E-03	0.1129	2.22E-07	2.596E-03
2-m-C5	13.8375	3.239E-06	3.758E-02	13.4156	3.007E-06	3.495E-02	13.5130	2.925E-06	3.405E-02	13.2883	2.743E-06	3.200E-02	12.0217	2.31E-06	2.897E-02	1.1437	2.25E-06	2.628E-02
3-m-C5	5.8087	1.360E-06	1.577E-02	5.3088	1.190E-06	1.383E-02	5.1459	1.114E-06	1.297E-02	4.9087	1.013E-06	1.182E-02	4.1047	7.87E-07	9.209E-03	0.3711	7.29E-07	8.529E-03
C6	1.4747	3.451E-07	4.005E-03	1.5119	3.389E-07	3.939E-03	1.5126	3.274E-07	3.811E-03	1.4922	3.081E-07	3.594E-03	1.3354	2.56E-07	2.996E-03	0.0306	6.01E-08	7.033E-04
C7-C8	1.4290	2.676E-07	3.105E-03	1.2447	2.232E-07	2.594E-03	1.1282	1.954E-07	2.274E-03	0.9797	1.616E-07	1.888E-03	0.6785	1.04E-07	1.218E-03	0.4348	8.83E-07	7.991E-03
2,3,5-tm-C6	0.0957	1.494E-08	1.733E-04	0.0531	7.940E-09	9.230E-05	0.0480	8.933E-09	8.071E-05	0.0312	4.297E-09	5.012E-05	0.0000	0.00E+00	0.000E+00			
2,2-dm-C7	0.2143	3.345E-08	3.881E-04	0.1424	2.128E-08	2.474E-04	0.1358	1.960E-08	2.282E-04	0.0975	1.342E-08	1.586E-04	0.0747	9.56E-09	1.118E-04			
2,4-dm-C7	1.3412	2.093E-07	2.428E-03	1.2093	1.807E-07	2.100E-03	1.0791	1.557E-07	1.813E-03	1.3350	1.837E-07	2.144E-03	0.7687	9.83E-08	1.150E-03			
4,4-dm-C7	0.1150	1.794E-08	2.081E-04	0.0841	1.257E-08	1.461E-04	0.0744	1.074E-08	1.250E-04	0.0536	7.373E-09	8.601E-05	0.0492	8.30E-09	7.364E-05			
2,6-dm-C7	0.1868	2.914E-08	3.382E-04	0.1417	2.117E-08	2.481E-04	0.1297	1.871E-08	2.179E-04	0.1095	1.506E-08	1.757E-04	0.0819	1.05E-08	1.225E-04			
2,5-dm-C7	1.2139	1.894E-07	2.198E-03	1.0654	1.592E-07	1.850E-03	0.9740	1.405E-07	1.636E-03	0.8517	1.172E-07	1.368E-03	0.6663	8.52E-08	9.965E-04			
3,5-dm-C7	0.5799	9.049E-08	1.050E-03	0.4687	7.003E-08	8.140E-04	0.3829	5.525E-08	6.433E-04	0.3237	4.456E-08	5.198E-04	0.2591	3.31E-08	3.875E-04			
3-e-2-m-C6	0.5661	8.834E-08	1.025E-03	0.3476	5.194E-08	6.038E-04	0.2644	3.816E-08	4.442E-04	0.1935	2.663E-08	3.106E-04	0.1535	1.96E-08	2.295E-04			
2,3,4-tm-C6	0.1476	2.303E-08	2.672E-04	0.0709	1.059E-08	1.231E-04	0.0629	9.070E-09	1.056E-04	0.0000	0.000E+00	0.000E+00	0.0000	0.00E+00	0.000E+00			
3-e-3-m-C6	0.0417	6.508E-09	7.551E-05	0.0000	0.000E+00	0.000E+00	0.0210	3.023E-09	3.520E-05	0.0000	0.000E+00	0.000E+00	0.0000	0.00E+00	0.000E+00			
2,3-dm-C7	1.2447	1.942E-07	2.254E-03	0.8986	1.343E-07	1.561E-03	0.7355	1.061E-07	1.236E-03	0.6282	8.646E-08	1.009E-03	0.4931	6.30E-08	7.374E-04			
3,4-dm-C7	1.7072	2.664E-07	3.091E-03	1.1610	1.735E-07	2.016E-03	0.9411	1.358E-07	1.581E-03	0.8101	1.115E-07	1.301E-03	0.6271	8.02E-08	9.379E-04			
4-e-C7	0.0928	1.449E-08	1.681E-04	0.0664	9.925E-09	1.154E-04	0.0520	7.506E-09	8.739E-05	0.0443	6.100E-09	7.116E-05	0.0000	0.00E+00	0.000E+00			
4-m-C8	1.1932	1.862E-07	2.160E-03	1.2680	1.895E-07	2.202E-03	1.1918	1.720E-07	2.002E-03	1.0606	1.460E-07	1.703E-03	0.9473	1.21E-07	1.417E-03			
2-m-C8	0.6916	1.079E-07	1.252E-03	0.7480	1.118E-07	1.299E-03	0.6904	9.961E-08	1.160E-03	0.8455	8.885E-08	1.036E-03	0.5107	6.53E-08	7.638E-04			
3-m-C8	1.3249	2.067E-07	2.399E-03	1.3635	2.037E-07	2.368E-03	1.2410	1.791E-07	2.085E-03	1.1442	1.575E-07	1.837E-03	0.9398	1.20E-07	1.406E-03			
C9	0.2521	3.933E-08	4.564E-04	0.2572	3.843E-08	4.467E-04	0.2439	3.519E-08	4.096E-04	0.2170	2.986E-08	3.484E-04	0.1862	2.38E-08	2.784E-04			
Total C9																0.3730	4.88E-07	5.715E-03
C12	2.6596	3.112E-07	3.611E-03	3.4223	3.835E-07	4.458E-03	2.7959	3.026E-07	3.522E-03	1.4772	1.525E-07	1.779E-03	1.4544	1.39E-07	1.631E-03	0	0.00E+00	0.000E+00
Total	100.00			100.00			100.00			100.00			100.00			100.00		
Conversion	5.3			4.8			4.4			3.9			3.1			2.9		
																Mass Balance: 99%		

Table E.7 - Propene Oligomerisation

Run No : 94

Catalyst : H-ZSM-5

Mass Catalyst,g : 0.06

Mass Sand,g : 3.0

Pretreatment : calcined at 500C in air overnight

Feed : 23 mol% N2, 77 mol% C3=

N2 flow, g/min : 0.058

C3= flow, g/min : 0.287

Molar density of feed mol/cm3 : 0.00120

Z Factor, feed : 0.956

Conc C3=, feed, mol/cm3 : 9.231e-4

Reaction Conditions : 250C, 5MPa

Internal Standard : Methane

Sample No.	1			2			3			4			5			8 (Mass Balance Sample)		
Bed Temp,C	249			249			249			249			250			249		
Time,min	97			152			195			237			282			332		
Compound (Hydrog.)	Mass%	Avg Conc mol/cm3	Rate mol/hr/g	Mass%	Avg Conc mol/cm3	Rate mol/hr/g	Mass%	Avg Conc mol/cm3	Rate mol/hr/g	Mass%	Avg Conc mol/cm3	Rate mol/hr/g	Mass%	Avg Conc mol/cm3	Rate mol/hr/g	Mass%	Avg Conc mol/cm3	Rate mol/hr/g
CH4	53.4043			59.7265			60.3286			60.6881			60.3045			6.3159		
C3		9.085E-04	-3.635E-01		9.117E-04	-2.810E-01		9.119E-04	-2.740E-01		9.120E-04	-2.699E-01		9.117E-04	-2.743E-01	90.4472	9.13E-04	-2.8E-01
C4	2.4901	1.007E-06	1.457E-02	2.9688	1.067E-06	1.553E-02	2.7755	9.671E-07	1.436E-02	3.3342	1.178E-06	1.717E-02	4.4692	1.569E-06	2.316E-02	0.0864	3.23E-07	4.70E-03
C5	1.0945	3.539E-07	5.123E-03	0.8076	2.322E-07	3.381E-03	0.7719	2.198E-07	3.199E-03	0.7107	2.009E-07	2.928E-03	0.6925	1.970E-07	2.871E-03	0.0566	1.69E-07	2.46E-03
2,3-dm-C4	2.4093	6.493E-07	9.399E-03	1.8076	4.331E-07	6.305E-03	1.7324	4.107E-07	5.982E-03	1.6420	3.868E-07	5.637E-03	1.5722	3.727E-07	5.431E-03	0.1461	3.64E-07	5.29E-03
2-m-C5	16.0006	4.312E-06	6.242E-02	15.5436	3.724E-06	5.422E-02	16.0184	3.798E-06	5.532E-02	16.0945	3.792E-06	5.525E-02	16.0598	3.607E-06	5.548E-02	1.5530	3.87E-08	5.63E-02
3-m-C5	6.5569	1.767E-06	2.558E-02	5.5893	1.339E-06	1.950E-02	5.6216	1.333E-06	1.941E-02	5.5390	1.305E-06	1.901E-02	5.4152	1.284E-06	1.871E-02	0.5055	1.26E-06	1.83E-02
C6	1.8167	4.896E-07	7.087E-03	1.9684	4.717E-07	6.866E-03	2.0931	4.963E-07	7.228E-03	2.1490	5.063E-07	7.377E-03	2.1598	5.120E-07	7.461E-03	0.2131	5.32E-07	7.72E-03
C7-C8	1.7788	3.835E-07	5.551E-03	0.8743	1.676E-07	2.440E-03	0.8184	1.552E-07	2.261E-03	0.7285	1.373E-07	2.001E-03	0.7763	1.472E-07	2.146E-03	0.0972	1.94E-07	2.82E-03
2,3,5-tm-C6	0.1341	2.408E-08	3.486E-04	0.0610	9.746E-09	1.419E-04	0.0495	7.826E-09	1.140E-04	0.0438	6.874E-09	1.002E-04	0.0421	6.652E-09	9.693E-05			
2,2-dm-C7	0.2430	4.366E-08	6.320E-04	0.1224	1.958E-08	2.847E-04	0.1115	1.782E-08	2.587E-04	0.0992	1.559E-08	2.271E-04	0.1112	1.758E-08	2.561E-04			
2,4-dm-C7	1.4911	2.679E-07	3.878E-03	1.1191	1.788E-07	2.602E-03	1.0582	1.673E-07	2.436E-03	0.9581	1.505E-07	2.193E-03	0.9255	1.463E-07	2.132E-03			
4,4-dm-C7	0.1377	2.474E-08	3.582E-04	0.0869	1.388E-08	2.020E-04	0.0887	1.402E-08	2.042E-04	0.0767	1.205E-08	1.755E-04	0.0825	1.303E-08	1.899E-04			
2,6-dm-C7	0.2197	3.948E-08	5.715E-04	0.1289	2.059E-08	2.997E-04	0.1270	2.007E-08	2.924E-04	0.1057	1.661E-08	2.420E-04	0.1163	1.839E-08	2.679E-04			
2,5-dm-C7	1.2028	2.161E-07	3.128E-03	0.9293	1.484E-07	2.161E-03	0.8765	1.385E-07	2.018E-03	0.7887	1.239E-07	1.805E-03	0.7917	1.251E-07	1.823E-03			
3,5-dm-C7	0.7052	1.267E-07	1.834E-03	0.4448	7.108E-08	1.034E-03	0.4133	6.533E-08	9.515E-04	0.3682	5.751E-08	8.380E-04	0.3059	4.835E-08	7.045E-04			
3-e-2-m-C6	0.6801	1.222E-07	1.769E-03	0.3681	5.880E-08	8.559E-04	0.3134	4.954E-08	7.215E-04	0.2695	4.233E-08	6.169E-04	0.2409	3.807E-08	5.548E-04			
2,3,4-tm-C6	0.1757	3.156E-08	4.569E-04	0.0626	1.000E-08	1.456E-04	0.0486	7.690E-09	1.120E-04	0.0477	7.487E-09	1.091E-04	0.0277	4.380E-09	6.383E-05			
3-e-3-m-C6	0.0484	8.687E-09	1.258E-04	0.0226	3.614E-09	5.261E-05	0.0000	0.000E+00	0.000E+00	0.0182	2.859E-09	4.165E-05	0.0000	0.000E+00	0.000E+00			
2,3-dm-C7	1.4054	2.525E-07	3.655E-03	0.8416	1.344E-07	1.957E-03	0.7568	1.196E-07	1.742E-03	0.6799	1.068E-07	1.556E-03	0.6248	9.875E-08	1.439E-03			
3,4-dm-C7	1.9716	3.542E-07	5.128E-03	1.1595	1.852E-07	2.696E-03	1.0367	1.639E-07	2.387E-03	0.9204	1.446E-07	2.106E-03	0.8841	1.397E-07	2.036E-03			
4-e-C7	0.1090	1.957E-08	2.834E-04	0.0533	8.519E-09	1.240E-04	0.0495	7.826E-09	1.140E-04	0.0429	6.738E-09	9.818E-05	0.0263	4.164E-09	6.068E-05			
4-m-C8	1.2775	2.295E-07	3.322E-03	1.2068	1.928E-07	2.806E-03	1.1542	1.824E-07	2.657E-03	1.0673	1.676E-07	2.443E-03	1.5995	2.528E-07	3.684E-03			
2-m-C8	0.6794	1.221E-07	1.767E-03	0.5919	9.455E-08	1.376E-03	0.6118	9.670E-08	1.408E-03	0.5811	9.127E-08	1.330E-03	0.0000	0.000E+00	0.000E+00			
3-m-C8	1.3815	2.482E-07	3.593E-03	1.1878	1.897E-07	2.762E-03	1.1792	1.864E-07	2.715E-03	1.0608	1.666E-07	2.428E-03	1.0398	1.643E-07	2.395E-03			
C9	0.2571	4.619E-08	6.686E-04	0.2121	3.388E-08	4.933E-04	0.2062	3.260E-08	4.747E-04	0.1894	2.974E-08	4.334E-04	0.1984	3.104E-08	4.523E-04			
Total C9																0.5790	9.83E-07	1.40E-02
C12	2.3297	3.139E-07	4.544E-03	2.1151	2.534E-07	3.689E-03	1.7591	2.085E-07	3.037E-03	1.7984	2.118E-07	3.087E-03	1.5359	1.821E-07	2.653E-03	0.0000	0.00E+00	0.00E+00
Total	100.00			100.00			100.00			100.00			100.00			100.00		
Conversion	5.3			4.1			4.0			3.9			4.0			4.1		
																Mass Balance: 91%		

Table E.8 - Propene Oligomerisation

Run No : 95

Catalyst : H-ZSM-5

Mass Catalyst,g : 0.06

Mass Sand,g : 3.0

Pretreatment : calcined at 500C in air overnight

Feed : 17 mol% N2, 83 mol% C3=

N2 flow, g/min : 0.052

C3= flow, g/min : 0.383

Molar density of feed mol/cm3 : 0.00120

Z Factor, feed : 0.942

Conc C3=, feed, mol/cm3 : 9.925e-4

Reaction Conditions : 250C, 5MPa

Internal Standard : Methane

Sample No.	1			2			3			4			5			6 (Mass Balance Sample)		
Bed Temp,C	249			249			253			253			253			249		
Time,min	95			138			176			218			254			332		
Compound (Hydrog.)	Mass%	Avg Conc mol/cm3	Rate mol/hr/g	Mass%	Avg Conc mol/cm3	Rate mol/hr/g	Mass%	Avg Conc mol/cm3	Rate mol/hr/g	Mass%	Avg Conc mol/cm3	Rate mol/hr/g	Mass%	Avg Conc mol/cm3	Rate mol/hr/g	Mass%	Avg Conc mol/cm3	Rate mol/hr/g
CH4	54.5059			55.3377			54.1787			57.7147			58.2432			4.5997		
C3		9.819E-04	-3.391E-01		9.821E-04	-3.279E-01		9.816E-04	-3.436E-01		9.830E-04	-2.976E-01		9.832E-04	-2.913E-01	92.7946	9.843E-04	-2.843E-01
C4	3.6082	1.116E-06	2.017E-02	3.9069	1.189E-06	2.151E-02	3.9137	1.217E-06	2.201E-02	3.6759	1.071E-06	1.941E-02	3.9314	1.134E-06	2.057E-02	0.0632	2.493E-07	4.514E-03
C5	0.9800	2.424E-07	4.383E-03	0.8613	2.097E-07	3.794E-03	0.8720	2.170E-07	3.923E-03	0.7649	1.783E-07	3.230E-03	0.7432	1.716E-07	3.110E-03	0.0438	1.382E-07	2.502E-03
2,3-dm-C4	2.3196	4.781E-07	8.644E-03	2.0260	4.110E-07	7.437E-03	1.9951	4.138E-07	7.480E-03	1.8038	3.503E-07	6.348E-03	1.7495	3.366E-07	6.102E-03	0.1203	3.164E-07	5.728E-03
2-m-C5	18.2753	3.767E-06	6.811E-02	18.8407	3.822E-06	6.916E-02	19.1740	3.976E-06	7.189E-02	18.6051	3.614E-06	6.548E-02	18.7221	3.602E-06	6.529E-02	1.3782	3.624E-06	6.561E-02
3-m-C5	6.3443	1.308E-06	2.364E-02	6.1907	1.256E-06	2.272E-02	6.4236	1.332E-06	2.408E-02	5.9882	1.163E-06	2.108E-02	5.8599	1.127E-06	2.044E-02	0.4182	1.100E-06	1.991E-02
C6	1.7935	3.697E-07	6.684E-03	2.1425	4.347E-07	7.864E-03	2.2794	4.727E-07	8.546E-03	2.2896	4.447E-07	8.058E-03	2.3184	4.460E-07	8.086E-03	0.1772	4.660E-07	8.436E-03
C7-C8	1.0738	1.771E-07	3.201E-03	0.8902	1.445E-07	2.614E-03	1.0014	1.661E-07	3.003E-03	0.7198	1.118E-07	2.027E-03	0.7163	1.102E-07	1.998E-03	0.0978	2.056E-07	3.723E-03
2,3,5-tm-C6	0.0672	9.238E-09	1.670E-04	0.0592	8.006E-09	1.449E-04	0.0573	7.922E-09	1.432E-04	0.0000	0.000E+00	0.000E+00	0.0445	5.704E-09	1.034E-04			
2,2-dm-C7	0.1218	1.674E-08	3.027E-04	0.1280	1.732E-08	3.133E-04	0.1271	1.758E-08	3.178E-04	0.0841	1.088E-08	1.972E-04	0.1081	1.386E-08	2.513E-04			
2,4-dm-C7	1.1618	1.597E-07	2.887E-03	1.0605	1.434E-07	2.595E-03	1.1088	1.533E-07	2.771E-03	0.9344	1.210E-07	2.192E-03	0.8916	1.143E-07	2.073E-03			
4,4-dm-C7	0.1011	1.389E-08	2.511E-04	0.0968	1.310E-08	2.369E-04	0.0900	1.244E-08	2.249E-04	0.0729	9.441E-09	1.711E-04	0.0796	1.021E-08	1.852E-04			
2,6-dm-C7	0.1426	1.959E-08	3.542E-04	0.1377	1.862E-08	3.369E-04	0.1316	1.820E-08	3.289E-04	0.0827	1.070E-08	1.940E-04	0.1019	1.307E-08	2.369E-04			
2,5-dm-C7	0.9520	1.308E-07	2.365E-03	0.8833	1.195E-07	2.162E-03	1.3035	1.802E-07	3.258E-03	0.7644	9.898E-08	1.794E-03	0.7602	9.750E-08	1.768E-03			
3,5-dm-C7	0.4638	6.374E-08	1.152E-03	0.3543	4.791E-08	8.669E-04	0.0000	0.000E+00	0.000E+00	0.3483	4.510E-08	8.173E-04	0.2741	3.515E-08	6.373E-04			
3-e-2-m-C6	0.4300	5.909E-08	1.068E-03	0.2978	4.028E-08	7.288E-04	0.2762	3.819E-08	6.903E-04	0.2369	3.067E-08	5.557E-04	0.2094	2.686E-08	4.870E-04			
2,3,4-tm-C6	0.0884	1.215E-08	2.197E-04	0.0592	8.006E-09	1.449E-04	0.0394	5.446E-09	9.846E-05	0.0376	4.871E-09	8.826E-05	0.0243	3.117E-09	5.651E-05			
3-e-3-m-C6	0.0253	3.472E-09	6.277E-05	0.0000	0.000E+00	0.000E+00	0.0000	0.000E+00	0.000E+00	0.0000	0.000E+00	0.000E+00	0.0000	0.000E+00	0.000E+00			
2,3-dm-C7	0.8704	1.196E-07	2.162E-03	0.6902	9.335E-08	1.689E-03	0.7050	9.747E-08	1.762E-03	0.5949	7.703E-08	1.396E-03	0.5477	7.024E-08	1.273E-03			
3,4-dm-C7	1.3022	1.789E-07	3.235E-03	0.9783	1.323E-07	2.394E-03	0.9709	1.342E-07	2.427E-03	0.8243	1.067E-07	1.934E-03	0.7514	9.637E-08	1.747E-03			
4-e-C7	0.0496	6.820E-09	1.233E-04	0.0367	4.965E-09	8.983E-05	0.0394	5.446E-09	9.846E-05	0.0316	4.089E-09	7.410E-05	0.0000	0.000E+00	0.000E+00			
4-m-C8	1.2110	1.664E-07	3.009E-03	1.2004	1.624E-07	2.938E-03	1.2400	1.714E-07	3.099E-03	1.0788	1.397E-07	2.531E-03	1.0990	1.409E-07	2.555E-03			
2-m-C8	0.6881	9.455E-08	1.709E-03	0.6420	8.683E-08	1.571E-03	0.7216	9.976E-08	1.804E-03	0.6321	8.184E-08	1.483E-03	0.5689	7.296E-08	1.323E-03			
3-m-C8	1.2652	1.739E-07	3.143E-03	1.1729	1.586E-07	2.870E-03	1.2655	1.750E-07	3.163E-03	1.1109	1.438E-07	2.606E-03	0.9976	1.279E-07	2.319E-03			
C9	0.2387	3.280E-08	5.930E-04	0.2161	2.923E-08	5.289E-04	0.2283	3.156E-08	5.706E-04	0.2016	2.610E-08	4.729E-04	0.1882	2.414E-08	4.377E-04			
Total C9																0.3070	5.383E-07	9.744E-03
C12	1.9203	1.979E-07	3.578E-03	1.7905	1.816E-07	3.286E-03	1.8577	1.926E-07	3.482E-03	1.4025	1.362E-07	2.468E-03	1.0695	1.029E-07	1.865E-03	0.0000	0.000E+00	0.000E+00
Total	100.00			100.00			100.00			100.00			100.00			100.00		
Conversion	3.7			3.6			3.8			3.3			3.2			3.1		
																Mass Balance: 93%		

Table E.9 - Propene Oligomerisation

Run No : 82

Catalyst : H-ZSM-5

Mass Catalyst,g : 0.06

Mass Sand,g : 3.0

Pretreatment : calcined at 500C in air overnight

Feed : 0 mol% N2, 100 mol% C3=

N2 flow, g/min : 0.0

C3= flow, g/min : 0.266

Molar density of feed mol/cm3 : 0.00268

Z Factor, feed : 0.896

Conc C3=, feed, mol/cm3 : 2.685e-3

Reaction Conditions : 250C, 5MPa

Internal Standard : Methane

Sample No.	1			2			3			4			5			6 (Mass Balance Sample)		
Bed Temp,C	247			249			250			253			252			254		
Time,min	97			149			188			210			273			338		
Compound (Hydrog.)	Mass%	Avg Conc mol/cm3	Rate mol/hr/g	Mass%	Avg Conc mol/cm3	Rate mol/hr/g	Mass%	Avg Conc mol/cm3	Rate mol/hr/g	Mass%	Avg Conc mol/cm3	Rate mol/hr/g	Mass%	Avg Conc mol/cm3	Rate mol/hr/g	Mass%	Avg Conc mol/cm3	Rate mol/hr/g
CH4	45.4849			47.3883			44.6922			44.9296			46.0187			5.8928		
C3		2.637E-03	-4.994E-01		2.640E-03	-4.626E-01		2.633E-03	-5.156E-01		2.635E-03	-5.107E-01		2.636E-03	-4.888E-01	87.8399	2.643E-03	-4.018E-01
C4	1.6857	2.569E-06	1.158E-02	1.6369	2.386E-06	1.079E-02	2.4266	3.765E-06	1.697E-02	1.7117	2.642E-06	1.191E-02	1.7210	2.588E-06	1.169E-02	0.0908	1.006E-06	4.588E-03
C5	1.0326	1.259E-06	5.675E-03	0.9510	1.109E-06	5.017E-03	0.9838	1.221E-06	5.503E-03	1.0660	1.316E-06	5.931E-03	0.9585	1.153E-06	5.207E-03	0.1127	1.001E-06	4.565E-03
2,3-dm-C4	2.8723	2.919E-06	1.316E-02	2.5425	2.470E-06	1.118E-02	2.6220	2.712E-06	1.222E-02	2.5370	2.611E-06	1.176E-02	2.4421	2.448E-06	1.106E-02	0.2997	2.220E-06	1.012E-02
2-m-C5	17.8331	1.812E-05	6.168E-02	18.5625	1.804E-05	8.161E-02	20.6378	2.135E-05	9.620E-02	19.6419	2.021E-05	9.108E-02	20.1720	2.022E-05	9.132E-02	2.5218	1.867E-05	8.514E-02
3-m-C5	6.8936	7.005E-06	3.157E-02	6.8652	6.670E-06	3.018E-02	7.4270	7.682E-06	3.462E-02	7.5683	7.788E-06	3.509E-02	7.4516	7.469E-08	3.373E-02	0.9189	6.804E-06	3.102E-02
C6	1.5699	1.595E-06	7.191E-03	1.9483	1.893E-06	8.565E-03	2.3069	2.386E-06	1.075E-02	2.4279	2.498E-06	1.126E-02	2.4638	2.470E-06	1.115E-02	0.3101	2.296E-06	1.047E-02
C7-C8	1.5543	1.264E-06	5.695E-03	1.1555	6.982E-07	4.064E-03	1.1318	9.365E-07	4.221E-03	1.2561	1.034E-06	4.659E-03	1.1128	8.924E-07	4.030E-03	0.1400	8.296E-07	3.783E-03
2,3,5-tm-C6	0.1821	1.233E-07	5.559E-04	0.1145	7.416E-08	3.356E-04	0.1041	7.181E-08	3.237E-04	0.1069	7.335E-08	3.305E-04	0.0918	6.134E-08	2.770E-04			
2,2-dm-C7	0.2933	1.987E-07	8.956E-04	0.2306	1.494E-07	6.759E-04	0.2115	1.459E-07	6.574E-04	0.2325	1.595E-07	7.186E-04	0.2092	1.398E-07	6.314E-04			
2,4-dm-C7	1.9297	1.307E-06	5.892E-03	1.8523	1.200E-06	5.429E-03	1.7944	1.237E-08	5.576E-03	1.9326	1.326E-06	5.974E-03	1.8094	1.209E-06	5.461E-03			
4,4-dm-C7	0.2270	1.538E-07	6.933E-04	0.1789	1.159E-07	5.245E-04	0.1642	1.132E-07	5.102E-04	0.1646	1.129E-07	5.089E-04	0.1523	1.018E-07	4.598E-04			
2,6-dm-C7	0.2408	1.631E-07	7.352E-04	0.1904	1.233E-07	5.579E-04	0.1812	1.250E-07	5.632E-04	0.2046	1.403E-07	6.323E-04	0.1788	1.195E-07	5.396E-04			
2,5-dm-C7	1.4166	9.597E-07	4.326E-03	1.3766	8.917E-07	4.035E-03	1.3236	9.127E-07	4.113E-03	1.5309	1.050E-06	4.732E-03	1.3746	9.186E-07	4.149E-03			
3,5-dm-C7	1.0245	6.940E-07	3.128E-03	0.8757	5.672E-07	2.567E-03	0.8161	5.628E-07	2.536E-03	0.8032	5.510E-07	2.483E-03	0.7712	5.154E-07	2.328E-03			
3-e-2-m-C6	1.0339	7.004E-07	3.157E-03	0.7229	4.682E-07	2.119E-03	0.6434	4.437E-07	2.000E-03	0.6569	4.506E-07	2.031E-03	0.5885	3.933E-07	1.776E-03			
2,3,4-tm-C8	0.2340	1.586E-07	7.147E-04	0.1368	8.860E-08	4.009E-04	0.1224	8.439E-08	3.803E-04	0.1261	8.649E-08	3.897E-04	0.1076	7.188E-08	3.246E-04			
3-e-3-m-C6	0.0587	3.977E-08	1.793E-04	0.0441	2.854E-08	1.291E-04	0.0388	2.678E-08	1.207E-04	0.0394	2.701E-08	1.217E-04	0.0344	2.296E-08	1.037E-04			
2,3-dm-C7	1.9160	1.298E-06	5.850E-03	1.5403	9.977E-07	4.515E-03	1.4072	9.703E-07	4.373E-03	1.4904	1.022E-06	4.607E-03	1.3555	9.058E-07	4.091E-03			
3,4-dm-C7	3.0057	2.036E-06	9.178E-03	2.3073	1.494E-06	6.762E-03	2.0933	1.443E-06	6.505E-03	2.1309	1.462E-06	6.587E-03	1.9710	1.317E-06	5.949E-03			
4-e-C7	0.1023	6.933E-08	3.125E-04	0.0843	5.461E-08	2.471E-04	0.0765	5.275E-08	2.377E-04	0.0900	8.172E-08	2.781E-04	0.0738	4.930E-08	2.227E-04			
4-m-C8	1.4317	9.699E-07	4.372E-03	1.7149	1.111E-06	5.026E-03	1.7285	1.192E-06	5.372E-03	1.8085	1.241E-06	5.590E-03	1.7131	1.145E-06	5.170E-03			
2-m-C8	0.7999	5.419E-07	2.442E-03	0.8270	5.357E-07	2.424E-03	0.8026	5.534E-07	2.494E-03	0.8830	6.058E-07	2.730E-03	0.8858	5.920E-07	2.674E-03			
3-m-C8	1.5457	1.047E-06	4.720E-03	1.7207	1.115E-06	5.043E-03	1.6755	1.155E-06	5.207E-03	1.8142	1.245E-06	5.608E-03	1.7117	1.144E-06	5.166E-03			
C9	0.2577	1.746E-07	7.870E-04	0.2760	1.788E-07	8.090E-04	0.2718	1.874E-07	8.448E-04	0.2907	1.994E-07	8.986E-04	0.2869	1.917E-07	8.660E-04			
Total C9																1.3869	6.847E-06	3.122E-02
C12	5.3738	2.730E-06	1.231E-02	4.7565	2.311E-06	1.046E-02	4.3166	2.232E-06	1.006E-02	4.5563	2.344E-06	1.056E-02	4.3439	2.177E-06	9.833E-03	0.4866	1.802E-08	8.215E-03
Total	100.00			100.00			100.00			100.00			100.00			100.00		
Conversion	7.9			7.3			8.1			8.1			7.7			6.3		
																Mass Balance: 105%		